Deeper into the dip: probing the ecophysiological implications of metabolic rate suppression in pulmonate limpets.

By: Sebbi Kankondi

ORCID: 0000-0002-2511-6590

Department of Zoology and Entomology

Rhodes University

Supervisor: Christopher D McQuaid

Department of Zoology and Entomology

Rhodes University

Co-supervisor: Dr Cristián Mónaco

French National Institute for Ocean Science and Technology

2025-07-30

A thesis submitted in fulfilment of the requirements for the PhD (Marine Biology) degree in the Department of Zoology and Entomology of Rhodes University

Abstract

Given the increasing threat posed by climate change, particularly in environments marked by extreme temperature fluctuations and desiccation stress, understanding the adaptive strategies that underpin thermal tolerance is crucial for predicting species resilience. Central to this investigation is the concept of metabolic rate suppression (hypometabolism), an energy-saving mechanism widespread among animals exposed to stressful climatic conditions. This thesis investigates the ecophysiological responses of two pulmonate limpets, *Siphonaria capensis* and *S. serrata*, to the dynamic thermal conditions characteristic of South Africa's rocky intertidal zones.

An integrative approach was employed to address this objective. Field surveys, utilizing transect-quadrat analysis and capture–mark–recapture experiments, quantified microhabitat use and preference across sites spanning distinct biogeographic regions (West, South, and East coasts of South Africa). Complementing these field studies, a laboratory-based thermal preference assay using an artificial thermal gradient elucidated the role of behavioural thermoregulation, via thermotaxis, in the micro-scale distribution of *S. capensis*. In parallel, non-invasive plethysmography was used to derive key physiological indices, including final breakpoint temperature, flatline temperature, and a proxy for hypometabolism, cardiac suppression range, from species-specific cardiac

responses to thermal stress. These parameters helped test the study's primary hypotheses: that limpets inhabiting thermally stressful microhabitats, or those unable to escape such conditions, would exhibit more pronounced hypometabolic activity and consequently greater thermal limits than conspecifics in cooler environments. This premise originated from the assumption that hypometabolism extends functional thermal limits under heat stress.

By integrating field observations, behavioural assays, and physiological measurements, this work contributes to a more nuanced understanding of how intertidal organisms mitigate thermal stress. Both species predominantly occupied, and exhibited pronounced preferences for, thermally benign microhabitats, such as crevices or coastal zones closer to the West coast. Neither species, however, exclusively avoided thermally suboptimal conditions. Furthermore, thermal history likely influenced these trends, with *S. capensis* demonstrating short-term thermal preferences linked to prior thermal acclimatization. This connection was corroborated by findings from the heart-rate analysis. Specifically, hypometabolism correlates with enhanced thermal tolerance, and through its transient and flexible nature, the consistency of this relationship is maintained across different thermal regimes.

In summary, the study provides compelling evidence that hypometabolism extends the upper thermal limits of pulmonate limpets, and that the hypotheses rooted in metabolic rate suppression (MRS) theory are supported. I therefore conclude that MRS theory serves as a valuable framework for predicting species thermal resilience across diverse environmental conditions.

Table of contents

List of tables

List of figures

Acknowledgements

Firstly, thank you to my supervisors, Prof. Christopher McQuaid and Dr. Cristián Mónaco. Prof. McQuaid, I truly would never have completed this thesis without your persistence and insistence that I find a way. Your guidance at crucial moments during my writing, especially when I had given up, is ultimately the reason I have come this far. Thank you again for your years of patience and belief in me.

To Dr. Mónaco, you set such a high standard as a scientist that it was difficult not to feel inspired after every conversation. You were the spark that lit my desire to tackle and understand challenging subjects in pursuit of personal growth.

This thesis would not have reached completion without the help of all current and former members of the coastal research group, and many of the students, researchers, and staff members at Rhodes University. Thank you to Ticia Swanepoel and Jaqueline Trassierra for making sure I always had a decent place to stay during my field trips along the South African coast. Thank you to my good friend, Siphosihle Wotshela, for joining me on my many field trips and assisting with all the fieldwork. I know more about philosophy than I ever intended to, thanks to our endless conversations. Thank you to all members of the Rhodes University Taekwondo and Mixed Martial Arts clubs. The camaraderie and countless hours in the dojo helped me hold on to my sanity.

Thank you to Dr Adam Smith of the School of Mathematical and Computational Sciences, Massey University, New Zealand, and Dr Jeremy Baxter of the Department of Statistics, Rhodes University, for reviewing my analytical approach. I truly appreciate the time you both took from your busy schedules to confirm that the statistical analysis was sound.

Thank you to the National Research Fund (NRF) for the financial support.

Finally, thank you to my parents, Dr. Lantine Harases-Kankondi and Petri Pekkarinen. You never stopped encouraging me to complete my work, you never stopped praying for me, and you never stopped believing that I could see this through.

Chapter 1

General introduction

1.1 Climate change impact on intertidal ecology

Climate change stands as one of the most pressing global challenges in modern times, driving shifts in ocean chemistry, sea level, environmental temperature regimes, and patterns of extreme weather events (IPCC 2018, 2021). This change primarily results from the accumulation of anthropogenically produced greenhouse gases, such as carbon dioxide and methane, that trap heat in the atmosphere and gradually raise global temperatures (IPCC 2018). Over the past century, the effects of anthropogenically mediated elevations in atmospheric and seawater temperatures in coastal and intertidal environments have been especially pronounced because these ecosystems are already subject to highly variable abiotic conditions (Harley & Helmuth 2003, Little et al. 2009). For intertidal organisms exposed to the oscillating tide, this includes fluctuating oxygen availability, desiccation, and particularly elevated thermal stress (Branch 1981, Garrity 1984, Denny & Harley 2006, Little et al. 2009). Organisms on rocky shores are frequently exposed to extreme daily changes in temperature, which are projected to intensify with ongoing climate warming (Williams & Morritt 1995, Denny et al. 2011, IPCC 2018). These extreme temperatures force organisms to the edge of their physiological capacity, driving significant changes in ecological processes across a range of spatial and temporal scales (Cossins & Bowler 1987, Schmidt-Nielsen 1997, Somero 2002, Perry et al. 2005, Parmesan 2006). Ecosystems with organisms that are chronically physiologically compromised experience changes in species dominance

interactions, or competition dynamics, potentially driving community-level restructuring (Parmesan 2006, Harley 2008, Menge et al. 2022). Furthermore, when temperatures increasingly reach or exceed the physiological tolerance thresholds of local fauna, this can lead to a rise in mass heat-induced die-offs, prompting changes in species' micro- and broad-scale distributions (Harley 2008, Soon & Ransangan 2019, McDowell & Sousa 2019, Menge et al. 2022, Heo et al. 2023). Central to understanding how intertidal species might endure or fail under various climate-change scenarios is pinpointing the ecological and physiological mechanisms that enable them to persist in environments of intense heat and desiccation stress. In this context, metabolic rate suppression (MRS) theory has been formulated to explore how organisms regulate their physiology to manage variable metabolic demands, thereby ensuring an appropriate thermal response capacity across thermally heterogeneous spatiotemporal scales (Storey & Storey 1990, Marshall & McQuaid 1991, Storey 1998, Pörtner 2010, Williams et al. 2011).

1.2 Metabolic Rate Suppression theory

Metabolic rate suppression, also referred to as metabolic depression or hypometabolism, is commonly interpreted as an energy-saving adaptation employed by animals that are typically exposed to potentially harmful abiotic conditions such as low oxygen concentrations, osmotic, thermal, and desiccation stress (Newell 1969, Sokolova & Pörtner 2001, Verberk et al. 2016), with the present study focusing on thermal stress. In their study, Marshall & McQuaid (2011) show that this concept challenges the universal temperature dependence (UTD) model, which explains the effect of increasing temperature on resting metabolic rate through the activation energy of biochemical reactions, as predicted by the Boltzmann-Arrhenius equation (Brown et al. 2004, Allen & Gillooly 2007). According to the UTD model, temperature increases continuously accelerate the rates of biochemical reactions and resting metabolism before the onset of acute or chronic thermal stress (Schulte 2015). This acceleration results in an initial boost in ATP production, primarily via oxidative phosphorylation, driven by increased membrane fluidity and heightened enzyme activity (Schulte 2015, Petrov & Razuvaeva

2018). The initial boost in ATP production, coupled with increased O_2 consumption rates, is necessary to meet the elevated energy demands associated with a sustained acceleration in reaction rates as aerobic metabolism intensifies.

As temperature continues to rise, the efficiency of ATP-producing biochemical processes begins to decline due to the thermal denaturation of enzymes, destabilization of protein structures, and disruption of cellular membranes (Angilletta 2009, Schulte 2015). The reduction in biochemical efficiency limits the availability of O_2 for energy production (Pörtner 2001). This limitation is further exacerbated by cardiorespiratory constraints and the reduced solubility of O_2 at high temperatures (Pörtner 2001). An energy deficit arises from the mismatch between the sustained, heightened ATP demand and the diminishing ATP supply that, if unresolved, can become fatal (Angilletta 2009). To address this energy deficit, cells may partially transition to anaerobic respiration (Houlihan et al. 1981, McMahon 1988, Simpfendörfer et al. 1995), which provides an alternative pathway for ATP production under challenging conditions (McMahon 1990, Donovan et al. 1999). While anaerobic respiration generates ATP without the need for oxygen, it is inefficient, producing only a fraction of the approximately 32 ATP molecules yielded through aerobic pathways (Granchi et al. 2010, Müller et al. 2012). Furthermore, it leads to the accumulation of potentially harmful by-products, which must be rapidly metabolized through elevated aerobic respiration rates once conditions normalize (Simpfendörfer et al. 1995, Donovan et al. 1999, Sokolova & Pörtner 2001). This is expressed as the enhanced catabolism of available substrates, placing significant strain on carbohydrate reserves, which are depleted more quickly (Gäde 1983, Babarro et al. 2007).

The resulting metabolic challenge, arising collectively from the low energy output and anaerobic by-product accumulation, shortens the time during which anaerobic pathways can sustain metabolic demands before organisms exceed their thermal tolerance limits. According to the MRS theory, however, organisms capable of hypometabolism mitigate reliance on anaerobic metabolism, along with the associated production of its by-products (Marshall & McQuaid 1992, Grieshaber et al. 1994, Curtis et al. 2000,

Sokolova & Pörtner 2001, Abele et al. 2002, Connor & Gracey 2012, Verberk et al. 2016). In marine intertidal gastropods, facultative hypometabolism likely arose in early lineages as a physiological safeguard against cyclical hypoxic or desiccation stress, triggered by shell withdrawal in response to predation and by tidal emersion, respectively (Marshall & McQuaid 1991, 2020). This inherent restriction of gas exchange selects for biochemical pathways that minimise the additional energetic burden imposed by limited ventilation (Marshall & McQuaid 1991, 2020). Over evolutionary time, the expansion of these lineages into warmer high-shore zones, driven by further ecological pressures such as intensified competition for space and food, likely fostered the exaptation of hypometabolism to buffer heat stress (Marshall & McQuaid 1991).

Hypometabolism is triggered within a specific temperature range that precedes the sub-lethal thermal thresholds of an animal (Hui et al. 2020, Liao et al. 2021). At this stage, a cascade of precisely coordinated regulatory mechanisms comes into play, involving adjustments to gene and protein activity to minimize energy expenditure while suppressing energetically costly activities such as protein synthesis (Storey & Storey 2004, Guppy & Withers 2007). Among these mechanisms, reversible protein phosphorylation plays a central regulatory role by inactivating key enzymes involved in metabolism and ion-transporting ATPases, which lowers ATP consumption and suppresses metabolic demand. This response presents an unusual pattern in how reaction rate changes with temperature, which deviates from the typical expectations of the Boltzmann-Arrhenius relationship (Storey & Storey 2004). Consequently, MRS theory provides a more explicit indication of a positive correlation between adverse environmental conditions, particularly heat stress, and the occurrence of hypometabolism in nature (Anestis et al. 2007, Marshall & McQuaid 2011, Li et al. 2021, Liao et al. 2021), that potentially plays a pivotal role in enhancing the survival of various species in the context of global warming.

1.3 Aims

This thesis therefore aims to build upon the MRS theory by determining the extent to which hypometabolism confers resilience to thermal stress in thermally variable environments. This is achieved by elucidating the potential relationship between temperature-mediated microhabitat distribution and the physiological responses of rocky intertidal animals to increasing temperatures. The rocky intertidal habitat is particularly relevant in this context, as animals in this zone routinely endure high-amplitude thermal stress over short temporal scales due to the oscillating tide (Lathlean et al. 2011, Gunderson et al. 2019, Moisez et al. 2020). These repeated cycles of air and water exposure, particularly under sunny conditions, drive highly variable temperature fluctuations across a thermally heterogeneous environment (Stephenson & Stephenson 1972, Menge 1976, Bustamante et al. 1997, Lathlean et al. 2015, Hoylman et al. 2018, Choi et al. 2019), offering a prime setting to explore hypometabolism as a buffering mechanism against acute heat stress. Field observations of microhabitat distribution patterns (Chapter 2 and 3), coupled with laboratory-derived data on thermal preferences (Chapter 4) and performance (Chapter 5), are applied together to clarify intertidal animals' biophysical responses to spatiotemporally variable abiotic conditions. Through this variability (Helmuth 2002, Harley & Helmuth 2003, Little et al. 2009), the rocky intertidal fosters a range of physiological and behavioural adaptations in organisms such as intertidal limpets (Gray & Hodgson 1998, Guppy & Withers 2007, Gleason & Burton 2015, Nuñez et al. 2018, Brahim et al. 2019, Brahim & Marshall 2020).

These limpets exhibit two broad heat-management (thermoregulatory) strategies, meant to control and mitigate against harmful deviations from optimal body temperature, that subsequently shape their ecological distribution (see Section 1.4 below). These include risk-avoidance, in which organisms physically evade adverse conditions, and endurance-based strategies that involve a greater reliance on physiological adjustments, such as hypometabolism, to survive heat stress when escape is impossible (Jones & Boulding 1999, Verberk et al. 2016). Nevertheless, organisms exhibit phylogenetic constraints, and not all groups are capable of employing hypometabolism. Based on the

MRS theory described above, it can be predicted that, among limpet populations from clades known to exhibit this adaptation, individuals experiencing thermally stressful environments will exhibit more prevalent hypometabolic activity compared to conspecific individuals in more benign conditions. This study, therefore, aims to provide explicit insights into the capacity of MRS to extend a species' thermal tolerance to higher temperatures, rather than serving solely as a mechanism that allows animals to endure high temperatures below their thermal tolerance limits for extended periods. Thermal tolerance in the current study refers to an organism's acute upper thermal limit i.e., the temperature at which rapid heating causes physiological failure (Cox et al. 1974, Boonstra 2013, Klepsatel et al. 2016). This concerns short-term heat stress lasting a maximum of several hours, rather than chronic exposure over days to weeks that allows acclimation (see Chapter 5 for a more detailed discussion on thermal tolerance).

1.4 Study animals and sample sites

South Africa's coastline spans approximately 3 650 km, from the Namibian border in the west to the Mozambican border in the east and encompasses three major bioregions across the intersection of the warm Indian and cool Atlantic oceans (Shillington & Wyndham Harris 1978, Bally et al. 1984, Griffiths et al. 2010). These are the sub-tropical Natal, warm-temperate Agulhas, and cool-temperate Namaqua regions occurring along the East, South, and West coasts, respectively (Stephenson & Stephenson 1972, Branch & Branch 1988, Stegenga & Bolton 1992, Bustamante & Branch 1996, Turpie et al. 2000, but see Bolton et al. 2004 for a more granular delineation of the East coast based on seaweed distributions). These contrasting conditions are primarily driven by the influence of the Agulhas and Benguela currents. The Agulhas carries warm oligotrophic water from the equatorial Indian Ocean southward, flowing close to the north-eastern shore of South Africa before it retroflects away from the coast further south (Gründlingh 1983, Schumann & Beekman 1984, Lutjeharms 2006, Lutjeharms 2007). Conversely, the Benguela transports relatively cooler, eutrophic water from the Southern Ocean northward along the western coastline (Shannon 1985, Shannon &

Nelson 1996, Griffiths et al. 2010). The South Coast is strongly influenced by the Agulhas Current, but this diverges from the coast as it follows the continental-shelf break, resulting in intermediary conditions along that stretch of coast (Figure 1.1).

Rocky intertidal habitats, predominantly consisting of quartzitic sandstone or aeolian calcarenite, comprise 30–40 % of South African shores, whereas the intervening stretches are predominantly wave-exposed sandy beaches (Shillington & Wyndham Harris 1978, Bally et al. 1984, Griffiths et al. 2010). These rocky habitats are primarily concentrated along the West and South coasts and are more sparsely distributed along the East coast. Rocky intertidal environments are characterized by thermal profiles that can vary as much as, or even more than, the variability observed at broader geographic scales during low tide (Helmuth 2002). Key among these is a vertical gradient of abiotic stressors from low to high shore, reflecting differences in aerial exposure (Stephenson & Stephenson 1972, Menge 1976, Bustamante et al. 1997). At a finer scale, rocky-intertidal microhabitats exhibit perceived differences in their low-tide thermal regimes due to variable insolation caused by aspect, slope, and overall sky-view factor (Holmer et al. 2001, Lima & Wethey 2009, Seabra et al. 2011, Lathlean et al. 2015, Hoylman et al. 2018, Choi et al. 2019), and exposure to splash linked to intertidal height during low tide (Williams & Morritt 1995, Lord et al. 2011). These microhabitats can be broadly categorized into crevices, rock pools, horizontal and vertical rock surfaces (Garrity 1984, Williams & Morritt 1995, Lord et al. 2011, Lathlean et al. 2015). Previous studies have also considered dimensional differences among rock pools (Underwood & Skilleter 1996, Martins et al. 2007, White et al. 2015), while aspect is important in studies of vertical rock surfaces (Chapperon et al. 2016, 2017).

Against this backdrop, three rocky-intertidal sites were selected to represent the bioregions: Zinkwazi (29°29′42″ S, 31°43′46″ E), Three Sisters (33°55′62″ S, 27°02′60″ E) and Kommetjie (34°14′09″ S, 18°32′04″ E) on the East, South, and West coasts, respectively. The sample site at Kommetjie features a north-westerly, gently sloping shore composed of hard quartzitic sandstone platforms interspersed with fields of small boulders (Deacon et al. 1992, Macdonald & Simmons 1996, Rensburg et al. 2021). A

dense offshore kelp bed of *Ecklonia maxima* forms a natural barrier, attenuating the impact of severe waves on this site (Tucker et al. 2017). Three Sisters comprises a wave-exposed aeolianite wave-cut platform on a rocky headland with a south-easterly scarp and a tall, seaward-facing cliff backdrop (Dower 1989, Garner 2013). Adjacent to these high-platform rocks within Three Sisters are sand-inundated, low-platform rocks or sandy beaches, dotted with cliff remnants (Garner 2013). The aeolianite rocky-shore headland at Zinkwazi forms a steeply sloping, sand-inundated platform facing south-easterly generated swells (Stow 2011, MacKay et al. 2012). Furthermore, the site at Zinkwazi is flanked by long stretches of sandy beach on either side.

Limpets, a type of marine gastropod mollusc, are characterized by their single, flattened or conical shell (Ponder & Lindberg 2008). They are prevalent in rocky intertidal zones worldwide, where they play an essential ecological role as grazers of intertidal flora and as a food source for numerous predators (Branch 1981). Along the South African coast, various limpet groups are present (Branch 1971, 1975, Branch et al. 2022). Among them are the genera *Scutellastra*, *Cymbula*, and *Helcion*, which comprise the true, gill-breathing limpets, and *Fissurella* and *Diodora*, which comprise the keyhole limpets. The present research, however, focuses on two pulmonate, or false limpets, *Siphonaria capensis* (Quoy & Gaimard 1833) and *S. serrata* (Fischer 1807; formerly *S. aspera* Krauss 1848). Along with the *Trimusculidae*, the *Siphonaridae* are commonly known as pulmonate limpets because they possess specialized respiratory adaptations that permit both aquatic and aerial respiration (Yonge 1952, Branch 1981). Other siphonariids on South African shores include *S. concinna*, *S. oculus*, *S. nigerrima*, *S. tenuicostulata* and *S. compressa* (Chambers & McQuaid 1994).

These siphonariid limpets are all simultaneous hermaphrodites, but they exhibit notable differences in reproductive and developmental strategies (Chambers & McQuaid 1994, Ansell et al. 1999). *S. capensis* undergoes pelagic development, releasing embryos that develop into free-swimming, planktotrophic larvae in the water column before settling and transforming into adults. In contrast, *S. serrata* follows a direct developmental strategy, with embryos completing development within the egg and hatching as

miniature adults (Chambers & McQuaid 1994). Other notable biological features include their secretion of noxious mucus containing polypropionate metabolites, which serves as a chemical defence against intertidal predators (McQuaid et al. 1999, Pinchuck & Hodgson 2009), and their tolerance of temperatures exceeding 40 °C (Kankondi et al. 2018, Connell et al. 2025) as well as variable salinities (Wilson et al. 2009).

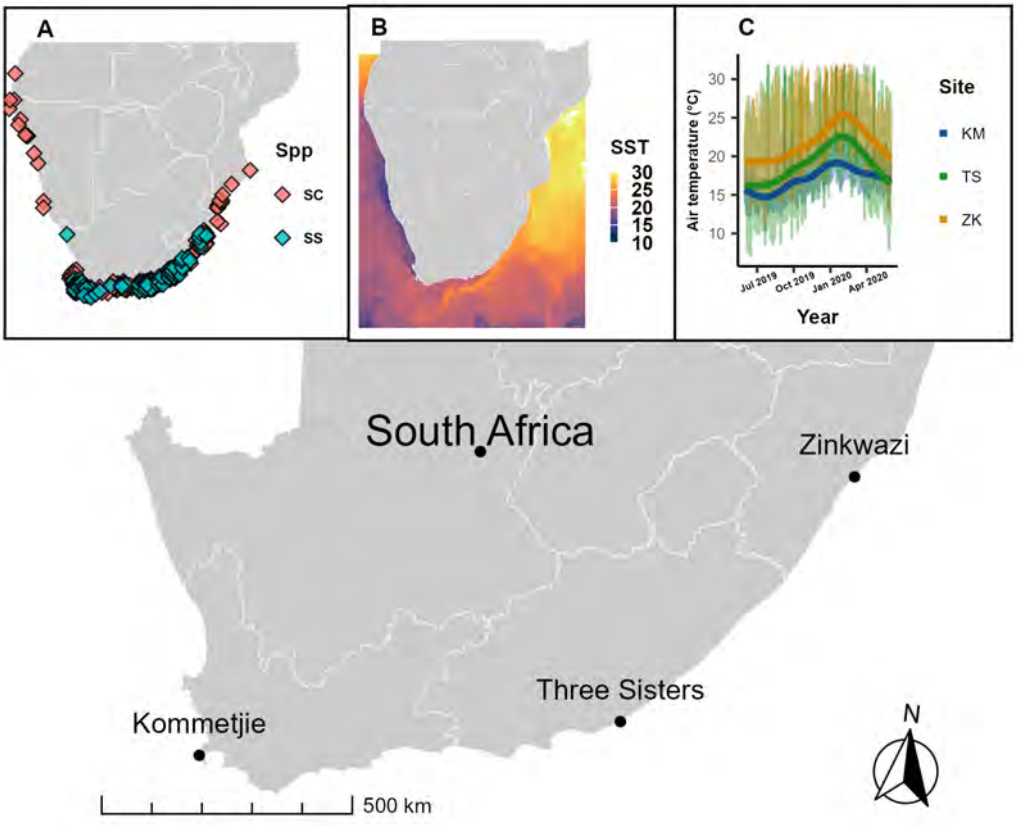

Figure 1.1: Map depicting (A) Sample species distributions (occurrence data obtained from (https://www.gbif.org); note that *Siphonaria capensis* points are obscured along the South coast, but both species do coexist there), (B) Mean sea surface temperature (SST) (data extracted from (https://upwell.pfeg.noaa.gov/erddap/index.html)), and (C) Mean daily air temperature displayed as curves and raw daily air temperature values as bars (data obtained from (https://www.ogimet.com)), at three sampling sites along the West (Kommetjie - KM), South (Three Sisters - TS), and East (Zinkwazi - ZK) coasts of South Africa. (SC - *S. capensis*; SS - *S. serrata*).

These traits underpin their extensive distribution along wide thermal gradients, across

South Africa's coastline (Figure 1.1) and throughout the intertidal. Although largely sympatric, *S. capensis* is found beyond South Africa's northern borders on both the West and East coasts (Allanson 1958, Branch & Griffiths 1994), whereas the distribution of *S. serrata* only extends northward past the Orange River on the West coast (Allanson 1958, Branch & Griffiths 1994).

At a more granular spatial resolution, vertical and micro-habitat partitioning is evident between the study species (Branch & Cherry 1985, Chambers & McQuaid 1994). Although their vertical distributions overlap in the upper mid-shore zone, *S. capensis* extends further into the high-shore zone, whereas *S. serrata* is more frequently found in the lower zones (Chambers & McQuaid 1994). Furthermore, *S. capensis* commonly inhabits cool, shallow rock pools with encrusting coralline algae in the high shore, or warmer, exposed rock surfaces (Garrity 1984, Branch & Cherry 1985, Chambers & McQuaid 1994). Conversely, *S. serrata* predominantly occupies bare rock surfaces or crevices, only occasionally occurring in crustose rock pools. The former habitat is generally warmer (Garrity 1984, Chambers & McQuaid 1994). This differential use of high-shore pools is likely driven by *S. capensis* greater tolerance of the variable salinity typical of these pools (Wilson et al. 2009). Consequently, the broader distribution of *S. capensis* into warmer environments may be partly facilitated by its more frequent pool use relative to *S. serrata*.

Given their wide geographic and microscale distributions, which expose them to highly variable thermal regimes, these two siphonariids are ideal model organisms for addressing the study's aims. By simultaneously examining their physiological responses to rising temperatures and their temperature-driven patterns of microhabitat distribution, this study explores the specific nature of the benefits likely afforded by their hypometabolic activity, when it occurs, in the context of a warming climate.

1.5 Hypotheses

The study hypothesizes that intertidal pulmonate limpets will exhibit responses consistent with MRS theory, thereby reinforcing its utility as a predictive framework for elucidating thermal tolerance across varying spatiotemporal scales. This is grounded on the premise that: 1. Thermally heterogeneous habitats drive differential hypometabolic responses within conspecific populations, which, in turn, influence distribution patterns at both broad geographic and localized micro-scales, and 2. Limpets exposed to warmer conditions exhibit enhanced hypometabolic activity, which is likely to facilitate greater thermal-tolerance limits compared with individuals subjected to cooler, more stable thermal ranges.

If populations do not display variations in hypometabolic capacity that reflect their exposure to different thermal conditions, this would suggest that MRS is not the principal mechanism driving their differential persistence and performance across thermally heterogeneous spatiotemporal scales. Furthermore, if limpets subjected to warmer conditions do not, on average, display both enhanced hypometabolism and markedly higher thermal tolerances, it would imply that increased hypometabolic activity does not necessarily confer greater resilience to high temperatures. Consequently, this would cast doubt on the general premise that MRS theory reliably explains, or forecasts, the thermal thresholds of intertidal pulmonate limpets across diverse environmental conditions.

1.6 Organization

This thesis is organized into six chapters. Chapter 1 serves as a general introduction, outlining the study species, study sites, and key concepts relevant to the research. Chapters 2 and 3 explore the patterns of distribution and dispersal of the study animals across the research sites. Chapters 4 and 5 examine, respectively, thermotaxis i.e., movement driven by thermal cues, in *Siphonaria capensis* and the cardiac response of

both species to rising temperatures. Lastly, Chapter 6 synthesizes the findings of the study and presents the general conclusions.

Chapter 2

Microhabitat use analysis

2.1 Abstract

Micro-scale thermal heterogeneity is a key, yet sometimes under-appreciated, driver of intertidal species' distributions. Here, I quantified the availability of daytime low-tide microhabitats, their thermal characteristics and their use by the pulmonate limpets *Siphonaria capensis* and *S. serrata* across cool-temperate (Kommetjie), warm-temperate (Three Sisters) and subtropical (Zinkwazi) rocky shores of South Africa. Point-intercept quadrats were deployed along 20m transects parallel to the shore to estimate the area of crevices, horizontal rock surfaces, rock pools, and vertical rock surfaces, and simultaneously to census limpet abundances within each microhabitat, while temperature loggers were used to record substratum temperatures at 30 minute intervals for up to nine months. Pools were consistently the coolest microhabitat, whereas horizontal and east- or north-facing vertical surfaces were the warmest, although seasonal and site effects modified these rankings. A zero-inflated Tweedie Generalized Linear Mixed Model (GLMM) showed that horizontal surfaces overwhelmingly dominated the sampled areas, followed by rock pools, crevices and the various vertical surface orientations, with crevices being absent at Three Sisters. Following these spatial patterns, zero-inflated Poisson GLMMs revealed that both limpets occurred more often in thermally benign refugia, such as pools and crevices, than availability alone would predict, yet neither species was confined to them. This reflects divergent risk-avoidance strategies. Furthermore, the direction of temperature-occurrence relationships varied among sites,

indicating local modulation by wave exposure, shoreline aspect and life-stage structure. Overall, microhabitat utilisation was non-random and linked to within-shore thermal regimes, supporting the hypothesis that fine-scale environmental mosaics influence limpet distributions, and providing the ecological backdrop for forthcoming physiological analyses.

2.2 Introduction

Behavioural thermoregulation is widespread across the animal kingdom, occurring in taxa from insects and other invertebrates to reptiles, birds, and mammals (Kearney et al. 2009, Akin 2011). Animals use this strategy to buffer their body temperature when physiological regulation is inadequate or energetically costly (Kearney et al. 2009, Akin 2011, Terrien et al. 2011). This behaviour is primarily induced by the need to avoid thermal stress, either through overheating or excessive cooling, and to keep body temperature within an optimal range for performance (Akin 2011, Terrien et al. 2011). This is particularly crucial for ectotherms, which lack substantial endogenous heat production and therefore rely on behavioural means of thermal control (Cowles & Bogert 2006, Akin 2011). For instance, desert lizards (e.g., *Dipsosaurus dorsalis* and *Varanus rosenbergi*) shuttle between sun and shade or adjust posture to modulate heat gain (Cowles & Bogert 2006, Kearney et al. 2009), butterflies (e.g., *Hesperia viridis*) orient their wings to absorb solar radiation and warm flight muscles (Clench 1966), and even endotherms such as emperor penguins (*Aptenodytes forsteri*) huddle to reduce individual heat loss in Antarctic winters (Terrien et al. 2011). Access to cooler microhabitats, such as shade, cool burrows, or rock pools, is therefore crucial for reducing thermal stress in ectotherms (Kearney et al. 2009, Janetzki et al. 2021). Consequently, behavioural thermoregulation shapes habitat selection and distribution, sometimes at centimetre scales, across a wide range of taxa and environments (Janetzki et al. 2021). This highlights how body size and habitat complexity set the spatial scale at which such behaviours operate (Kearney et al. 2009, Janetzki et al. 2021).

Several intertidal gastropods utilize behavioural thermoregulation to minimize heat stress during emersion (Wolcott 1973, Garrity 1984, Raimondi 1990, Williams & Morritt 1995, Lord et al. 2011). Good examples of these gastropods include some limpets (Garrity 1984, Branch & Cherry 1985, Williams & Morritt 1995, Gray & Hodgson 1998, Vat 2000, Seabra et al. 2011, Lord et al. 2011). During low tide, they can often be found in rock pools, crevices, and shaded vertical rock surfaces, where conditions are usually cooler compared with the surrounding more exposed environment (Chambers 1995, Gray & Hodgson 1998, Lord et al. 2011). Limpets, particularly juveniles among various species, also frequent biogenic microhabitats provided by aggregations of other species, including bivalves, ascidians, or macroalgae (Harper & Williams 2001, Castilla et al. 2004, Cartwright & Williams 2012). Among the thermoregulatory behaviours of limpets is an atypical behaviour known as homing, wherein they return to the same resting spot after foraging during high tide (Santina 1994, Gray & Hodgson 1998, Nuñez et al. 2014). Philopatry facilitates the formation of small depressions at their resting locations, known as home scars, which closely resemble the outline of the shell (Santina 1994, Gray & Hodgson 1998, Jakob et al. 2001, Shanks 2002, Nuñez et al. 2014). The primary function of the home scar is to alleviate desiccation stress by minimizing water loss during periods of emersion (Verderber et al. 1983). The tight seal created between the shell and the rock surface, however, also offers some thermal insulation to limpets, providing a degree of protection against extreme temperature fluctuations (Santina 1994, Shanks 2002). In addition to these behavioural adaptations, limpets also employ physiological adaptations to heat, including the expression of thermal tolerance plasticity (Marshall et al. 2018, Brahim et al. 2019, Brahim & Marshall 2020), and an elevated heat shock response (Tomanek 2010, Dong & Williams 2011, Gleason & Burton 2015), as well as the capacity for hypometabolism (Newell 1969, Marshall & McQuaid 1991, Guppy & Withers 2007).

The current study focuses on limpets at three rocky shores, Kommetjie, the Three Sisters, and Zinkwazi Beach, as described in Chapter 1, to examine how microhabitat structure and temperature heterogeneity relate to limpet distribution and habitat use. I quantified within-shore variation in microhabitat availability and the fine-scale

temperature regimes, using quadrat–transects and temperature loggers, respectively (Wethey 2002, Harley & Helmuth 2003, Hill & Wilkinson 2004), across the intertidal zone. By mapping limpet occurrences onto these microhabitats (Chapter 1), I assess how each species uses pools, crevices, and open rock surfaces. Many studies have shown that microhabitat temperature heterogeneity influences intertidal organisms' behaviour and physiology (Williams & Morritt 1995, Helmuth & Hofmann 2001, Lord et al. 2011, Chapperon et al. 2017, Moisez et al. 2020), underscoring the importance of fine-scale temperature differences in shaping species' performance and tolerance.

The aim of this study is to elucidate the potential association between microhabitat utilization and local thermal regimes, to provide a framework for understanding how these factors may influence limpet physiology (e.g., thermal tolerance) in later work. This stems from evidence that, through thermoregulatory adaptations, recent thermal history can strongly influence thermal tolerance (Bjelde & Todgham 2013, Verberk et al. 2016, Chapperon et al. 2017, Moisez et al. 2020). Therefore, it is hypothesized that the variations in microhabitat utilization would yield a negative relationship with microhabitat temperature, which may dictate species thermoregulation and the subsequent intraspecific variation in thermal tolerance for both species in a downstream study.

2.3 Methods

2.3.1 Sample sites and animals

The study examines the utilization of intertidal microhabitats by the two limpet species mentioned earlier, across three sites located on the East, South, and West coasts of South Africa (Figure 1.1).

2.3.2 Near surface thermal regimes

Several temperature data loggers (EnvLogger T2.4, Electricblue, Portugal), encased in hard grey acrylic, were deployed across three sites in seven high-shore intertidal microhabitats. These microhabitats included rock pools, crevices, and horizontal as well as vertical rock surfaces facing the four cardinal directions. An exception was made at the Three Sisters site, which lacked a suitable crevice microhabitat. To prepare for logger attachment, sections of rock surface relatively free of algae and other biogenic materials were cleaned by scraping off any debris with a hammer and chisel. This process ensured an optimal bond between the substratum and resin. The loggers were affixed to the rock surfaces using a mixture of Z-spar and epoxy resin, with three loggers deployed per combination of site and microhabitat, totalling 60 loggers (N) for the study. These data loggers were programmed to record temperature with a precision of 0.001 °C at 30 minute intervals using their associated companion application (EnvLogger Viewer, v1.18), for one year, from 01 June 2019 to 29 February 2020. Due to a temporary shortage of loggers, however, there was a delayed start of data collection at Three Sisters, which only began on 26 October 2019.

2.3.3 Sample area selection

To ascertain the microhabitat use of the study species at selected sites, their abundances within available microhabitats were quantified at each location. Selection criteria for sample sites included a continuous stretch of rocky intertidal coastline known to have representative samples of the study species (Chambers & McQuaid 1994, Vat 2000). Additionally, selected areas measuring 20m along the shore by 20m across the shore, from high to low intertidal zones, were chosen, ensuring they were not predominantly covered by sand or characterized by large, deep pools (Table 2.1). This consideration was crucial, as such features would have greatly impeded the effectiveness of sampling based solely on visual means.

2.3.4 Sampling method

Sampling was conducted during the spring low tides of November – December 2019 at all three sites (13/11 at Zinkwazi, 28/11 at Kommetjie, and 9/12 at Three Sisters), under clear and sunny weather conditions. Tide information was sourced from the South African Navy Hydrographic Office. To maximise sampling efficiency, activities commenced two hours before low tide during the outgoing tide, allowing sufficient time to complete sampling within a single low-tide period. Microhabitat availability and limpet species' abundances were assessed using point-intercept quadrats along transect lines at each site, following methodologies described by Hill & Wilkinson (2004). Prior to sampling, two 20m reference lines were established parallel to the coast at each site, marking the high and low shore sample limits with 50m measuring tapes (Figure 2.1). The high shore limit was set 1m above the highest observed individual of *Siphonaria capensis*, chosen as the reference because it typically occupies higher shore levels than other intertidal limpets (Chambers & McQuaid 1994), with the low-shore limit positioned 20m below.

Figure 2.1: Computer-generated image, using (https://www.midjourney.com/explore), illustrating the use of reference lines (blue) and the direction (yellow arrows) in which the quadrat and transect line was shifted during the microhabitat use sampling procedure, with the yellow-shaded area indicating the type of large sandy area typically avoided.

Once the reference lines were in place, a 20m measuring tape was laid from the high shore to the low shoreline to serve as the transect. This tape was then moved sequentially at 2m intervals, from the 2m to the 18m points along the reference lines, creating a parallel series of nine transects (Figure 2.1). At each 2m interval along a transect, a 50 × 50cm quadrat, sub-divided into four equal squares with fishing line, was placed so that the point where the fishing lines crossed aligned precisely with the interval mark. Within each quadrat, the microhabitats defined in Table 2.1 were identified, and their percentage cover was visually estimated in each of the four sub-quadrats. The percentages were then converted to area (cm^2) and summed for the entire quadrat. Dividing the quadrat into four smaller viewing windows reduced the visual field at any one time, allowing more accurate estimation of microhabitat cover. Slope measurements of the microhabitats were taken to a precision of 10° using a clinometer.

Table 2.1: Physical descriptions and abbreviations for each microhabitat type.

Type	Abbreviation	Description
Horizontal rock	HR	Rock surfaces with an incline between 0° - 30°
Vertical rock	VR	Rock surfaces with an incline between 71° - 90°, in all four cardinal directions
Crevice rock	CR	A slit or pock-like recess in the rock
Rock pool	RP	A rock pool < 20cm deep

Rock surfaces with inclines between 31° and 70° were generally not encountered during the sampling process.

Cardinal directions for VR included north-, south-, east-, and west-facing rock surfaces.

RP > 20cm deep were avoided. RP depth was determined using a meter stick.

This method, however, presented a limitation when assessing quadrats containing both horizontal and non-horizontal surfaces, such as crevices and vertical surfaces. Due to the quadrat's horizontal alignment and the overhead view adopted for cover estimation

(Figure 2.2), it was sometimes difficult to accurately gauge the coverage of non-horizontal surfaces. As shown in Figure 2.2, this resulted in the non-horizontal surfaces appearing to cover a smaller portion of the area under the quadrat than they actually did.

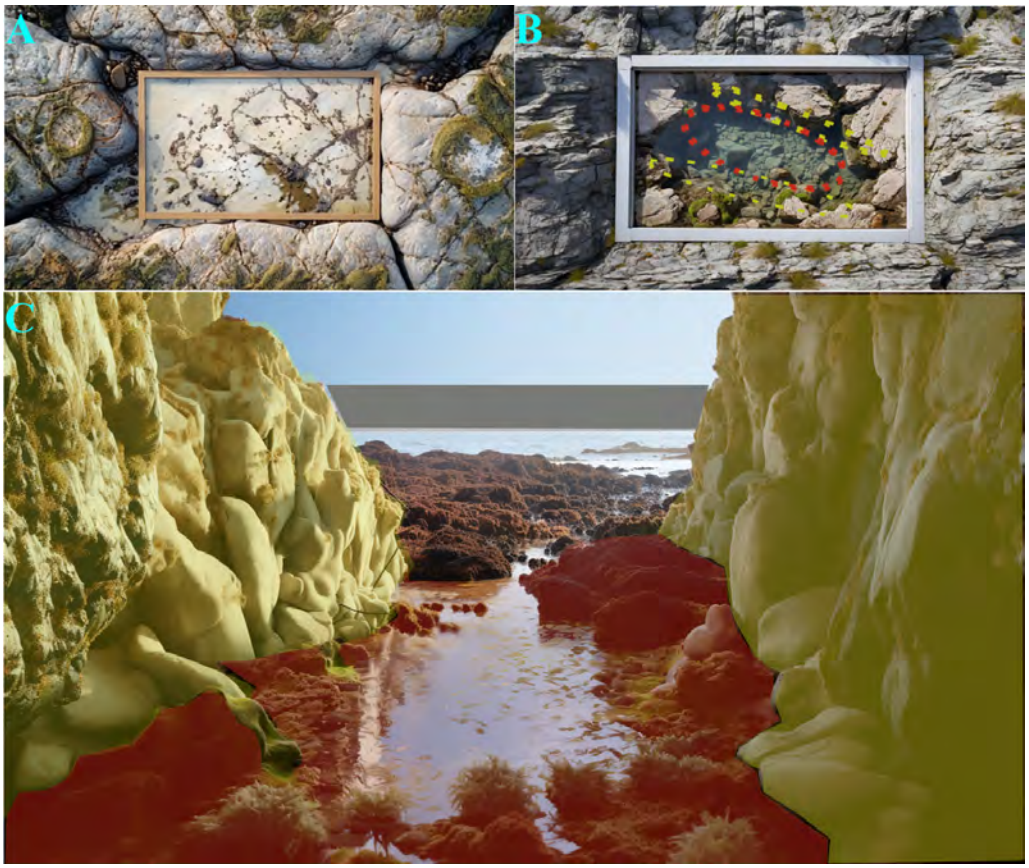

Figure 2.2: Computer-generated images, using (https://www.midjourney.com/explore), illustrating the estimation problem of non-horizontal microhabitats due to their co-occurrence with horizontal ones in the same quadrat (B and C), in contrast to quadrats with only horizontal microhabitats (A). *A - Top view of a flat rock pool, B - Top view of a rock pool with steep edges, C - Eye-level view under a quadrat showing a flat rock pool flanked by vertical rock surfaces. Yellow marks vertical edges and red denotes horizontal surfaces.*

Abundances of the study species were then estimated by counting the number of individuals present in each available microhabitat within each quadrat. The sampling procedure yielded a final dataset comprising seven variables, including five categorical ones: species (2 levels), site (3 levels), transect (9 levels), microhabitat (4 levels), and

quadrat (9 levels). In addition, the dataset contained one discrete, zero-inflated count variable for occurrences and one continuous, zero-inflated variable for area (cm^2). Zero-inflation in the two numeric variables manifests as pronounced spikes at 0 in their respective frequency histograms (Figure 2.3).

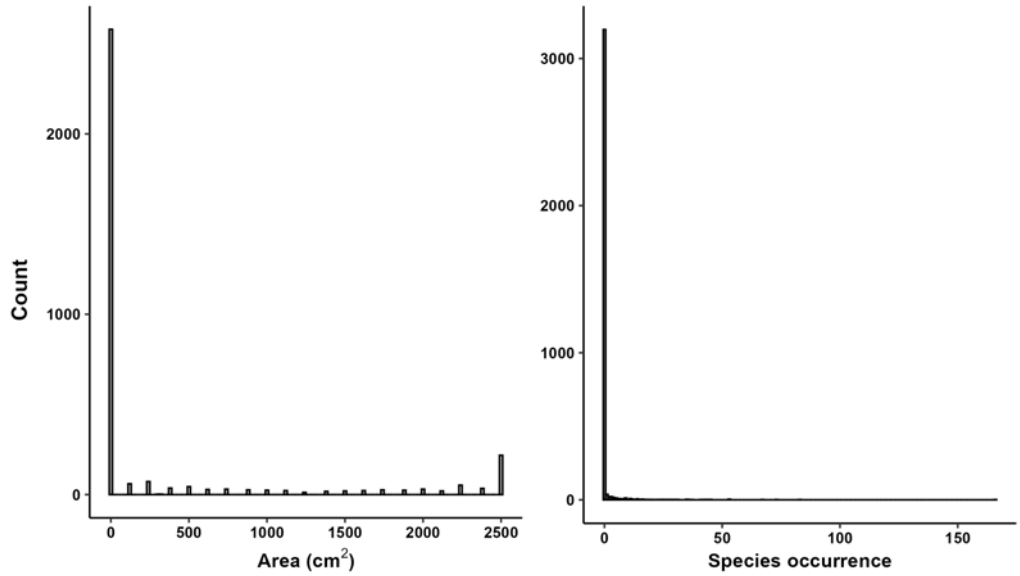

Figure 2.3: Frequency histograms of the numeric variables generated by the study sampling procedure.

2.3.5 Statistical analysis

Unless stated otherwise, data analyses and visualisations were conducted using R version 4.4.0 (R Core Team 2021). The analysis of logger data to identify statistical differences in daytime low-tide temperatures across microhabitats, both within and between sites, was not feasible due to substantial gaps in the data. These gaps resulted from the frequent removal of loggers by the public at Zinkwazi and Three Sisters, compounded by an inability to replace lost loggers and by the delayed arrival of a replacement batch. Consequently, the reduced number of loggers rendered the dataset insufficient for viable statistical analysis (Figure 2.4). Logger data were therefore plotted with ggplot from the ggplot2 package (Wickham 2016) and examined qualitatively after filtering the dataset to include only the peak two hours of daytime temperature observations. These peak

observations, amounting to five per day of available data, were specifically chosen to focus exclusively on day-time low-tide conditions. All mean temperature records, termed ‘surface temperature’ throughout, are derived from these peak observations in this thesis. Critically, such averages alone are not the preferred metric for linking habitat conditions to species ecology (Helmuth et al. 2006, Sunday et al. 2019, Li et al. 2021). Mean values, even when taken at peak times, smooth over the brief but intense extremes that set physiological limits, trigger stress responses, and shape distribution patterns (Li et al. 2021). For this reason, most studies on ecophysiology favour the inclusion of absolute daily maxima and minima, which help better represent the full range of thermal challenges faced by intertidal organisms (Helmuth et al. 2006, Sunday et al. 2019). Nevertheless, averaging peak low-tide temperatures captures the period of most pronounced variation in upper temperature extremes among rocky intertidal microhabitats.

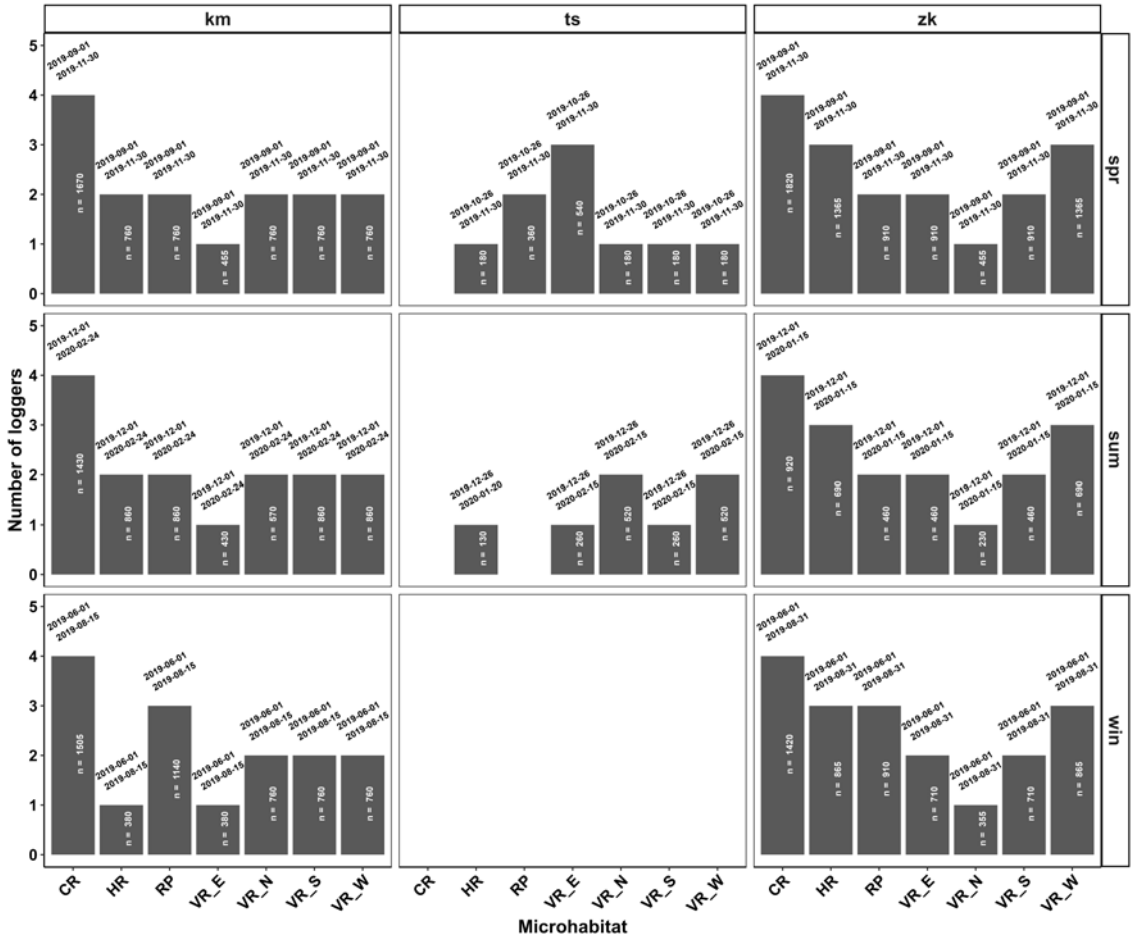

Figure 2.4: Bar plot showing differences in the number of loggers deployed across different microhabitats (CR – crevice, HR – horizontal rock, RP – rock pool, VR_E - east-facing vertical rock, VR_N - north-facing vertical rock, VR_S - south-facing vertical rock, VR_W - west-facing vertical rock), within each site (ZK - Zinkwazi, TS - Three Sisters, K, - Kommetjie) and season (sum - Summer, spr - Spring, win - Winter). *The deployment date range, following the extraction of peak daytime temperature data, for each combination of nominal variables are displayed within the respective bars*.

Generalised Linear Mixed Models (GLMMs), all fitted with the function glmmTMB in the package of the same name (Brooks et al. 2017), were chosen as the final models to evaluate the influence of the study predictors on the outcomes specified below. GLMMs are recommended when modelling relationships involving non-normal response variables and their covariates, especially when the data exhibit dependencies or hierarchical structure (Bolker et al. 2009). This approach effectively handles the

variability both within and between groups, providing a more nuanced and accurate analysis of complex datasets (Bolker et al. 2009).

A Tweedie GLMM, an effective method for analysing zero-inflated continuous data (Dunn & Smyth 2018), was used to model variation in the response variable area as a function of microhabitat, irrespective of site. Because equal areas were sampled at each site, and because variation in area across sites or among microhabitats within sites was not a primary focus of the current paper, site was excluded from the model. Furthermore, zero-inflation was not explicitly modelled as a function of any predictors. Instead, including microhabitat as a predictor in the dispersion component was sufficient to account for potential overdispersion (Equation 2.1) and zero-inflation, as the Tweedie distribution naturally accommodates both. Additionally, this model incorporated random effects for quadrats in the conditional component.

$$
\begin{aligned}
\mathrm{Y}_i &\sim \text{Tweedie}(\mu_i, \phi_i, \pi_i, \mathrm{p}) \\
\log(\mu_i) &= \alpha_0 + \alpha_1 \mathrm{X}_{1j} + v_j + \varepsilon_{j[i]} \\
\log(\phi_i) &= \theta_0 + \theta_1 \mathrm{X}_{1i} \\
\operatorname{logit}(\pi_i) &= \zeta_0 \\
&\text{where} \\
\varepsilon_{j[i]} &\sim \mathcal{N}(0, \sigma^2) \\
v_j &\sim \mathcal{N}(\mu_j, {\sigma_j}^2), \quad \text{for quadrat } j = 1, \ldots, J
\end{aligned}
\tag{2.1}
$$

In Equation 2.1, Y_i represents the response variable area for the i-th observation, modelled as a Tweedie distribution with mean (μ_i), dispersion (ϕ_i), zero-inflation (π_i), and power parameter (p). The model specifies $Y_i \sim \text{Tweedie}(\mu_i, \phi_i, \pi_i, \mathrm{p})$, where the mean variation in area is captured by the conditional component as $\log(\mu_i) = \alpha_0 + \alpha_1 X_{1j} + v_j + \epsilon_{j[i]}$. Here, v_j is the random intercept for the j-th level of quadrat, α_0 is the grand intercept, and α_1 is the regression coefficient for the average area in different (X_{1j}) microhabitats. The dispersion (ϕ_i) is modelled as $\log(\phi_i) = \theta_0 + \theta_1 X_{1i}$, and the zero-inflation probability (π_i) is modelled using a logit link function $\operatorname{logit}(\pi_i) = \zeta_0$. The random intercept ($v_j$) follows a normal distribution $v_j \sim N(\mu_j, {\sigma_j}^2)$. The residual variance ($\epsilon_{j[i]}$) represents the individual-level variability not explained by the model, and it is assumed to have a mean of 0 and a variance of σ^2.

To analyse the variation in the response variable occurrence in relation to site and microhabitat, the dataset was divided by species before fitting two separate zero-inflation Poisson GLMMs. This approach is an effective way to analyse discrete data with excess zeros (Zuur & Ieno 2016). The fitting of the conditional component involved incorporating an offset of log-transformed area, adjusted by adding a small constant to address zero-inflation in the predictor, and random effects for quadrats. These steps were taken to control for the effect of area, without explicitly modelling area as a predictor, and to manage data dependencies on species occurrence. Running two separate models for each species helped avoid problems typically associated with overly complex models, such as convergence issues (Barr et al. 2013). Here, zero-inflation in the response variable was not modelled as dependent on any predictors, instead a uniform zero-inflation component was applied across all observations in the model (Equation 2.2). This follows the approach applied to the Tweedie GLMM (Equation 2.1) without including a dispersion component.

$$
\begin{aligned}
\mathrm{Y}_i &\sim \text{Poisson}(\lambda_i, \pi_i) \\
\log(\lambda_i) &= \alpha_0 + \alpha_1 \mathrm{X}_{1j} + \alpha_2 \mathrm{X}_{2j} + \log(A_i + \delta) + v_j + \varepsilon_{j[i]} \\
\text{logit}(\pi_i) &= \zeta_0 \\
&\text{where} \\
\varepsilon_{j[i]} &\sim \mathcal{N}(0, \sigma^2) \\
v_j &\sim \mathcal{N}(\mu_j, {\sigma_j}^2), \quad \text{for quadrat } j = 1, \dots, J
\end{aligned}
\tag{2.2}
$$

In Equation 2.2, the response variable occurrence for each observation, denoted as Y_i, is modelled using a zero-inflated Poisson distribution. The mean of this distribution, represented as λ_i, is adjusted for zero-inflation by the factor π_i, formulated as $Y_i \sim \text{Poisson}(\lambda_i, \pi_i)$. The model's grand intercept is defined by α_0, with the predictors site (X_{1j}) and microhabitat (X_{2j}) linked to the regression coefficients α_1 and α_2, respectively. An offset for area is incorporated as $\log(A_i + \delta)$. The probability of zero-inflation, π_i, is modelled using the logit link function $\text{logit}(\pi_i) = \zeta_0$. A random intercept, v_j, accounts for variability across the j-th level of quadrat, following a normal distribution $v_j \sim N(\mu_j, {\sigma_j}^2)$. The residual variance ($\epsilon_{j[i]}$) represents all unexplained stochastic variability, assumed to have a mean of 0 and a variance of σ^2.

The final structure of the statistical models were generally determined using a forward-step model selection procedure, facilitated by the Likelihood Ratio Test (LRT), which can be implemented using the anova function in base R (Zuur et al. 2009). Initially, null Generalized Linear Models (GLMs), comprising only the conditional component, were fitted. These models were then progressively modified to increase complexity by adding interactions between variables, incorporating random effects, adjusting the distributional component, and including zero-inflation and dispersion components where required. The goodness of fit between reduced and more complex models was compared stepwise. Alongside, various statistical and visual model validation checks were conducted at each step, aiding decisions to either include additional variables or model terms or to retain the simplest model under scrutiny (Section A1). Model validation procedures included checks for issues with dispersion, zero-inflation, significant outliers, significant within-group deviation from uniformity, and between-group deviation from homogeneity (Section A1). The variable transect was not included in either of the models represented by the equations. This omission was due to the unlikely event of along-shore variations in species occurrence within a 20m span at different sites, which was not a primary focus of this study.

For the Tweedie GLMM on area, *post hoc* testing was conducted by calculating contrasts between the estimated marginal means across each level of the categorical predictor. These *post hoc* tests were performed using the emmeans function from the package of the same name (Lenth 2023). To control for type I error inflation, the false discovery rate (FDR) adjustment method was applied to the p-values. Initial *post hoc* analysis for the zero-inflated Poisson GLMMs on species occurrence was carried out using the same approach as for the Tweedie GLMM. To examine intra-site differences in species occurrences among microhabitats, however, the data were split by site for each species *a priori* due to convergence challenges encountered when attempting to fit models to the full dataset for each species. This allowed for more reliable parameter estimation and improved model stability. Models fitted to the data after this split underwent the same model selection and validation procedure previously discussed, with the objective of identifying suitable substantive models without including the site variable as a

predictor.

2.4 Results

2.4.1 Surface temperature

Throughout this study, the overall low-tide surface temperature recorded by all loggers was 25.1°C, with a range of 36.5°C, spanning from a minimum of 13.5°C to a maximum of 50°C. Summer emerged as the warmest season with surface temperatures of 28.7°C (±5.7°C), followed by spring at 26°C (±5.5°C) and winter at 20.4°C (±4.5°C). In terms of site comparisons, Three Sisters, surprisingly, had the highest recorded low-tide temperatures, averaging 26.3°C (±5.7°C), closely followed by Zinkwazi at 25.9°C (±5.6°C), while Kommetjie had the lowest surface temperatures at 24.1°C (±6.7°C). Analysing differences among microhabitat rock temperatures, regardless of site or season, the highest surface temperatures were observed on horizontal 27.8°C (±6.7°C), east-facing 27.2°C (±6.1°C), and north-facing 27.1°C (±6.6°C) vertical rock surfaces, with negligible differences among these categories. This was followed by west-facing 24.6°C (±5.4°C) and south-facing 24.4°C (±5.9°C) vertical rock surfaces, and crevices (23.8°C ±5.8°C), all of which also differed minimally. Finally, the lowest temperatures of 22.9°C (±5.6°C) were consistently recorded in rock pools

It is crucial to note the absence of temperature data for Three Sisters during winter, for crevices at Three Sisters throughout the study, and for rock pools at Three Sisters during summer (Figure 2.4). When analysing data grouped by season, deviations emerged from the general trends in low-tide surface temperatures across both sites and microhabitats (Figure 2.5). During summer, contrary to the general trend of Three Sisters being warmest, the highest surface temperatures were recorded at both Zinkwazi (28.9 ±5.8°C) and Kommetjie (28.9 ±5.6°C), followed by Three Sisters (27.6 ±5.6°C). Regarding microhabitats, the trend deviated slightly: horizontal rocks (31.9 ±6°C) remained the warmest, but north-facing vertical rocks (29.9 ±6.2°C) were warmer than east-facing

vertical rocks (29.6 ±5.4°C), a reversal from the general trend. Crevices (28 ±5.3°C), which were typically cooler than all vertical rocks in the general trend, followed next, then west- (28 ±4.6°C) and south-facing vertical rocks (27.7 ±5°C), with the lowest temperatures consistently recorded in rock pools (26.2 ±5.8°C). In spring, the highest surface temperatures were also noted at Zinkwazi (27.2 ±5°C), deviating again from the general trend by ranking above Three Sisters (25 ±5.5°C), which was followed by Kommetjie (24.5 ±5.6°C). The sequence for microhabitats was horizontal rocks (28.3 ±5.6°C), followed by east- (27.9 ±6°C), north- (27.4 ±6°C), and south-facing vertical rocks (26 ±5.3°C), crevices (25 ±4.9°C), west-facing vertical rocks (24.3 ±3.8°C), and rock pools (24 ±5.4°C). In winter, the general trend for sites was maintained. For microhabitats, however, the highest temperatures were in east- (23.5 ±5.5°C) and north-facing vertical rocks (23.4 ±6.1°C), followed by horizontal rocks (21 ±3.5°C), west-facing vertical rocks (20.6 ±5.4°C), rock pools (19.6 ±3.4°C), crevices (19.2 ±3.4°C), and lastly south-facing vertical rocks (18.9 ±2.7°C), which diverged from the general trend as well.

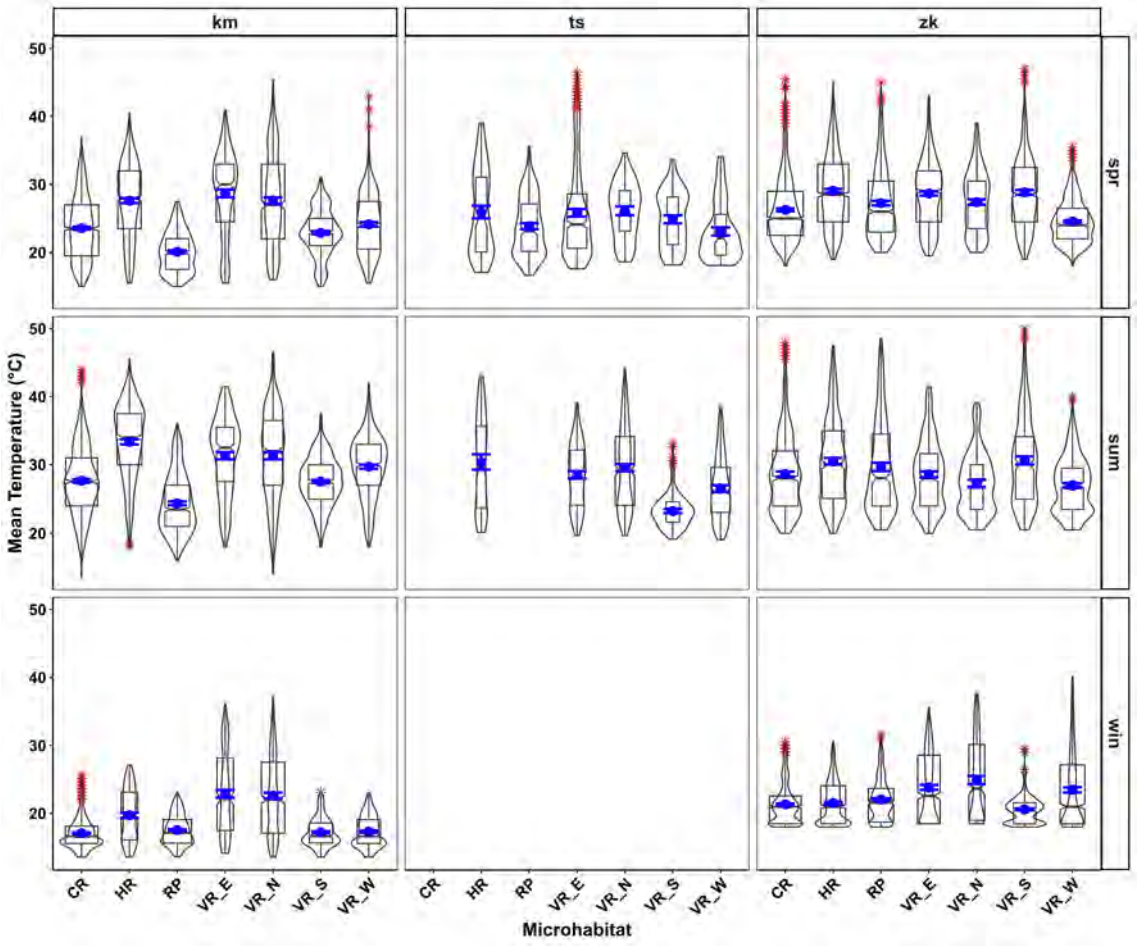

Figure 2.5: Violin plots superimposed on box and whisker plots illustrating seasonal variations (spr - spring; sum - summer; win - winter) in daytime low-tide temperatures (°C) across microhabitats (CR - crevices, HR - horizontal surfaces, RP - rock pools, VRE - east-facing vertical surfaces, VRN - north-facing vertical surfaces, VRS - south-facing vertical surfaces, VRW - west-facing vertical surfaces) at different sites (zk - Zinkwazi; ts - Three Sisters; km - Kommetjie). The plot features the mean (blue circles) ± standard deviation, median (central horizontal line), confidence intervals of the median (box plot notch), interquartile range, as well as minimum and maximum values (whiskers), and outliers (values falling beyond 3x the interquartile range) are represented by red symbols.

An analysis of low-tide surface temperatures, comparing different sites within the same season and contrasting the variations at each site across different seasons, underscored differences in microhabitat temperature trends (Figure 2.5). For instance, at Zinkwazi during summer, the highest temperatures were observed on south-facing vertical rock

surfaces (30.6 ±6.4°C). This was followed in descending order by horizontal rock surfaces (30.5 ±6.2°C), rock pools (29.7 ±6.7°C), crevices (28.6 ±5.7°C), and then east- (28.6 ±5°C), north- (27.3 ±4.4°C), and west-facing rock surfaces (27 ±4.1°C). In spring, however, the temperature hierarchy at Zinkwazi shifted dramatically, with horizontal rock surfaces emerging as the warmest (29.1 ±5.4°C), followed by south- (28.8 ±5.3°C), east- (28.7 ±5°C), and north-facing vertical rock surfaces (27.4 ±4.5°C), and then rock pools (27.3 ±5.2°C), crevices (26.3 ±4.8°C), and west-facing vertical rock surfaces (24.6 ±3.2°C) in that order. In stark contrast to Zinkwazi during summer, at Kommetjie, the highest temperatures were not on south-facing but rather on horizontal rock surfaces (33.4 ±5.5°C), followed by north- (31.3 ±6.4°C), east- (31.3 ±5.6°C), and west-facing vertical rock surfaces (29.7 ±4.5°C). Furthermore, at Kommetjie, the lowest temperatures were observed in rock pools (24.4 ±4.3°C), with slightly higher temperatures in south-facing vertical rocks (27.5 ±3.5°C) and crevices (27.6 ±5°C). This pattern markedly differs from that of Zinkwazi, where the lowest rock temperatures in summer were found in west-, north-, and east-facing vertical rock surfaces (Figure 2.5).

2.4.2 Microhabitat availability

In the zero-inflated Tweedie GLMM (Table 2.2), analysing the variations in area (cm^2) as a function of microhabitat, a significant effect ($p < 0.0001$) of microhabitat on the outcome was revealed.

Table 2.2: Analysis results from a zero-inflated Tweedie GLMM assessing variations in area (cm^2) among microhabitats irrespective of site. Microhabitat was treated as a fixed effect and quadrat as a random effect.

term	Chisq	Df	p.value
(Intercept)	975.7721	1	< 0.0001
mh	417.9793	6	< 0.0001

Model terms: mh - microhabitat

Horizontal rock surfaces were the dominant feature in the surveyed areas, irrespective of

site, averaging 1825.6 ± 66 cm^2 of the area in the quadrats used to estimate microhabitat cover. This difference in area was significantly ($p < 0.0001$) greater than that of any other microhabitat (Figure 2.6). This is further reflected in the total area sampled at each site, with 13.5 m^2 at Three Sisters, 12.54 m^2 at Kommetjie, and 10.57 m^2 at Zinkwazi, out of a total 22.5 m^2 (Figure 2.7).

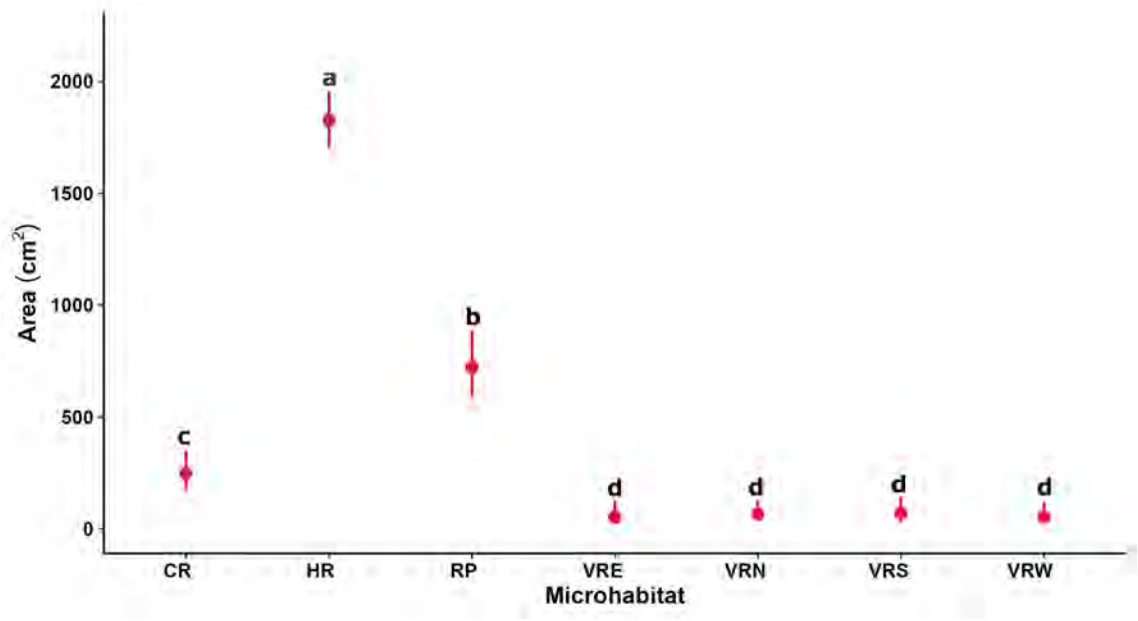

Figure 2.6: Dot and whisker plot showing variations in total area (cm^2), represented as point estimates (± CI), averaged across all sites for various microhabitats (CR - crevices, HR - horizontal surfaces, RP - rock pools, VRE - east-facing vertical surfaces, VRN - north-facing vertical surfaces, VRS - south-facing vertical surfaces, VRW - west-facing vertical surfaces). Homogenous groups are shown as lowercase letters.

After horizontal rock surfaces, rock pools, averaging 722.5 ± 74.7 cm^2 per quadrat (Figure 2.6), constituted the second-largest area regardless of the site. This was significantly ($p < 0.0001$) more than the area covered by the remaining microhabitats. Specifically, rock pools accounted for 5.14 m^2, 3.41 m^2 and 5.82 m^2 of the sampled area at Three Sisters, Kommetjie and Zinkwazi, respectively (Figure 2.7). Crevices followed rock pools in terms of area coverage, comprising a significantly ($p < 0.05$) greater amount than all microhabitats except horizontal rocks and rock pools. While crevices comprised 2.8 m^2 and 2.17 m^2 of total area at Zinkwazi and Kommetjie, respectively,

they were notably absent at Three Sisters (Figure 2.7). When considering the orientation of vertical rock surfaces as distinct microhabitats, each direction contributed a relatively minor portion of the total area surveyed at each site, and there were no significant differences among these microhabitats.

Furthermore, the extremely low variability in area (m^2) among quadrats (Table A1) indicates that including quadrat as a random effect contributes minimal additional variability to the model intercepts. This was displayed as a negligible variance component for area in the random effects structure, which suggests that its inclusion does not significantly improve model fit or explanatory power. Despite this, the random effect for quadrats was retained to preserve the methodological rationale for addressing hierarchical data dependencies described in Section 2.3.5.

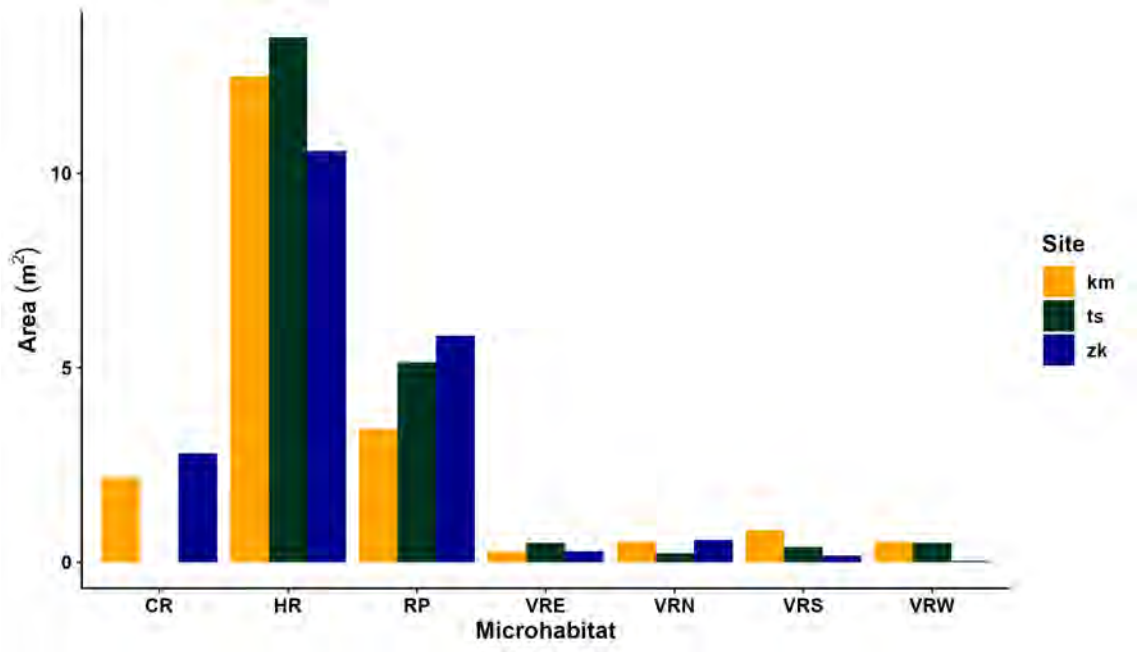

Figure 2.7: Bar graph showing differences in total area (m^2) covered by various microhabitats (CR - crevices, HR - horizontal surfaces, RP - rock pools, VRE - east-facing vertical surfaces, VRN - north-facing vertical surfaces, VRS - south-facing vertical surfaces, VRW - west-facing vertical surfaces) across sites (Zinkwazi, (zk), Three Sisters (ts), and Kommetjie (km)).

2.4.3 Microhabitat use

In the two zero-inflated Poisson GLMMs evaluating the occurrence of both species across sites and microhabitats (Table 2.3), significant main effects ($p < 0.0001$) were observed in both models for both species.

Table 2.3: Results from two zero-inflated Poisson GLMMs assessing variations in *Siphonaria capensis* and *S. serrata* occurrences (counts/cm^2) separately. Site, microhabitat, and the log of area (cm²) were treated as fixed effects, while quadrat was treated as a random intercept.

spp	term	Chisq	Df	p.value
sc	(Intercept)	259.3417	1	< 0.0001
	site	90.2977	2	< 0.0001
	mh	146.3526	6	< 0.0001
ss	(Intercept)	116.3503	1	< 0.0001
	site	367.2768	2	< 0.0001
	mh	283.5843	6	< 0.0001

Model terms: Spp - Results from separate models split by species, sc - S. capensis, ss - S. serrata, mh - Microhabitat.

Both study species, *Siphonaria capensis* and *S. serrata*, were present at all three sites. Their overall abundances, however, varied across sites when microhabitat was not considered (Figure 2.8). At Zinkwazi, both species had low total abundances (*S. capensis*, n=19; *S. serrata*, n=18), particularly when compared to Kommetjie, where the mean occurrence rate of *S. capensis* (0.96 ± 0.3 counts/cm^2, $p < 0.0001$) and *S. serrata* (2.88 ± 1.1 counts/cm^2, $p < 0.0001$) were significantly greater (Figure 2.9). The occurrence rate of *Siphonaria capensis* at Three Sisters was significantly higher ($p < 0.0001$) than at the other two sites (Figure 2.9). Conversely, the mean occurrence of *S. serrata* at Three Sisters was significantly lower ($p < 0.0001$) than at Kommetjie, which had the highest total abundance, and was not significantly ($p = 0.22$) different from Zinkwazi.

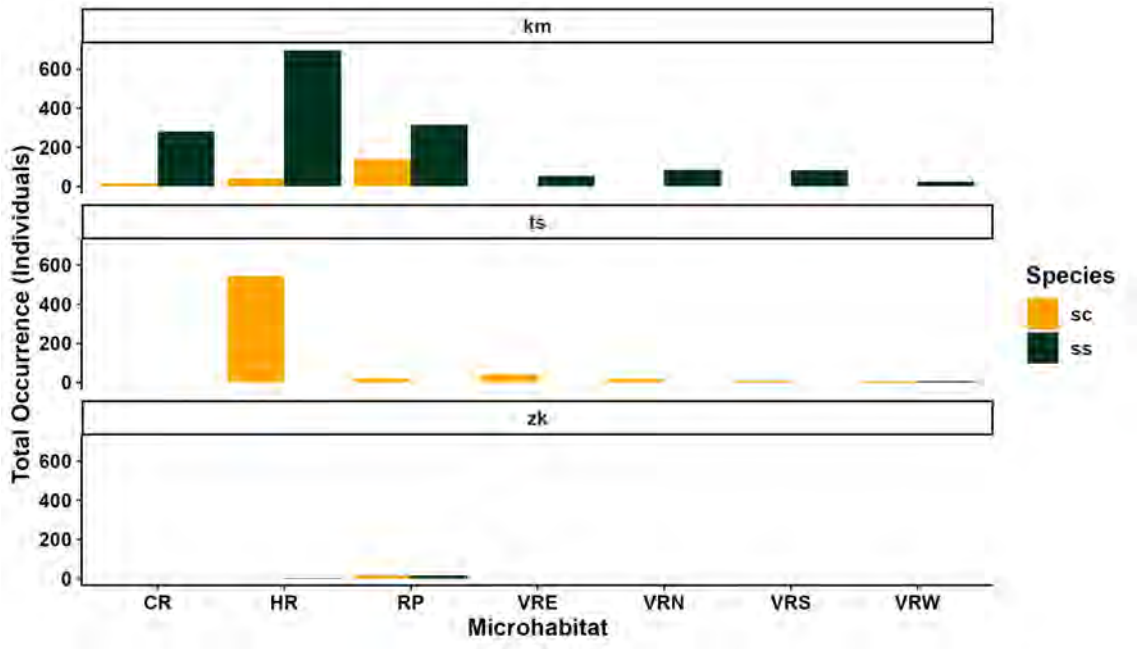

Figure 2.8: Bar graph showing total counts for the species *Siphonaria capensis* (sc) and *S. serrata* (ss) across microhabitats (CR - crevices, HR - horizontal surfaces, RP - rock pools, VRE - east-facing vertical surfaces, VRN - north-facing vertical surfaces, VRS - south-facing vertical surfaces, VRW - west-facing vertical surfaces) at Zinkwazi (zk), Three Sisters (ts) and Kommetjie (km).

Across various microhabitats (Figure 2.8), irrespective of the site, most *Siphonaria capensis* individuals were observed on horizontal rocks (n=589), followed by rock pools (n=178), east- (n=43) and north-facing (n=20) vertical rocks, crevices (n=18), south- (n=12), and west-facing vertical rocks (n=7). When accounting for the area (cm^2) and the non-independence of data points within quadrats, a slightly different pattern emerged in the average occurrence rates of *S. capensis* across microhabitats compared to what simple comparisons of total abundances suggest (Figure 2.8). The general occurrence rate of *S. capensis* on horizontal rocks was significantly lower compared to rock pools ($p < 0.0001$), east- ($p < 0.0001$), and north-facing vertical rocks ($p < 0.0001$), with no statistical difference observed between horizontal rocks and the remaining microhabitats (Figure 2.9). In fact, *S. capensis* had its highest occurrence rates on north- and east-facing vertical rocks and rock pools, with no significant differences among these microhabitats (Figure 2.9).

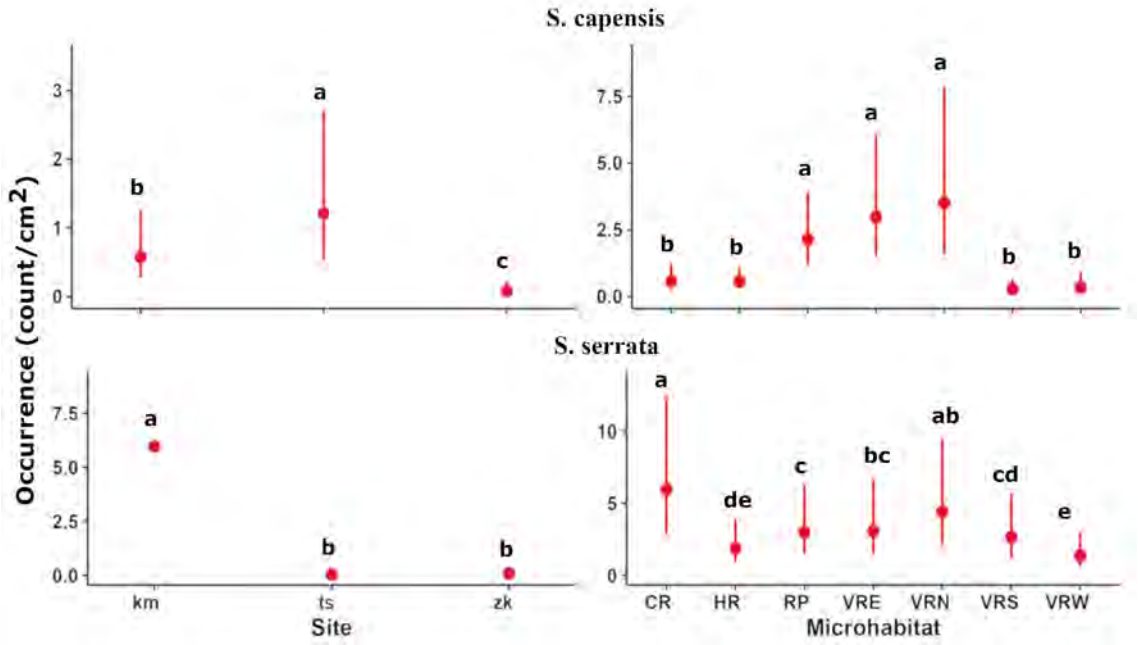

Figure 2.9: Dot and whisker plot displaying variations in overall occurrence (counts/cm²) for *S. capensis* and *S. serrata*, represented as point estimates (± CI), across microhabitats (CR - crevices, HR - horizontal surfaces, RP - rock pools, VRE - east-facing vertical surfaces, VRN - north-facing vertical surfaces, VRS - south-facing vertical surfaces, VRW - west-facing vertical surfaces) and sites at Zinkwazi (zk),Three Sisters (ts), and Kommetjie (km). Homogenous groups indicated as lowercase letters.

Siphonaria serrata exhibited a slightly different pattern of simple abundance across sites compared to *S. capensis*, as shown in Figure 2.8. Similar to *S. capensis*, *S. serrata* was most commonly found on horizontal surfaces (n = 698) and in rock pools (n = 331). This was followed, in order of decreasing abundance, by crevices (n = 281), north- (n = 85), south- (n = 82), east- (n = 54), and west-facing vertical surfaces (n = 33). Echoing the results for *S. capensis*, there was a slight deviation in the mean occurrence rates for *S. serrata* from the pattern shown for simple abundance (Figure 2.9). Specifically, mean occurrence rates for *S. serrata* were highest in crevices and on north-facing surfaces, with no significant difference between these two microhabitats ($p = 0.24$), rather than on horizontal surfaces or rock pools. This was indicated by significantly ($p < 0.001$) greater occurrence rates of *S. serrata* in crevices compared to the other microhabitats and significantly ($p < 0.05$) greater occurrence rates on north-facing surfaces compared to all

other microhabitats except east-facing surfaces (Figure 2.9). For the remaining microhabitats, mean occurrences on east-facing surfaces, rock pools and south-facing surfaces were not significantly different from each other (Figure 2.9). The occurrence rates on east-facing surfaces and in rock pools, however, were both significantly greater than on horizontal and west-facing surfaces. In contrast, mean occurrence rates for *S. serrata* on south-facing surfaces were only significantly greater than on west-facing surfaces and not significantly different from horizontal surfaces. Finally, there were no significant differences in mean occurrences between horizontal surfaces and west-facing surfaces, the two microhabitats where mean occurrence of *S. serrata* was the lowest.

Moderate variability in occurrence (counts/cm^2) across quadrats was detected for both species (Table A2 and A3). *Post hoc* analysis of the random effects was not conducted, however, as understanding species occurrence patterns among individual quadrats was not of direct interest. This is because quadrats were included as random effects solely to account for within-group non-independence while also preventing overfitting due to its numerous levels (Section 2.3.5).

The multiple zero-inflated Poisson GLMMs, which assessed variations in occurrence as a function of microhabitat within each site, revealed significant effects ($p < 0.0001$) of microhabitat on the mean occurrence rates for both species at each site (Table 2.4).

Table 2.4: Results from five zero-inflated Poisson GLMMs assessing variations in mean occurrences of both species as a function of microhabitat at each site, separately. Microhabitat and the log of area were treated as fixed effects, while quadrat was treated as a random intercept.

spp	term	site	Chisq	Df	p.value
sc	mh	km	35.80291	3	<0.0001
	mh	ts	45.62305	5	<0.0001
	mh	zk	26.94837	1	<0.0001
ss	mh	km	54.24069	6	<0.0001
	mh	zk	26.94837	1	<0.0001

Model terms: Spp - Results from separate models split by species (sc - Siphonaria capensis, ss - S. serrata), Site – Results from separate models for each site, km – Kommetjie, ts – Three Sisters, zk – Zinkwazi, mh - Microhabitat.

2.4.3.1 Microhabitat use at Zinkwazi

Except for two individuals of each species found on horizontal rock surfaces, *Siphonaria capensis* (n=17) and *S. serrata* (n=16) were predominantly found in rock pools, and in no other microhabitat, at Zinkwazi (Figure 2.8). This was demonstrated by significantly ($p < 0.0001$) greater mean occurrence rates in rock pools compared to horizontal surfaces for both species (Figure 2.11). Regarding their distribution across different shore heights, at Zinkwazi both species were present at all levels (Figure 2.10). *S. capensis*, however, was more frequently observed on the mid-shore, while *S. serrata* was more commonly found lower down.

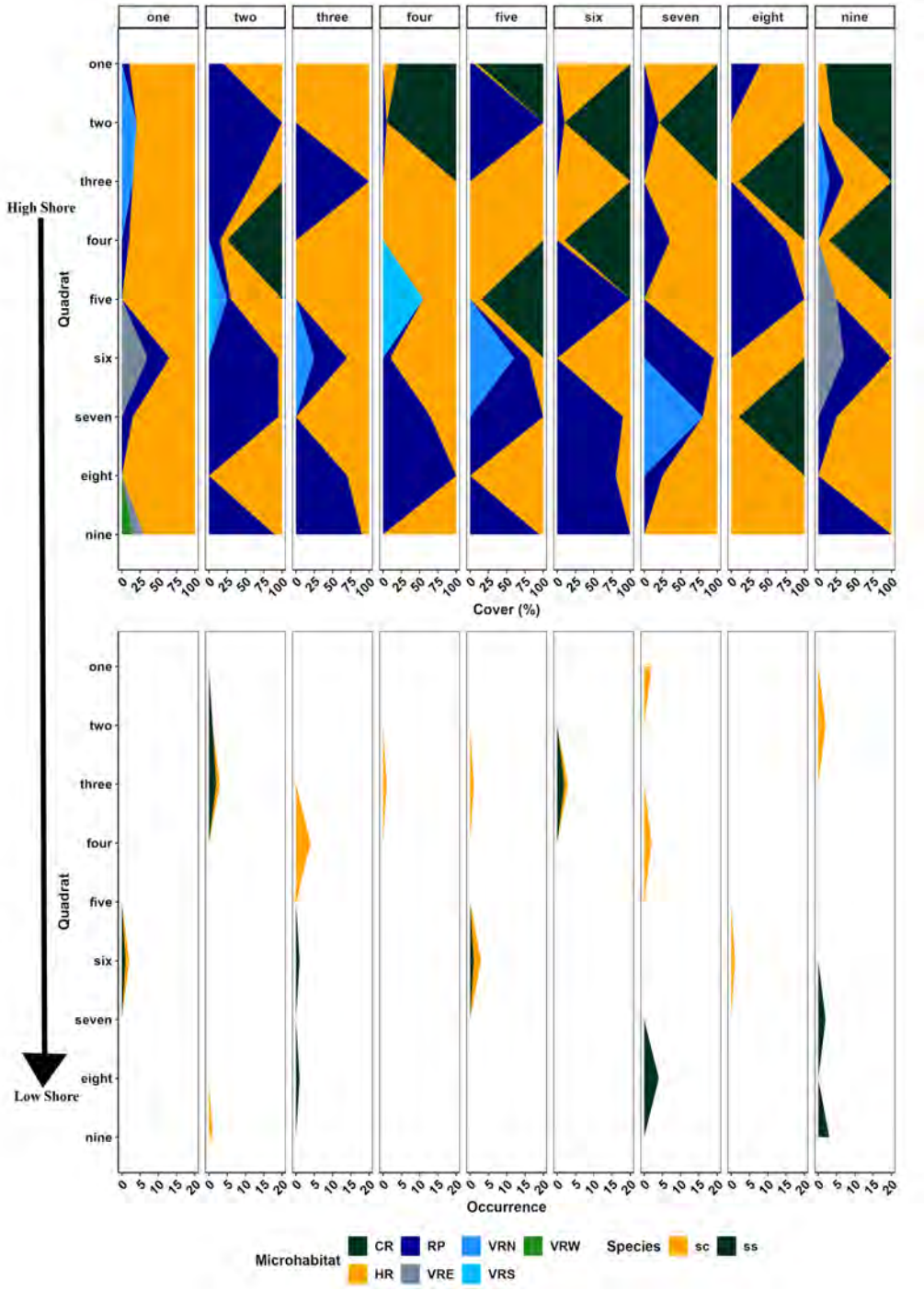

Figure 2.10: Base map illustrating microhabitat coverage (%), shown in the top panel, and limpet counts, presented in the bottom panel, at Zinkwazi. The species are denoted as sc for *Siphonaria capensis* and ss for *S. serrata*. The microhabitats are CR - crevices, HR - horizontal surfaces, RP - rock pools, VRE - east-facing vertical surfaces, VRN - north-facing vertical surfaces, VRS - south-facing vertical surfaces, VRW - west-facing vertical surfaces.

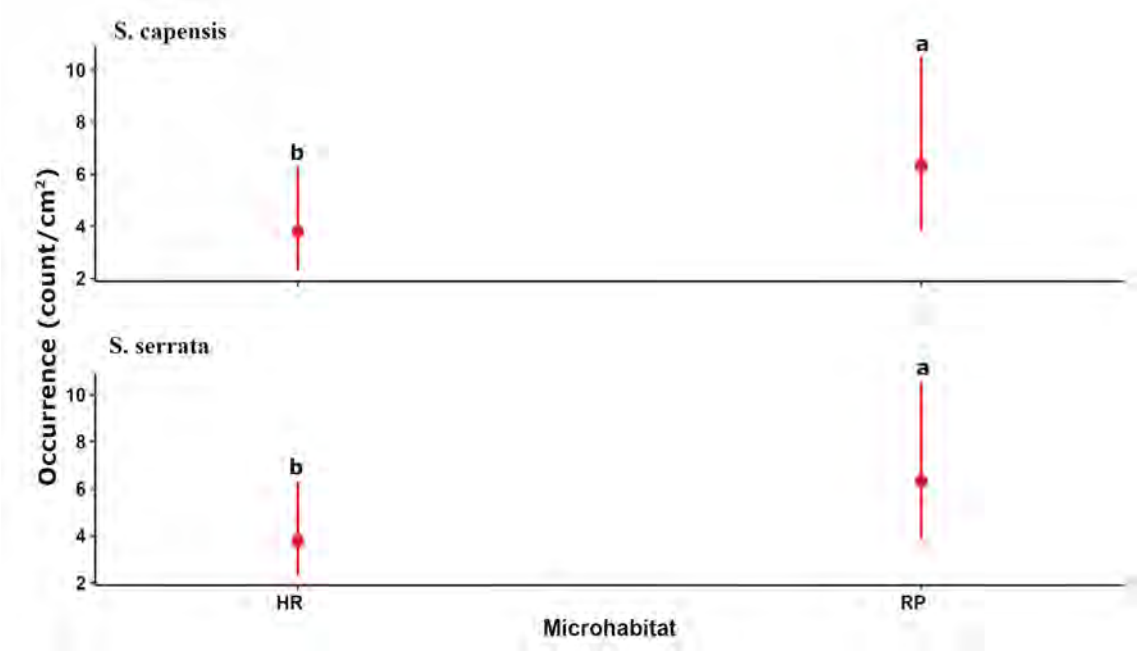

Figure 2.11: Dot and whisker plot displaying variations in occurrence (counts/cm²) for *S. capensis* and *S. serrata*, represented as point estimates (± CI), across various microhabitats (HR - horizontal surfaces, RP - rock pools) for both species at Zinkwazi. Homogenous groups are shown as lowercase letters.

2.4.3.2 Microhabitat use at Three Sisters

At Three Sisters, unlike Zinkwazi where both species were predominantly found in rock pools, *Siphonaria capensis* was more frequently observed on horizontal rocks than in any other microhabitat, while *S. serrata* was found exclusively on west-facing vertical rock surfaces (Figure 2.8). The prevalence of *S. capensis* on horizontal rocks was followed, in descending order of abundance, by east-facing vertical rocks (n=41), rock pools (n=22), north- (n=20), south- (n=12), and west-facing vertical rock surfaces (n=7), respectively. Despite the high numbers on horizontal rocks at Three Sisters, north-facing surfaces, east-facing surfaces and rock pools had significantly ($p < 0.01$) higher mean occurrence rates than all other microhabitats, and no significant differences among them (Figure 2.13). Furthermore, mean occurrence rates of *S. capensis* were not significantly different among the remaining three microhabitats. This highlights a distinct habitat preference for *S. capensis* at Three Sisters. While *S. capensis* exhibited a distribution

from high- to mid-shore only, *S. serrata* was confined to just the one high-shore microhabitat at Three Sisters (Figure 2.12).

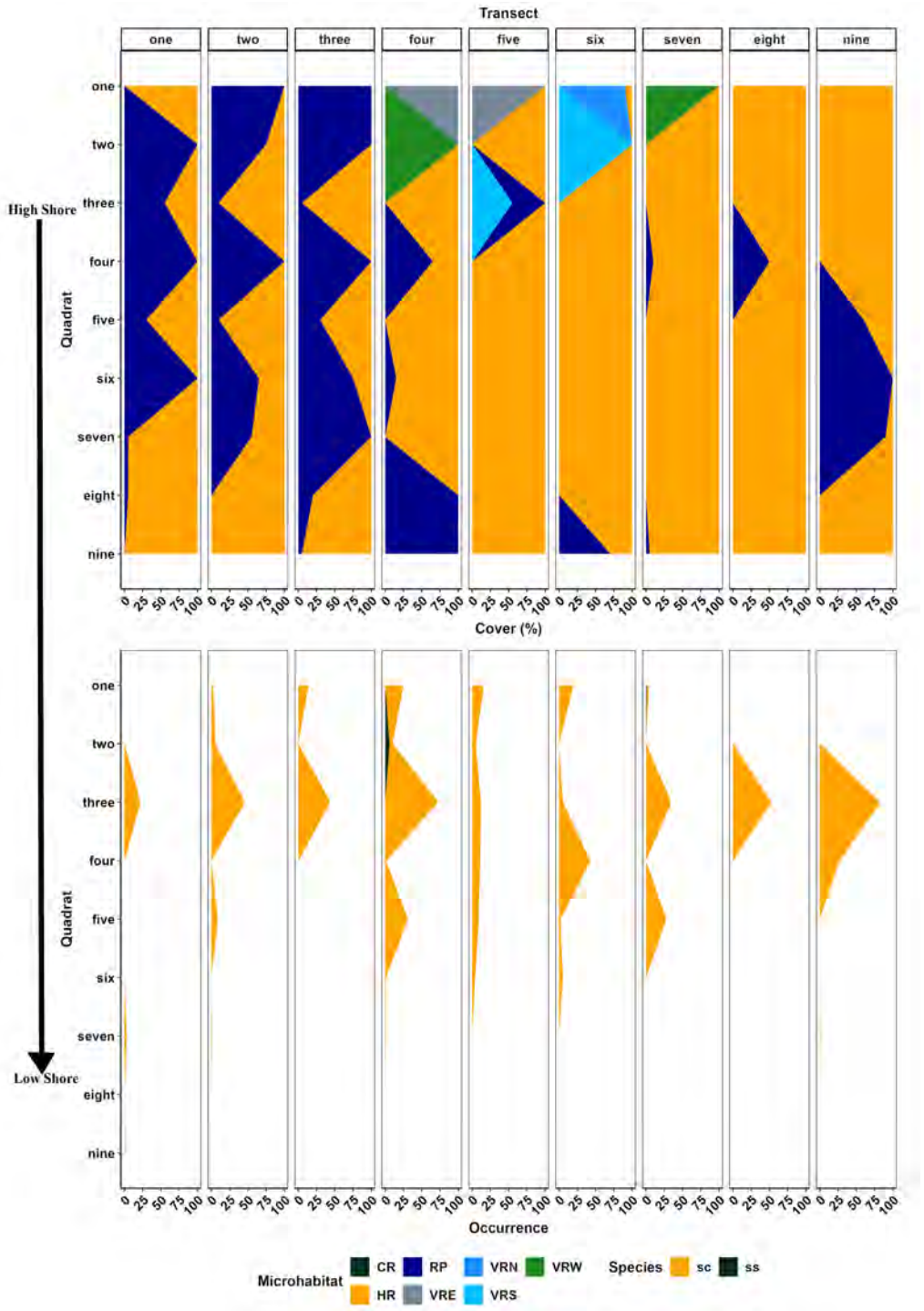

Figure 2.12: Base map depicting the percentage of microhabitat coverage in the top panel and the distribution of limpet populations in the bottom panel at Three Sisters. The species are indicated as sc for *Siphonaria capensis* and ss for *S. serrata*. The microhabitats are CR - crevices, HR - horizontal surfaces, RP - rock pools, VRE - east-facing vertical surfaces, VRN - north-facing vertical surfaces, VRS - south-facing vertical surfaces, VRW - west-facing vertical surfaces.

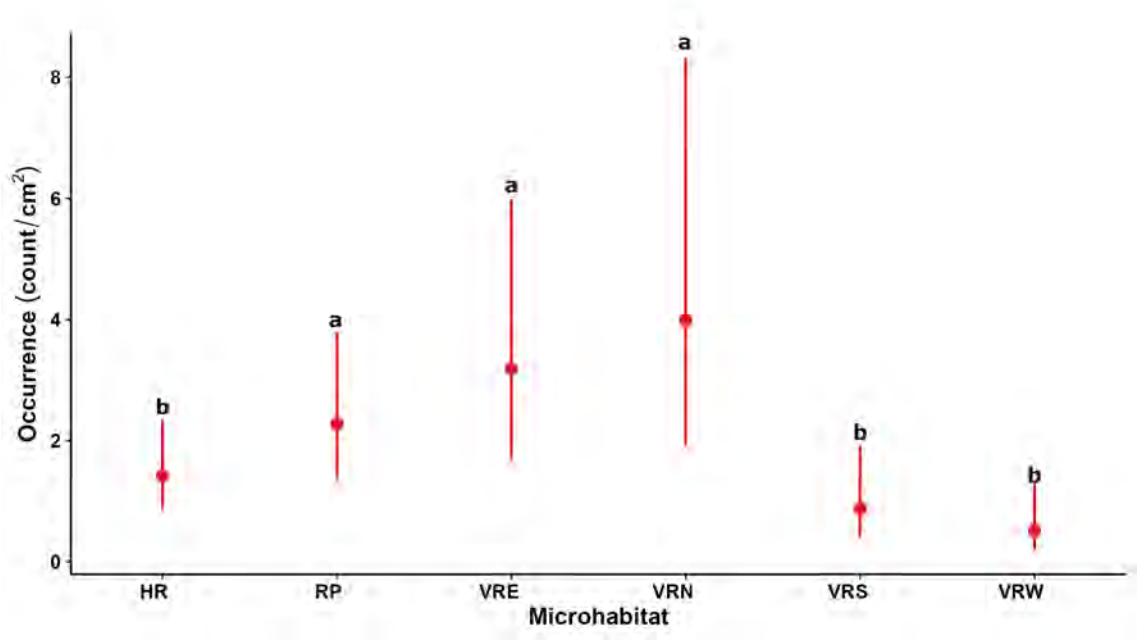

Figure 2.13: Dot and whisker plot displaying variations in occurrence (counts/cm²), represented as point estimates (± CI), across various microhabitats (HR - horizontal surfaces, RP - rock pools, VRE - east-facing vertical surfaces, VRN - north-facing vertical surfaces, VRS - south-facing vertical surfaces, VRW - west-facing vertical surfaces) for *S. capensis* at Three Sisters. Homogenous groups are shown as lowercase letters.

2.4.3.3 Microhabitat use at Kommetjie

The vertical distribution of *Siphonaria capensis* and *S. serrata* at Kommetjie mirrored that at Zinkwazi, in that both species occupied all shore levels (Figure 2.14). *S. serrata* was, however, more abundant in the mid- to low-shore zones, primarily on horizontal rock surfaces and in rock pools (Figure 2.8). In contrast, *S. capensis* favoured high- to mid-shore zones (Figure 2.14), most notably in rock pools, while also appearing to a lesser extent on horizontal rock surfaces (Figure 2.8). *S. serrata* was also found in crevices (n=281) and across various vertical rock surfaces, with north (n=85), south (n=82), east (n=54), and west (n=26) orientations. Conversely, *S. capensis* was mainly confined to crevices (n=18) and east-facing vertical rocks (n=2), while being absent on north-, south-, and west-facing vertical microhabitats. Reflecting the findings from Three Sisters, there were deviations in the pattern for *S. capensis* occurrence rates and

total abundances among microhabitats (Figure 2.15). At Kommetjie, *S. capensis* had significantly ($p < 0.01$) higher occurrence rates on east-facing surfaces and in rock pools than on horizontal surfaces and in crevices, with no significant differences between microhabitats within each pair. For *S. serrata*, mean occurrence rates on north-facing surfaces, east-facing surfaces, and in rock pools were significantly greater ($p < 0.05$) than on the remaining microhabitats, with no significant differences among these three (Figure 2.15). Additionally, there were no significant differences in mean occurrence rates of *S. serrata* in the remaining microhabitats.

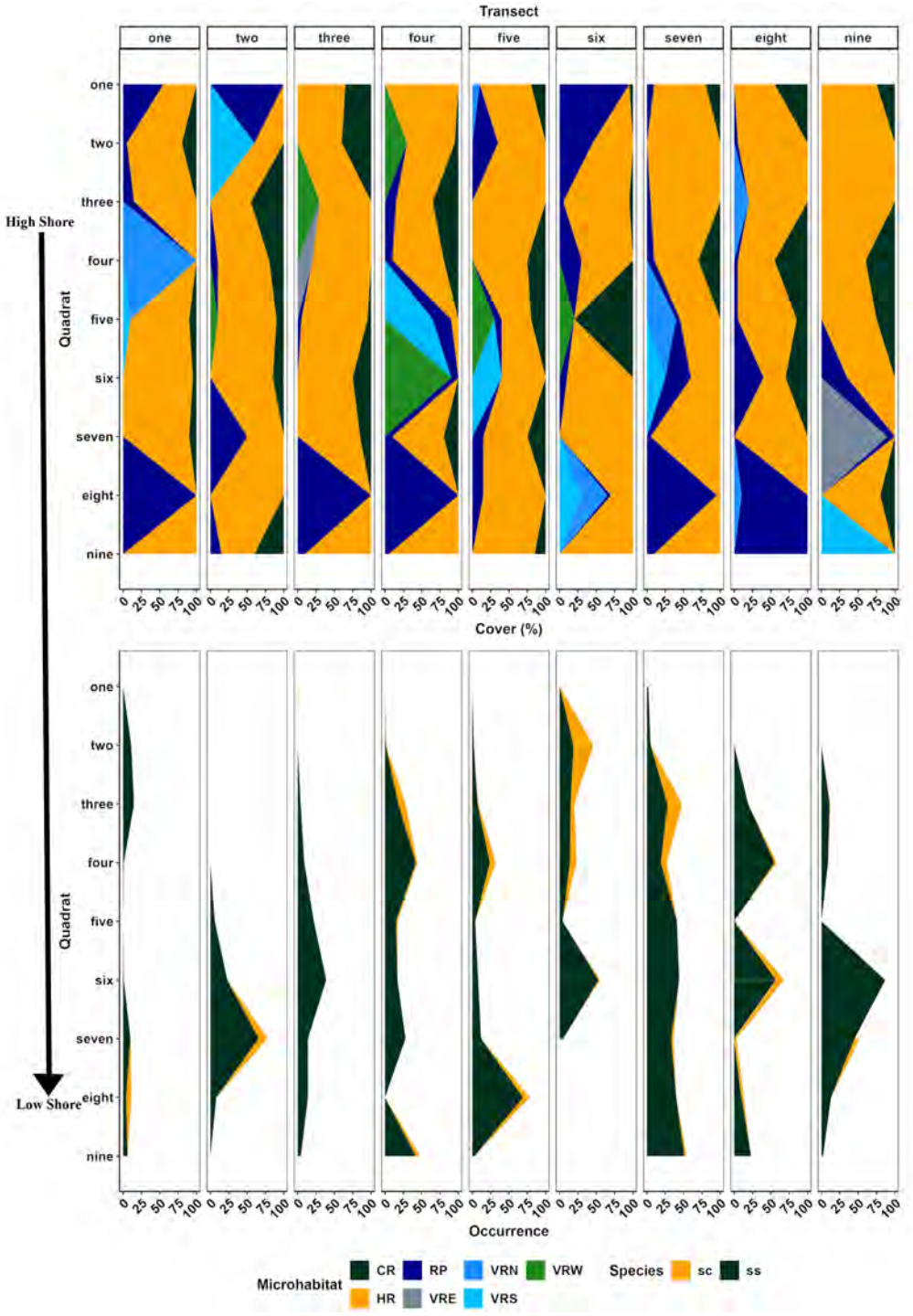

Figure 2.14: Base map displaying the percent microhabitat cover in the top panel and the distribution of limpet populations in the bottom panel at Kommetjie. The species are indicated as sc for *Siphonaria capensis* and ss for *S. serrata*. microhabitats are abbreviated as: HR - horizontal surfaces, RP - rock pools, VRE - east-facing vertical surfaces, VRN - north-facing vertical surfaces, VRS - south-facing vertical surfaces, VRW - west-facing vertical surfaces.

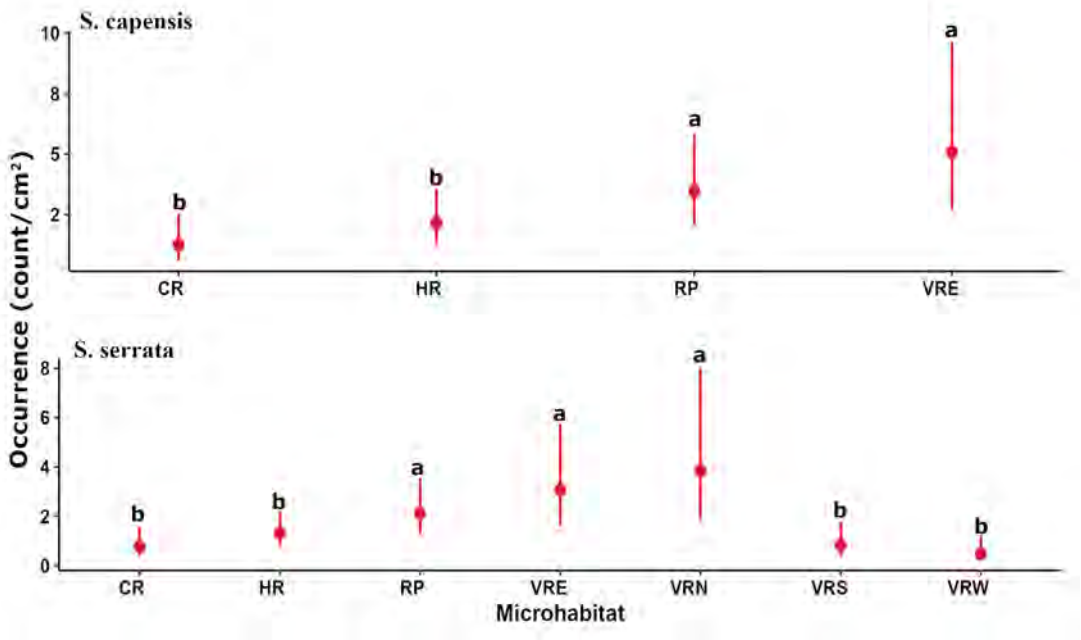

Figure 2.15: Dot and whisker plot showing variations in occurrence (counts/cm²), represented as point estimates (± CI), as a function of microhabitat (CR - crevices, HR - horizontal surfaces, RP - rock pools, VRE - east-facing vertical surfaces, VRN - north-facing vertical surfaces, VRS - south-facing vertical surfaces, VRW - west-facing vertical surfaces) for both species at Kommetjie. Homogenous groups are shown as lowercase letters.

2.5 Discussion

2.5.1 Overview and guiding hypotheses

This chapter investigated patterns in microhabitat utilisation by the pulmonate limpets *Siphonaria capensis* and *S. serrata* at Zinkwazi, Three Sisters and Kommetjie on the East, South, and West coasts of South Africa, respectively. The primary objectives were to determine how these limpets are distributed among different microhabitats based on the thermal properties of these habitats and to relate these patterns to their potential physiological responses in subsequent studies. I predicted a negative relationship between limpet occurrence and stressful microhabitat thermal regimes, which should subsequently manifest as a reduced reliance on physiological adaptations to heat stress.

If the results showed a positive relationship between microhabitat utilization and stressful thermal regimes, then these predictions would not hold true.

2.5.2 Summary of key findings

The study found noteworthy variations in low-tide temperatures across different microhabitats and sites. Three Sisters had the highest average low-tide temperatures, while the lowest were recorded at Kommetjie. In descending order, the general trend for temperatures recorded among microhabitats was horizontal surfaces, east-, north-, west-, and south-facing vertical surfaces, crevices, and rock pools. These patterns, however, varied between seasons for sites and there were within-season and site variations in the trend for microhabitats. For instance, during summer, instead of the highest temperatures being recorded at Three Sisters, they were tied at Zinkwazi and Kommetjie, whereas the lowest were at Three Sisters. During summer at Kommetjie, the microhabitat temperature trend largely aligned with the general trend, except that north-facing vertical surfaces were warmer than east-facing ones, and crevices were warmer than south-facing vertical surfaces. This was not the case, however, for the trend in temperatures recorded among microhabitats during summer at Zinkwazi. Here, the highest temperatures were recorded on south-facing vertical surfaces, followed by horizontal surfaces, rock pools, crevices, east-, north-, and west-facing vertical rocks. Due to gaps in the temperature data for Three Sisters during summer, particularly for crevices and south-facing surfaces, making comparisons of temperature patterns among microhabitats involving Three Sisters was difficult. Aside from these omissions, however, the pattern of temperature variation among microhabitats at Three Sisters was identical to Kommetjie.

Horizontal rock surfaces were the most prevalent microhabitat at each site, covering significantly more area than other types. Rock pools followed, covering the second-largest area, while crevices were less common. Vertical rock surfaces, characterized by direction, contributed minor portions to the total surveyed area with no significant differences among them. Both *S. capensis* and *S. serrata* were present at all three sites, but their abundances, that is number per unit area, varied. They were both

rare at Zinkwazi. The highest abundances of *S. capensis* were observed at Three Sisters, while *S. serrata* had its highest abundance at Kommetjie. *S. capensis* showed higher occurrence rates in rock pools and on east- and north-facing vertical rocks at Kommetjie and Three Sisters, and in rock pools at Zinkwazi. *S. serrata* occurrence rates were also highest in rock pools at Zinkwazi. It was only found on west-facing vertical surfaces at Three Sisters and, like *S. capensis*, was predominantly found in rock pools and on east- and north-facing vertical rocks at Kommetjie.

2.5.3 Microhabitat availability

Research explicitly quantifying differences in the area covered by intertidal rocky shore microhabitats, as defined in this study, is largely unavailable. The findings from this study deviate from those in a similar study by Garrity (1984) conducted on rocky shores off the Pacific mouth of the Panama Canal. In both studies, it was found that the largest area of the rocky intertidal sample sites consisted of horizontal rock surfaces. Unlike the current study, however, Garrity (1984) found that horizontal surfaces were followed by vertical surfaces, crevices, and rock pools in terms of area coverage. Note that the criteria used to define horizontal surfaces in the current study were used to distinguish horizontal from sloped surfaces by Garrity (1984). Furthermore, the lower ranking of vertical surfaces in the trend for microhabitat cover in the current study is likely due to Garrity (1984) treating vertical surfaces as a single microhabitat irrespective of cardinal direction, whereas cardinal direction was considered in the current study.

2.5.4 Near surface thermal regimes

2.5.4.1 Near-surface temperatures defy the regional air/sea-temperature gradient

The overall trend in broad geographical, emerged intertidal rock temperatures for the current study, derived from summary statistics without performing any statistical analyses, differs from the general trend of increasing surface temperatures from the West

to the East coast of South Africa (Griffiths et al. 2010, Smit et al. 2013, Tagliarolo et al. 2016, Lathlean et al. 2017). Most research contrasting thermal regimes along the South African coastline does not distinguish aerial or sea-surface temperatures from temperatures recorded near the surface of emerged intertidal rocks (Smit et al. 2013, Tagliarolo et al. 2016). In Tagliarolo et al. (2016), where the aerial component of temperature logger data was explicitly isolated, the average temperature data logged near intertidal rock surfaces indicated insignificant differences in general surface temperature among the West, South, and East coasts of South Africa. Studies like the current one and that by Tagliarolo et al. (2016), where the surface temperature was isolated and analysed, are likely to display patterns in broad geographic thermal trends that differ from most previous research of this type in South Africa.

2.5.4.2 Local atmosphere and geomorphology affect site-specific temperatures

Central to this difference between the two types of studies are the more consistent thermal profiles observed in datasets consisting entirely of temperature data for submerged environments or for a combination of submerged and emerged environments, resulting from the distinct oceanographic features of each coast (Lutjeharms et al. 2000, Fawcett 2006, Griffiths et al. 2010). These attributes include the combined cooling effects of the Benguela current and frequent upwelling along the West coast, compared to the South and East coasts, where upwelling is less frequent and the influence of cold currents is less prominent, or where upwelling is scarce and the nearshore Agulhas current is warm, respectively (Andrews & Hutchings 1980, Lutjeharms 2006, Smit et al. 2013, Tagliarolo et al. 2016). In contrast, the more complex patterns observed in surface temperature data for South African coasts could be attributed to several factors. These include variations in local atmospheric conditions such as rain, fog, cloud cover, timing of low tide at different latitudes, and wind intensity, as well as disparities in intertidal rock characteristics like varying rock porosity or albedo (Dower 1989, Helmuth 1998, Vat 2000, Harley 2008, Helmuth et al. 2011, Zhao et al. 2015, Helmuth et al. 2016, Putra et al. 2023). Additionally, fluctuations in the overall slopes and orientation of the

intertidal rocky shores at each site, along with their interaction with the average angles of solar radiation, also play a significant role (Zhao et al. 2015, Barbosa et al. 2022, Putra et al. 2023). These factors have previously been shown to drive large-scale variations in the thermal characteristics of environmental substrata. The unexpectedly higher overall temperatures at Three Sisters compared to Zinkwazi in the current study may thus be attributed to the interplay of local atmospheric conditions and rocky shore characteristics, with the likely greater overall rainfall at Zinkwazi during the sample period potentially playing a central role (Reason et al. 2006, Griffiths et al. 2010, Jury 2013, Mashao et al. 2023, Tim et al. 2023).

2.5.4.3 Seasonal modifiers of coastal thermal patterns

The misalignment of season-mediated shifts in the general thermal patterns among coasts in this study with the more consistent patterns across seasons observed in previous research (Andrews & Hutchings 1980, Lutjeharms et al. 2000, Smit et al. 2013) can be attributed to some of the aforementioned factors. For example, seasonal shifts in average cloud cover or wind intensity can differentially modulate the amount of solar radiation reaching the intertidal zone or influence the amount of heat transferred from the air to the rock surfaces, thus affecting rock temperatures to different degrees across seasons along the coast (Harley 2008, Choi et al. 2019, Mieszkowska et al. 2021). The interaction of wind with sand surrounding the intertidal zone can further impact the amount of heat transferred to intertidal rocks. By retaining greater levels of moisture during low tide compared to exposed rock surfaces, sand inundation is known to reduce intertidal rock temperatures (Branch 1976, Dower 1989). Fluctuating wind patterns associated with various seasons can differentially alter the degree of sand inundation at a site (Colosimo et al. 2020). Furthermore, as mentioned earlier in this paragraph, the angle at which solar radiation strikes a surface also has a notable effect on the magnitude of heat energy transferred to that surface. Surfaces angled perpendicularly to the sun at any given time receive greater solar energy input than surfaces angled away from the sun (Putra et al. 2023). This effect can vary seasonally as the sun's path changes, altering which slopes

receive more direct sunlight (Putra et al. 2023).

2.5.4.4 Thermal regime differences between rock pools and crevices

When considering general patterns in high-shore microhabitat thermal regimes irrespective of site and season, the findings from this study deviate only slightly from those in Garrity (1984) and Williams & Morritt (1995). For instance, in contrast to the current study, Garrity (1984) recorded greater surface temperatures in rock pools than in crevices, but the trend in surface temperature for the remaining microhabitats matched that of the current study. Without detailed information regarding the geomorphological features of either rock pools or crevices sampled in both studies, it is challenging to determine accurately the possible reasons for the discrepancies between studies. This challenge is further compounded by the fact that I could find no previous research on intra-microhabitat variations in temperature among crevices. Previous research on rock pools (Morris & Taylor 1983, Legrand et al. 2018, Buasakaew et al. 2021) however suggests that the discrepancies in the placement of rock pools in patterns of inter-microhabitat thermal regime for each study may be driven by differences in surface temperature associated with variations in the dimensions of the rock pools sampled in the different studies. Morris & Taylor (1983) also note that rock pool temperature in deep pools, as defined in (Table 2.1) of this chapter, is influenced by the depth at which the temperature logger is placed in the pool.

2.5.4.5 Aspect and wave splash influence vertical surface thermal profiles

In their study where aspect-influenced differences in thermal profiles among vertical surfaces were also considered, Williams & Morritt (1995) found that east-facing vertical surfaces generally served as thermal refuges at their four sample sites. In contrast, the current study identified east-facing surfaces as having some of the highest temperatures. Differences among studies in the thermal profiles of vertical microhabitats can be attributed to the interplay between temporal and site-specific factors, the latter of which

was not considered in the study by Williams & Morritt (1995). For instance, east-facing surfaces are typically cooler than west-facing surfaces because they receive higher solar irradiance in the morning, when temperatures are generally lower than in the afternoon, when west-facing surfaces receive peak solar irradiance (Putra et al. 2023). Furthermore, changes in the overall shoreline aspect relative to the sea and the cooling effect of wave splash on surfaces facing the sea can influence thermal profiles among vertical microhabitats (McQuaid & Branch 1984, Harley 2008, Mieszkowska et al. 2021, Hayes et al. 2024). At the wave-exposed Zinkwazi, the relatively low temperatures recorded on east-facing surfaces were likely due to the combined effects of peak solar exposure coinciding with cooler morning conditions, frequent wave splash, and the general seaward orientation of these surfaces. Conversely, when these surfaces are angled away from the sea or where wave activity and splash are relatively limited, as observed at Kommetjie and, to a lesser extent, Three Sisters, they tend to exhibit comparatively higher temperatures.

2.5.5 Species distribution patterns

2.5.5.1 Decoupling of abundance patterns from the regional temperature gradient

The patterns of abundance for both species were not aligned with the large-scale, average surface temperature gradient across sites in the current study. It is important to note that with only one site sampled per region, no conclusions can be drawn about the broader effects of coastal regions or biogeography. Nonetheless, along the South African coast, *Siphonaria serrata* exhibited patterns of distribution consistent with patterns of general rocky shore biota abundance observed in the study by Bustamante et al. (1997). In their research on the effects of physical factors on the distribution of South African rocky shore communities, Bustamante et al. (1997) described a general decrease in biomass of these communities from the West to East coasts of South Africa. This trend correlates with similar gradients of nutrient availability and intertidal epilithic microalgae biomass, as well as the inverse gradient of average sea water temperatures along the South African

coast (Bustamante et al. 1997). It differs, however, from the findings for *S. capensis* in the current study, where abundance peaked at the site, Three Sisters, on the South coast.

2.5.5.2 Within-site effects modulate regional abundance gradients

The discrepancy in the abundance pattern of *S. capensis* in the current study compared to the general patterns reported in other studies cannot be attributed to biogeographical effects due to key limitations in sampling methodology, particularly the selection of only one site per region. Instead, site-specific factors likely played a significant role. For instance, the lower biomass of *S. capensis* at the West coast site compared to the South coast site in this study may be due to the fact that Kommetjie is a sheltered site (Tucker et al. 2017, Rensburg et al. 2021), whereas Three Sisters is an exposed site (Dower 1989, Garner 2013), respectively. As shown in studies by McQuaid & Branch (1984) and Bustamante et al. (1997), wave-exposed sites generally maintain higher intertidal organism biomass regardless of region. The differing effects of sheltered versus exposed sites on the biomass of *S. serrata* compared to *S. capensis* may result from the interaction of wave-exposure with the general patterns of vertical shore distribution of these species. Bustamante et al. (1997) demonstrated that intertidal organism biomass decreases exponentially with shore height on sheltered shores and peaks at mid-shore on exposed shores. Consequently, as the general consensus from both the current study and earlier research (Chambers 1995, Hodgson 1999) that *S. capensis* typically occupies higher shore zones than *S. serrata*, wave exposure is likely to have a greater impact on the overall biomass of *S. capensis* compared to *S. serrata*. Therefore, within-shore effects play a significant role in shaping the patterns of occurrence of the sample species among sites along the South African coast. Further evidence supporting this is provided by Chambers (1995). In his doctoral dissertation on the ecological and phylogenetic influences on the reproductive strategies and evolution of *Siphonaria* species, he found no substantial differences in biomass for species between the South and East coasts. This contrasts with what would be expected if large-scale patterns of occurrence followed the

general thermal regime gradient along South Africa's coast.

2.5.5.3 Site-specific shifts in temperature mediated micro-scale distribution patterns

Micro-scale variations in day-time intertidal rock temperatures can be substantial, sometimes exceeding those observed over larger geographic distances (Helmuth et al. 2006, Denny et al. 2011, Janetzki et al. 2021). This is driven by discrepancies between the temperatures of exposed rock surfaces and the surrounding air, with differences often exceeding 15°C, with rock temperatures generally being higher (Bertness 1989, Helmuth 1998, Helmuth & Hofmann 2001, Judge et al. 2018, but see Wang et al. 2020). Because the body temperatures of intertidal gastropods, including limpets, are closely correlated with the temperatures of the rock surfaces they inhabit, these variations can significantly influence their within-shore distribution patterns across different microhabitats (Denny & Harley 2006, Fraser et al. 2016, Pound et al. 2020, Moisez et al. 2020, Janetzki et al. 2021). Many studies indicate that intertidal gastropods either prefer, are more common in, or perform better in cooler microhabitats (Denny & Harley 2006, Pound et al. 2020, Janetzki et al. 2021), suggesting a potential negative correlation between gastropod abundance and microhabitat temperature. In contrast, findings from this study demonstrate that, although microhabitat temperature influenced limpet distribution, there was no consistent pattern linking limpet abundance to the thermal conditions of those microhabitats. Whether the limpets were more common in warmer or cooler microhabitats varied depending on the sample site. For example, *Siphonaria capensis* was equally abundant in two warm and one cool microhabitat at Kommetjie and it was most abundant in a warm microhabitat at Zinkwazi. Similarly, *S. serrata* was equally abundant in two warm and one cool microhabitat at Kommetjie, most abundant in a cool microhabitat at Three Sisters, and most abundant in a warm microhabitat at Zinkwazi. In their study on *Littorina littorea* and *Patella vulgata*, Moisez et al. (2020) observed comparable results to those of this study, though instead of site-dependent effects on the patterns of occurrence, they found that both species exhibited season-dependent

preferences for microhabitats based on their thermal conditions. Namely, they showed that both species favoured warmer microhabitats during cooler months and cooler microhabitats during warmer months. In the present study, however, both species were equally likely to occur in warm or cool microhabitats at the coolest site but were more common in intermediate to cool microhabitats at the warmer site.

2.5.5.4 Life-stage effects on microhabitat use

As discussed in Moisez et al. (2020), a preference for cooler microhabitats when atmospheric conditions are warm may be an active avoidance of lethal or sub-lethal temperatures, which can be transferred to them by conduction from the warm substrate to the gastropod's foot. A weaker preference for cooler microhabitats, on the other hand, at cool sites may be driven by several interacting factors. Foremost among these are ontogeny-based differences in patterns of microhabitat occurrence. For instance, text from Chambers (1995) implies that ontogeny-related differences in food preferences could lead to interspecific differences in microhabitat preferences for *Siphonaria serrata* in the mid-intertidal zone. Specifically, juvenile *S. serrata* were more common in crustose rock pools, whereas adults were more frequently found on bare rocks. Although data correlating ontogeny and microhabitat were not quantitatively analysed for the current study, small individuals of both species were predominantly confined to rock pools (pers. obs.). This observation aligns with previous research (Diederich & Pechenik 2013, Truebano et al. 2018, Delorme et al. 2024) and suggests that ontogeny may have influenced microhabitat distribution in the study species, potentially shaping their distribution among thermally variable microhabitats. Other factors contributing to the patterns of occurrence at the cooler site may include a reduced incentive for limpets to avoid warmer microhabitats because they possess larger thermal safety margins, i.e., a wider temperature buffer between their upper thermal limit and routine body temperatures (Liao et al. 2021, Leeuwis & Gamperl 2022), lower post-settlement mortality in warmer microhabitats (Wethey 1983, Lathlean & Minchinton 2012), and possibly due to reduced localized thermal stress, as well as interspecific variations in

their morphological and physiological adaptations to thermal stress (Vermeij 1972, Harley et al. 2009, Sangphueak et al. 2024).

2.5.6 Methodological constraints and potential solutions

2.5.6.1 Unmeasured confounders

For a chapter primarily aimed at determining whether the microhabitat distribution patterns of the study species were correlated with intertidal microhabitat thermal regimes, other factors such as food availability (Chambers & McQuaid 1994, Thompson et al. 2000, Lord et al. 2011, Monaco et al. 2016), which can confound temperature effects on species distribution, were not sufficiently considered during sampling and analysis. Addressing such a variable would require prior knowledge of the food sources relevant to the study animals, followed by the recording and analysis of presence, absence or coverage data. This, however, would further increase the sampling effort needed to collect sufficient data, a challenge commonly encountered with the traditional sampling methods used in the current chapter (Godet et al. 2009, Casal et al. 2013, Rhodes et al. 2015, Estes et al. 2018).

2.5.6.2 Limits of traditional sampling techniques

As highlighted by others (Casal et al. 2013, Estes et al. 2018, Balado et al. 2021), conventional sampling techniques largely based on the use of point quadrats, transects, and manual counts of target spatial features and organisms, either *in situ* or from photographs taken with hand-held cameras, are often time-consuming and labour intensive. Consequently, for intertidal data that must be collected within a single low-tide event to be considered a complete sampling effort (Miller & Ambrose 2000), accounting for an exhaustive list of potentially confounding variables and groups per variable would not have been feasible. Several studies suggest using modern image data collection and processing techniques to enhance the sampling and analysis of species

distribution (Weinstein 2018, Wäldchen & Mäder 2018, D'Urban Jackson et al. 2020, Barbosa et al. 2022, Tallam et al. 2023). These methods include the use of equipment such as unmanned aerial vehicles equipped with ventrally mounted cameras for rapid and autonomous data capture, and image processing techniques that apply photogrammetry alongside advanced computer vision systems for rapid object identification and counting.

2.5.6.3 Benefits of advanced sampling techniques

Implementing these methods in future studies could enable more frequent sampling across seasons and at multiple sites on each coast (East, West, and South), potentially allowing for statistically robust inferences regarding variations in patterns of species microhabitat distribution among coasts and across seasons (Weinstein 2018, Barbosa et al. 2022). In the current study, data were collected from one site per coast during a single sampling event in summer. While the primary aim of this work was to investigate microhabitat utilization patterns across sites, expanding sampling efforts across additional sites and seasons would enhance the representation of each coast and allow additional conclusions to be drawn regarding spatiotemporal variability in these patterns. Moreover, due to data gaps arising from challenges detailed in Section 2.3.5, statistical analyses on the temperature logger data were limited. Future studies on similar topics must consider prioritizing the early availability of, and sufficient redundancy in, hardware and equipment to avoid the issues encountered in the current study, such as the frequent loss of key hardware components like the temperature loggers.

2.5.7 Linking physiology with micro-scale distribution

The use of microhabitats by intertidal organisms has been extensively studied by numerous researchers (Garrity 1984, Raimondi 1990, Vat 2000, Helmuth & Hofmann 2001, Lord et al. 2011), with some attributing their distribution to microscale variations in heat stress (Pound et al. 2020, Moisez et al. 2020, Janetzki et al. 2021) and associated

performance limits (Lord et al. 2011, Chapperon et al. 2017, Han et al. 2020, Moisez et al. 2020). Additionally, a closely related body of research has explored hypometabolism in several marine organisms and its relationship with prevailing environmental conditions (Newell 1969, Marshall & McQuaid 1991, 2020, Guppy & Withers 2007, Verberk et al. 2016). By identifying species' microscale distribution patterns and linking these to within-shore temperature variability, the current chapter lays the groundwork for investigating how these thermal landscapes translate into physiological tolerance.

2.5.8 Conclusion

Based on the findings presented here, I fail to reject the hypothesis that a negative relationship exists between the microhabitat utilization of the sample species and warm, intertidal microhabitat thermal regimes. Specifically, both species were more frequently found in thermally benign microhabitats, such as rock pools and crevices. Their distributions, however, were not entirely confined to these areas, suggesting variability in their responses to thermal stress. In conclusion, the findings from this chapter support the claim that variable environmental conditions at the micro-scale influence the distribution of pulmonate limpets. The implications of these patterns for physiological responses, including hypometabolism and thermal tolerance, will be addressed in a later chapter.

Chapter 3

Microhabitat preference analysis

3.1 Abstract

Behavioural refuge selection can mitigate the thermal extremes that intertidal ectotherms face within the fine-scale mosaics described in Chapter 2, yet the strength and consistency of such preferences remain insufficiently resolved. I quantified daytime low-tide microhabitat preference and homing tendencies in the pulmonate limpets *Siphonaria capensis* and *S. serrata* during winter and summer, on the rocky shores at Kommetjie and Zinkwazi, in South Africa. This was done to test whether risk-avoidance (preference for cool refugia) outweighs endurance strategies (i.e., persistence in warmer microhabitats). Using a multi-state capture–mark–recapture sampling design 6 822 individuals were marked across all sample microhabitats (Chapter 2), yielding 3 633 recovered individuals, located after a two week dispersal period, for the analysis of homing behaviour. Zero-inflated Beta-binomial GLMMs showed that the proportion of recaptured *S. serrata*, but not *S. capensis*, depended on relocation direction, while a Binomial GLM revealed strong homing in both species that was weaker under displacement and differed among species-treatment combinations. Furthermore, Multinomial GLMs revealed significant preferences for crevices in both species with only minor site- and season-specific exceptions. Taken together, these findings demonstrate non-random, risk-averse microhabitat selection coupled with high site fidelity, reinforcing the proposition that refuge selection underpins limpet resilience and

providing essential context for analyses of their physiological responses to climate warming.

3.2 Introduction

The rocky intertidal zone presents a myriad of environmental stressors, systematically arranged along a pronounced vertical gradient (Helmuth 2002, Harley & Helmuth 2003, Little et al. 2009). These include, but are not limited to, wave-induced mechanical stress, marked risk of desiccation, competition for resources, predation pressure, and severe temperature fluctuations (Little et al. 2009). The stressor-generated effects on intertidal fauna are generally dictated by vertical shore position, that is, competition, hydrodynamic forces and predation decrease with increasing elevation, while desiccation and thermal stressors increase simultaneously (Denny & Harley 2006, Finke et al. 2007, Little et al. 2009). Consequently, distribution limits for animals in the high and low shore regions of the intertidal zone are differentially influenced by the interplay of these biotic and abiotic stressors (Harley & Helmuth 2003, Pörtner & Farrell 2008, Miller et al. 2009, Robles et al. 2009, Little et al. 2009).

Rocky intertidal environments, being topographically complex and varied, offer a variety of habitats with relatively homogeneous biophysical attributes at spatial scales particularly pertinent to the resident macrofauna (Morris 1987). Through differential habitat utilization, these microhabitats not only confer varying degrees of protection against environmental stressors but also facilitate access to preferred trophic resources for organisms (Mackay & Underwood 1977, Pinna et al. 2012, Martínez-Laiz et al. 2018). Given this, the intricacy of the topography of many rocky intertidal systems can modulate an otherwise stark vertical gradient in stressors (Monaco et al. 2015, Monaco et al. 2017, Rensburg et al. 2021), thus, further complicating species distribution patterns across these intertidal environments.

Among the physical stressors, this study emphasizes thermal stress, as it is known to have a direct influence on species physiology and distributions (Angilletta 2009, Monaco

et al. 2015, Moyen et al. 2020, Dong et al. 2021, Li et al. 2021), and is expected to have even stronger effects on species due to the projected anthropogenic increase in global temperatures of 1-4°C by the end of the 21st century (IPCC 2018). Elevated temperatures can compromise various biological processes, such as organismal metabolism (Ganser et al. 2015, Tagliarolo et al. 2018, Somero 2020), phenological events (Pankhurst & Munday 2011, Paxton et al. 2016) and reproductive capabilities (Tropea et al. 2015, Wright et al. 2017), potentially leading to reduced aquatic animal viability (Somero 2010). This is especially true in low-latitude regions, where acclimation capacities are generally diminished due to relatively warm yet stable macrohabitat thermal regimes (Stillman & Somero 1996, Deutsch et al. 2008, Nguyen et al. 2011, Faulkner et al. 2014, Campos et al. 2021). Such concerns are also significant in fringe aquatic environments like the rocky intertidal, where inhabitants typically possess narrow thermal safety margins. Because the vast majority of intertidal species have marine origins, they are especially vulnerable to high air temperatures, leaving them susceptible to increased thermal stress (Vinagre et al. 2019, Campos et al. 2021, Dong et al. 2021).

Characterized by their intricate topography, rocky intertidal environments form thermally heterogeneous landscapes during low tide exposure (Lathlean et al. 2015, Lathlean et al. 2017, Dong et al. 2017). During low tide, organisms within these environments frequently endure rapid temperature increases that often exceed 20°C before re-submersion, a fluctuation primarily governed by factors such as tidal elevation and microhabitat characteristics (Lathlean et al. 2011, Gunderson et al. 2019, Moisez et al. 2020). Notably, the body temperatures of marine ectotherms, including sessile and sedentary species such as mussels, barnacles, and limpets, are closely aligned with rock substratum temperatures, as they gain most of their heat from the substratum rather than the direct effects of insolation (Garrity 1984, Chapperon & Seuront 2011, Hayford et al. 2021). This results in the formation of thermal stress gradients across available microhabitats, with temperature differences within-shores often reported to be more intense than those experienced by intertidal ectotherms separated by thousands of kilometres (Denny & Dowd 2012, Marshall et al. 2015, Monaco et al. 2015, Seabra et al. 2015). This emphasizes the importance of thermoregulatory adaptations, such as altered

reproductive seasonality (Pinchuk et al. 2008, Riesgo & Maldonado 2008), geographic range shifts (Mieszkowska et al. 2006, Wethey & Woodin 2008, Lenoir & Svenning 2015), enhanced thermal-tolerance physiology (Ravaux et al. 2016, Harada & Burton 2019), and, most crucially for the current study, active selection of thermal refugia in the intertidal environment (Jones & Boulding 1999, Cartwright & Williams 2012, Monaco et al. 2015, Hayford et al. 2021, Lam et al. 2022).

Active habitat selection, referred to as microhabitat preference throughout this study, denotes a deliberate choice by animals consistently to occupy specific environments from among several other possibilities (Krebs & Davies 1987, Herrendörfer 1993, Crowe & Underwood 1998). This behavioural trait exhibits ontogenetic shifts, size-dependent differentiation and multiscale spatial variation (Olabarria et al. 2002, Monaco et al. 2015, Lam et al. 2022). Importantly, microhabitat preference is not merely a consequence of differential mortality rates reducing populations in less desirable habitats (Levins 1968, Russo 1987), but rather an active selection of favourable sites. Furthermore, it is crucial to distinguish this concept from the closely associated ideas of microhabitat use and microsite fidelity. The former, microhabitat use, is characterized by passive access to microhabitats, primarily dictated by physical microscale barriers – essentially, "there is no choice and therefore no preference" (Olabarria et al. 2002, p 160). Conversely, microsite fidelity, which is typically referred to as "homing," represents an organism's repeated return to the same location, transcending a simple preference for a certain type of microhabitat, thus demonstrating a higher degree of specificity in the organism's habitat selection strategy (Santina 1994, Gray & Hodgson 1998, Nuñez et al. 2014).

My focus centers on the daytime low-tide microhabitat preferences of adult *Siphonaria capensis* and *S. serrata* at the chosen sampling sites (Chapter 2), using a multi-state capture-mark-recapture (CMR) study design (Lebreton et al. 1992, Brownie et al. 1993, Nichols & Kendall 1995). This approach allows for the investigation of disparities in survival rates stemming from variability in intertidal conditions and the likelihood of transitions among different habitat types by employing individual-specific data (Brownie

et al. 1993, Nichols & Kendall 1995). Prior research on microhabitat use by the study species indicates potential differences in overall preferences, with *S. capensis* seemingly favouring shallow rock pools supporting crustose macroalgae and *S. serrata* demonstrating an inclination for crevices (Branch & Cherry 1985, Chambers & McQuaid 1994). Contemporary research presents compelling evidence linking numerous ecological factors to microhabitat selection patterns in intertidal organisms, encompassing size-related effects (Kovach & Tallmon 2010, Monaco et al. 2015), responses to vertical zonation (Monaco et al. 2015), food availability (Pinna et al. 2012, Martínez-Laiz et al. 2018), and adjustments to seasonal climatic shifts (Cartwright & Williams 2012). The underlying mechanisms regulating these environmental processes include diverse sensory modalities that help intertidal ectotherms navigate complex environments and optimize their habitat selection (Doering & Phillips 1983, Perea et al. 2007, Pinna et al. 2012, Camacho & Thacker 2013, Lam et al. 2022).

Building on Chapter 2, which established the relationship between microhabitat temperature heterogeneity and species occurrence patterns, this chapter aims to determine the study animals' microhabitat preferences as a measure of their risk-avoidance predisposition. For instance, limpets may leverage visual and thermally-mediated cues to avoid thermally stressful microhabitats, as seen in intertidal snails like *Chlorostoma funebralis* and *Littorina sitkana* (Jones & Boulding 1999, Tepler et al. 2011). Certain barriers, however, may prevent individuals of a certain species from consistently occupying its preferred microhabitats during extreme low tides. These include the interrelated effects of slow-moving gastropods not being able to return to their favoured environments in time after foraging during tidal transitions, given that limited food resources necessitate extended foraging trips away from desired sites (Jones & Boulding 1999), as well as intraspecific competition for scarce resources within these preferred areas (Nuñez et al. 2014). Limpets trapped in unfavourable microhabitats might be forced to rely on energy-saving strategies to alleviate the impacts of thermal stress (Jones & Boulding 1999, Monaco et al. 2015, Verberk et al. 2016, Marshall & McQuaid 2020). This underscores the challenges encountered by organisms striving to strike a balance between resource requirements, employing endurance-based strategies,

and risk-avoidance tactics in thermally taxing environments.

Hence, this study aims to quantify how pulmonate limpets navigate thermally adverse intertidal environments during daytime low tides and how these behavioural responses might affect their survival and distribution. It is therefore hypothesized that those pulmonate limpets, which display a potentially restricted capacity for microhabitat preference during escalating temperatures, may be predisposed to favour endurance-based strategies, thereby shaping their population persistence.

3.3 Methods

3.3.1 Sample sites and animals

This study explores the microhabitat preferences of *Siphonaria capensis* and *S. serrata* across four distinct intertidal microhabitat types (Table 2.1) within previously designated sample areas (Chapter 2) on the East and West coasts of South Africa (Figure 1.1).

3.3.2 Sampling method

Fieldwork was carried out at Zinkwazi and Kommetjie during spring low tides from May to June and November to December 2019. Sampling was confined to sunny days, commencing two hours prior to low tide, to maximize efficiency as detailed in Chapter 2. Following methodologies similar to those described by Crowe & Underwood (1998), I assessed microhabitat preferences using three treatments. Limpets were either relocated to different microhabitats in the displacement treatment, temporarily lifted and then returned to their initial location for the disturbance treatment, or left entirely undisturbed. Using a coarse scalpel, limpets were carefully removed from their substratum during the displacement and disturbance treatments, taking care to avoid injuring them. Displacement was constrained to within one meter of the original microhabitat to align with the documented limited ranging behaviour of *Siphonaria spp*. (Creese & Underwood 1982). To trace limpet movements between original and subsequent

microhabitats, I implemented a colour-coded marking system using car body paint whose toxicity in such applications has previously been shown to be negligible (Henry & Jarne 2007). Microhabitats were marked to reflect this coding, and the apex of the limpets' shells were marked to correspond with their original microhabitats, ensuring accurate tracking. Importantly, for all three relocation treatments, the location where the limpets were first marked is referred to as the original microhabitat, while the location where the limpets were placed or left immediately after marking is referred to as the new microhabitat. This distinction is crucial because new microhabitats always matched original microhabitats in the disturbance and undisturbed treatments, whereas they generally differed in the displacement treatment. Furthermore, specific symbols were assigned to denote each relocation treatment (Table 3.1).

Table 3.1: Description of the colour coded marking scheme used to help trace movement of the study species, *Siphonaria capensis* and *Siphonaria serrata*, among the microhabitats (HR - Horizontal rock, VR - Vertical rock, CR - Crevice, RP - Rock pool) of interest.

rel_treat	**symbol**	**mh_type**	**colour**
displacement	-	HR	red
		VR	yellow
		CR	green
		RP	blue
disturbance	=	HR	red
		VR	yellow
		CR	green
		RP	blue
undisturbed	+	HR	red
		VR	yellow
		CR	green
		RP	blue

Variables: rel_treat - relocation treatment, mh_type - Microhabitat type

The marking process, referred to throughout as “mark events,” involved tagging 20 individuals of each species per microhabitat (original and new) and relocation treatment at each site in each season (Figure 3.1). Each instance of this process constituted a single mark event. To maintain the integrity of the study, marked individuals were left in their sample areas throughout the study to prevent resampling of the same individuals between trials and seasons. Occasionally, limitations in limpet numbers precluded marking in specific microhabitats, particularly during mark events in summer (November/December). This issue was exacerbated by attempts made to avoid tagging the same individuals more than once. Notably, *Siphonaria capensis* was scarce on vertical rock surfaces at both sites (Chapter 2), leading to the exclusion of this class from the original microhabitat variable in subsequent analyses. Conversely, as long as the limpets could successfully attach or “home” to a rock surface, that rock surface could be sampled as a new microhabitat. Therefore, vertical surfaces remained part of the displacement treatment for *S. capensis*. Furthermore, spatial distribution of mark events was carefully managed within the sample area to prevent overlapping and confusion during later recapture efforts. Post-marking, limpets were left to disperse naturally for two weeks before recapture attempts commenced. The recapture phase involved documenting the combination of the relocation treatment, original and new microhabitat for each limpet, and their recapture microhabitat. Notably, a limpet’s recapture microhabitat could be its original microhabitat, its new microhabitat, or another of the study’s defined microhabitat categories.

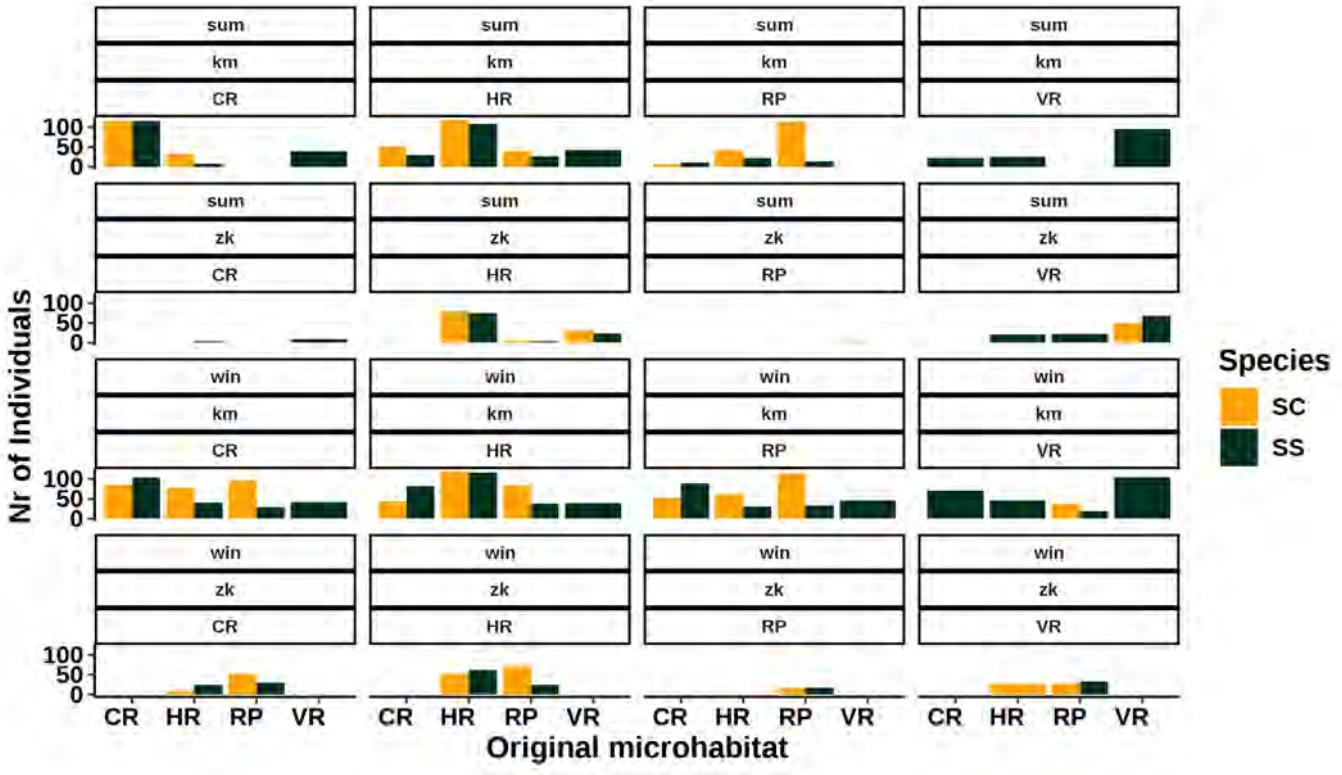

Figure 3.1: Bar graph depicting the number of sampled individuals for each species (SC - *S. capensis*, SS - *S. serrata*) across original microhabitats (HR - Horizontal rock, VR - Vertical rock, CR - Crevice, RP - Rock pool), faceted by new microhabitats at both sites (km - Kommetjie, zk - Zinkwazi) during winter (win) and summer (sum)).

The entire mark/recapture process, which includes marking limpets, allowing them to disperse for two weeks, and then attempting recapture, was replicated three times per season at each site. This approach enriched the data collection, resulting in a comprehensive dataset of fourteen variables and 3633 observations, with *S. serrata* (n = 1909) sampled more than *S. capensis* (n = 1724) throughout. The dataset featured seven categorical variables. This included the species (2 levels), site (2 levels), season (2 levels), trial (3 levels), relocation treatment (3 levels), original microhabitat (3 levels for *S. capensis* and 4 levels for *S. serrata*) and new microhabitat (4 levels for both species) variables. Furthermore, two datetime (mark and recapture dates) and one numerical explanatory variable (mark event) were included as well. The dataset also included three response variables, namely, a binary categorical variable for homing status (yes/no)

defined in the introduction as an organism consistently returning to the same spot, a categorical variable for recapture microhabitat (4 levels for both species), and a continuous zero-inflated variable representing the proportion of individuals recaptured.

3.3.3 Statistical analysis

All statistical analyses and data visualizations were carried out in R version 4.4.0 (R Core Team 2021). Generalized linear models (GLMs) and Generalized linear mixed models (GLMMs) were employed to assess the effects of selected predictors on three target response variables. These models were implemented through the glmmTMB function discussed in (Chapter 2) and multinom_reg from the tidymodels package (Kuhn et al. 2024), as detailed below. GLMs, and their extensions GLMMs, are highly recommended for analyzing relationships involving response variables with non-normal distributions (Zuur et al. 2009, Bolker et al. 2009), which are characteristic of the ecological data examined in this study. These models are advantageous because they extend beyond traditional linear regression, which assumes normally distributed errors, by accommodating a variety of distribution families. For instance, the use of the distribution families detailed below allows for a more accurate representation and analysis of the study data. This approach circumvents the need for *a priori* transformation of outcome variables to meet normality assumptions, a method that is not always viable (Zuur et al. 2009, Dunn & Smyth 2018).

To analyse the variation in the proportion of recaptured individuals in relation to season, and the interaction between original and new microhabitat, the dataset was divided by species before fitting two separate zero-inflation Beta-binomial GLMMs. As described in Chapter 2, separate models were specified to guard against issues associated with overly complex models. Random effects were modelled to account for data dependencies arising from separate mark events in the conditional model component, and a zero-inflation component was included to address the excess zeros in the data (Equation 3.1). Finally, specifying a compound error structure such as the Beta-binomial

provides an effective way to analyse count data with an upper bound and excess variability (Harrison et al. 2018).

$$
\begin{aligned}
\mathrm{Y}_i &\sim \text{BetaBinomial}(\mathrm{n}_i, \mathrm{p}_i, \phi) \\
\text{logit}(\mathrm{p}_i) &= \alpha_0 + \alpha_1 \mathrm{X}_{1j} + \alpha_2 \mathrm{X}_{2j} \mathrm{X}_{3j} + v_j + \varepsilon_{j[i]} \\
\text{logit}(\pi_i) &= \zeta_0 \\
&\text{where} \\
\varepsilon_{j[i]} &\sim \mathcal{N}(0, \sigma^2) \\
v_j &\sim \mathcal{N}(\mu_j, {\sigma_j}^2), \quad \text{for mark instance } j = 1, \ldots, J
\end{aligned}
\tag{3.1}
$$

In Equation 3.1, the response variable Y_i, representing the proportion of individuals recaptured for each observation, is modelled using a Beta-binomial distribution. This distribution is characterized by parameters n_i, p_i, and ϕ, which denote the total number of individuals marked, the probability of recapture, and the overdispersion, respectively. The model's grand intercept, α_0, is influenced by the predictors: season (X_{1i}), and the interaction between new and original microhabitat ($X_{2i}X_{3i}$), each contributing to the linear predictor for p_i through the regression coefficients α_1 and α_2. The probability p_i is transformed using the logit link function as $\text{logit}(p_i) = \alpha_0 + \alpha_1 X_{1i} + \alpha_2 X_{2i} X_{3i} + v_j + \epsilon_{j[i]}$, where v_j denotes the random intercept for each mark event j, adhering to a normal distribution $v_j \sim N(\mu_j, {\sigma_j}^2)$. The probability of zero-inflation, π_j, is modelled with the logit link function $\text{logit}(\pi_i) = \zeta_0$. The residual variance $\epsilon_{j[i]}$ represents the individual-level noise, assumed to be normally distributed with zero mean and a variance of σ^2.

A Bernoulli GLM was used to model the effect of the interaction between species and the relocation treatment on the homing response variable (Equation 3.2), given its proficiency in analysing binary outcomes (Dunn & Smyth 2018). Before running the model, records without recaptured individuals were removed from the primary dataset to ensure the analysis focused exclusively on the intended phenomena rather than on the processes that generate lost individuals.

$$
\begin{aligned}
\mathrm{Y}_i &\sim \text{Bernoulli}(\pi_i) \\
\text{logit}\left(\frac{\pi_i}{1-\pi_i}\right) &= \alpha_0 + \alpha_1 X_{1i} X_{2i} + \epsilon_i \\
&\text{where} \\
\varepsilon_i &\sim \mathcal{N}(0, \sigma^2)
\end{aligned}
\tag{3.2}
$$

In Equation 3.2, Y_i is the binary response variable representing the homing status for the i-th individual, modelled with a Bernoulli distribution with success probability π_i. The logit link function $\text{logit}(\pi_i/(1-\pi_i))$ linearly relates the predictors and the log odds of the outcome. The grand intercept is represented by α_0 and, α_1 is the coefficient for the interaction between species (X_1) and relocation treatment (X_2), respectively. Individual-level variability not accounted for by the model is represented by the residual variance ϵ_i, which is assumed to exhibit a variance of σ^2 and a mean of 0.

Similar to the analysis of recapture rate (Equation 3.1), the dataset was segregated by species before modelling the probability of appearing in a recapture microhabitat, as a function of season, site, and the interaction between original and new microhabitats, by employing a Multinomial logistic regression (Equation 3.3). A Multinomial GLM was used because it extends Binomial GLMs by accommodating categorical outcomes with more than two classes (Urban et al. 1987).

$$
\begin{aligned}
\text{logit}\left(\frac{P(P_i = y)}{P(P_i = \text{ref})}\right) &= \alpha_y + \beta_{1y} X_{1i} + \beta_{2y} X_{2i} + \beta_{3y} X_{3i} X_{4i} + \epsilon_i \\
&\text{where} \\
\varepsilon_i &\sim \mathcal{N}(0, \sigma^2)
\end{aligned}
\tag{3.3}
$$

The log-odds of individual i being in recapture microhabitat y relative to the reference habitat is expressed as
$\text{logit}(P(P_i = y)/P(P_i = ref)) = \alpha_y + \beta_{1y} X_{1i} + \beta_{2y} X_{2i} + \beta_{3y} X_{3i} X_{4i} + \epsilon_i$ in Equation 3.3. Here, P_i is the categorical response for the microhabitats, horizontal rocks, crevices, and rock pools, with vertical rocks acting as the reference level. The intercept α_y represents the baseline log-odds of being in microhabitat y when all predictors are zero. The coefficients β_{1y}, β_{2y}, and β_{3y} quantify the effects of the predictors original

microhabitat (X_{1i}), new microhabitat (X_{2i}) and, the interaction between season (X_{3i}) and site (X_{4i}) on the log-odds of each microhabitat category compared to the reference. The error term ϵ_i accounts for the variability in individual i's microhabitat choice not explained by the model, following a normal distribution with a mean of 0 and a variance of σ^2.

The final model configuration, including the inclusion or exclusion of model terms such as interactions, was determined using forward-step model selection and validated through various model diagnostic checks (Section A2), as described in (Chapter 2). These model validation and selection procedures, including checks for over/under-dispersion, zero-inflation, outliers, and deviations from uniformity within and between groups, were applied to the Beta-binomial GLMM (Figures A17, A19, A18 and A20, and Tables A4 and A5), assessing recapture proportion of the limpets. Because Bernoulli and Multinomial GLMs typically assume two or three (or more) categories, respectively, they can introduce complexities that render certain standard GLM validation techniques inadequate. In the case of Multinomial GLMs, these complexities arise from each outcome category having its own set of regression coefficients, resulting in intricate likelihood surfaces and interdependent probability structures that necessitate specialized validation methods (Wang & Tsodikov 2010, Van Hoorde et al. 2014). For Bernoulli GLMs, the usual concerns about normal errors and homogeneous variances from linear models do not apply, since the response data are binary (Peng et al. 2002). Moreover, each residual is the observed outcome minus its predicted probability, resulting in an unusual residual pattern. Additionally, the variance is directly tied to the predicted probability and is not assumed to be constant.

To assess the performance of the Bernoulli and Multinomial GLM in distinguishing between the binary homing outcomes and categorizing recapture microhabitats of limpets, respectively, several category-specific metrics were used (Section A2). These included the area under the receiver operating characteristic curve and overall model accuracy for both, the Hosmer–Lemeshow test and Brier score for the Bernoulli GLM and a confusion matrix for the Multinomial GLM (Brier 1950, Hosmer 2000, Lloyd &

Frommer 2008, Steyerberg et al. 2010). The area under the receiver operating characteristic curve evaluates the model's ability to discriminate among levels of the outcome by comparing the proportion of true positives correctly identified to the proportion of false positives, across various thresholds. The receiver operating characteristic curve (roc) visually represents the relationship between true and false positive rates, with the area under the roc curve (auc) value quantifying overall model performance. Model accuracy quantifies the proportion of correctly classified observations in the response variable, offering a comprehensive measure of the model's performance. The Hosmer–Lemeshow test is a Pearson statistic that determines how well a model's predicted probabilities match its actual outcomes. For binary data, this is achieved by grouping the data and comparing the proportion of observed versus predicted positive outcomes in each group. The Brier score is a quadratic scoring rule that evaluates the accuracy of probabilistic predictions in binary models. It quantifies this accuracy by calculating the mean squared difference between predicted probabilities and observed outcomes. A confusion matrix helps determine misclassification rates across recapture microhabitat levels, indicating the number of correct predictions made by the model compared to the actual classifications. This matrix provides a straightforward visualization of the model's effectiveness in distinguishing among the response categories. The two datetime variables and the trial factor were excluded from the final analyses. The former was used solely to denote mark and recapture dates, while the latter was not expected to be a significant contributor to variation, nor was it considered a variable of interest.

As described in Section 2.3, the *post hoc* analysis for the Beta-binomial GLMM also entailed calculating contrasts between the estimated marginal means for each level of the categorical predictors. In the case of the Bernoulli and Multinomial GLMs, however, these analyses involved computing contrasts between the estimated marginal proportions for different outcome classes. These *post hoc* tests were performed, and any error inflation was adjusted for, using the same approach described for the Tweedie GLMM (see Equation 2.1).

3.4 Results

3.4.1 Recapture rate

Of the 6822 limpets marked in total across 339 marking events, 52.58% were recaptured. The recapture rate varied among sites, seasons, and species. At Kommetjie, a higher recapture rate of 69.07% was observed compared to 29.81% at Zinkwazi. Seasonally, 56.7% of the limpets marked in winter were recaptured, exceeding the 47.68% recapture rate in summer. *Siphonaria capensis* exhibited a slightly higher recapture rate of 55.26% than *S. serrata* at 50.32%. Variations in recapture rates were also influenced by both the limpets' original microhabitat and the new microhabitat to which they were relocated. In terms of original microhabitats, limpets that were initially found in crevices before being marked, relocated and allowed to disperse naturally had the highest recapture rate of 69.18%. Limpets initially found on horizontal surfaces had the next highest recapture rate (54.48%), followed by those initially found in rock pools (40.9%). For new microhabitats, limpets that were relocated to horizontal surfaces after the initial catch and mark effort had the highest recapture rate (63.29%). The next highest recapture rate of 56.71% was for limpets relocated to vertical rocks, followed by limpets relocated to crevices (50.25%), and finally those that were relocated to rock pools (38.53%). Considering the non-independence of data points within mark events and the zero-inflation in the recapture-rate data, the influence of explanatory variables was weaker than suggested by direct comparisons of the recapture rates across different levels of these variables. This is made evident in the following paragraph.

The Beta-binomial GLMM analysis for *S. capensis*, examining the effects of season and the interaction between original and new microhabitat on the recapture rate, found that these factors did not significantly affect the recapture rate of *S. capensis* (Table 3.2). Furthermore, the extremely low variability associated with mark events (Table A6) suggests that this random effect does not contribute much additional variability to the intercepts of the model.

Table 3.2: Results from a Beta-binomial GLMM analysis of the recapture rate for *S. capensis*, with zero-inflation considered. Original microhabitat (omh), new microhabitat (nmh), their interaction and season (SZN) were analysed as fixed effects, with mark events treated as a random effect.

predictor	Chisq	Df	p.value
(Intercept)	94.3463	1	<0.0001
omh	4.0750	2	0.1304
nmh	4.0111	2	0.1346
SZN	1.4860	1	0.2228
omh:nmh	8.8347	4	0.0654

Predictors: omh - original microhabitat, nmh - new microhabitat, SZN - season.

In contrast to *S. capensis*, the model for *S. serrata* revealed a significant effect of the interaction between original and new microhabitat on its recapture rate (Table 3.3), while sample season did not have a significant effect. Similar to *S. capensis*, the differences in intercepts among mark events for *S. serrata* were negligible (Table A7), indicating that the random effect did not substantially influence the fixed effect estimates.

Table 3.3: Results from a Beta-binomial GLMM analysis of the recapture rate for *S. serrata*, accounting for zero-inflation. Original microhabitat (omh), new microhabitat (nmh), their interaction, and season (SZN) were evaluated as fixed factors, with mark events included as a random factor.

predictor	Chisq	Df	p.value
(Intercept)	107.3387	1	<0.0001
omh	8.5227	3	<0.05
nmh	2.6897	3	0.442
SZN	3.6880	1	0.0548
omh:nmh	18.3992	9	<0.05

Predictors: omh - original microhabitat, nmh - new microhabitat, SZN - season.

The *post hoc* analysis results from the Beta-binomial GLMM of *S. serrata* recapture rates are best read by holding the levels of each original microhabitat constant while

assessing contrasts between levels of the new microhabitats (Figure 3.2). Recapture rates did not differ significantly among new microhabitats for limpets originally found in crevices, on horizontal rock or in rock pools. By contrast, limpets that originated on vertical rocks showed different patterns. Individuals moved to rock pools were recaptured most often, those moved to horizontal rocks and crevices less often, and those left on vertical rocks only rarely. *Post hoc* tests confirmed significant ($p < 0.05$) differences between limpets relocated to rock pools and all other microhabitats, and, among the remaining microhabitats, between horizontal and vertical rocks. Conversely, when the *post hoc* analysis results are read by holding the levels of each new microhabitat constant (not graphically displayed), there were no significant contrasts between any levels of the original microhabitat.

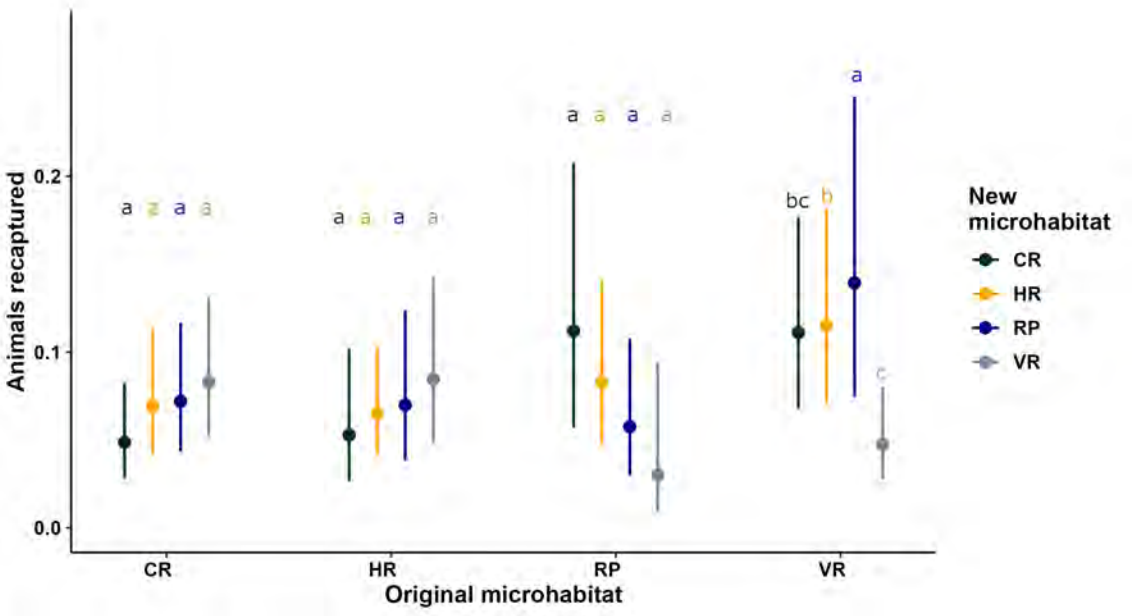

Figure 3.2: Dot and whisker plot illustrating recapture rates as point estimates (± CI) for *S. serrata* relocated from and to different original and new microhabitats, respectively. CR - crevices, HR - horizontal surfaces, RP - rock pools, VR - vertical surfaces. Homogeneous groups, indicated by lowercase letters, are considered within each original microhabitat level only.

3.4.2 Homing

Among the 3633 recaptured limpets examined, 88.93% demonstrated homing behaviour. Specifically, within the *Siphonaria capensis* population, 89.5% exhibited homing, while 88.4% of the *S. serrata* population showed this behaviour. The homing rates also differed by relocation treatment. Undisturbed limpets had the highest homing rate at 98%, followed by those subjected to simple disturbance at 94.7%, and displaced limpets at 81.6%.

Further statistical analysis highlighted significant differences in homing rates across predictors (Table 3.4), with proportions exceeding 50% indicating a tendency toward homing behaviour in the limpets (Figure 3.3). In the Bernoulli GLM analysis, examining the effect of species, relocation treatment, and their interaction on homing rates, a significant influence was found for species interaction with relocation treatment ($p < 0.05$), while species ($p = 0.5068$) showed no significant effects.

Table 3.4: Analysis results from a Bernoulli GLM of the homing rate for both study species. Species (spp), relocation treatment (rel_treat) and their interaction were treated as fixed effects.

predictor	Chisq	Df	p.value
(Intercept)	294.9806	1	<0.0001
spp	0.4407	1	0.5068
rel_treat	76.2047	2	<0.0001
spp:rel_treat	7.5140	2	<0.05

In the analysis of homing rates, the mean rates for displaced *Siphonaria capensis* were significantly lower compared to undisturbed ($p < 0.0001$) and disturbed individuals ($p < 0.0001$). Similarly, the mean homing rates for displaced *S. serrata* were significantly lower in both comparisons ($p < 0.0001$) (see Figure 3.3). Furthermore, undisturbed *S. serrata* individuals exhibited a significantly higher homing rate than their disturbed counterparts ($p < 0.001$). In contrast, there was no significant difference in homing rates between undisturbed and disturbed *S. capensis* (Figure 3.3). Worth noting, however, is

that the homing rate of undisturbed limpets was significantly higher for *S. serrata* than for *S. capensis* ($p < 0.05$).

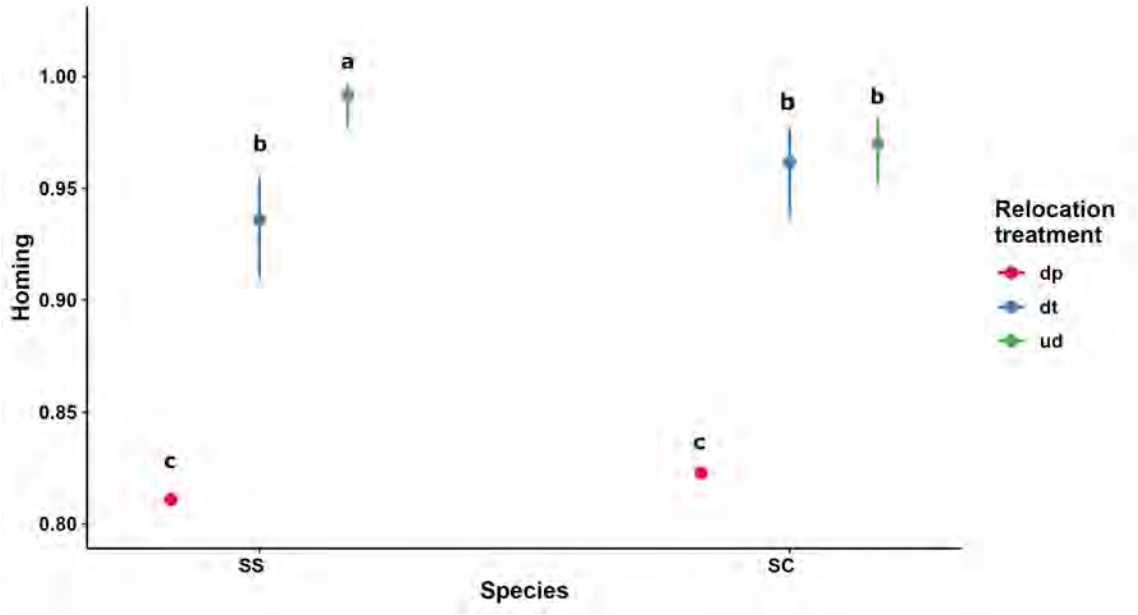

Figure 3.3: Dot and whisker plot illustrating homing rates as point estimates (± CI) of two species (SC - *S. capensis*, SS - *S. serrata*) under different relocation treatments (dp - displacement, dt - disturbance, ud - undisturbed). Homogeneous groups are indicated by lowercase letters.

3.4.3 Recapture microhabitat

In the total recaptured limpet population of 3633 individuals, the microhabitat showing the highest recapture rate was crevices (30.88%), followed by horizontal rock surfaces (30.42%), vertical surfaces (20.07%) and rock pools (18.63%), but the order differed between coasts (Figure 3.4). Kommetjie exhibited this sequence of crevices (36.13%), followed by horizontal surfaces (26.88%), rock pools (19.4%) and vertical surfaces (17.6%). At Zinkwazi, however, limpets were most often recaptured on horizontal surfaces (41.92%), followed by vertical surfaces (28.1%), rock pools (16.16%), and crevices (13.82%).

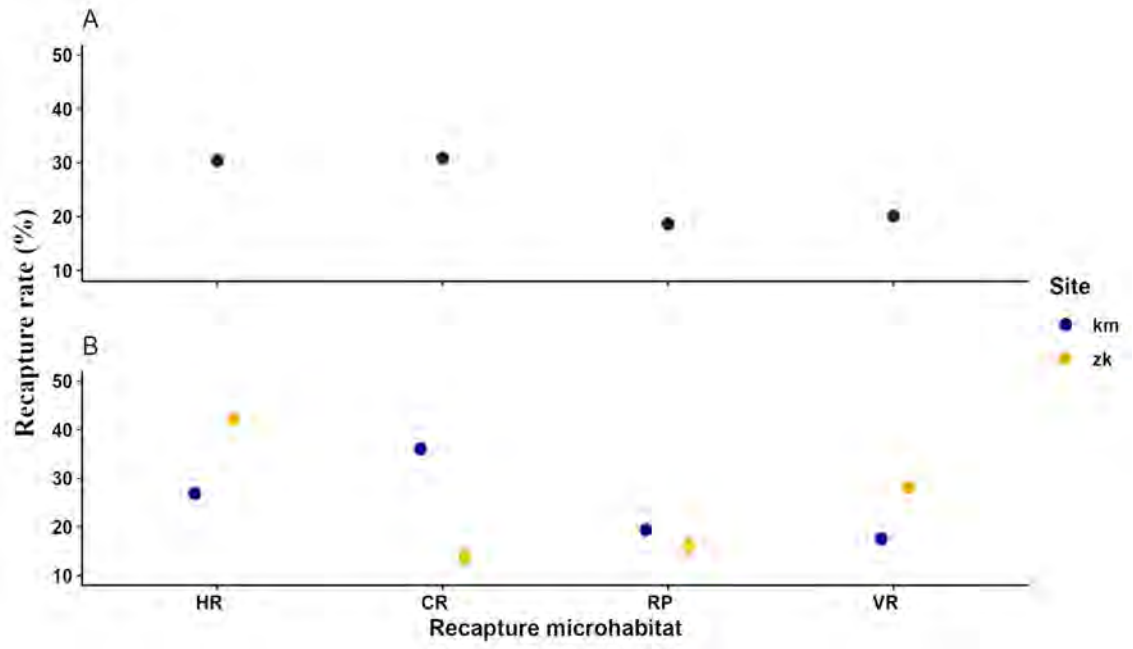

Figure 3.4: Dot plot displaying recapture rates (%) of the two species combined: A) overall, and B) by site (zk - Zinkwazi, km - Kommetjie), across various recapture microhabitats (HR - horizontal rocks, CR - crevices, RP - rock pools, VR - vertical rocks).

3.4.3.1 *Siphonaria capensis*

In the Multinomial GLM analysis evaluating the distribution of *S. capensis* among recapture microhabitats (Table 3.5), significant effects were identified for season ($p < 0.05$) and the interaction between original and new microhabitat ($p < 0.0001$). For instance, *S. capensis* was recaptured at significantly higher rates from crevices ($p < 0.001$) compared to both horizontal surfaces and rock pools during winter (Figure 3.5). During summer, however, there were no significant differences in recapture rates among recapture microhabitats. While the effect of site in the Multinomial GLM was non-significant ($p = 0.1950$; Table 3.5), *post hoc* contrasts revealed significant differences among recapture microhabitats within each site. For instance, *S. capensis* recapture rates from specific microhabitats were significantly, albeit marginally ($p < 0.05$), greater in crevices compared to horizontal surfaces and rock pools at both sites (Figure 3.5). In describing the remaining results for *S. capensis*, emphasis is placed on

the relocation direction. This term, as outlined previously, refers to the experimental placement of the limpets that allows us to trace their movement post-relocation.

Table 3.5: Results from a Multinomial GLM analysis of the distribution of *Siphonaria capensis* among recapture microhabitats throughout the study. Original microhabitat (omh), new microhabitat (nmh), their interaction, site and season (SZN) were set as fixed effects.

predictor	LR Chisq	Df	p.value
omh	79.0293	4	<0.0001
nmh	109.2331	6	<0.0001
SZN	7.6192	2	<0.05
site	3.2691	2	0.195
omh:nmh	52.0985	12	<0.0001

When considering relocations involving crevices, *S. capensis* were recaptured in crevices at significantly higher rates (at least $p < 0.05$) than all other microhabitats, except for relocations from crevices to vertical surfaces. For this final relocation direction, *S. capensis* individuals were not recaptured in crevices at significantly different rates from those on horizontal surfaces, but it was recaptured at significantly higher rates than in rock pools (Figure 3.5).

For the six relocations involving horizontal surfaces, *S. capensis* were recaptured on horizontal surfaces at significantly ($p < 0.0001$) higher rates compared to all other microhabitats for only two of the six relocations (Figure 3.5). Specifically, *S. capensis* was recaptured at significantly greater rates on horizontal surfaces when individuals were relocated from horizontal to horizontal surfaces and from horizontal to vertical surfaces. Finally, when individuals were moved from horizontal surfaces to rock pools, from crevices to horizontal surfaces, and from rock pools to horizontal surfaces, the individuals were recaptured at significantly greater ($p < 0.0001$) probabilities on horizontal surfaces only when compared to crevices, rock pools, and crevices, for those relocations, respectively (Figure 3.5).

As for relocations related to rock pools, the recapture rate within specific microhabitats for *S. capensis* was significantly higher ($p < 0.0001$) in rock pools, than in all other microhabitats, for only two of the six relocations (Figure 3.5). This was observed when individuals were moved from rock pools to rock pools and from rock pools to horizontal surfaces. When individuals were moved from horizontal surfaces to rock pools, from rock pools to crevices, and vice versa, they were recaptured in rock pools at significantly higher rates (at least $p < 0.01$) compared only to crevices and horizontal surfaces, respectively, for both cases.

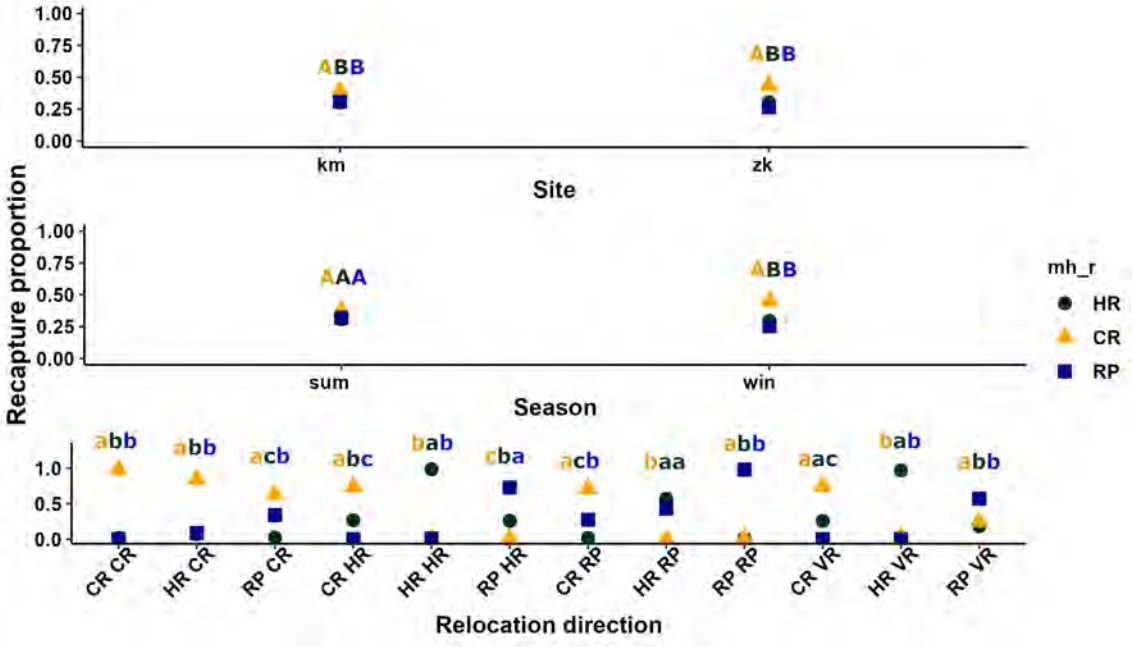

Figure 3.5: Dot plot of recapture proportions by recapture microhabitat (mh_r) of *Siphonaria capensis* as point estimates, spanning seasons (sum - summer, win - winter), sites (zk - Zinkwazi, km - Kommetjie) or each original and new microhabitat combination (relocation direction). HR - horizontal rock, CR – crevices, RP – rock pools, VR – vertical rocks. Homogeneous groups are indicated for site/season combinations (upper case letters) and relocation direction (lower case letters) only.

3.4.3.2 *Siphonaria serrata*

Contrasting slightly with the findings for *S. capensis* (Table 3.5), the Multinomial GLM analysis for *S. serrata* (Table 3.6) indicated significant effects for all predictors on the

recapture distribution, including site ($p < 0.0001$). At Zinkwazi, *S. serrata* recapture rates within specific microhabitats were significantly greater ($p < 0.0001$) for crevices than for all other microhabitats. Here, apart from being recaptured at a greater rate ($p < 0.05$) on horizontal surfaces compared to rock pools, there were no differences in *S. serrata* recapture rates among the remaining microhabitats. Regarding Kommetjie, however, *S. serrata* were recaptured at significantly greater ($p < 0.0001$) rates on both horizontal surfaces and in crevices than on vertical surfaces and rock pools, with no significant differences within either of these two microhabitat pairs (Figure 3.6).

During summer, *S. serrata* recapture rates within specific microhabitats were significantly higher ($p < 0.0001$) for both horizontal rocks and crevices compared to vertical rocks and rock pools. *S. serrata* was not recaptured at significantly different ($p = 0.5465$) rates between horizontal rocks and crevices, but individuals were recaptured at significantly higher rates ($p < 0.01$) on vertical rocks than in rock pools (Figure 3.6). In winter, *S. serrata* recapture rates within specific microhabitats were highest ($p < 0.0001$) for crevices, followed by horizontal surfaces and rock pools, where individuals were recaptured at significantly greater (at least $p < 0.05$) rates in both microhabitats than on vertical surfaces. Individuals of *S. serrata* were not recaptured at significantly different rates between horizontal surfaces and rock pools (Figure 3.6). For the remaining results for *S. serrata*, a similar approach to that used for *S. capensis* was taken, where emphasis was placed on relocations to analyse their distribution post-relocation.

Table 3.6: Outcomes of a Multinomial GLM assessment on the distribution of *Siphonaria serrata* across recapture microhabitats during the study. Fixed effects include original microhabitat (omh), new microhabitat (nmh), their interaction, site, and season (SZN).

predictor	LR Chisq	Df	p.value
omh	132.0539	6	<0.0001
nmh	275.7000	9	<0.0001
SZN	28.2491	3	<0.0001
site	19.7446	3	<0.001
omh:nmh	63.8510	18	<0.0001

For relocations involving crevices, *S. serrata* were recaptured in crevices at significantly higher rates ($p < 0.05$) than for all other microhabitats, except for relocations from crevices to vertical surfaces or from horizontal surfaces to crevices (Figure 3.6). In particular, *S. serrata* were significantly more likely ($p < 0.05$) to be found on vertical rocks when relocated from crevices to vertical surfaces, and there was no significant difference in the likelihood of being found in crevices compared to horizontal rocks following relocation from horizontal rocks to crevices ($p = 0.4414$).

Not too dissimilar to the relocations associated with crevices, the likelihood of recapturing *S. serrata* on vertical surfaces significantly exceeded that in all other microhabitats for all three relocations involving vertical surfaces (Figure 3.6). Moreover, these differences were marked by high levels of significance ($p < 0.001$) for all comparisons across microhabitats, except for relocations from crevices to vertical surfaces, which had a significance level of $p < 0.05$.

Compared to relocations involving crevices and vertical surfaces, fewer relocations involving horizontal rocks or rock pools exhibited significantly ($p < 0.0001$ for both) higher likelihoods of recapture on horizontal surfaces ($n = 2$) or in rock pools ($n = 1$), respectively, compared to all other recapture microhabitats (Figure 3.6). Specifically, when considering relocations for horizontal surfaces, *S. serrata* recapture rates within specific microhabitats were highest for horizontal surfaces when individuals were

relocated between horizontal surfaces, or from horizontal surfaces to rock pools. For relocations concerning rock pools, *S. serrata* was only recaptured at its highest rate in rock pools for relocations between rock pools.

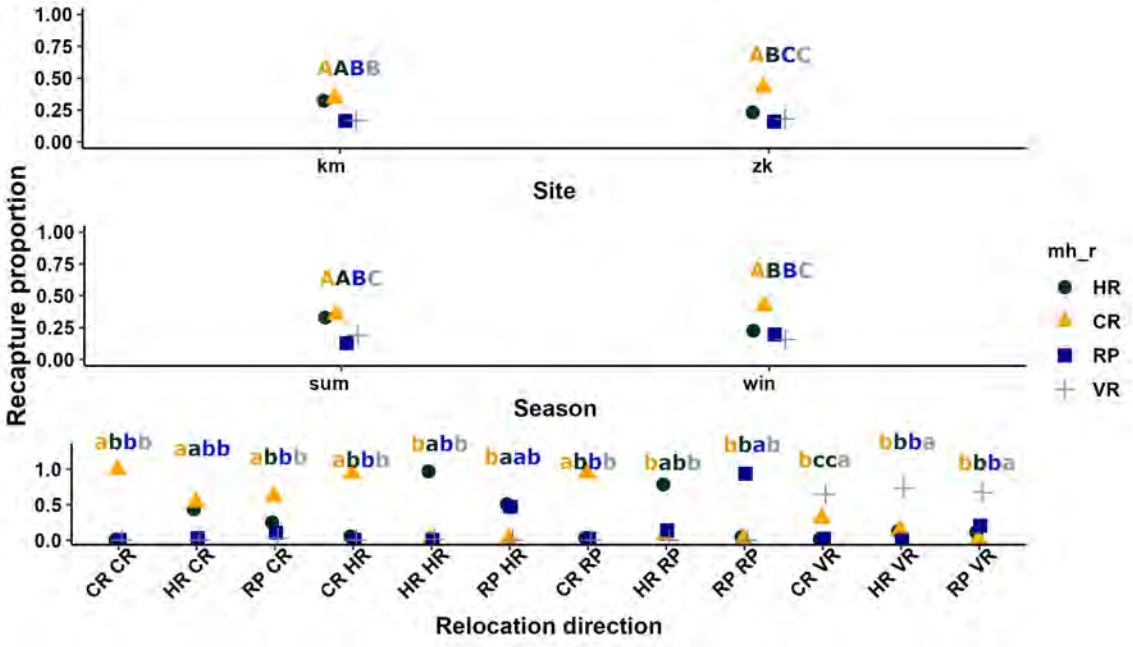

Figure 3.6: Dot plot depicting point estimates of recapture proportion for *Siphonaria serrata* across different recapture microhabitats (mh_r), categorized by season (sum - summer, win - winter), site (zk - Zinkwazi, km - Kommetjie), and every original and new microhabitat combination (relocation direction). HR - horizontal rocks, VR - vertical rocks, RP - rock pools, CR - crevices. Homogenous groups are indicated for site/season combinations (upper case letters) and relocation direction (lower case letters.

3.5 Discussion

3.5.1 Overview and guiding hypotheses

The current chapter examined the microhabitat preferences of two pulmonate limpets, *Siphonaria capensis* and *S. serrata*, at rocky intertidal sites on the East and West coasts of South Africa. The main objectives were to evaluate the limpets' movement patterns primarily in response to variations in micro-scale thermal regimes as an indicator of their risk-avoidance tendencies in thermally challenging intertidal environments. I predicted a

negative relationship between limpet microhabitat preference and exposure to thermally stressful microhabitats, signifying an increased reliance on risk-avoidance strategies and a reduced dependence on physiologically mediated endurance. Any clear evidence of preferential selection for more thermally stressful microhabitats would invalidate this hypothesis.

3.5.2 Summary of key findings

The study revealed significant variations in overall recapture rates only for *S. serrata*. More precisely, *S. serrata* individuals originating from vertical rocks had higher recapture rates when relocated to rock pools and horizontal surfaces, than when relocated to vertical rocks. No significant differences were observed for *S. serrata* originating from or relocated to any other microhabitat. Both limpets demonstrated strong homing tendencies, with the highest and lowest rates of homing by *S. serrata* occurring in undisturbed and displaced individuals, respectively. Homing rates for *S. capensis*, however, showed notable differences only for displaced individuals. Microhabitat preferences for recapture varied by site, season, and relocation direction for both species. *S. capensis* preferred crevices during winter, irrespective of site or relocation direction. *S. serrata* favoured crevices in winter and horizontal surfaces in summer, irrespective of site or relocation direction. When emphasizing relocation direction, both species preferred crevices after relocation, with some instances of preference for horizontal surfaces or rock pools, and several cases where *S. serrata* preferred vertical surfaces depending on relocation origin or release site.

3.5.3 Recapture rate

3.5.3.1 Species specific patterns and environmental influences

Overall recapture rates in the current study, of 55.3% for *Siphonaria capensis* and 50.3% for *S. serrata*, can be considered to fall within a moderate range when compared to

research on other intertidal organisms using similar capture-mark-recapture (CMR) study designs (Gray & Hodgson 1998, Ruiz Sebastián et al. 2002, Nuñez et al. 2014, Montecinos et al. 2020, Compaire et al. 2022). Apart from the exceptional 100% recapture rate reported for the rocky shore limpet *Helcion pectunculus* by Gray & Hodgson (1998), these studies document recapture rates ranging from 25% to 92%. The recapture rates observed for limpets in the current study, however, are relatively low compared to rates of 80% or higher recorded for other limpets (Gray & Hodgson 1998, Ruiz Sebastián et al. 2002, Nuñez et al. 2014). Variations in recapture rates across studies could potentially be ascribed to several factors, including geographically influenced differences in average environmental conditions during sampling (Nuñez et al. 2014, Nuñez et al. 2018, Moura et al. 2022), various species-specific traits (Compaire et al. 2022) and differences in key methodological parameters used across the studies (Nuñez et al. 2014, Nuñez et al. 2018), all of which function by disproportionately affecting organism mortality rates or the probability of them leaving the sample site. When examining the relationship between recapture rates and spatiotemporally influenced variations in environmental conditions, Nuñez et al. (2014) reported significantly higher recapture rates for *Siphonaria lessoni* individuals when climatic conditions at a site were more stressful. Despite summer often being more stressful, Nuñez et al. (2014) still found similar recapture rates. Although this may appear contradictory, their findings suggest that the seasonal differences in environmental stress during the study were not substantial enough to significantly affect recapture rates. In the present study, differences in recapture rates between sites were ultimately not incorporated into the relevant statistical model (Equation 3.1). Surprisingly, however, temporally driven variations in recapture rates for both species remained nonsignificant, even though the shift from winter to summer (Kwiecien et al. 2022) is typically more pronounced than the moderate spring-to-autumn transition reported by Nuñez et al. (2014).

3.5.3.2 Methodological considerations

A likely explanation for the variations in recapture rates among studies lies in the differences in key methodological parameters used across the studies. To illustrate, in their study on burrow fidelity behaviour of the intertidal crab *Neohelice granulata*, Nuñez et al. (2018) observed substantial disparities in recapture rates for different mark-recapture intervals, reflecting a response to the time elapsed between marking and recapture efforts. Notably, they found a negative correlation between crab recapture rates and the duration of these intervals, where even a modest increase of 48 hours, from 24 to 72 hours, substantially lowered recapture rates. The difference in overall recapture rates between the current study and that of Gray & Hodgson (1998) serves as a broader example of how variations in methodological factors can affect results. In addition to species-specific traits, such as differences in attachment strength or microhabitat utilization, a seven-day difference in the mark-recapture interval between the current study and Gray & Hodgson (1998) likely accounts for the approximately 46% lower recapture rates observed in the current study.

Further methodological considerations that could account for differences in recapture rates among studies include the study design in the current research, which involved the deliberate disturbance of the sample animals, as opposed to other studies (Gray & Hodgson 1998, Ruiz Sebastián et al. 2002, Nuñez et al. 2014), where efforts were made to avoid disturbing the limpets during sampling. Dislodging and displacing limpets increases the likelihood of injury to their large muscular foot, particularly when improper techniques are used (Ellem et al. 2002). Limpets injured in experiments where they have been displaced or disturbed are more susceptible to predation, heat stress and desiccation, and are at greater risk of being dislodged by wave activity due to an impaired ability to clamp adequately to the substratum (McAlister & Fisher 1968, Branch & Cherry 1985). As a result, they are subject to higher rates of mortality and are less likely to be recaptured compared to limpets in studies where disturbance is minimized (Castejón et al. 2022).

3.5.3.3 Relocation direction and life history effects

Other researchers have also shown that relocation origin and release site influence animal recapture rates in CMR experiments (Crowe & Underwood 1998, Rochette & Dill 2000, Rochette et al. 2003, Seuront et al. 2018, Compaire et al. 2022). For most of these studies, however, variation in recapture rates is closely linked to changes in biotic and abiotic factors, such as predation risk, desiccation stress, wave exposure, food availability, competition for space and heat stress, associated with shifts in shore height, rather than the transplantation of study animals between different microhabitats within the same shore-zone (Rochette & Dill 2000, Rochette et al. 2003, Seuront et al. 2018, Compaire et al. 2022). Notably, Rochette & Dill (2000) reported reduced recapture rates for high-shore *Littorina sitkana* and *L. scutulata* transplanted to low-shore environments, due to the increased predation in low-shore areas, compared to the reverse relocation direction. In contrast, similar to the current study, Crowe & Underwood (1998) found that the recapture rates of the intertidal gastropod *Bembicium auratum* were influenced by its relocation origin and release site, without considering shore height. In their study, however, the potential mechanisms driving the differential effect of relocation direction on recapture rates were not elucidated but are likely related to variations in some of the same factors listed as influencing the relationship between recapture rate and shore height above.

Differences in the influence of relocation direction on the recapture rates of two intertidal congeners were previously demonstrated in the study by Rochette & Dill (2000). In their research, Rochette & Dill (2000) highlighted variations in life history traits and behavioural responses to predation risk between the two sample species as plausible factors for the distinct responses of *L. sitkana* and *L. scutulata* to relocation direction. They explained that the greater dispersal of *L. sitkana* away from its low-shore release site, compared to *L. scutulata*, was driven by stronger local adaptations linked to its benthic development, in contrast to the pelagic development of *L. scutulata*. This, combined with a heightened reaction to chemical cues signalling the presence of predators, reduced the mortality risk and ultimately increased the recapture rate of *L.*

sitkana for that relocation direction. The interplay of the aforementioned factors may explain the varying effects of relocation direction on recapture rates between *Siphonaria capensis* and *S. serrata*. It is important to note, though, that neither species is known to actively disperse in response to predators. Instead, they excrete a noxious mucus containing polypropionate metabolites as their primary defence against predation (Hodgson 1999, McQuaid et al. 1999, Davies-Coleman 2006, Darias et al. 2006, Pinchuck & Hodgson 2009). Therefore, the influence of mortality due to predation is unlikely to explain a distinctive effect of relocation direction on the recapture rates of these species. Nonetheless, following the logic of Rochette & Dill (2000) the differences in developmental strategies between the species, with *S. serrata* being a direct developer and *S. capensis* a pelagic developer (Chambers & McQuaid 1994), suggest that relocation direction would have a more pronounced impact on *S. serrata*. This is due to its more limited dispersal and stronger attachment to local environmental conditions (Chambers & McQuaid 1994), particularly to fluctuating heat stress, leading to greater variation in its recapture rates compared to *S. capensis*.

3.5.4 Homing

3.5.4.1 Species specific and methodological effects

Like many other intertidal organisms (Chapman 1986, Gray & Hodgson 1998, Ruiz Sebastián et al. 2002, Nuñez et al. 2014, Nuñez et al. 2018, Montecinos et al. 2020, Compaire et al. 2022), both sample species in this study display homing behaviour. Site fidelity, characterized by returning to specific home scars or sites, has previously been described for *S. capensis* and *S. serrata* (Branch & Cherry 1985, Hodgson 1999). In contrast to the current study, numerical values for the homing rates of these siphonariids were not provided by these researchers. The high homing rates determined for the limpets in this analysis are comparable to the average rates of 100% and 91% observed for *Helcion pectunculus* (Gray & Hodgson 1998) and *S. lessoni* (Nuñez et al. 2014), respectively, but exceed the average rates of 30.4% for *Scutellastra argenvillei* (Ruiz

Sebastián et al. 2002). Beyond inherent species-specific differences mentioned previously, the difference in homing rates between this study and that of Ruiz Sebastián et al. (2002) likely arises due to differences in the mark-recapture intervals and environmental variations related to shore height at which sampling occurred. As previously noted, mark-recapture intervals are negatively correlated with recapture rates, making it reasonable to assume a similar reduction in homing rates with increased mark-recapture intervals. In Ruiz Sebastián et al. (2002), the homing rate of 30.4% was determined after four weeks, while the homing rates in this study, as well as those in Nuñez et al. (2014) and Gray & Hodgson (1998), were determined after 14, 10, and 7 days, respectively. Moreover, Ruiz Sebastián et al. (2002) reported a sharp decline in homing rates between mark-recapture intervals of 12hours and four weeks.

3.5.4.2 Environmental effects

More relevant to the specific aims of this analysis is the evaluation of potential temperature-driven variations in homing rates across studies. The harsher microclimates experienced by limpets in high-shore areas in this study, as well as the studies by Nuñez et al. (2014) and Gray & Hodgson (1998), may contribute to the higher homing rates observed compared to the findings of Ruiz Sebastián et al. (2002), that sampled *Scutellastra argenvillei* from the more benign low shore. Although they did not make a comparison across different shore heights, Nuñez et al. (2014) observed notably higher homing rates for *Siphonaria lessoni* individuals at the warmer Las Grutas than at the cooler Mar del Plata, Argentina. This aligns with several other studies that attribute homing behaviour to challenging environmental conditions such as desiccation and heat stress (Branch & Cherry 1985, Iwasaki 1992, Aguilera & Navarrete 2012, Nuñez et al. 2018).

Homing helps intertidal organisms reduce the adverse effects of desiccation and heat stress in their immediate environment. Using chemical cues, these organisms consistently return to home scars or specific resting sites (Branch 1981, Aguilera & Navarrete 2012, Montecinos et al. 2020). These resting sites, often located in

microhabitats like crevices, offer more favourable conditions compared to surrounding areas (see Chapter 2), although home scars can also be found in less favourable microhabitats (Branch & Cherry 1985). Through isolating the limpet's soft tissue from the external environment, home scars provide several benefits to limpets that utilize them (Garrity 1984, Branch & Cherry 1985). These benefits include a reduced risk of being dislodged by waves, protection from predators, and most importantly, protection from overheating. Isolating the soft tissue from external conditions allows limpets to retain moisture and slow heat absorption from the environment, promoting the effective regulation of their body temperature, even in challenging microhabitats such as horizontal surfaces (see Chapter 2). Other factors influencing homing behaviour include wave activity (Branch & Branch 1988, Gray & Hodgson 1998), predation pressure (Branch 1978, Iwasaki 1992, Iwasaki 1993), food availability (Jenkins & Hartnoll 2001), intraspecific competition (Mackay & Underwood 1977, Iwasaki 1995) and size variation (Jenkins & Hartnoll 2001). As mentioned earlier in the discussion on recapture rates, the application of different methods in assessing organism site fidelity must also be considered. For example, in this analysis, undisturbed limpets exhibited higher homing rates compared to disturbed limpets. This is likely due to the increased likelihood of injury during disturbance, which impairs a limpet's ability to attach firmly to the substratum and successfully home.

3.5.5 Microhabitat preference

3.5.5.1 Ecological benefits

Overall, recapture rates within specific microhabitats, at both sites and during both seasons for both siphonariids suggest clear preferences at the micro-scale for favourable environmental conditions, particularly for the cooler-temperature habitats provided by crevices (see Chapter 2). This corresponds to findings from similar studies on the microhabitat preferences of the common periwinkle *Littorina littorea* by Seuront et al. (2018), the land snails *Placostylus ambagiosus* and *P. hongii* by Stringer et al. (2018),

the gold-mouthed conniwink *Bembicium auratum* by Crowe & Underwood (1998), and the littorinid gastropods *Littorina sitkana* and *L. scutulata* by Rochette & Dill (2000). In all four studies, the sample animals demonstrated "true habitat preferences" by actively selecting certain sections of their environment while avoiding others, following deliberate displacement by the respective researchers. These preferred habitats generally provide benefits compared to the areas they avoid, such as increased food availability (Seuront et al. 2018) and protection from environmental stressors like desiccation (Crowe & Underwood 1998) and predation pressure (Rochette et al. 2003). For example, Seuront et al. (2018) found that *Littorina littorea* favoured a high-shore vertical seawall, where food was more abundant, instead of a lower-shore horizontal platform. Similarly, Rochette et al. (2003) demonstrated that *L. sitkana* exhibited a strong preference for the high-intertidal zone along the rocky shore at Bamfield Inlet in Barkley Sound, Canada, driven by predation pressure from the red rock crab *Cancer productus* in the low-intertidal zone. In both cases, the consistent, directional return of these intertidal animals to their preferred habitats is probably mediated by info-chemicals related to the presence of conspecifics, food sources, and predators (Finke et al. 2007, Chapperon & Seuront 2009, Seuront & Spilmont 2015), but may also involve sensory cues underlying geotaxis (Petraitis 1982, Thain et al. 1985), phototaxis (Seyer et al. 1998, Nilsson 2009), and rheotaxis (Gendron 1977, Murray et al. 1992).

3.5.5.2 Temperature effects

In this investigation, it is reasonable to suggest that temperature shapes the broader habitat preference patterns of both siphonariid species, specifically driving their preference for crevices, where average low-tide temperatures are generally lower than in most other microhabitats examined in this study (see Chapter 2). Previous research (Williams & Morritt 1995, Crowe & Underwood 1998, Chapman 2000, Harper & Williams 2001, Cartwright & Williams 2012, Silva et al. 2014, O'Dwyer et al. 2014) provides compelling evidence for the preference of intertidal organisms for cooler microhabitats compared to their immediate surroundings. More specifically, some of

these studies imply that various rocky shore limpets, including *S. serrata* (Chambers & McQuaid 1994), prefer crevices (Garrity 1984, Williams & Morritt 1995, Gray & Hodgson 1998). In contrast, the studies by Branch & Cherry (1985) and Chambers & McQuaid (1994) reported that *S. capensis* shows a preference for rock pools rather than crevices. Interestingly, however, these findings are consistent with the observations in Chapter 2, where *S. capensis* was most frequently found in rock pools. Unlike the current investigation, which explicitly addresses true microhabitat preferences characterized by the deliberate selection of optimal environments, these earlier findings likely reflect a different interpretation, where high species abundance was mistakenly considered indicative of habitat preference. In fact, many of these researchers (Garrity 1984, Branch & Cherry 1985, Chambers & McQuaid 1994, Williams & Morritt 1995, Harper & Williams 2001), when attempting to determine habitat preferences in intertidal species, often incorrectly equate abundance with preference. As highlighted previously (Levins 1968, Russo 1987, Olabarria et al. 2002, Moura et al. 2022), abundance patterns typically represent incidental site occupancy, driven by differential mortality between more and less suitable habitats and unequal dispersal influenced by microscale physical barriers.

3.5.5.3 Explaining the reduced preference for rock pools

Since rock pools generally provide the lowest surface temperatures (Chapter 2) and offer the greatest buffer against desiccation among rocky shore microhabitats (Newell 1979, Femino & Mathieson 1980, Jackson et al. 2013), both study animals were expected to show a stronger preference for rock pools over any other microhabitat. As mentioned above, this would have aligned with findings from Chapter 2 that indicate greater overall limpet densities in rock pools compared to any other microhabitat. Based on the reasoning outlined earlier, the reduced or similar recapture rates of both siphonariids in rock pools compared to crevices, and particularly to horizontal surfaces, was therefore largely unexpected. Factors such as highly variable salinity levels (Firth & Williams 2009, Buasakaew et al. 2021), however, may either discourage the animals from

favouring mid- to high-shore rock pools or, through increased mortality, negatively affect their recapture rates in these areas, in comparison to microhabitats that are less favourable in terms of temperature and desiccation. Without specific evidence of the harmful effects from hyposaline rock pool conditions on siphonariid limpets, an alternative explanation for the lower recapture rates of both siphonariids in rock pools must be considered.

As previously discussed, disturbances during experimental procedures can lead to increased mortality and consequently lower recapture rates. In their study on the behaviour and adaptive strategies of *Siphonaria capensis*, Branch & Cherry (1985) observed that the predatory whelk *Burnupena catarrhacta* circumvents the chemical defences of, and effectively preys on, *S. capensis* individuals whose muscular foot has been damaged in rock pools. The increased predation of *S. capensis* by *B. catarrhacta* in rock pools occurs because the initial defensive release of mucus in response to disturbance can be depleted by repeated stimulation (McQuaid et al. 1999) and washed away by the water. This could lead to high mortality of limpets after translocation to rock pools, resulting in lower recapture rates in this microhabitat. It is important to note, however, that the distribution of *B. catarrhacta* does not extend to the East coast of South Africa (Dempster & Branch 1999), making it unlikely that predation by this species accounts for the lower-than-expected recapture rates of *S. capensis* in rock pools at Zinkwazi on that coast. Nevertheless, empty shells of marked *S. capensis* individuals have been found trapped in rock pools at both study sites (pers. obs.), suggesting that similar opportunistic predation by another limpet predator, possibly the *B. catarrhacta* congener, *B. lagenaria*, which is found on both coasts (Dempster & Branch 1999), could explain the comparatively lower preference of *S. capensis* for rock pools at Zinkwazi. Although there are no records of *S. serrata* being preyed upon in this manner, it lacks the same capacity for producing predator-repelling mucus as *S. capensis* (Pinchuck & Hodgson 2009). Therefore, it is plausible that disturbed *S. serrata* individuals are similarly preyed upon at both sites, which may account for their similarly reduced preference for rock pools compared to other microhabitats, particularly at Zinkwazi. Furthermore, the observation that surface temperatures in rock pools at Zinkwazi are

higher than those in crevices (see Chapter 2) may also explain the diminished or comparable preference for rock pools shown by both siphonariids at Zinkwazi.

3.5.5.4 Importance of rock pool edges

Since horizontal surfaces were generally the most unfavourable microhabitat sampled in terms of temperature stress, and densities of both study animals were among the lowest in this microhabitat (see Chapter 2), where preferences for it surpass those for rock pools and vertical surfaces, it is possible that the study animals actually prefer "rock pool edges." Rock pool edges are described as a distinct, transitional microhabitat between rock pools and horizontal surfaces, where organisms may benefit from a combination of moisture retention from the pool and access to the air, reducing the risk of desiccation and exposure to temperature extremes (Noël et al. 2009, Seabra et al. 2023). There are previous records of *Siphonaria serrata* utilizing rock pool edges (Chambers 1995) and both sample animals have been observed near rock pools (pers. obs.). In the present study, however, rock pool edges were not explicitly treated as a distinct microhabitat but rather included as part of the horizontal surface category. Consequently, current findings suggesting a preference for horizontal surfaces rather than rock pools or vertical surfaces may, in fact, reflect a preference for this more favourable transitional microhabitat. This indicates that future studies on organism dispersal patterns among microhabitats in the rocky intertidal should consider more granular representations of these microhabitats, while simultaneously assessing the conditions within them.

3.5.6 Methodological constraints and potential solutions

3.5.6.1 Relocation direction effects

As evidenced throughout this discussion, careful consideration of specific methods used to elucidate limpet dispersal patterns and, ultimately, to generate robust inferences regarding variations in their microhabitat preference is essential. Variations in

microhabitat preferences across or between studies can arise from suboptimal translocation techniques (Ellem et al. 2002) and/or variations in mark-recapture intervals (Nuñez et al. 2018). Moreover, this study shows that relocation direction during animal displacement can also be considered alongside the two aforementioned methodological aspects that influence microhabitat preference. There appears to be a relationship between relocation direction and species' microhabitat preferences, such that the limpets' preferred microhabitats often correspond with either their relocation origin or release site. For example, in cases where *Siphonaria capensis* or *S. serrata* exhibited a preference for crevices or horizontal surfaces, their relocation direction often involved crevices or horizontal surfaces, respectively. This outcome was expected, as both the current study and previous research (Branch & Cherry 1985, Hodgson 1999) report homing behaviour in these limpets. Although not explicitly examined in prior studies, stronger homing tendencies likely correspond to higher recapture rates in the associated microhabitats. The limpets' stronger preferences for crevices post-relocation to or from crevices compared to other microhabitats (Figure 3.5 and 3.6) aligns with the broader findings of this study, which indicate an overall preference for crevices regardless of site or season. These results are further substantiated with horizontal surfaces following crevices in this trend.

3.5.6.2 Advanced tagging to reduce sample loss and bias

In intertidal environments, other challenges not previously discussed that could affect the outcomes of CMR studies involve improper or inadequate tagging, typically associated with more traditional methods such as the use of plastic tags or paint (Hayford et al. 2015, Hayford et al. 2018, Mace et al. 2018), as in the current study. This often results in inflated tag-loss rates because intertidal organisms tagged using conventional methods are usually harder to detect (Judge et al. 2018). These detection difficulties occur because tags exposed to the harsh conditions of the intertidal zone are often washed away or obscured by biological growth. Additionally, studies using conventional approaches may experience higher rates of marked-animal loss or mortality (Judge et al.

2018). This can happen due to increased visibility of the tags, making tagged animals more susceptible to predation, or due to behavioural changes induced by the chemicals used to apply these tags that may cause them to move out of the study area. High tag and animal loss, in turn, reduces the pool of tagged individuals available for data analysis, which consequently biases the results of CMR studies. Several researchers recommend using modern computer-readable tags, such as Passive Integrated Transponder (PIT) or passive Radio Frequency Identification (RFID) tags, to mitigate the limitations of conventional tagging methods used in small invertebrate dispersal studies (Lahoz-Monfort & Magrath 2021, Schtickzelle 2024, Folk & Mennerat 2024). These tags, which can be as small as 10µg and 5mm in length, are robust, submersible electronic devices that can transmit real-time location data via electromagnetic induction to transceivers through air or water at distances below 1m (Gibbons & Andrews 2004, Robinson et al. 2009, Bonter & Bridge 2011, Lahoz-Monfort & Magrath 2021). Their small size, mode of data transmission, and multiple deployment options facilitate efficient tracking, reduce detection errors and animal stress, and enable continuous monitoring of small intertidal invertebrates in CMR study designs (Hayford et al. 2018, Mace et al. 2018, Judge et al. 2018).

3.5.7 Temperature-linked temporal shifts in preference

Seasonal variations in the microhabitat preference patterns of *Siphonaria capensis* and *S. serrata* may be influenced by changes in the interaction between temperature and other environmental factors discussed previously. These factors include temperature-driven changes in competition for resources and food availability between seasons. As temperatures rise from winter to summer, the overall abundance of common food sources for both animals, including several crustose algae found in the intertidal zone (Iwasaki 1993, McQuaid et al. 1999, Jenkins & Hartnoll 2001), generally decreases. This decline is attributed to the co-occurring effects of increased desiccation and heightened UV exposure, which can inhibit algal growth and reduce photosynthetic efficiency (Tâmega & Figueiredo 2019). Higher summer temperatures also typically

lead to a greater preference for benign rocky shore microhabitats (Williams & Morritt 1995, Harper & Williams 2001, Cartwright & Williams 2012, Virgin & Schiel 2023), such as crevices, where already limited macroalgal food resources are further strained by grazing from sedentary organisms (Mackay & Underwood 1977, Jones & Boulding 1999, Davies et al. 2007, Nuñez et al. 2014). Consequently, increased population densities and competition for space in these preferred microhabitats reduce their benefits, particularly due to the lower availability of food resources compared to winter. This may compel parts of the limpet population to inhabit less favourable nearby microhabitats, such as horizontal surfaces, during summer, which eventually manifests behaviourally as equal dispersal among microhabitats by *S. capensis* (Section 3.4.3.1).

3.5.8 Trade-offs between heat management strategies

This occasional selection of thermally unfavourable microhabitats occurs nearly as often as the selection of more favourable ones by the sample animals. Such a pattern suggests a compromise between minimizing thermal stress and meeting nutritional demands (Santini et al. 2014, Monaco et al. 2015, Crickenberger et al. 2020). Thus, a slightly larger proportion of individuals favour risk avoidance over endurance, though endurance strategies remain part of both limpets' thermoregulatory approach. Due to the proposed influence of hypometabolism on their capacity to withstand thermal stress (Chapter 1), the variable adoption of heat management strategies in the thermally heterogeneous rocky intertidal suggests the variable expression of hypometabolism in both limpet populations. This observation is supported in the study by Liao et al. (2021) on the role of hypometabolism in heat tolerance among 26 intertidal mollusc species, where the researchers established a significant link between environmental thermal variability and hypometabolic variation. Specifically, Liao et al. (2021) found that individuals or species in thermally stressful zones exhibited greater capacities for heat tolerance through hypometabolism compared to those in more benign zones. The findings from the current study reflect the effective pursuit of the research objective to explore limpets' movement patterns in response to microscale thermal variations and their implications

for their heat management strategies and ultimately, hypometabolism, as stipulated by MRS theory (see Chapter 1). By fulfilling these objectives, I build upon various ideas and findings from studies that have explored microhabitat utilization (Helmuth & Hofmann 2001, Lord et al. 2011), examined temperature-mediated microscale distribution patterns (Pound et al. 2020, Janetzki et al. 2021), linked these patterns to species thermal tolerance (Chapperon et al. 2017, Han et al. 2020), and determined how adverse abiotic conditions induce hypometabolism in marine organisms (Guppy & Withers 2007, Verberk et al. 2016, Marshall & McQuaid 2020).

3.5.9 Conclusion

Based on these findings, I reject the hypothesis that the sampled species prioritize endurance-based approaches over risk-avoidance strategies. Both species preferred thermally favourable microhabitats such as crevices, although this did not prevent them from using less favourable ones. In conclusion, these results show that centimetre-scale thermal mosaics dictate the movement and settlement of *S. capensis* and *S. serrata* across the intertidal. How these behavioural choices intersect with their capacities for metabolic rate depression and thermal resilience will be examined in upcoming chapters.

Chapter 4

Thermal preference analysis

4.1 Abstract

Rocky shore ectotherms are exposed to micro-scale thermal mosaics that dictate their survival, nevertheless, the extent to which thermal history shapes their temperature-driven dispersal remains unclear. This study hypothesised that limpets acclimatized to warmer habitats would either prefer higher temperatures on an experimental gradient or show a muted tendency to leave warm areas. To test this, the thermotactic behaviour of the pulmonate limpet *Siphonaria capensis* was compared between animals from chronically warm horizontal rock and conspecifics from cooler rock pools at Kommetjie, South Africa. Two hundred adults, 100 from each microhabitat, were placed on an aluminium tank spanning 25–35 °C, and their movement and final position were logged after one hour. A Bernoulli GLM analysis demonstrated that pool-origin individuals were significantly more likely to move, while a Chi-square test on temperature-shift direction showed they settled disproportionately in cooler sections, whereas limpets originating from horizontal rocks mostly remained stationary within the warmer half of the gradient. A separate Chi-square analysis confirmed that starting temperature did not influence these patterns. These results show that *S. capensis* exhibits low but non-random thermotactic activity governed by prior microhabitat thermal history, implying acclimatory modulation of behavioural risk-avoidance. The findings supply a behavioural link between the microhabitat distribution patterns

reported in Chapter 2 and 3, and the physiological performance explored later in the thesis.

4.2 Introduction

Marine animals exhibit a diverse range of responses to external stimuli that are extensively documented in the scientific literature (Crickenberger et al. 2020, Brumley et al. 2020, Bandara et al. 2021, Teske et al. 2021, Raina et al. 2022, Letendre et al. 2024). This includes responses at the population level, such as mass spawning events triggered by changing lunar light in reef-building corals, specifically *Acropora millepora* (Kaniewska et al. 2015, Zoccola & Tambutté 2015), mass migrations in response to thermal cues in the sardine *Sardinops sagax* (Lo et al. 2011, Teske et al. 2021), diel vertical migrations in herbivorous zooplankton driven by light availability (Bandara et al. 2021, Hobbs et al. 2021), and coordinated bioluminescence displays in dinoflagellates such as *Noctiluca scintillans* due to mechanical disturbance (Letendre et al. 2024). Such responses affect species distributions, population densities, and predator–prey interactions, among others.

At a more granular level, researchers have focused their efforts on understanding how environmental cues influence marine animal behaviour, aiming to elucidate broader species behavioural patterns from individual responses (Hamilton 1978, Davies & Beckwith 1999, Diaz et al. 2011, Raw et al. 2013, Ng et al. 2013, Lewis & Ayers 2014, Morley et al. 2022). For example, the marsh periwinkle *Littorina irrorata* exhibits visually mediated anti-predator behaviour by moving toward on-shore or nearby vegetation when released onto bare sand (Hamilton 1978). Similarly, the common periwinkle *Littorina littorea* responds to chemical cues when following the mucus trails left by other snails during foraging (Davies & Beckwith 1999). Both response behaviours, broadly referred to as phototaxis and chemotaxis, respectively, contribute to the clumped natural distributions of these species that provide ecological advantages, such as reduced exposure to thermal stress and increased foraging success.

Body temperature plays a crucial role in determining the performance of ectotherms, influencing their behaviour, physiology, and overall fitness (Somero 2002, Angilletta 2009). Many ectotherms, including marine organisms, exhibit behavioural thermoregulation to maintain their body temperatures within an optimal range, thereby enhancing their survival and performance in varying thermal environments (Kearney et al. 2009, Clusella-Trullas et al. 2011, Hui et al. 2022, Morley et al. 2022). A key component of behavioural thermoregulation is the capacity for thermal preference displayed by several marine ectotherms, such as the sea cucumber *Cucumaria georgiana* (Morley et al. 2022), the purple sea urchin *Strongylocentrotus purpuratus* (Salas et al. 2012), and the Atlantic cod *Gadus morhua* (Behrens et al. 2012, Schakmann et al. 2023). Thermal preference, also known as thermal *preferenda*, refers to the behaviour of animals actively seeking specific temperature ranges that maximize their physiological performance when presented with a choice (Fry 1947, Reynolds & Casterlin 1979, Hertz et al. 1993, Angilletta et al. 2002). Studies on thermotaxis have been key in enhancing our collective understanding of the interplay between the physiological and ecological adaptations of marine ectotherms, particularly those that inhabit the thermally heterogeneous intertidal zone, where they are subjected to significant thermal fluctuations due to tidal cycles and, especially, microhabitat variability (Crickenberger et al. 2020).

The focus here is on determining the thermal preference of the intertidal pulmonate gastropod *Siphonaria capensis* collected from horizontal surfaces and rock pools at Kommetjie (see Chapter 2). To achieve this, I use the Eulerian approach (Tepler et al. 2011, Lewis & Ayers 2014, Padilla-Ramírez et al. 2015), as discussed by Crickenberger et al. (2020). This analysis entails studying species distributions along an artificially constructed temperature gradient, in contrast to a control without the gradient (Crickenberger et al. 2020). Consequently, this allows one to relate species body temperatures directly to distribution patterns in the context of climate change, which is expected to exacerbate temperature extremes and variability in coastal environments (Easterling et al. 2000, Helmuth et al. 2014, Seabra et al. 2015). *S. capensis* is the ideal model species for this study due to its broad geographic distribution along the South

African coastline, where it experiences significant temperature differences between the warm Indian and cool Atlantic Oceans (Lutjeharms 2006, Lutjeharms 2007). Additionally, its distribution from mid- to high-shore and among various microhabitats exposes it to a complex array of temperatures (see Chapter 2). In Chapter 3, it was noted that *S. capensis* displays distinct preferences for specific microhabitats with different thermal regimes. Understanding the thermal preferences of *S. capensis* can thus provide insights into the mechanisms underlying its adaptive strategies and potential resilience to climate change-induced temperature variation.

Key findings from previous studies provide important insights into the relationship between thermal acclimation and the behavioural responses of intertidal marine ectotherms to thermal cues, and how this relates to their biological performance (Mcgaw 2003, Lagerspetz & Vainio 2006, Lewis & Ayers 2014, Padilla-Ramírez et al. 2015, Crickenberger et al. 2020). For instance, research on the Jonah crab *Cancer borealis* and the amphibious purple shore crab *Hemigrapsus nudus* demonstrated a significant effect of acclimation on the thermal preferences of these crabs (Lewis & Ayers 2014, Padilla-Ramírez et al. 2015). Generally, crabs acclimated to higher temperatures tend to prefer warmer temperatures, while those acclimated to lower temperatures show preferences for cooler temperatures. These studies further imply that by adjusting their thermal preferences through acclimation, these crabs optimize their physiological functions to better suit their environments, enhancing their overall fitness. The current text, however, compares the thermal preferences of *Siphonaria capensis* individuals acclimatized to naturally warmer versus cooler habitat conditions. This helps clarify micro-scale, temperature-driven patterns of species occurrence and microhabitat preference, as determined in Chapter 2 and 3.

Therefore, this study aims to quantify the effect of acclimatization on the thermotactic response of *Siphonaria capensis* to thermal stress. It is hypothesized that individuals acclimatized to warmer conditions, may exhibit preferences for such conditions or show potentially subdued thermotactic responses to rising temperatures. This behaviour may represent a trade-off: a preference for warmer regimes could help match physiological

optima in warm environments but may also require physiological adjustments (e.g., hypometabolism) to survive until conditions improve.

4.3 Methods

4.3.1 Sample sites and animals

This study investigates the thermal preferences of *Siphonaria capensis*, collected from the study site on the West coast of South Africa (Figure 1.1; see Chapter 2 for further site details).

4.3.2 Collection and maintenance

A grand total of 200 individuals of *Siphonaria capensis* were collected from horizontal rock surfaces and rock pools (Table 2.1), at a rate of 50 individuals per Spring low tide from March to April 2020. Limpets were detached from rock substrata and immediately placed in moistened, pre-marked 500mL containers identified by individual collection microhabitat, within an insulated box at 20 – 22°C. Specimens were transported to a climate-controlled environment room (temperature – 20°C; lighting regime – 12 hours light/dark) within 12 hours, where they were housed in 50L tanks for another 12 hours while maintaining separation by microhabitat. Thus, experiments commenced within 24 hours of collection. A 6-hour tidal cycle was simulated in the holding tanks using constantly aerated seawater, an adjacent 50L tank, WACO plug-in timers, and flow-restricted (20L/h) mini submersible water pumps, each fitted with a filter sponge (NEWA MN404, NEWA, Italy). The pumps were programmed to run automatically for 30 minutes at the end of each simulated tidal cycle, ensuring a total transfer volume of 10L of water between the adjacent tanks.

4.3.3 Sampling method

Thermal preferences were measured for *Siphonaria capensis* individuals that remained firmly attached to the inner surfaces of the tanks in the climate-controlled room described above. This was done using a 0.6mm thick, 35cm wide, aluminium sample tank shaped like a canoe (Figure 4.1). This setup follows a modified experimental procedure, consolidated from previously established protocols for the assessment of thermal preference (Licht 1965, Dillon et al. 2009, Tepler et al. 2011). The rounded corners of the tank helped mitigate potential aggregatory behaviour by the limpets at otherwise angular edges that has been observed in similar animals, such as *Chlorostoma funebralis* (Tepler et al. 2011). A 20mm wide strip of copper tape (Advance Tapes, Leicester, United Kingdom) was used to line the inner boundary walls of the tank, serving as a barrier to contain the limpets within a pre-defined experimental area of 130cm by 15cm (Schüder et al. 2003, Roda et al. 2018).

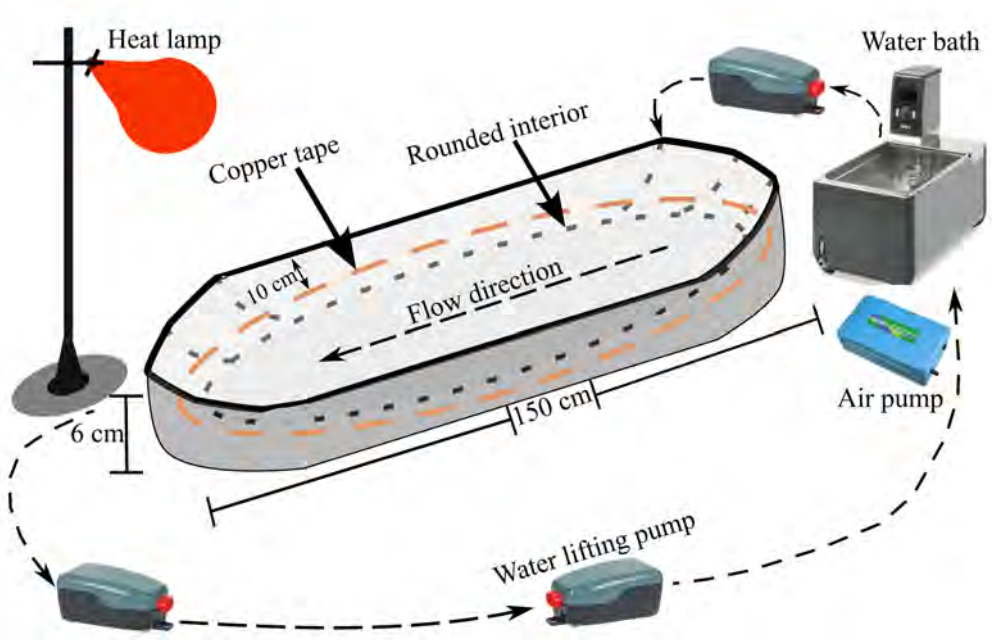

Figure 4.1: Image displaying the layout, equipment and materials used for the sample tank in the thermal preference assessment of *Siphonaria capensis*.

To establish a temperature gradient from 20°C to 40°C, one end of the tank was heated

using two 250-watt heat lamps (Haining Hongxin Electrical, Haining, China), kept approximately 30cm above the tank, while the opposite end was cooled using water from a 10L container in a programmable water bath (Grant Optima TXF200-R4). This gradient, which falls within the typical intertidal temperature range encountered by these limpets (see Chapter 2) and remains below their acute lethal limit (Kankondi et al. 2018), was maintained by circulating aerated seawater from the water bath through the tank (Figure 4.1). This circulation was accomplished using flow-restricted (500 mL/h) Toms 5-watt aqua-lifter dosing pumps. The outer surface of the tank was insulated with foam to stabilize the temperature gradient, which was allowed to settle for 30 minutes before initiating each trial.

Starting temperatures of 25.6°C, 27°C, 28.7°C, 30°C, and 34°C were established using T-type thermocouples, positioned at least 10cm apart and 40cm from the ends of the tank. These points were marked with 7cm lines drawn across the gradient using a permanent marker. At the beginning of each trial, two limpets, one from each of the two different microhabitats, were placed at either end of the five lines, totalling ten limpets per trial. Mark–recapture data (Chapter 3) show homing in over 90% of undisturbed limpets, thus confirming that these limpets were exposed to their collection microhabitats for at least two weeks. Limpets were allowed to move freely for one hour before the temperature at their final positions was recorded. To track limpet movement, the car paint applied in Chapter 3 was used in a colour-coded system to distinguish between limpets from different microhabitats and those placed at the pre-set starting temperatures. This procedure was repeated 20 times. After each trial, the tank was cleaned to eliminate potential biases from lingering chemical cues or mucous trails left by the limpets (Davies & Beckwith 1999, Edwards & Davies 2002, Raw et al. 2013, Ng et al. 2013). To ensure unbiased responses to the temperature gradient, fresh limpets were collected after every five trials, and the temperature settings at the ends of the tank were alternated to minimize local substrate effects (Tepler et al. 2011). The water level was maintained 5mm below the copper tape to eliminate copper leaching (Krull & Newman 2022).

This experimental procedure produced the penultimate dataset, which comprised four

variables: one numerical (start temperature) and two categorical predictor variables (trial and microhabitat). Additionally, it included the numerical response variable end temperature. Subsequently, four additional variables were created to form the final dataset with a total of eight variables. These included a categorical predictor, start temperature status, which ranked the start temperatures from coldest to hottest. Three outcome variables were also generated: a zero-inflated continuous variable for temperature change (reflecting differences between end and start temperatures); a categorical temperature shift variable indicating whether limpets moved to a warmer or colder position on the thermal gradient or showed no change; and movement status (1 = moved, 0 = stationary) as a binary measure of micro-scale dispersal during the experiment. Here, dispersal refers specifically to the centimetre-scale displacement of an individual along the experimental thermal gradient during each trial, not to large-scale demographic migration.

4.3.4 Statistical analysis

All statistical analyses and data visualizations were conducted using R version 4.4.0 (R Core Team 2021). A Generalized Linear Model (GLM) and a Chi-square test were employed to assess the effects of predictors on the response variables of interest. These models were implemented using either the glmmTMB function, as discussed in Chapter 2 and 3, or the ggbarstats function from the ggstatsplot package (Patil 2021).

A Bernoulli GLM was utilized to model limpet movement status as a function of microhabitat (Equation 4.1). Although the interaction between microhabitat and start temperature status was initially considered in this study, it was not included in the final model because it did not significantly improve model fit ($p = 0.76$), as determined by the Likelihood Ratio Test (Table A15) conducted with base R's anova function (Zuur et al. 2009).

$$
\begin{aligned}
Y_i &\sim \text{Bernoulli}(\pi_i) \\
\text{logit}\left(\frac{\pi_i}{1-\pi_i}\right) &= \alpha_0 + \alpha_1 X_{1i} + \epsilon_i \\
\text{where } \epsilon_i &\sim N(0, \sigma^2)
\end{aligned}
\tag{4.1}
$$

In Equation 4.1, Y_i represents the binary response variable for the movement status of the i-th individual, modelled using a Bernoulli distribution with success probability π_i. The logit link function $\text{logit}(\pi_i/(1-\pi_i))$ linearly relates the predictor to the logarithm of the odds ratio (log odds) of the outcome, which indicates the ratio of the probability of the outcome occurring relative to its complement. The grand intercept is denoted by α_0, and α_1 is the coefficient for the predictor microhabitat (X_{1i}). The residual variance ϵ_i, representing individual-level variability not accounted for by the model, is assumed to have a variance of σ^2 and a mean of 0.

The primary research question aimed to identify differences in the direction of temperature changes for animals from perceived cooler versus warmer microhabitats, rather than their magnitude per se. This led to the creation of the new temperature shift variable introduced earlier in this chapter. Consequently, two separate Pearson's Chi-square tests of independence were conducted to determine the influence of microhabitat and start temperature status on the direction of thermal change associated with animal movement. Chi-square tests of independence are appropriate in scenarios where the impact of one categorical variable on another must be statistically assessed. However, using the non-parametric Chi-square test may not be as efficient, powerful, or precise as its parametric counterparts (Vickers 2005, Hopkins et al. 2018, Gerald & Patson 2021). For example, employing the Multinomial GLM would have allowed for a single analysis model to test the effects of the two categorical predictors on temperature shift status, rather than conducting two separate tests. Nevertheless, the Chi-square test was utilized because it does not adhere to the strict assumptions required by the Multinomial GLM, as discussed in Chapter 3, and can therefore be applied more reliably.

Model validation procedures, as outlined in Chapter 2 and 3, were applied to the

Bernoulli GLM assessing the movement status of the limpets. These procedures involved determining the area under the receiver operating characteristic curve, overall model accuracy, the Hosmer–Lemeshow test and Brier score (Section A3). A similar method utilized for evaluating the main effects of the Bernoulli model in Chapter 3 was employed here, using a Type II test appropriate for simpler or balanced designs where interactions are not a primary concern (Shaw & Mitchell-Olds 1993). For the Chi-square tests examining variation in limpet temperature shift status (Figure 4.3 and 4.4), the assumptions for independent observations, mutually exclusive cells, and categorical variables could only be qualitatively verified (Bolboacă et al. 2011, McHugh 2013, Singhal & Rana 2015). The final assumption, that all expected values for all levels of the combination of predictors must be above 5 (Table A16 and A17), was satisfied as determined using the chisq.test function from the stats package (R Core Team 2021).

Post hoc analyses for the Bernoulli GLM involved generating contrasts between the estimated marginal proportions for different outcome classes, as detailed in Chapter 2 and 3. For the Chi-square test, the chisq.posthoc.test function in base R facilitated direct pairwise comparisons between the proportions of animals associated with each level of temperature shift status. To reduce the likelihood of Type I errors, the Bonferroni adjustment was applied to these multiple pairwise comparisons for the Chi-square test.

4.4 Results

4.4.1 Movement status

Overall, only 41.5% of the *Siphonaria capensis* sampled in this study moved during the thermal preference treatments. Among these individuals, a higher percentage was observed in those collected from rock pools (60.2%) compared to those from horizontal surfaces (39.8%).

The Bernoulli GLM analyzing the influence of microhabitat on the movement status of *S. capensis* during treatments revealed a significant tendency for the limpets not to move,

as indicated by an overall rate below 50% (Figure 4.2).

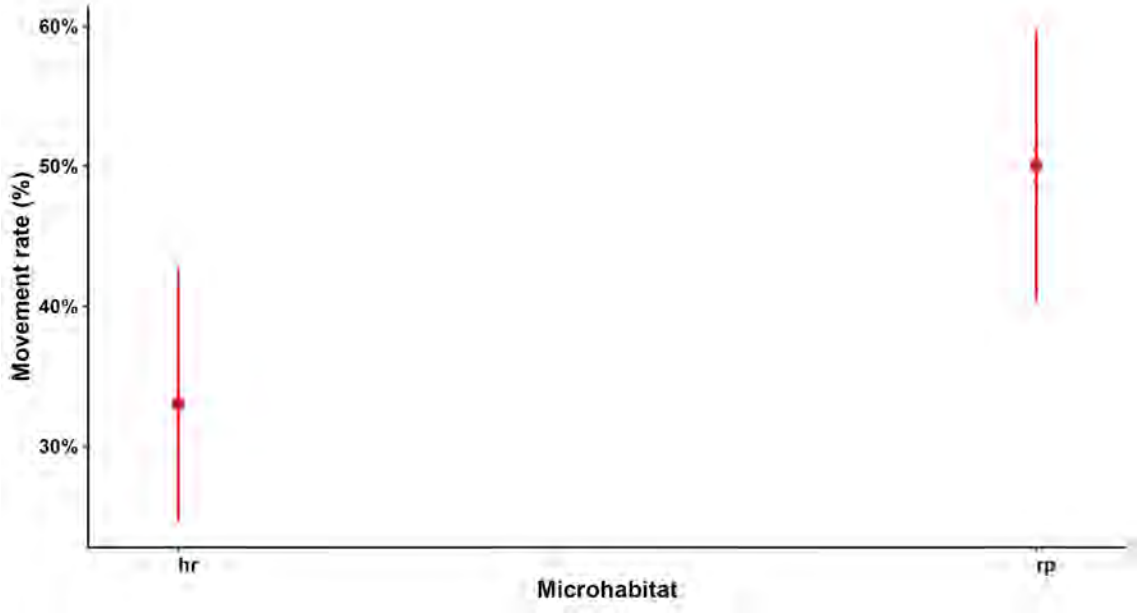

Figure 4.2: Dot and whisker plot illustrating the shift in movement status between *S. capensis* individuals collected from horizontal surfaces (hr) and rock pools (rp), represented as point estimates (± CI).

Additionally, limpet sample microhabitat significantly affected their movement status ($\chi^2 = 5.88$, df = 1, $p < 0.05$), as shown in Table 4.1. In particular, when comparing the movement status between microhabitats (Figure 4.2), *S. capensis* collected from horizontal rocks were less likely to move compared to individuals collected from rock pools (0.49, $p < 0.05$).

Table 4.1: Analysis results from a Bernoulli GLM on the movement status of *Siphonaria capensis*. Microhabitat was treated as a fixed effect.

predictor	Chisq	Df	p.value
mh	5.8845	1	0.0153

Predictor: mh - Microhabitat.

4.4.2 Temperature shift status

Out of the 200 limpets sampled for thermal preference, raw proportions indicate that the majority (58.5%) showed no inclination to move towards either the warmer or cooler sections of the thermal gradient after being placed at their starting temperature. Among the remainder, a larger proportion preferred warmer temperatures (23.5%) as opposed to cooler ones (18%).

4.4.2.1 Collection microhabitat

In the Pearson's Chi-square test analyzing the impact of *Siphonaria capensis* collection microhabitats on their temperature-driven movement, a significant probability of dependence ($\chi^2 = 19.51$, df = 2, $p < 0.0001$) was identified, along with a moderate effect size (Cramér's V = 0.30; Figure 4.3). *Post hoc* analyses show that limpets collected from horizontal rocks were significantly less likely to move to cooler sections of the gradient than expected ($p < 0.0001$). In contrast, limpets from rock pools were significantly more likely to move towards cooler sections ($p < 0.0001$). Finally, for both microhabitats, the movement rates for the remaining temperature-shift categories were consistent with expectations ($p = 0.0882$ for warmer sections and $p = 1$ for no change; Figure 4.3).

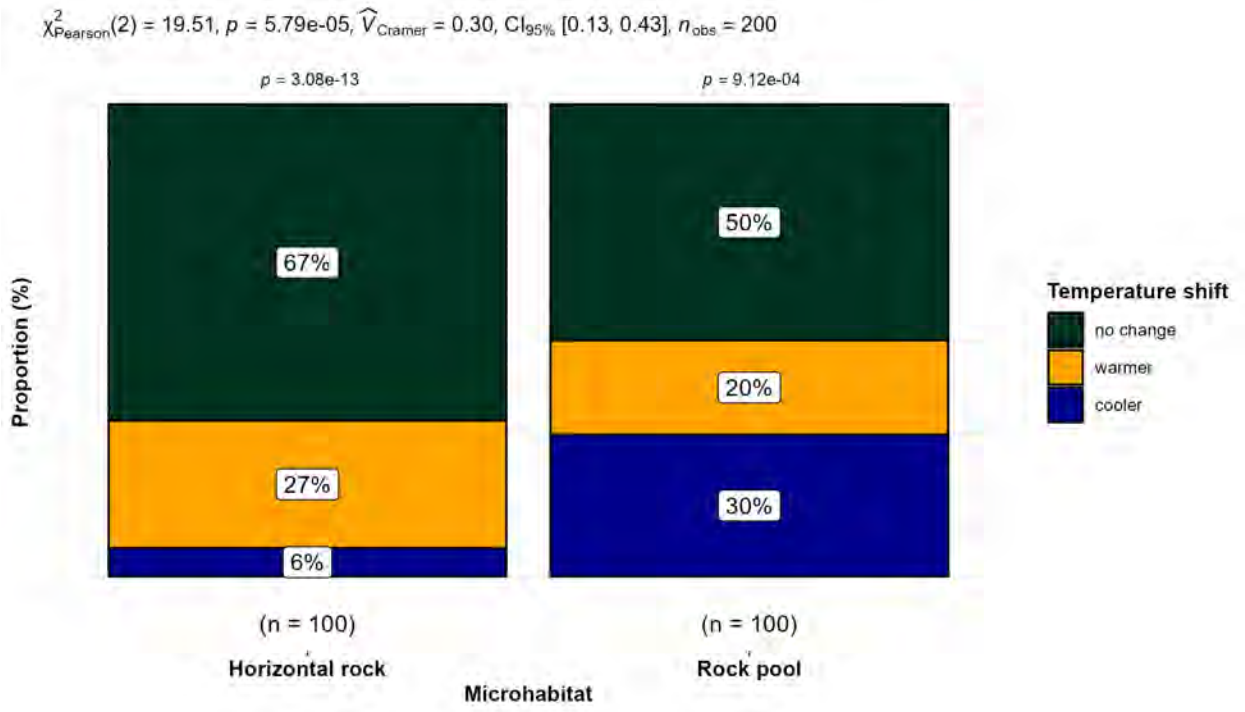

Figure 4.3: Stacked bar chart depicting the results of a Pearson's chi-square test of independence on the relationship between microhabitat and temperature shift status in *S. capensis*. The chart overlays the proportion of observations within each category. Frequentist statistics are presented at the top of the chart.

4.4.2.2 Initial temperature status

The Pearson's Chi-square test, which assessed the effect of initial temperature status on limpet temperature-driven movement, indicated an insignificant probability of dependence ($\chi^2 = 5.30$, df = 8, p = 0.73) with a negligible effect size (Cramér's V = 0; Figure 4.4). Despite this, significant differences in expected temperature-driven movement rates were detected within all groups of temperature status, except for the 'warm' category (Figure 4.4). It is important to note, however, that these findings of significant deviations from expected movement rates were not corroborated by further *post hoc* tests (Table A19).

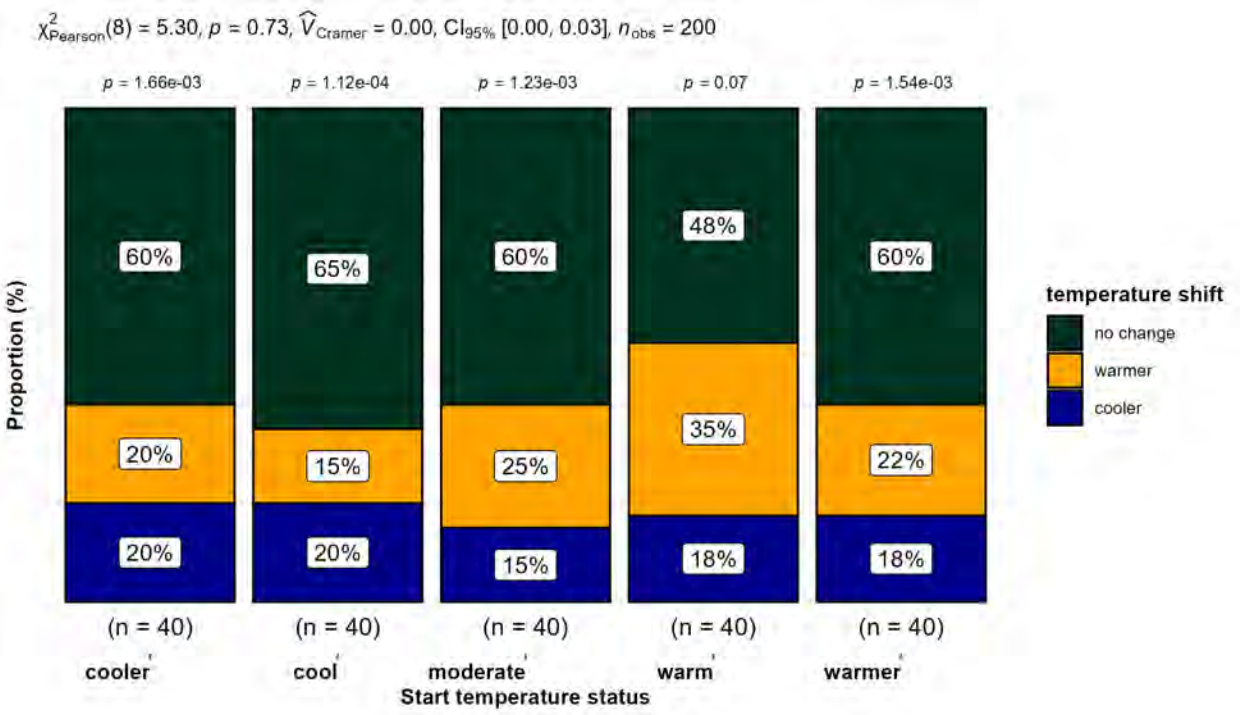

Figure 4.4: Stacked bar chart presenting the results of a 3x5 Pearson's Chi-square test of independence, examining the relationship between the initial temperature and temperature shift status of *S. capensis*. The bars are annotated with the proportion of observations, while Frequentist statistics are displayed above the chart.

4.5 Discussion

4.5.1 Overview and guiding hypotheses

The present chapter explored thermotaxis in the pulmonate limpet *Siphonaria capensis* collected at Kommetjie on the West coast of South Africa. The primary objectives were to examine temperature-driven dispersal of *S. capensis* acclimatized to contrasting microhabitat thermal profiles during low tide and to link this to their distribution patterns, heat-management strategies (as discussed in Chapter 2 and Chapter 3), and potential physiological responses addressed in Chapter 5. I hypothesized that *S. capensis* would favour warmer conditions, potentially reflecting acclimatization to elevated temperatures. Conversely, if no preference for higher temperatures is observed, these

hypotheses would not be supported.

4.5.2 Summary of key findings

Overall, *Siphonaria capensis* exhibited low frequencies of micro-scale dispersal during the thermal preference treatments, which varied based on the sample microhabitat. Specifically, limpets originating from rock pools had substantially higher dispersal frequencies than those from horizontal surfaces. Further analysis showed that, regardless of their collection microhabitat, *S. capensis* generally followed temperature-driven patterns of dispersal consistent with random movement, highlighting its overall low dispersal frequency. Limpets from rock pools, however, occasionally demonstrated notable preferences for cooler temperature zones, while those from horizontal surfaces tended to avoid cooler areas. Furthermore, the results were not affected by the initial placement of individuals along the experimental temperature gradient, indicating that dispersal patterns were shaped by the microhabitat of origin and inherent thermal preferences, rather than the starting point of experiment trials.

4.5.3 Dispersal frequency

4.5.3.1 Relationship between dispersal frequency and heat management strategies

Many gastropods including *Siphonaria spp*., are relatively slow-moving (Creese & Underwood 1982, Herrera et al. 1996). For example, Herrera et al. (1996) reported average dispersal rates of 2–14cm/h for the sea snail *Bulla gouldiana*, while Creese & Underwood (1982) documented even slower rates for *S. denticulata* and *S. virgulata* (0.2–6cm/day). Although dispersal rates were not quantified here, the consistently low dispersal frequencies observed in *S. capensis* fit these benchmarks and likely result from ecological drivers rather than morphological constraints. Restricted dispersal may serve as a risk-avoidance strategy, keeping limpets near home scars or in favourable microhabitats during foraging at high tide (Hui et al. 2022) and reducing exposure to

lethal heat or desiccation at low tide (Chapters 2 - 3). Where access to cooler refuges is limited by barriers, space, or food, however, limpets may instead rely on endurance tactics such as clamping, metabolic depression, and related physiological adjustments to survive (Jones & Boulding 1999, Monaco et al. 2015, Verberk et al. 2016, Marshall & McQuaid 2020). This constitutes unaccounted for intraspecific variation in *S. capensis* employment of thermoregulatory adaptation strategies, which are only elucidated through more granular analyses.

4.5.3.2 Effects of acclimatization to harsh conditions

The results from the current study, together with several field and laboratory studies (Jones & Boulding 1999, Chester et al. 2015, Deldicq et al. 2021, Hui et al. 2022), but see Bonte et al. (2012) and Raina et al. (2022), show that animals acclimatized to thermally harsh habitats disperse less than conspecifics from benign sites. For instance, the drought-exposed small caddisfly *Agapetus sp*. limits its dispersal in response to increased drying during droughts (Chester et al. 2015). Similarly, *S. capensis* individuals adapted to unfavourable microhabitats may adjust their behaviour to limit their dispersal, facilitating faster clamping behaviour at ebb tide to conserve moisture (Wolcott 1973). Comparable thermal cues trigger burrowing in the protozoan *Haynesina germanica* (Deldicq et al. 2021), preventing body temperatures from reaching critical thermal maxima, the temperature at which marine organisms experience neuromuscular inhibition and a loss of presynaptic functionality due to thermal stress (White 1983). Because clamping alone does not fully mitigate heat stress in limpets, it may instead prompt metabolic depression, which could help them endure extended exposure to high temperatures (Chapter 2 and 3). Such links between inactivity and hypometabolism are well documented in animals adapted to high temperatures (Storey & Storey 2004, 2012, Navas & Carvalho 2010, Storey 2015, Jiang et al. 2023).

Thermoregulatory responses associated with restricted limpet movement can only be sustained for finite periods. Prolonged reliance on them leads to harmful metabolic by-products and other adverse effects (see Chapter 1), including the buildup of

nitrogenous waste, reduced foraging and escape capacity, and increased molecular damage due to restricted energy availability for repair (Storey 2015, Marshall & McQuaid 2020, Leeuwis & Gamperl 2022). Therefore, there is ample incentive for *S. capensis* to avoid these costs by maintaining higher dispersal frequencies in cool microhabitats, where stressful thresholds are seldom reached. This is corroborated by previous research (Santina 1994, Gray & Hodgson 1998, Nuñez et al. 2014), where increased dispersal of the study animals was typically observed under relatively cool rock shore conditions.

4.5.4 Thermal preference

4.5.4.1 Drivers of interspecific variation in thermal preference

Other taxa show the opposite pattern to *Siphonaria capensis* when thermal preferences are compared between animals acclimatized to warm and cool microhabitats (García-Guerrero et al. 2013, Johansson 2015). Warm-acclimated juvenile red claw crayfish (*Cherax quadricarinatus*) selected cooler areas, whereas the cool-acclimated freshwater snail (*Radix balthica*) generally preferred the warmer regions of a gradient. Along with the present study's finding that *S. capensis* from cool microhabitats preferred cooler sections while those from warm microhabitats remained stationary, these cases suggest distinct but comparable physiological drivers of thermal preference. Cooler water may limit heat stress and conserve energy in the warm-acclimatized *C. quadricarinatus*, whereas moving to 17°C on the thermal gradient places *R. balthica* near its 20°C growth optimum (Johansson 2015).

The differences in thermal preferences observed between warm- and cold-adapted *S. capensis* and the other two species, *C. quadricarinatus* and *R. balthica*, probably arise from contrasting evolutionary histories, body size, locomotor anatomy, and sample location (Crickenberger et al. 2020). The large crayfish *C. quadricarinatus*, with carapace lengths ranging from 50 to 250mm (Ahyong & Yeo 2007, Patoka et al. 2016, Douthwaite et al. 2018, Liu et al. 2024), uses jointed appendages for rapid, efficient

movement (McCormack 2012), whereas the much smaller *S. capensis* and *R. balthica*, which reach shell lengths of up to 28mm (Chambers & McQuaid 1994, Schniebs et al. 2011), rely on a muscular foot and disperse slowly (Miller 1974, Creese & Underwood 1982, Lai et al. 2010, Tyrakowski et al. 2012). Consequently, the decapod can readily track cooler refuges, while *S. capensis* may have to rely more heavily on behavioural thermoregulation, such as clamping. Although *R. balthica* and *S. capensis* are similar in size and locomotor anatomy, they differ in thermal preference among cool-origin individuals. Cool-origin *S. capensis* appear predisposed to avoid warmer conditions on the high-shore rocky intertidal to mitigate the risk of thermal stress and the need to employ sub-optimal physiological adaptations for survival. In contrast, cool-acclimated *R. balthica*, from the stable environment of sub-Arctic Lake Mývatn in Iceland (Johansson 2015), likely seeks slightly warmer water to optimize metabolic processes like growth and digestion, illustrating how habitat and morphology jointly shape thermal preference strategies.

4.5.4.2 Drivers of intraspecific variation in thermal preference

These interspecific differences echo reports that species prefer either cooler conditions (González et al. 2010, Tepler et al. 2011, Deldicq et al. 2021, Hui et al. 2022, Ripley et al. 2022, Morley et al. 2022, Helmond et al. 2023) or warmer ones (Herrera et al. 1996, Diaz et al. 2006, Dillon et al. 2012), regardless of acclimatization status. Although risk-avoidance strategies dominate (Crickenberger et al. 2020), intraspecific variation is common (Bovbjerg 1975, Clusella-Trullas et al. 2011, Salas et al. 2012, Behrens et al. 2012, Padilla-Ramírez et al. 2015, Truitt et al. 2018, Strunov et al. 2023, Schakmann et al. 2023), including in *S. capensis*. Key drivers include body size (Clusella-Trullas et al. 2011, Schakmann et al. 2023), food-resource induced chemotaxis (Bovbjerg 1975), temporal fluctuations in environmental conditions (Salas et al. 2012, Padilla-Ramírez et al. 2015), and animal-health status (Truitt et al. 2018). For example, *Drosophila melanogaster* infected with the endosymbiotic bacterium *Wolbachia* prefer cooler temperatures than uninfected flies (Truitt et al. 2018), while larger squamate ectotherms

tend to select warmer sites to offset their greater thermal inertia (Clusella-Trullas et al. 2011). Furthermore, despite efforts to minimize size differences during sampling, *S. capensis* remains size-segregated between microhabitats, with larger individuals typically found on horizontal surfaces rather than in rock pools (pers. obs.). This suggests that size-linked physiology may underlie its broad thermal preferences.

4.5.5 Methodological constraints and potential solutions

Assessments of thermal preference based on the manual observation and tracking of specimens are prone to bias and can introduce spurious intraspecific variation (Myrick et al. 2004, Dillon et al. 2009, Diaz et al. 2011, Chen et al. 2011, Reiser et al. 2013, Touska et al. 2016). Consequently, small, subtle movements are easily missed, and errors in maintaining or logging stable thermal gradients further skew results. Precision in detecting minor changes can be enhanced using high-resolution video paired with automated tracking systems (Pérez-Escudero et al. 2014, Truitt et al. 2018, Henry et al. 2022, Strunov et al. 2023, Schakmann et al. 2023), which can record movement frequency, speed, direction, course adjustments, and distances travelled. This approach minimizes bias, allows finer scale quantification of temperature-driven dispersal, and detects minute behaviours such as subtle shifts in body orientation (Reiser et al. 2013, Touska et al. 2016, Henry et al. 2022). Therefore, integrating such tracking with feedback-controlled temperature gradients (Reiser et al. 2013) would yield more accurate assessments of thermotactic behaviour in future studies.

4.5.6 Thermal preference links distribution and physiological expression

The broad range of thermal preference determined here echoes findings for *Siphonaria capensis* in Chapter 2 and 3, where its distribution between favourable and less favourable microhabitats suggests an equilibrium between two primary heat management strategies. This variation reflects differences in energy requirements among individuals and their capacity to regulate these demands under conditions that fluctuate

across spatial and temporal scales, potentially contributing to differing heat tolerances. As in many ectotherms (Crickenberger et al. 2020), limpet thermal preferences are shaped by the need to access resources or maintain optimal conditions for physiological functions as climatic conditions alternate between being hospitable and challenging. This may require differing propensities for hypometabolism across the *S. capensis* population to conserve energy and maintain thermal tolerance across highly variable thermal conditions. The proposed links among thermotaxis, microhabitat distribution, dispersal, and hypometabolic capacity are only inferred, because they are drawn from separate studies (Salas et al. 2012, Padilla-Ramírez et al. 2015, Crickenberger et al. 2020, Pound et al. 2020, Liao et al. 2021, Janetzki et al. 2021). The influence of temperature on micro-scale distribution (Pound et al. 2020, Janetzki et al. 2021) appears to shape dispersal patterns through thermal preference (Padilla-Ramírez et al. 2015, Crickenberger et al. 2020) and hypometabolism-mediated thermal tolerance (Liao et al. 2021).

4.5.7 Conclusion

Building on these results, I fail to reject the hypothesis that *in situ* acclimatization to higher temperatures fosters a preference for elevated temperatures, which could amplify hypometabolic responses and enhance thermal tolerance in *Siphonaria capensis* when behavioural thermoregulation is chronically restricted. While a clear preference for warmer conditions was observed, thermal preferences were context-dependent, with individuals from warmer habitats favouring higher temperatures and those from cooler habitats preferring lower temperatures. Ultimately, the findings of this chapter underscore that variable thermal histories create cascading effects on the thermal tolerance of pulmonate limpets, shaped by their distribution, dispersal patterns, and capacity for hypometabolic activity.

Chapter 5

Thermal limit analysis

5.1 Abstract

Intertidal organisms face rapid, tide-driven temperature oscillations that can push body temperatures to physiological extremes within hours, yet the extent to which hypometabolism modulates their absolute thermal tolerance has not been comprehensively established. In this chapter I assessed whether energy-saving hypometabolism enhances heat tolerance in two South African limpets, *Siphonaria capensis* (n = 240) and *S. serrata* (n = 160), collected in spring and summer from Kommetjie, Three Sisters and Zinkwazi. Guided by metabolic rate suppression (MRS) theory, I hypothesized that (i) the link between hypometabolism and sub-lethal limits would strengthen under warmer regimes, and that (ii) lethal and sub-lethal limits would covary more tightly in cooler conditions. Non-invasive plethysmography was used to log heart rate across controlled heat ramps (20 – 55°C at 0.25°C/min) to generate cardiac thermal response curves. From these curves, final breakpoint temperature (FBT), flatline temperature (FLT) and cardiac suppression range (CSR) were derived as proxies for sub-lethal limits, lethal limits and hypometabolic activity, respectively. Mixed effects models showed that CSR and FBT were positively correlated, an association that was only steeper at the warmer site for *S. serrata*, whereas the correlation between FLT and FBT was weaker and inconsistent across sites particularly for *S. serrata*. These results indicate that individuals expressing stronger hypometabolism attained higher sub-lethal limits, while lethal thresholds remained comparatively inflexible. Additionally, mean

FBTs peaked at the warmest sites and during the warmest conditions, whereas limpets were largest at the coolest site, with minor size differences among microhabitats reflecting local thermal heterogeneity. Collectively, these findings confirm that hypometabolism not lethal limit plasticity, principally underpins heat endurance in these pulmonate limpets, supporting metabolic suppression theory as a predictive framework for intertidal resilience under climate warming.

5.2 Introduction

Various factors are likely to govern the ability of intertidal ectotherms to survive extreme, tide driven temperature fluctuations under climatic warming. Of these, access to thermally heterogeneous environments, at different spatial scales, and specialized physiological adaptations are often discussed (Marshall & McQuaid 1991, Dong et al. 2017, Monaco et al. 2017, Choi et al. 2019, Rilov et al. 2019, Moyen et al. 2020, Liao et al. 2021). Individuals that mitigate costly metabolic responses to acute and/or sustained temperature increases, by tandem physiological/behavioural processes, are generally predicted to fare better than those that do not (Richards 2010, Marshall & McQuaid 2011, Choi et al. 2019, Hui et al. 2020, Li et al. 2021). As discussed in Chapter 1, metabolic rate depression is an energy saving adaptation to harmful abiotic conditions (Newell 1969, Sokolova & Pörtner 2001, Guppy & Withers 2007, Verberk et al. 2016) that reduces respiratory costs during severe thermal stress (Abele et al. 2002), preventing energy deficits and extending thermal tolerance (Hand & Hardewig 1996). Attempts have been made to establish patterns of the incidence of metabolic depression in thermally variable environments (Li et al. 2021) and to predict the onset of metabolic depression using autocorrelative environmental cues (Hui et al. 2020). However, past studies fall short of making substantial links between metabolic depression and thermal tolerance. By utilizing a range of physiological parameters derived from heart rate measurements (described below), this study aims to investigate the potential effect of metabolic depression on thermal tolerance and the degree to which lethal limits are plastic, replicating the analysis in two congeneric intertidal pulmonate limpets,

Siphonaria capensis and *S. serrata*, that experience similar shore temperatures along the South African coast (see Chapter 2).

Organismal response to increasing temperatures are normally represented by thermal performance curves (TPC), which commonly exhibit a left-skewed pattern (Huey & Kingsolver 1989, Angilletta Jr. et al. 2006, Angilletta 2009, Sunday et al. 2011, Woods et al. 2018). Generally, TPCs describe an increase in the rate of some fitness related trait (e.g., growth, locomotion, etc) with temperature, followed by a sudden crash after reaching peak performance at the optimum temperature (T_{opt}), and a flatline, or failure to respond to increasing temperatures, at the critical maximum temperature (CT_{max}). Deviations from the rate-temperature norm have, however, been described for some species (McMahon & Russell-Hunter 1977, Fangue et al. 2008, Fangue et al. 2009, Marshall & McQuaid 2011, Verberk et al. 2016). This is shown in regions of the TPC where animals exhibit a plateau in performance (performance thermoneutrality) or a drop in performance (metabolic rate depression), below T_{opt}, that varies in temporal extent depending on the species and environmental conditions (Storey & Storey 2004, Guppy & Withers 2007, Marshall & McQuaid 2011).

Along with their thermal limit indicators, cardiac thermal response curves or TRCs, which relate heart rate to temperature, are commonly used to study metabolic patterns in intertidal ectotherms (Stenseng et al. 2005, Dong & Williams 2011, Tagliarolo & McQuaid 2015). TRCs are similar in shape and features to TPCs at higher temperatures. Specifically, TRCs also display a rapid and usually non-lethal drop in cardiac function at the peak of the curve, which is often referred to as the Arrhenius breakpoint temperature (ABT) in TRCs with a single breakpoint (Stillman & Somero 1996, Stenseng et al. 2005, Dong & Williams 2011, Huang et al. 2015, Tagliarolo & McQuaid 2015, Xing et al. 2016, Monaco et al. 2017, Kankondi et al. 2018, Han et al. 2020). In this study, however, I use the term 'final breakpoint temperature' (FBT) instead of ABT, as it provides a more accurate representation of peak performance for TRCs that deviate from the rate-temperature norm, specifically those with multiple breakpoint temperatures (BPT) before the FBT (see Figure 5.1). Multiple breakpoints have been identified in the

TRCs of several intertidal ectotherms (Bjelde et al. 2015, Pasparakis et al. 2016) and it has previously been implied that they contribute to energy conservation at elevated temperatures (Bjelde & Todgham 2013). This study defines regions segmented by two of the multiple breakpoints, one of which could be the FBT (Figure 5.1 E), as the cardiac activity suppression range (CSR), where cardiac response either plateaus or drops before recovering (Pasparakis et al. 2016). After this, FBTs are typically followed in close succession by the flatline temperature, or FLT (Figure 5.1), a critical point at which the heart ceases to function, often leading to fatal consequences for the organism. As shown by Bjelde & Todgham (2013) and Wang et al. (2023), several ectotherms exhibit considerable variability in breakpoint temperatures, and consequently in the overall shape of their TRCs (Figure 5.1). This variation is likely driven by fluctuating energy states before thermal stress events (Pasparakis et al. 2016), differences in individual thermal history, and the extent to which various physiological safeguards against heat stress are deployed (Wang et al. 2023). Following several other studies (Stillman & Somero 1996, Dong & Williams 2011, Bjelde & Todgham 2013, Tagliarolo & McQuaid 2015, Pasparakis et al. 2016, Kankondi et al. 2018, Marshall et al. 2018, Hann 2021), I used the final breakpoint temperature (FBT) and flatline temperature (FLT) as markers for thermal tolerance. Specifically, FBT, along with the CSR, which serves as a proxy for metabolic depression in this study, was employed to investigate the relationship between metabolic depression and thermal tolerance across different spatiotemporal scales (Bjelde & Todgham 2013, Bjelde et al. 2015, Giomi et al. 2019, Hui et al. 2020, Hann 2021, Li et al. 2021).

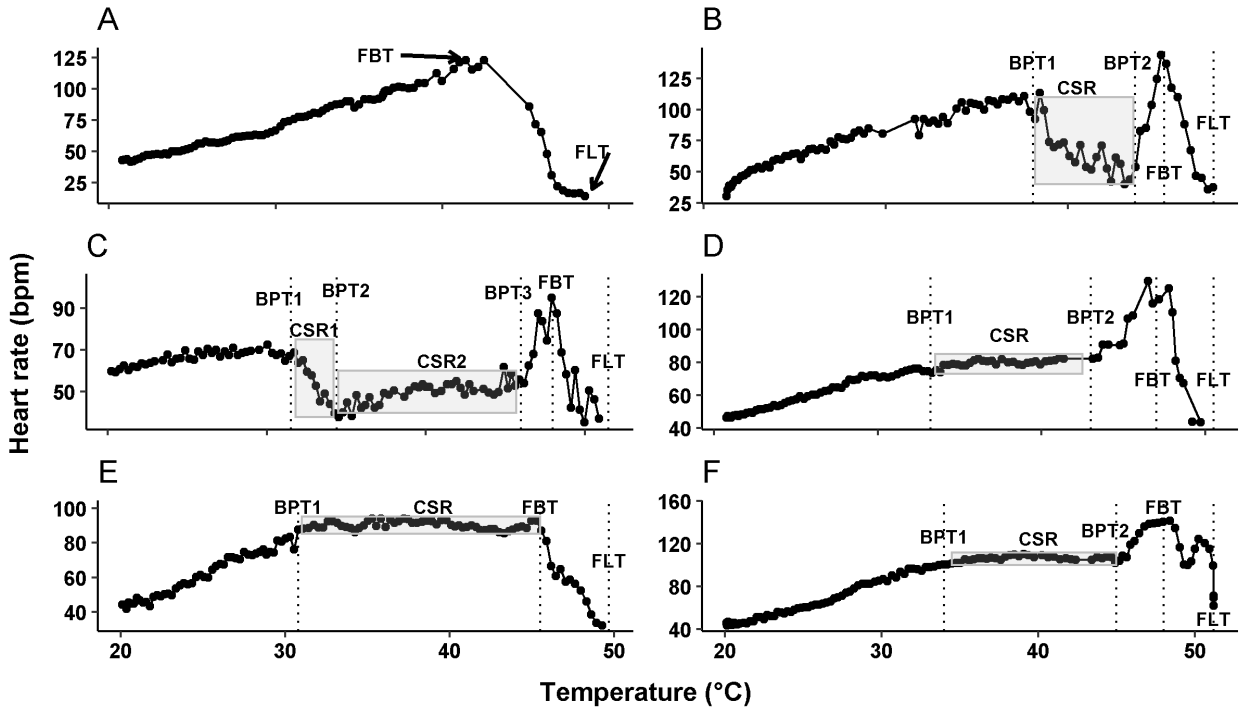

Figure 5.1: Cardiac thermal response curves with cardiac activity suppression range (CSR), flatline temperature (FLT), final (FBT) and preceding breakpoint temperatures (BPT) shown for six individual *Siphonaria capensis*.

Final breakpoint temperatures represent maximal upregulation of heat induced protective molecules (i.e., Heat Shock Proteins and Heat Shock Transcription Factors) after their steady accumulation in cellular systems (Han et al. 2013, Zhang et al. 2014). Thermal injury associated with FBT is typically reversible through the action of Heat Shock Proteins (HSPs) that facilitate protein refolding following proteolysis (Lindquist 1986, Feder & Hofmann 1999, Richter et al. 2010). At somatic temperatures above FBT, protein damage extends beyond the capacity of the organism for cellular repair often resulting in the formation of cytotoxic aggregates and excessive apoptosis closer to FLT (Kultz 2005, 2020, Gracey et al. 2008). Neural damage of this extent to the visceral ganglia could disrupt the neurotransmission responsible for cardio-modulation (Carlson 1905, Zhuravlev & Safonova 1984, Beninger & Le Pennec 2006), ultimately resulting in death due to failure of the heart's electrical system or asystole. This lethality and irreversibility is thought to contribute to the reputation of FLTs as being physiologically rigid (Stenseng et al. 2005, Moyen et al. 2020), particularly when compared to FBT,

which is believed not to be as tightly conserved (Pasparakis et al. 2016, Dong et al. 2017, Li et al. 2021, Moyen et al. 2022, but see Drake et al. 2017). Comparisons of plasticity in animals' lethal limits have generally been made by acclimating differentially acclimatized individuals to contrasting temperature regimes and reporting any subsequent differences. Here, I used a simpler approach by examining covariance in limpet FLT∼FBT to examine comparative, inter-population plasticity of FLT across time and space.

The study hypothesizes that: 1. Cardiac activity suppression range (CSR) will be positively correlated with final breakpoint temperature (FBT), with this relationship predicted to be strongest in warmer environments and in limpets typically exposed to higher temperatures, where a more pronounced CSR is anticipated. 2. Flatline temperature (FLT) will show greater variability, and tighter covariance with FBT in limpets from cooler environments, where a greater scope for FLT acclimatization is predicted.

5.3 Methods

5.3.1 Sample sites and animals

I examined the aerial thermal response metrics of two pulmonate limpets, *Siphonaria capensis* and *S. serrata* with the potential for metabolic rate depression (Marshall & McQuaid 1991) from three and two sites, respectively, along the South African coast (Figure 1.1).

5.3.2 Collection and maintenance

A grand total of 240 individuals of *Siphonaria capensis* and 160 of *S. serrata* were collected across all microhabitats at each species respective site, throughout spring low tides, specifically during spring (September 2019 – November 2019) and summer (December 2019 - February 2020). To minimize overlap and potential ambiguity

between seasons, collection was spaced such that the first spring low tide of each month was reserved for collections from Kommetjie, while the second spring low tide was reserved for collections from Zinkwazi and Three Sisters. This ensured roughly a month between sample collections for each site between levels of season. The remaining collection, transportation, and initial handling procedures for these specimens followed those detailed in Section 4.3.2, with experiments commencing within 24 hours of collection.

5.3.3 Heart rate measurements

Heart rates were recorded using non-invasive plethysmography (Depledge & Andersen 1990, Burnett et al. 2013), as a proxy for metabolic activity (Armstrong 1986, Green 2011). Optoelectronic sensors (CNY70, Vishay, Germany) were attached to 4 limpet shells, near their hearts, using Pattex super glue (Henkel (Pty) Ltd, South Africa), before moving them to 4 dampened 500mL containers. Limpet movement within the containers was restricted using mesh netting, secured to the bottom with melted polyvinyl chloride plastic. There was a 1 hour pause at 20°C in the container before starting each heat ramp, to allow for heart rate recovery. Heat ramps (20 - 55 °C at 0.25°C min^{-1}), as in Kankondi et al. (2018), were then generated using a programmable water bath (Grant Optima TXF200-R4), whilst simultaneously recording temperature with a 4-channel data logging thermometer (Gilson Company, USA) and T-type thermocouples (Fluke Corporation and Cromega) set beneath each limpet's foot. The impedance signals were amplified (custom-built pre-amplifier), smoothed (Triangular-Bartlett), filtered and logged using PowerLab 4/30 and 2/26 (LabChart version 8, ADInstruments, Australia).

Each ramp, combined with the preliminary 1h pause, lasted 200 minutes, with 2-3 ramps being run each day for 72h after collection. This constituted a single trial, with six trials conducted per season over a total of two seasons. The order in which samples from each microhabitat was analysed, was randomized within and between trials, and between trials for each site. Individual shell lengths (mm) were measured immediately after each ramp, with the entire dataset consisting of 240 measurements for *Siphonaria capensis*

and 160 for *S. serrata*. For subsets of the data, shell heights were measured for 156 *S. capensis* individuals and 104 *S. serrata* individuals, shell widths were measured for 156 *S. capensis* individuals and 104 *S. serrata* individuals, shell weight was recorded for 101 *S. capensis* individuals and 83 *S. serrata* individuals, and shell thickness was measured for 60 *S. capensis* individuals and 35 *S. serrata* individuals. Subsets were used because these variables were considered only at different stages after the experimentation began. Vernier callipers (0.02mm precision) were used to measure length, height and width. A micrometer screw gauge (0.01mm precision) and electric lab measuring scale (precise to 0.0001g) were used to measure thickness and weight, respectively.

5.3.4 Data analysis

Unless stated otherwise, data analyses and visualizations were conducted using R version 4.4.0 (R Core Team 2021). TRCs were visualized using ggplot from the ggplot2 package (Wickham 2016), and data producing plots with no clear trend, approximately 42% and 34% of all heart rate measurements for *Siphonaria capensis* and *S. serrata*, respectively, were considered missing and treated as discussed in Section 5.3.5 below. The remaining data were treated by log transforming heart rate LN(HeartRate) and calculating inverse (1/T) temperature (K). Final and preceding breakpoint temperatures (BPT) were derived by back transforming breakpoints (Figure 5.1), obtained using segmented regressions (Muggeo 2008). Total numbers of breakpoints were then determined according to the lowest Bayesian information criterion (BIC) score, between models fitted with different numbers of breakpoints, using the selgmented function (Muggeo 2020). The calculation of the cardiac suppression range (CSR) varied depending on the number of breakpoints identified. When there were two breakpoints, the CSR was determined as the difference between them, thereby giving a single value that represents the span of this range. In cases where there were more than two breakpoints, the CSR was calculated as the cumulative difference between all the breakpoint temperatures (BPTs), creating a cumulative range value (Figure 5.1 C). Flatline temperatures (FLTs) were determined by first fitting natural cubic splines,

developed by Hastie & Tibshirani (2017), to back-transformed cardiac response data. Then, the regression model was extrapolated beyond the FBT until the predicted heart rate (y) reached 0 bpm, a method similar to the one described in Hui et al. (2020). The degrees of freedom needed to generate the "best fit" spline, was determined using K-fold cross-validation (K=10) with the boot package (Canty et al. 2017).

In order to ensure the accuracy of the FLTs derived from my spline regression models, the estimated flatline temperatures (FLTs) for 20 randomly selected individuals were validated by comparing them with FLTs calculated using a more established reference method. This reference method, described in the supplementary information provided by Marshall et al. (2018), determines FLTs based on the detection of a "loss of periodicity within a one-minute band" of the heart rate data. Two multilevel datasets, one for each species, were generated. These datasets included five numerical level 1 covariates, length, height, width, weight, and thickness. Additionally, three explanatory categorical variables were incorporated. This included the level 2 variable microhabitat that consisted of four groups, nested within the level 3 variable site with two groups for *S. serrata* and three for *S. capensis*, and crossed with the level 3 variable season that had two groups. Finally, the dataset included three level 1 response variables, namely the continuous variables FBT, FLT, and CSR. These response variables were collectively referred to as 'thermal limit' variables while the rest of the continuous data were termed size variables, where it was syntactically convenient to do so.

5.3.5 Missing data

Data gaps present a pervasive and often overlooked challenge in many research fields, especially in ecological and evolutionary studies (Nakagawa & Freckleton 2008, Ginkel et al. 2010, Eekhout et al. 2012, Ellington et al. 2015, Nakagawa 2015, Hossie et al. 2021). The problem manifests as missing values in a dataset, usually attributed to potential issues with sample and data collection procedures (Enders 2010), but can be the result of planned missing data designs (Graham et al. 2006, Noble & Nakagawa 2018, Hossie et al. 2021, Noble & Nakagawa 2021). Here, missing thermal limit data arose

when thermal limits could not be derived from TRCs, for environments where finding more sample animals for additional tests was prohibitively time consuming. Missing data were generated for size variables as indicated in Section 5.3.3. When implemented, missing data "solutions" generally involve the wholesale exclusion of incomplete cases from data analyses via listwise or pairwise deletion (Enders 2010). This often produces biased parameter estimates and can reduce the statistical power of affected studies (Nakagawa & Freckleton 2008, Graham 2009, Little et al. 2014). An extensive body of research over the past decade has coincided with the emergence of modern missing data techniques and the enhancement of their associated theoretical frameworks (Graham et al. 1996, Enders 2001, Graham 2003, Buuren & Groothuis-Oudshoorn 2011, Buuren 2018, Heymans & Eekhout 2019). At the forefront of this research are the advanced techniques, multiple imputation and full information maximum likelihood (Rubin 1976, Graham 2009, Enders 2010).

5.3.5.1 Missing data inspection

The original datasets for both species had missing values across all continuous variables except shell length. In this study, to address the issue of missing data, I employed multiple imputation. Before implementing this on the original datasets of both species, I conducted a simulation study as a "proof of concept." This simulation was broadly informed by the missing data patterns observed in the incomplete *Siphonaria capensis* dataset but was not an exact replication. It is important to note that the imputation of the actual datasets for both species was set to follow the imputation methods and specifications detailed for the simulation in the rest of Section 5.3.5.1 and 5.3.5.2 below. This did not, however, include any steps involved in determining the accuracy of imputed parameter estimates. Any discrepancies in the methods used for the simulation and actual datasets, particularly for *S. serrata*, are stated explicitly. For the simulation study, I generated a complete dataset using faux for factorial designs (DeBruine 2021) to "mimic" the intraclass correlations, correlation coefficients (Table 5.1), and frequency distributions of the continuous variables (Figure 5.2). Numeric values for all variables

were generated from normal distributions except for CSR. The zero-inflated (24.2%), positive skewed distribution for CSR, as evidenced from the summary statistics of its non-zero values (minimum 2.35, mean 9.98, maximum 19.74), was derived by sampling from a gamma distribution. Finally, an integer Cluster ID variable was added to the simulated dataset. This variable assigned a unique identifier to each cluster that was derived from the unique combinations of the season, site, and microhabitat variables.

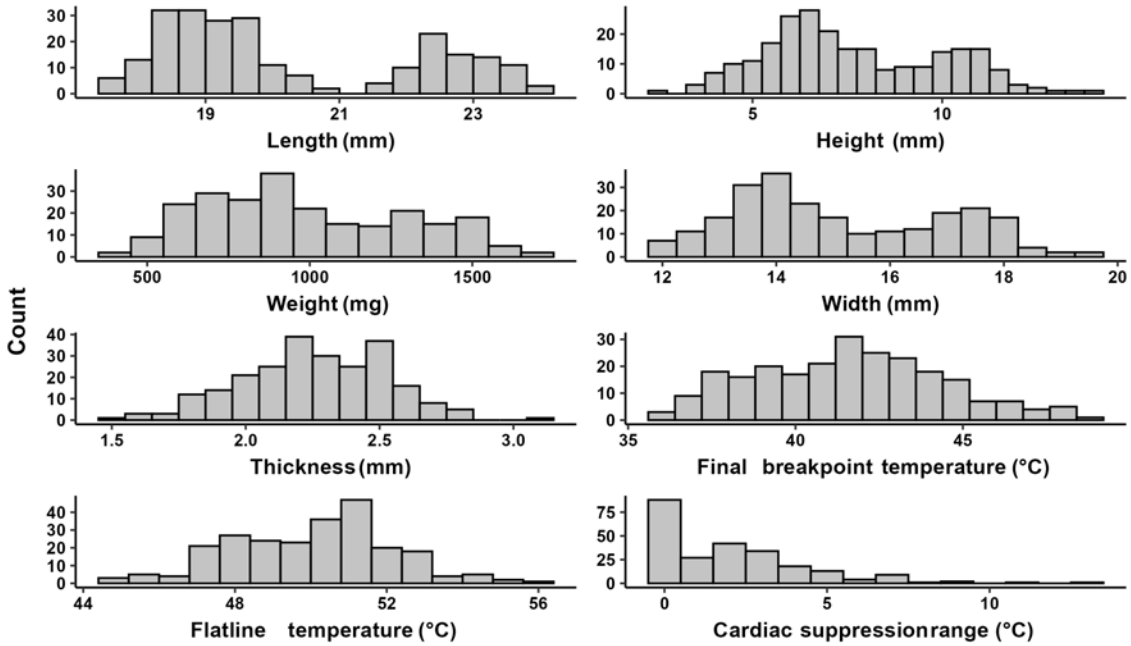

Figure 5.2: Frequency distributions of all continuous variables in the simulated complete dataset of *Siphonaria capensis*.

Table 5.1: Correlation matrix of all continuous variables used in a simulated missing data analysis based on *Siphonaria capensis* data.

Var	FBT	FLT	CSR	L	H	W	Wt	Th
FBT	1	0.5964	0.2274	-0.2063	-0.2175	-0.1927	-0.1901	0.0631
FLT		1.0000	0.0904	-0.1308	-0.0957	-0.1405	-0.0477	0.0116
CSR			1.0000	-0.0596	-0.0838	-0.0163	-0.0345	0.1861
L				1.0000	0.8494	0.9421	0.8674	0.0076
H					1.0000	0.7694	0.9204	0.0320
W						1.0000	0.7887	-0.0092
Wt							1.0000	-0.0032
Th								1.0000

Var - Variables; FBT - final breakpoint temperature (°C); FLT - flatline temperature (°C); CSR - cardiac suppression range (°C); L - length (mm); H - height (mm); W - width (mm); Wt - weight (mg); Th - thickness (mm)

An incomplete dataset with data missing at random (MAR), with a similar missing data pattern (Table 5.2) and mechanism to the original dataset, was produced from the complete dataset using the missMethods package (Rockel 2022). The missing data pattern describes the distribution of missing and observed data in a dataset, whereas missing data mechanisms (referred to as "missingness" throughout) refer to the underlying processes that lead to data being missing. Missingness details the possible relationships between measured variables and the probability of missing data (Rubin 1976, Enders 2010). There are three types of missingness, namely, data missing completely at random (MCAR), missing at random (MAR), and missing not at random (MNAR). Including variables with more than 50% missing data in imputation models is generally discouraged (Collins et al. 2001, Marshall et al. 2010), as rates exceeding this threshold can introduce biased parameter estimates. This exclusion criterion, however, is not an absolute rule, and variables with missing data rates marginally above 50% may still be retained. For instance, in the simulation exercise, weight (58%) and thickness (75%) were excluded from the main analyses. In contrast, height and width, which had

missing data rates of 55% and 56% in the *Siphonaria capensis* and *S. serrata* data, respectively, were retained for final analysis.

Table 5.2: Induced missing data patterns for the simulated incomplete data of *Siphonaria capensis*, displayed as frequencies of missing (0) and observed (1) data.

NrC	IND	CID	L	SZN	SITE	MH	FLT	FBT	CSR	H	W	Wt	Th	I_C
60	1	1	1	1	1	1	1	1	1	1	1	1	1	**0**
41	1	1	1	1	1	1	1	1	1	1	1	1	0	**1**
55	1	1	1	1	1	1	1	1	1	1	1	0	0	**2**
63	1	1	1	1	1	1	1	1	1	0	0	0	0	**4**
21	1	1	1	1	1	1	0	0	0	0	0	0	0	**7**
Tot	**0**	**0**	**0**	**0**	**0**	**0**	**21**	**21**	**21**	**84**	**84**	**139**	**180**	**NA**
Pcnt	**0**	**0**	**0**	**0**	**0**	**0**	**9**	**9**	**9**	**35**	**35**	**58**	**75**	**NA**

IND - Individual; CID - Cluster ID; L - length (mm); SZN - season; MH - microhabitat; FLT - flatline temperature (°C); FBT - final breakpoint temperature (°C); CSR - cardiac suppression range; H - height (mm); W - width (mm); Wt - weight (mg); Th - thickness (mm).

NrC - Number of cases with a specific pattern; Tot - Total missing values in each variable; Pcnt - Percent of total cases that are missing; I_C - Number of incomplete variables in that pattern.

Data are MAR when the probability of missing data in an incomplete variable Y is dependent on other measured variables, but not on data within Y, representing a systematic relationship between one or more variables and missing data in Y. This is in contrast to MNAR missingness, where missing values in Y are dependent on other measured variables and are correlated with observed and unobserved values in Y (Biro & Dingemanse 2009). In MCAR data, the probability of missing values in Y is the same for all cases and unrelated to data in all measured variables (Rubin 1976, Graham 2009) but, see Enders (2010) pp. 24-27 for a more detailed explanation. Truly distinguishing the missingness of an incomplete dataset, particularly the difference between MAR and MNAR, is not always possible because the information needed to achieve that is often held in the missing cases. However, several tests (Little 1988, Ridout & Diggle 1991, Buuren 2018) and graphic functions are available to help develop an idea about potential

missingness, e.g., logistic regression analysis, t -tests and Little's MCAR test from the naniar package (Tierney et al. 2021). In this study, the MCAR test indicated significant differences (χ^2=56.2484 , p<0.001) between observed and estimated means in each missing data pattern, suggesting that missingness for the incomplete data were not MCAR (Table 5.3).

Table 5.3: Littles' MCAR test statistic for continuous variables in the simulated incomplete data of *Siphonaria capensis*.

statistic	**df**	**p.value**
56.2484	13	0.0001

Figure 5.3 and 5.4 serve as visual diagnostic tools to help determine the likelihood that data may be MAR, by determining if missing data in Y depend on other variables (Buuren 2018). Here (Figure 5.3), the missing data rate for FBT was not equally distributed across site, microhabitat, or season. This indicates an MAR dependence of FBT on the explanatory variables that also applies to the other thermal limit variables because the missing data pattern and rate were exactly the same (Table 5.2). By this logic, missingness in shell height and width were also likely MAR (Figure 5.4), despite a more severe missing data problem for these two variables.

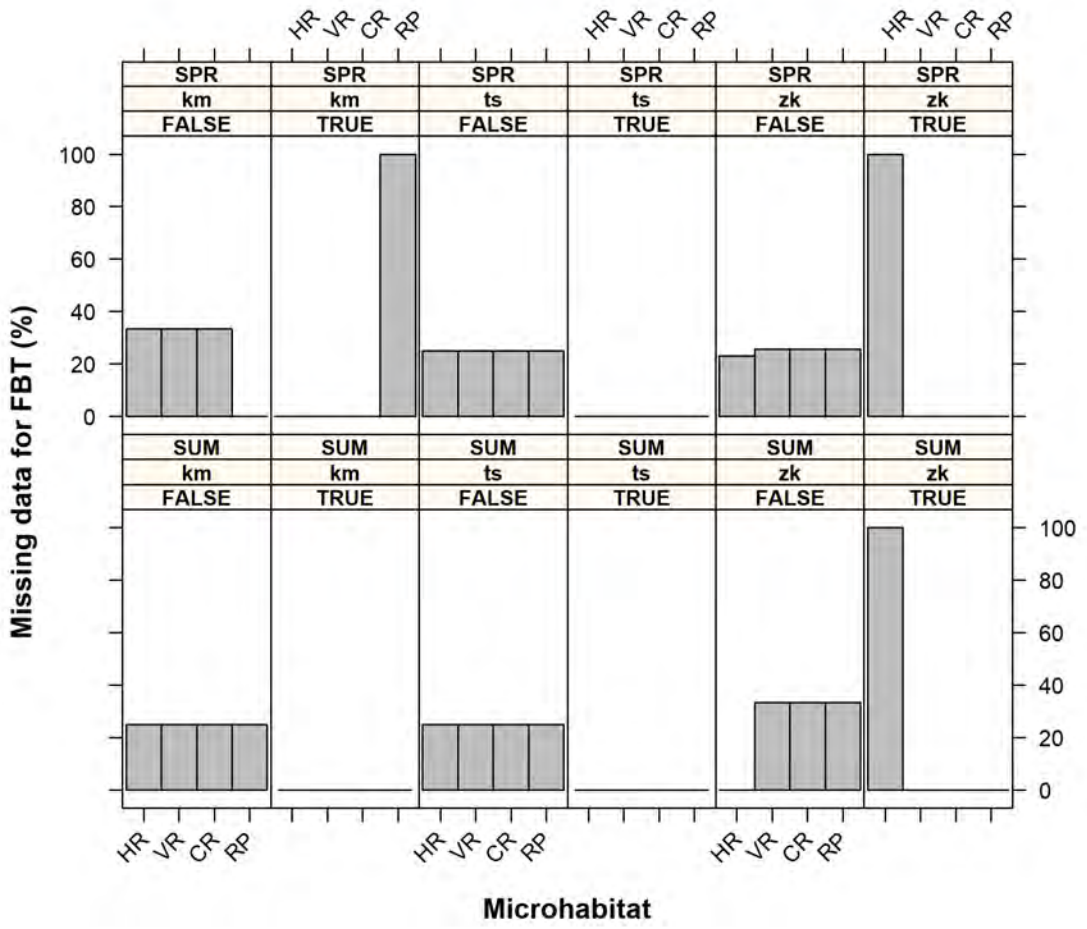

Figure 5.3: Bar plots displaying the missing data rate (%) for the variable FBT (final breakpoint temperature °C) for *Siphonaria capensis* across microhabitats (HR - horizontal rock; VR - vertical rock; CR - crevice; RP - rock pool), sites (zk - Zinkwazi; ts - Three Sisters; km - Kommetjie) and seasons (SUM - summer; SPR - spring) in the incomplete dataset. Panels with the facet label 'true' indicate that values are missing.

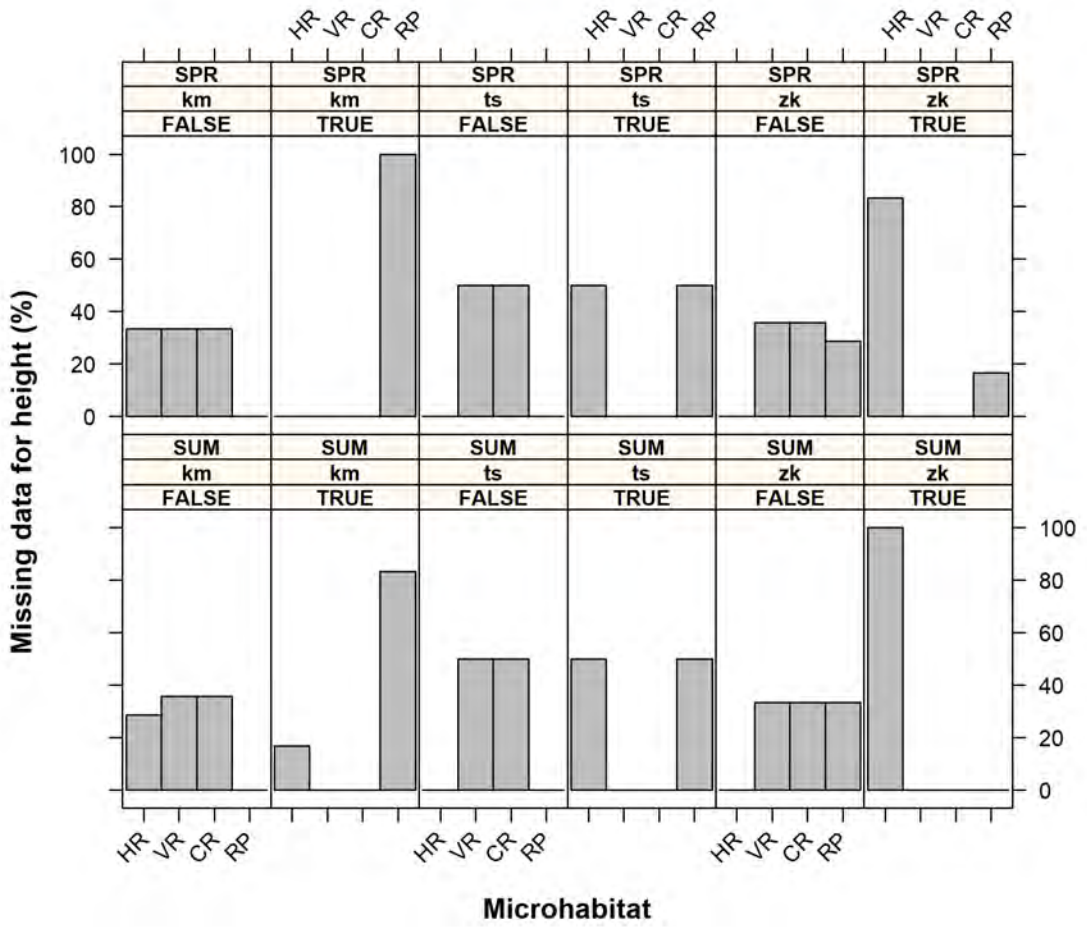

Figure 5.4: Bar plots displaying the missing data rate (%) for the shell height variable in *Siphonaria capensis* across microhabitats (HR - horizontal rock; VR - vertical rock; CR - crevice; RP - rock pool), sites (zk - Zinkwazi; ts - Three Sisters; km - Kommetjie) and seasons (SUM - summer; SPR - spring) in the incomplete dataset. Panels with the facet label 'true' indicate that values are missing.

5.3.5.2 Data Imputation

A clear idea regarding the missing data mechanism is important because that governs how missing data problems are handled. Traditional techniques (e.g., single imputation methods, listwise and pairwise deletion) are heavily reliant on the assumption that incomplete data are MCAR (Little 1988, Peugh & Enders 2004). Using these techniques when the data are MAR or MNAR invariably generates distorted parameter estimates

and, in the case of single imputation, attenuated standard errors. Even where MCAR holds, traditional deletion-based techniques are considered wasteful and result in reduced statistical power (Schafer & Graham 2002). For these reasons, many researchers advise against their use (Brown 1994, Arbuckle 1996, Wothke 2000, Enders 2001) and instead advocate for more advanced techniques (e.g., multiple imputation and maximum likelihood estimation) that yield unbiased results in MAR or MCAR scenarios (Little 1988, Carpenter & Kenward 2012).

MNAR cases present more complex problems, with few substantive options available to deal with them (Buuren & Groothuis-Oudshoorn 2011). Possible solutions for MNAR often involve finding more data to clarify potential causes of missingness or performing a sensitivity analysis (Little 2008, Verbeke & Davidian 2009). Despite their robustness (Carpenter & Kenward 2012), applying multiple imputation or maximum likelihood estimation under MNAR will likely also lead to biased estimates, underlining the importance of clearly understanding the missingness problem. Overall, the tests and diagnoses performed here provide sufficient evidence to suggest MAR missingness. Consequently, the missing data were addressed using "multiple imputation by chained equations" with the mice package (Buuren & Groothuis-Oudshoorn 2011). Through multiple imputation, several completed (m) datasets are produced by repeatedly sampling from the Bayesian posterior distributions of the missing data, based on observed values and parameters from the imputation model. Each of these m datasets undergo individual analysis using conventional data analysis techniques. Subsequently, the results are combined using Rubin's rules to provide a consolidated inference (Rubin 1987, Enders 2010). Keeping the imputation and analysis phase separate allows for the inclusion of auxiliary variables (e.g., Cluster ID in Table 5.2) in the multiple imputation model to improve its predictive power and help ensure MAR (Collins et al. 2001), without sacrificing parsimony in the substantive analysis model. A multilevel model with random intercepts (Snijders & Bosker 2011), including interaction terms, represented the model of interest in this case (Equation 5.1).

$$
\begin{aligned}
Y_{ij} = \alpha_0 &+ \beta_0 X_{1ij} + \alpha_1 Z_{1j} + \alpha_2 Z_{2j} + \beta_1 Z_{1j} X_{1ij} \\
&+ \beta_2 Z_{2j} X_{1ij} + \beta_3 X_{2ij} + \beta_4 Z_{1j} X_{2ij} + \beta_5 Z_{2j} X_{2ij} \\
&+ \beta_6 X_{3ij} + v_j X_{1ij} + v_j X_{2ij} + u_j + \epsilon_{ij}
\end{aligned}
$$

where (5.1)

$$
\begin{aligned}
\epsilon_{ij} &\sim N(0, \sigma^2) \\
u_j &\sim N(0, \sigma_u^2) \\
v_j &\sim N(0, \sigma_v^2)
\end{aligned}
$$

In Equation 5.1, Y_{ij} is the response variable FLT, where α_0 is the grand intercept, and the equation symbols α_1 and α_2 represent regression coefficients for the average FLT in different sites (Z_{1j}) and seasons (Z_{2j}). The symbols β_0, β_3 and β_6 denote regression slopes for the continuous predictors FBT (X_{1ij}), CSR (X_{2ij}) and shell length (X_{3ij}), correspondingly. β_1 and β_2 account for FBT's interactions with the categorical predictors site and season, respectively, while β_4 and β_5 capture CSR's interactions with site and season. Residual variance ϵ_{ij} represents the individual-level variability not explained by the model, and it's assumed to have a mean of 0 with a variance of σ^2. The microhabitat level introduces the random effects u_j, $v_j X_{1ij}$ and $v_j X_{2ij}$. These random effects are assumed to be independent of the residuals and each other, and they all have a mean of 0. Specifically, u_j has a variance of σ_u^2, while the terms involving v_j have a variance of σ_v^2. microhabitats are denoted by subscript j ($1 \ldots J$) and individual limpets by subscript i ($1 \ldots n_i$).

By imputing in repeated sequential cycles, updating current imputed estimates with values from the previous cycle each time, the uncertainty involved in replacing missing values is incorporated into the multiple imputation process (Buuren & Groothuis-Oudshoorn 2011). The fully conditional specification feature implemented in mice allows for the handling of multilevel data (Buuren & Groothuis-Oudshoorn 2011). Multiple imputation models must be as or less structurally complex than the substantive model to ensure valid statistical inferences (Schafer 2003, Hippel 2009, Andridge 2011, Drechsler 2015, Enders et al. 2016). This is achieved using fully conditional specification by permitting the imputation of each incomplete/target variable separately,

using some or all of the remaining variables as predictors in the imputation model. Utilizing dummy indicator variables to represent each categorical predictor group helps account for multilevel structure during multiple imputation (White et al. 2011, Ludtke et al. 2017).

A “fluxtable” (Table 5.4), generated from the fluxplot function in mice, was used to determine model predictors by comparing influx and outflux values among variables (Buuren 2018). Influx refers to the dependence of a variable on other variables for imputation, while outflux refers to the dependence of other variables on a given variable for imputation. A high influx indicates a high rate of missing data in a given variable, whereas a high outflux means the variable has substantial influence in the imputation of other variables. Relatively high influx (0.2808) and low outflux values (0) are observed for both height and width. Moreover, they exhibit strong correlations with length, with correlation values of 0.8494 for height and 0.9421 for width (Table 5.1). This highlights both height and width as low-quality predictors that should not be used. Additionally, the similar influx and outflux values observed among groups of variables, such as the thermal limit variables FBT, CSR, and FLT (Table 5.4), can be attributed to the shared missing data pattern (Table 5.2) and similar missingness among them. As mentioned previously in Section 5.3.5 for the analysis of missing data, missing values were predominantly generated when thermal response curves could not be used for heart rate analyses. This leads to simultaneous missingness and results in similar influx and outflux values across these variables.

Table 5.4: Influx and outflux statistics for the simulated missing data of *Siphonaria capensis*.

Var	influx	outflux
IND	0.0000	1.0000000
L	0.0000	1.0000000
SZN	0.0000	1.0000000
SITE	0.0000	1.0000000
MH	0.0000	1.0000000
FLT	0.0484	0.5454545
FBT	0.0484	0.5454545
CSR	0.0484	0.5454545
H	0.2808	0.0000000
W	0.2808	0.0000000

Var - Variables; IND - Individual; CID - Cluster ID; L - length (mm); SZN - season; MH - microhabitat; FLT - flatline temperature (°C); FBT - final breakpoint temperature (°C); H - height (mm); W - width (mm)

Added advantages of full conditional specification are its non-dependence on the assumption of multivariate normality and the reduction of group level bias through the inclusion of pre-calculated group means (Buuren 2018, Grund et al. 2018). These, along with any product terms in interactions, were accounted for by using passive imputation which, facilitates the recalculation of interaction terms after the imputation of their constituents (Royston 2004, Enders et al. 2016, Buuren 2018). The target variables FBT and FLT were imputed using the 2l.pan imputation method from the pan package (Grund et al. 2016), to allow for variance and covariance at level 1 and level 2 (Andridge 2011). Both size variables, height and width, were imputed using the general purpose imputation method, predictive mean matching (pmm) in mice, because it does not rely on the normality assumption (Little 1988, Buuren 2018). Predictive mean matching can also be used on data with skewed distributions, because it preserves the distribution of the data (White et al. 2011), making it ideal for the imputation of cardiac suppression

range (CSR). Prior to its imputation, a constant +1 was added to CSR before log-transformation to mitigate problems faced log transforming zeros (Lee & Carlin 2010, White et al. 2011, Buuren 2018). This has been shown to yield favourable results for zero-inflated data with skewed distributions by MacNeil-Vroomen et al. (2016). Contrary to MacNeil-Vroomen et al. (2016), however, I chose not to back-transform the data prior to analysis, thus maintaining a linear relationship between the predictor and response variables. In the study by MacNeil-Vroomen et al. (2016), they used a Generalized Linear Mixed Model with a gamma distribution specifically to address the skewed nature of the response variable in the analysis. Considering other variables with distributional issues, such as the bimodality observed in length (Figure 5.2), the primary concern is ensuring overall model fit and meeting model assumptions. Since the model assumptions for the mixed effects model are met (see Section A4), and because mixed effects models are generally robust to bimodal distributions (Schielzeth et al. 2020), the bimodality of length is unlikely to pose a significant issue. As a rule of thumb, White et al. (2011) suggest that the number of imputations should at least equal the highest percentage of missing cases in the incomplete data. In this instance, the number of imputations was set to 100 with 5 iterations, far surpassing 35%, the highest missing data rate for the eligible dataset (Table 5.2). Notably, this specified amount also exceeds the highest missing data rates observed for the real *Siphonaria capensis* and *S. serrata* datasets, allowing for the same number of imputations and iterations to be applied during the imputation of the actual data.

5.3.5.3 Imputation diagnostics

Several graphic diagnostic tools are provided by mice to assess the quality of imputed data. These tools focus on distributional discrepancies, where similar distributions between imputed and observed data signify good imputations (Buuren 2018). Convergence plots (Figure 5.5 and 5.6), fit using autocorrelation and trace functions, helped assess the appearance of any trends in the imputed thermal limit and size variables (Schafer & Olsen 1998, Enders 2010). Variance between the imputation chains

were equal to variance within chains and there were no clear signs of autocorrelation for either set of variables, which is indicative of unproblematic convergence.

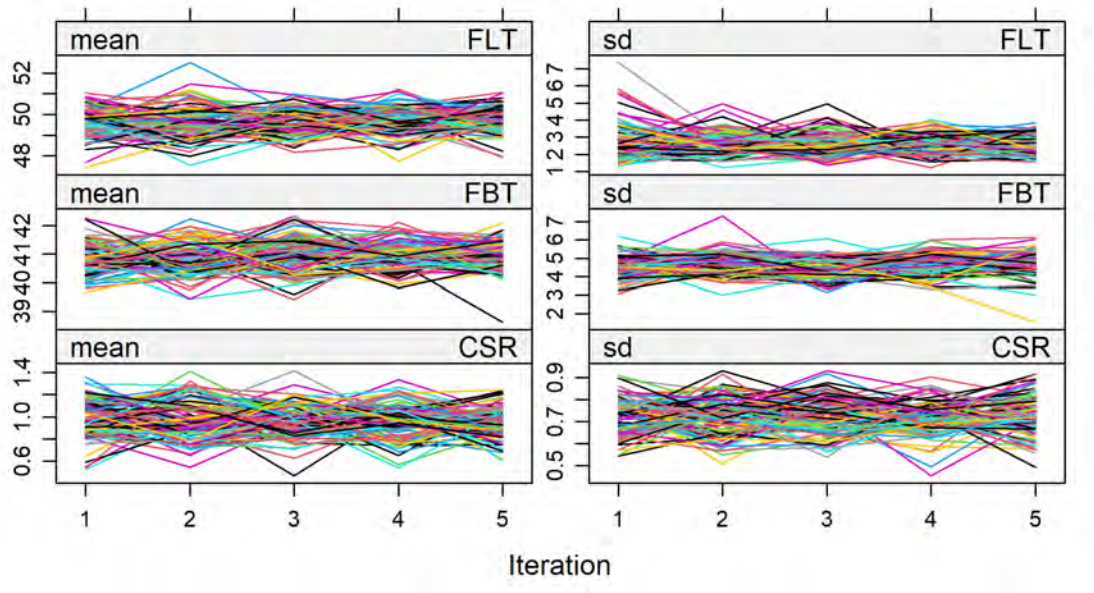

Figure 5.5: Convergence plots displaying mean and standard deviation (SD), for the thermal limit variables of *Siphonaria capensis* data, plotted against 5 iterations of the imputed data. *FBT - final breakpoint temperature (°C); FLT - flatline temperature (°C); CSR - cardiac suppression range (°C).*

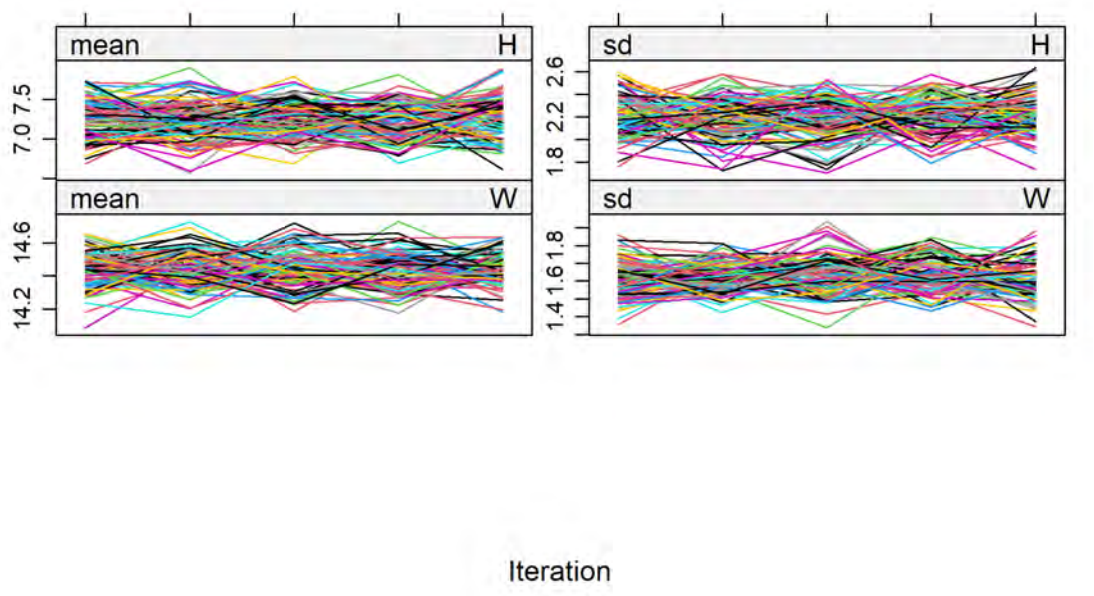

Figure 5.6: Convergence plots displaying mean and standard deviation (SD), for the size variables of *Siphonaria capensis* data, plotted against 5 iterations of the imputed data. *H - height (mm); W - width (mm).*

The bwplot function was used to evaluate distributions among datasets, with "side-by-side" box-and-whisker plots for the observed and imputed data (Figure 5.7). These revealed potential systematic differences for the FBT outcome, where imputed data values were slightly larger than observed data. This is usually associated with MNAR or a problem with the multiple imputation model (Buuren & Groothuis-Oudshoorn 2011). It can, however, be seen from Figure 5.3 that missing values for FBT were mostly linked to warmer microhabitats, sites and/or seasons. This implies that the higher imputed values reflect an expected positive relationship between these thermal limits and spatiotemporal thermal conditions (Somero 2002, Norin et al. 2014, Xing et al. 2016), offering a reasonable explanation for larger imputed FBT values.

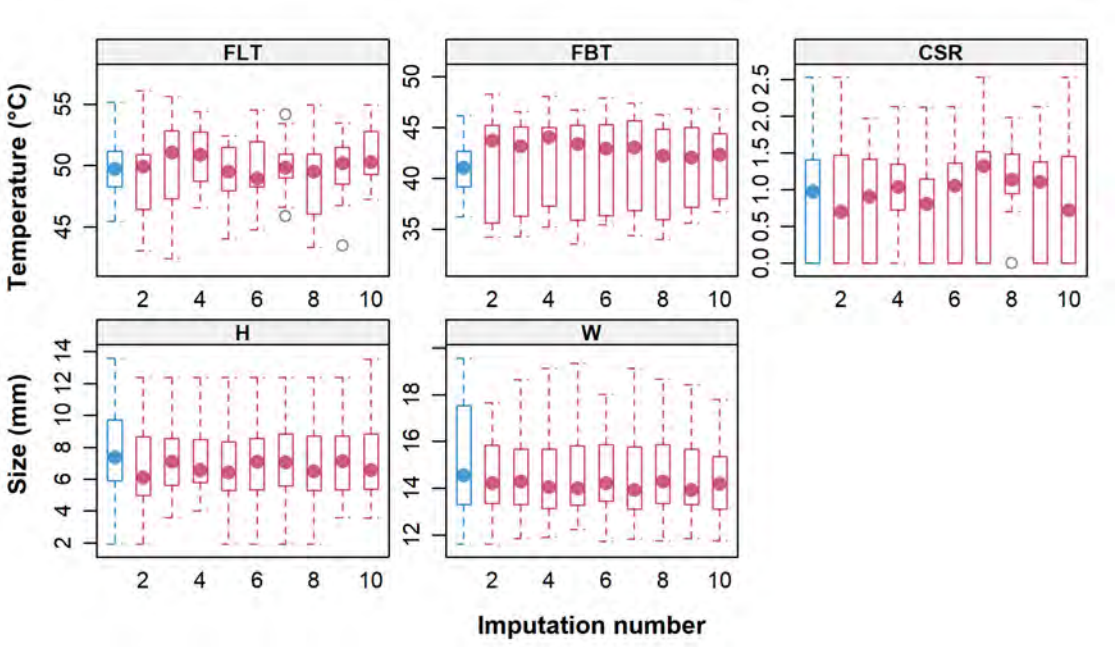

Figure 5.7: Box-and-whisker plots comparing the distribution within variables of the first 9 multiply imputed datasets (in pink) with the incomplete dataset (in blue) for *Siphonaria capensis*. *FBT - final breakpoint temperature (°C), FLT - flatline temperature (°C), CSR - cardiac suppression range (°C), H - height (mm), W - width (mm).*

Further exploration shows that the relationships between FLT and FBT, and between FBT and CSR, were preserved in the imputed data (Figure 5.8 and 5.9). The distribution of imputed values for both sets of variables was on the high and low end of observed values i.e., missing values were imputed according to their missing data patterns. This lends more credence to the MAR assumption and provides evidence that there were no substantial problems with the multiple imputation model.

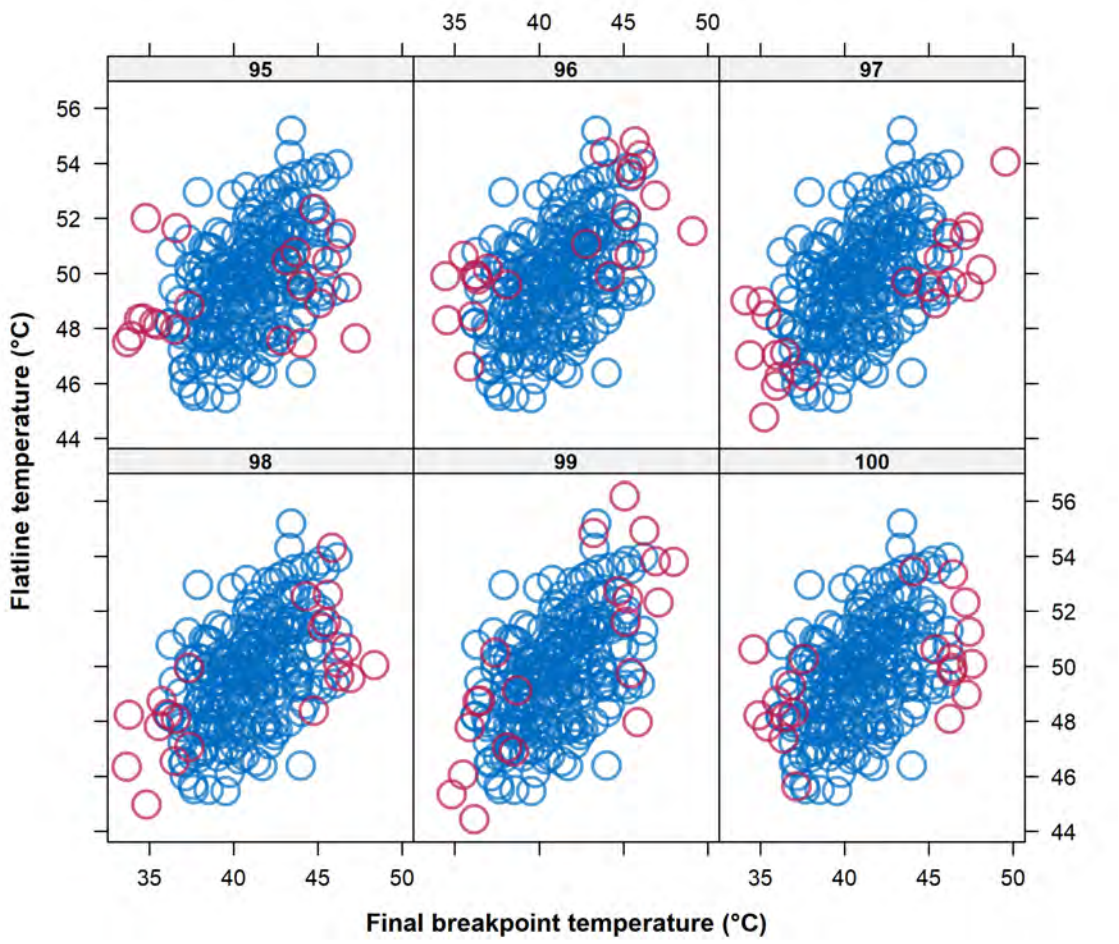

Figure 5.8: Scatterplots illustrating the relationship between flatline (FLT) and final breakpoint (FBT) temperatures (°C) in the last six multiple imputations (number displayed in strip panel), contrasting imputed (pink) with incomplete (blue) data for *Siphonaria capensis*.

The persistent presence of zero values in the imputed data involving CSR, as shown in Figure 5.9, reflects the fact that the available analytical strategies for addressing zero-inflated data do not directly eliminate these zeros. Instead, these strategies account for and model the prevalence of zeros within the data. Their overarching goal is to generate normalized residuals, whilst concurrently tackling the heteroscedasticity typically associated with the non-zero portions of right-skewed, zero-inflated datasets (MacNeil-Vroomen et al. 2016, Liu et al. 2019).

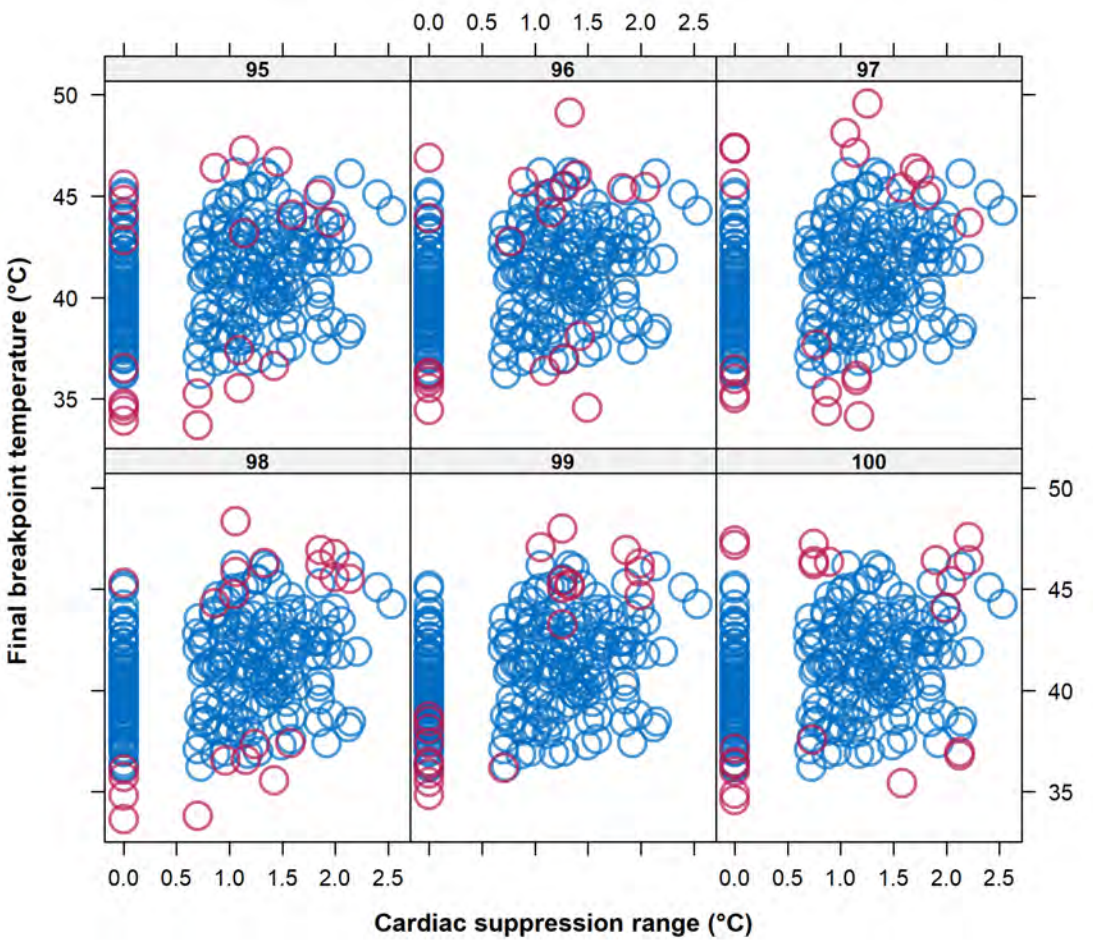

Figure 5.9: Scatterplots illustrating the relationship between cardiac suppression range (CSR) and final breakpoint temperature (FBT) in the last six multiple imputations (number displayed in strip panel), contrasting imputed (pink) with incomplete (blue) data for *Siphonaria capensis*.

5.3.6 Statistical analysis

A principal components analysis (PCA) was used to help reduce the dimensionality of the imputed datasets (Section A4.1.2) by omitting redundant variables prior to the main analysis (Zuur 2007). The prcomp function was used to compute the PCA, with data zero centred and scaled to unit variance, and the associated biplot was produced using the biplot function from the stats package (R Core Team 2021).

Three main analysis models were specified for the complete, incomplete and imputed

data (incomplete and imputed data are collectively referred to as "test data"), to compare parameter estimate accuracy between the test data, with the complete data analysis results set as the reference. First, variations in the effect of the continuous predictor FBT on the response variable FLT were compared using a multivariate linear mixed effects model. This is the recommended modelling method to account for data dependencies, borne out of nested structures, by including random effects (Goldstein 2011, Snijders & Bosker 2011). Building on the same rationale, I used a linear mixed model (LMM) to elucidate the covariance between the semi-continuous predictor CSR and the response variable FBT in the second analysis model. The variable microhabitat was treated as a random intercept for all LMMs because microhabitats represent a random sample from the broader set of rocky intertidal habitats in this study, individual observations are nested within these microhabitats (Gomes 2022), and model diagnostics did not reveal any major issues with this specification (Section A4). Meanwhile, season and site were treated as fixed categorical variables, and length was controlled for as specified in Equation 5.1. The intraclass correlation coefficient ICC1 was also determined using the equation below, as a measure of non-independence within microhabitat observations. High ICC1 values (>0.1) necessitate the use of multilevel models (Bliese 2000).

$$p = \frac{\tau_{00}}{(\tau_{00}+\sigma^2)}$$

Here, the proportion of variance (p) was calculated with τ_{00} representing between-group variance and σ^2 representing within-group variance. Finally, FBT was compared between seasons and among three sites for the *Siphonaria capensis* data and between two sites for the *S.serrata* data for each season, using a factorial analysis of variance (ANOVA), with a three-way interaction between microhabitat, site and season. Limpet sizes (length) were also compared among the three sites for *S.capensis* data and two sites for *S.serrata* data using a factorial ANOVA, with an interaction between microhabitat and site.

All linear mixed models were run using the lmer function in the lme4 package (Bates et al. 2015). Mixed model statistics for the multiply imputed data were pooled using the standard pool function from mice. For the ANOVAs, base R's aov function was used for

the complete and incomplete data, and the mi.anova function in the miceadds package was used to analyse the imputed data and to test for differences in length (Robitzsch & Grund 2022). The mi.anova function's default D2 statistic was used to pool ANOVA results, because it is easily implemented and suitable for most ANOVA applications (Grund et al. 2016).

Raw coefficient bias and root mean square error (RMSE) were used to assess parameter accuracy, while comparisons of the significance outcome determined if effect significance in the complete data analysis corroborated that of the test analyses (Buuren 2018). The significance outcome refers to whether the p-values for the parameter estimates indicate that the effects of the predictors are statistically significant or not ("Yes"/"No"). Together, these key performance indicators (KPI) were used to evaluate the test analyses against each other. Bias was estimated by calculating the difference between the parameter estimates from the test analyses and the true population parameters. The RMSE was determined by calculating square difference from the square root of estimates and true parameters, providing an overall measure of parameter estimate accuracy. Optimal estimators had a bias below 0.1, a comparatively small RMSE, and accurately assigned significance outcomes (Grund et al. 2018). The diagnostic summary of the multiple imputation indicates that the analyses based on the imputed data produced parameter estimates that are within acceptable limits, and therefore statistically reliable (see Section A4.1.1).

Only the imputed versions of the actual datasets were considered for *post hoc* analyses. Treatment coding (or dummy coding) systems are automatically used to represent categorical variable groups in linear mixed models (Dalgaard 2002, Zuur et al. 2009, Brown 2021). Spring and Zinkwazi were set as the initial reference levels (represented by the intercept where dummy code = 0) for season and site against which the magnitude and direction of subsequent mean estimates were assessed. *Post hoc* testing for linear mixed models consisted of changing the reference levels for season and site to ensure all relevant contrasts were included in the model interpretation (Dalgaard 2002, Zuur et al. 2009). Thereafter, a Benjamini–Hochberg false discovery rate (FDR) correction was

used to adjust p-values for multiple testing. Pairwise, Tukey adjusted contrasts were computed for the multiply imputed ANOVA, using the estimated marginal means emmeans package (Lenth 2023), as described in Section 2.3.5 and 3.3.3, to determine where significant differences in FBT and length lay.

5.4 Results

5.4.1 Relationship between flatline and final breakpoint temperature

It is evident from Figure 5.10 that there was a positive correlation between FLT and FBT for *Siphonaria capensis* (Table 5.5). For spring at Zinkwazi, Three Sisters and Kommetjie, each unit increase in FBT led to a significant average FLT increase of 0.66°C ($p < 0.0001$), 0.51°C ($p < 0.0001$) and 0.49°C ($p < 0.0001$), respectively, with no significant differences in the slopes among sites. In summer, however, the positive effect of FBT on average FLT was only significant at Zinkwazi ($p < 0.01$) and Three Sisters ($p < 0.05$), with no significant differences in slope among sites or for any of the remaining predictors (Table 5.5).

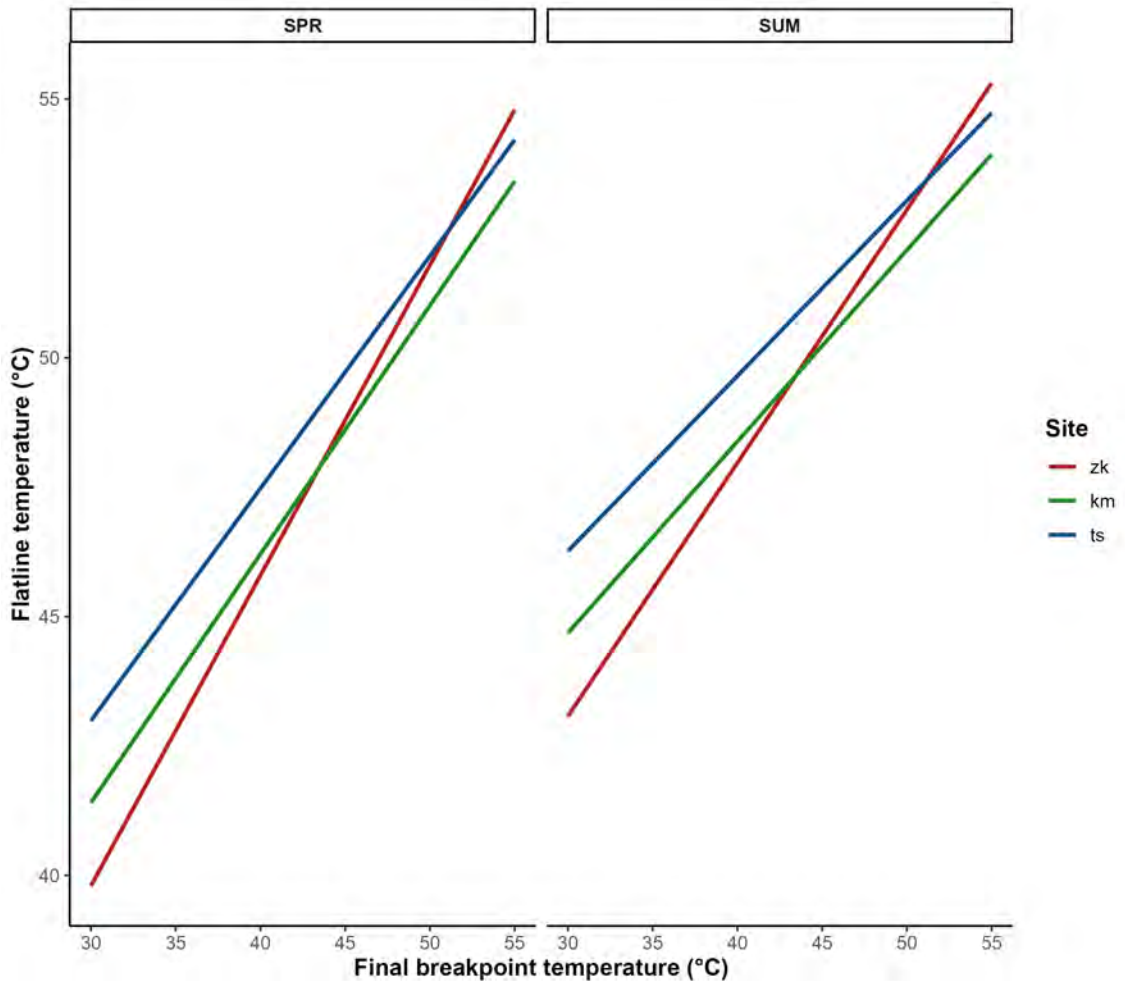

Figure 5.10: Relationship between FLT (°C) and FBT (°C) across seasons (SUM - Summer; SPR - Spring) and sites (zk - Zinkwazi; ts - Three Sisters; km - Kommetjie) for *S. capensis*.

The variance estimates for the microhabitat random effect, in the *S. capensis* dataset, indicates that FLT varied around the average intercept by about 0.09°C, less than the residual variance of 8.32°C. This pattern, coupled with an ICC of 0.01 (Bliese 2000), signifies higher within-group than between-group variation.

Table 5.5: Summary of the pooled linear mixed model (LMM) analysing the influence of FBT (°C), season, and site on FLT (°C) variation in *S. capensis*, while accounting for the effect of length (mm). The model incorporates season, site, and their interactions with FBT as fixed effects, with microhabitat treated as a random effect. Only predictors with estimates that have non-adjusted p-values less than 0.05 are displayed.

lmm	term	estimate	std.error	statistic	df	p.value	p.FDR
or_LMM	**Intercept1**	21.6391	6.6318	3.2629	98.8213	0.0015	< 0.01
	FBT	0.6593	0.1434	4.5982	96.9922	0.0000	< 0.0001
re1_LMM	**Intercept2**	28.7034	5.7742	4.9710	118.4413	0.0000	< 0.0001
	FBT	0.5129	0.1160	4.4206	127.6505	0.0000	< 0.0001
re2_LMM	**Intercept3**	29.5029	5.4708	5.3928	120.4419	0.0000	< 0.0001
	FBT	0.4947	0.1059	4.6699	134.2267	0.0000	< 0.0001
re3_LMM	**Intercept4**	30.9131	5.9583	5.1882	98.1589	0.0000	< 0.0001
	FBT	0.4848	0.1290	3.7592	95.0835	0.0003	< 0.01
re4_LMM	**Intercept5**	37.9773	6.2330	6.0929	107.0856	0.0000	< 0.0001
	FBT	0.3384	0.1274	2.6557	110.2125	0.0091	< 0.05
re5_LMM	**Intercept6**	38.7769	6.5550	5.9156	118.2336	0.0000	< 0.0001
	FBT	0.3202	0.1296	2.4711	128.2200	0.0148	0.0665
All	**Intercept|MH**	0.0943	NA	NA	NA	NA	NA
	Residual	8.3200	NA	NA	NA	NA	NA
	ICC|MH	0.0111	NA	NA	NA	NA	NA

FLT - flatline temperature (°C); FBT - final breakpoint temperature (°C); Intercept|MH - microhabitat random effect.

Model includes Benjamini-Hochberg, false discovery rate, corrected p.values (p.FDR).

The variable LMM specifies LMMs fit with different reference levels for the categorical predictors season and site.

or_LMM - Spring and Zinkwazi; re1_LMM - Spring and Three Sisters; re2_LMM - Spring and Kommetjie; re3_LMM - Summer and Zinkwazi; re4_LMM - Summer and Three Sisters; re5_LMM - Summer and Kommetjie.

As for *Siphonaria capensis* (Figure 5.10), there was some evidence of a positive

relationship between the FLT and FBT of *S. serrata* (Figure 5.11). In this case, however, the effect of FBT on FLT was non-significant for all seasons, across sites, except for Kommetjie in summer ($p < 0.05$). The effects of all other predictors of FLT variation for *S. serrata* were non-significant (Table 5.6).

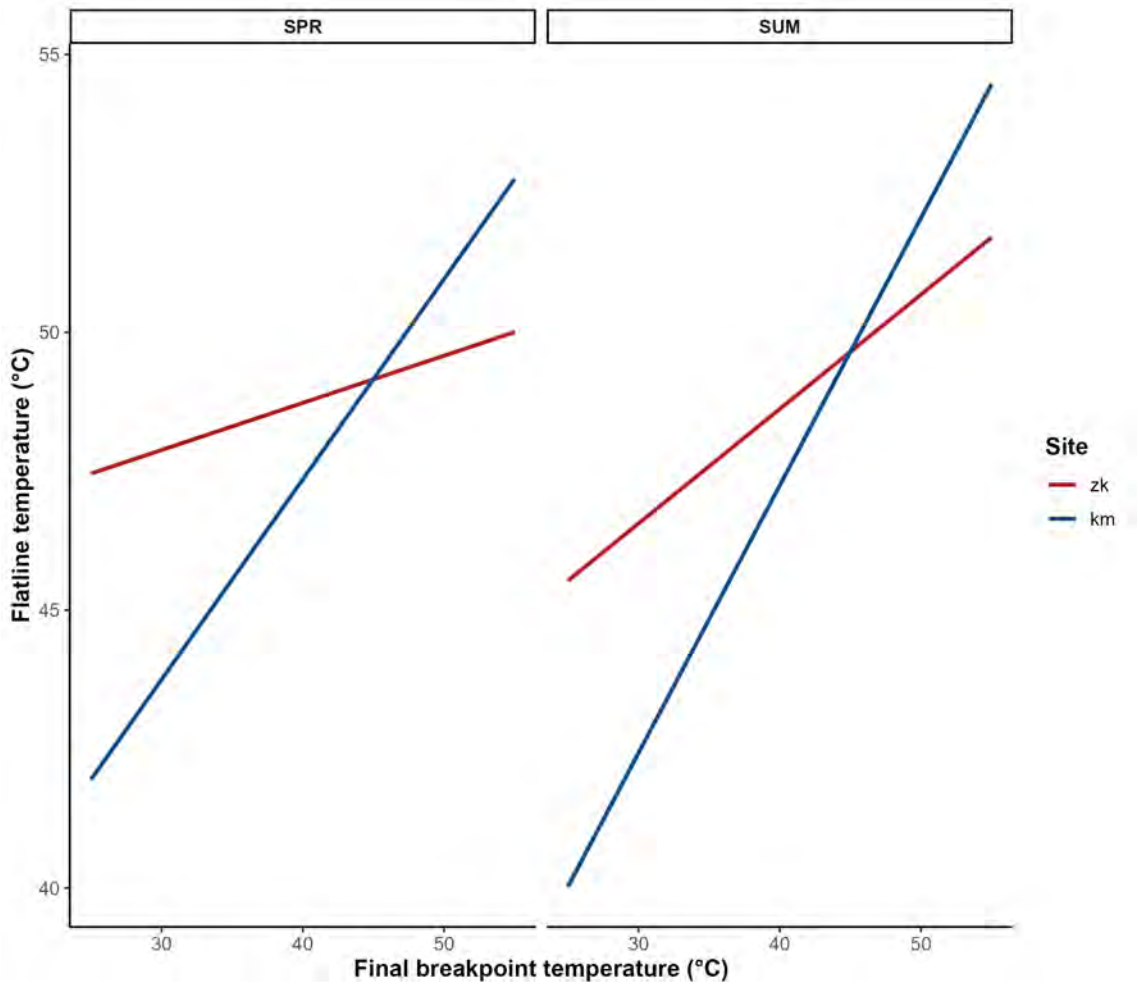

Figure 5.11: Variation in the Relationship between FLT (°C) and FBT (°C) across seasons (SUM - Summer; SPR - Spring) and sites (zk - Zinkwazi; km - Kommetjie) for *S. serrata*.

A residual variance of 12.8°C, similar to the high residual variance of the random intercept for the linear mixed model on *S. capensis* (Table 5.5), suggests minimal clustering by microhabitat for *S. serrata* (Table 5.6).

Table 5.6: Summary of the pooled linear mixed model (LMM) analysing the influence of FBT (°C), season, and site on FLT (°C) variation in *S. serrata*, while accounting for length (mm). The model incorporates season, site, and their interactions with FBT as fixed effects, with microhabitat treated as a random effect. Only predictors with estimates that have non-adjusted p-values less than 0.05 are displayed.

lmm	term	estimate	std.error	statistic	df	p.value	p.FDR
or_LMM	**Intercept1**	44.9478	7.0930	6.3370	81.6858	0.0000	< 0.0001
re1_LMM	**Intercept2**	35.9246	6.7765	5.3013	111.5881	0.0000	< 0.0001
	FBT	0.3511	0.1528	2.2985	108.7524	0.0234	0.1094
re2_LMM	**Intercept3**	40.2223	6.5995	6.0947	89.3116	0.0000	< 0.0001
	FBT	0.2851	0.1411	2.0198	84.5299	0.0466	0.1863
re3_LMM	**Intercept4**	31.1990	7.7765	4.0120	102.7510	0.0001	< 0.001
	FBT	0.4768	0.1630	2.9242	103.5910	0.0042	< 0.05
All	**Intercept|MH**	0.0577	NA	NA	NA	NA	NA
	Residual	12.7953	NA	NA	NA	NA	NA
	ICC|MH	0.0040	NA	NA	NA	NA	NA

FLT - flatline temperature (°C); FBT - final breakpoint temperature (°C); Intercept|MH - microhabitat random effect.

Model includes Benjamini-Hochberg, false discovery rate, corrected p.values (p.FDR).

The variable LMM specifies LMMs fit with different reference levels for the categorical predictors season and site.

or_LMM - Spring and Zinkwazi; re1_LMM - Spring and Kommetjie; re2_LMM - Summer and Zinkwazi; re3_LMM - Summer and Kommetjie.

5.4.2 Relationship between final breakpoint temperature and cardiac suppression range

Figure 5.12 shows a positive relationship exists between FBT and CSR for *Siphonaria capensis*, although this relationship was context-dependent (Table 5.7). For instance, during spring and summer, the overall effect of CSR on FBT was non-significant at Zinkwazi ($p = 0.1409$), whereas CSR had a significant positive effect on FBT at Three

Sisters and Kommetjie in both seasons ($p < 0.05$ for all significant effects). There were no significant effects for any of the other predictors of FBT variation (Table 5.7).

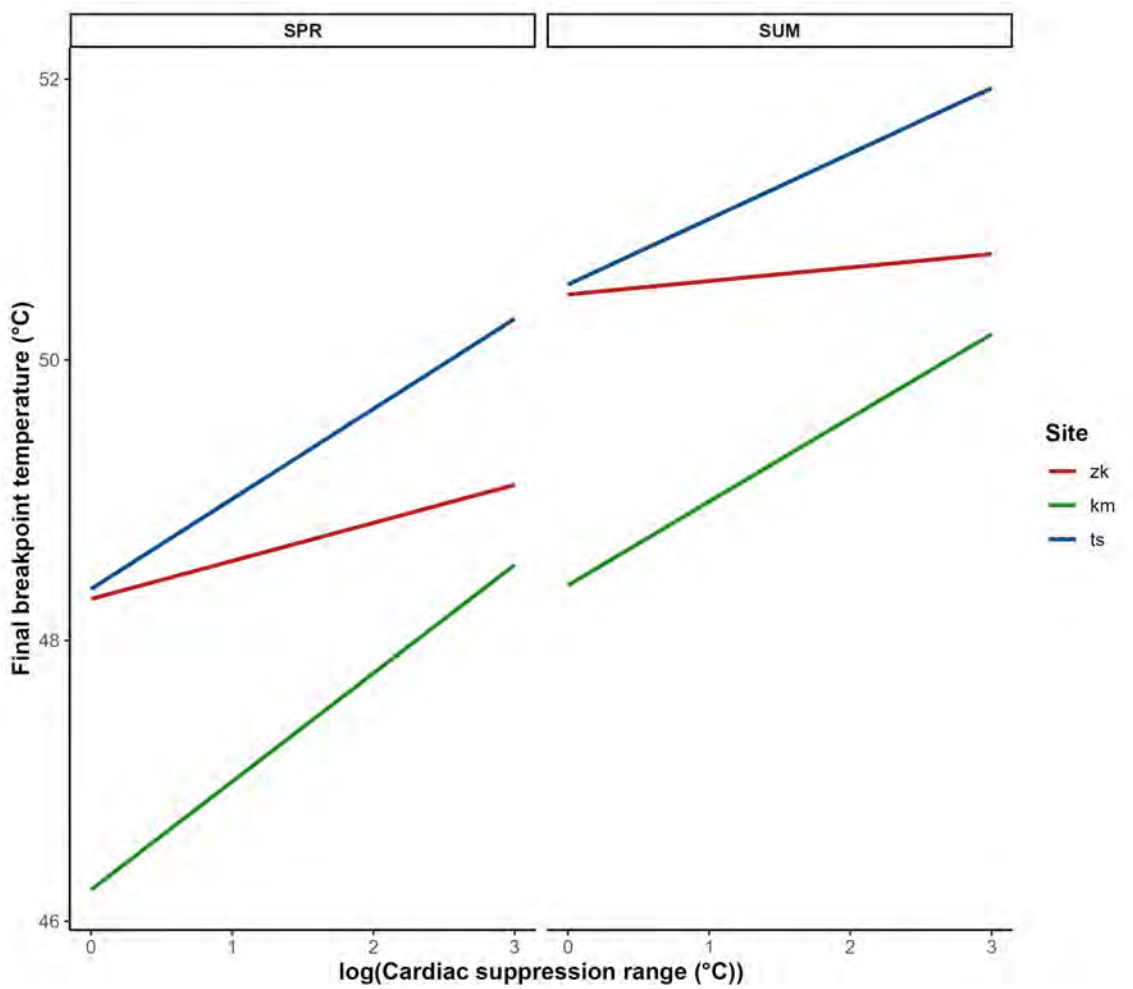

Figure 5.12: Variation in the relationship between FBT (°C) and the natural log of CSR (°C) across seasons (SUM - Summer; SPR - Spring) and sites (zk - Zinkwazi; ts - Three Sisters; km - Kommetjie) in *Siphonaria capensis*.

The microhabitat random effect suggests that the variations in the FBT of *S. capensis* around the mean intercept of about 0.33°C, was much less than the 12.93°C residual variance (Table 5.7).

Table 5.7: Summary of the pooled linear mixed model (LMM) analysing the influence of CSR (°C), season, and site on FBT (°C) variation in *Siphonaria capensis*, while accounting for length (mm). The model incorporates season, site, and their interactions with FBT as fixed effects, with microhabitat treated as a random effect. Only predictors with estimates that have non-adjusted p-values less than 0.05 are displayed.

lmm	term	estimate	std.error	statistic	df	p.value	p.FDR
or_LMM	**Intercept1**	39.0155	3.1329	12.4535	114.7585	0.0000	< 0.0001
	CSR	1.0588	0.4844	2.1860	124.9329	0.0307	0.1409
re1_LMM	**Intercept2**	38.2142	3.2864	11.6281	119.9467	0.0000	< 0.0001
	CSR	1.3929	0.5164	2.6973	113.8760	0.0081	< 0.05
re2_LMM	**Intercept3**	36.2345	4.0464	8.9547	114.3383	0.0000	< 0.0001
	CSR	1.4637	0.5027	2.9118	114.7426	0.0043	< 0.05
re3_LMM	**Intercept4**	40.2864	3.1746	12.6904	106.5029	0.0000	< 0.0001
	CSR	1.1887	0.5438	2.1858	94.2276	0.0313	0.1409
re4_LMM	**Intercept5**	39.4851	3.3114	11.9238	113.5577	0.0000	< 0.0001
	CSR	1.5228	0.5243	2.9047	104.1738	0.0045	< 0.05
re5_LMM	**Intercept6**	37.5053	4.0266	9.3143	112.9243	0.0000	< 0.0001
	CSR	1.5936	0.4908	3.2471	141.7288	0.0015	< 0.05
All	**Intercept|MH**	0.3241	NA	NA	NA	NA	NA
	Residual	12.9391	NA	NA	NA	NA	NA
	ICC|MH	0.0243	NA	NA	NA	NA	NA

FBT - final breakpoint temperature (°C); CSR - cardiac suppression range (°C); Intercept|MH - microhabitat random effect.

Model includes Benjamini-Hochberg, false discovery rate, corrected p.values (p.FDR).

The variable LMM specifies LMMs fit with different reference levels for the categorical predictors season and site.

or_LMM - Spring and Zinkwazi; re1_LMM - Spring and Three Sisters; re2_LMM - Spring and Kommetjie; re3_LMM - Summer and Zinkwazi; re4_LMM - Summer and Three Sisters; re5_LMM - Summer and Kommetjie.

A positive relationship between FBT and CSR was evident for *Siphonaria serrata*

(Figure 5.13). Unlike *S. capensis*, the effect of CSR on FBT was significant at both Zinkwazi ($p < 0.0001$) and Kommetjie ($p < 0.05$) in spring (Table 5.8). In summer, however, this effect was only significant at Zinkwazi ($p < 0.01$).

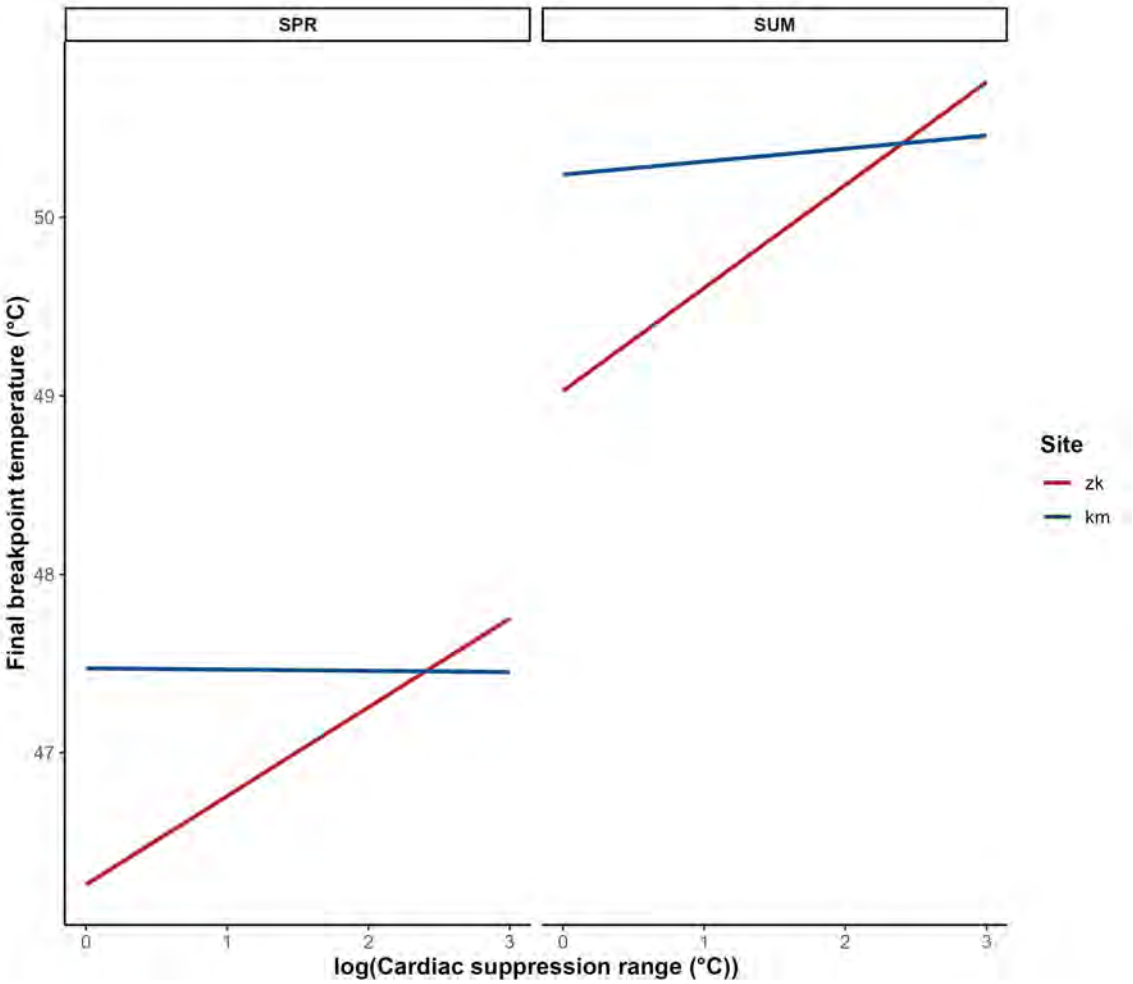

Figure 5.13: Variation in the relationship between FBT (°C) and the natural log of CSR (°C) across seasons (SUM - Summer; SPR - Spring) and sites (zk - Zinkwazi; km - Kommetjie) for *Siphonaria serrata*.

At Zinkwazi during summer, the intercept for FBT increased significantly by 3.6°C ($p < 0.01$) compared to spring, but there was no significant change in the slope ($p = 0.3130$). This indicates higher initial FBTs for *S. serrata* during summer, but no change in the effect of CSR on FBT between seasons. At Kommetjie, the intercept was significantly higher ($p < 0.01$), and the slope was significantly ($p < 0.05$) reduced compared to Zinkwazi. This indicates higher initial FBTs but a diminished effect of CSR on FBT at

Kommetjie in general. Furthermore, similar to *S. capensis*, the effect of length on FBT was generally non-significant. In terms of microhabitat variation, there was more within-group variability in the FBT values of *S. serrata* than between-group variability (Table 5.8), which was consistent with the patterns for *S. capensis* (Table 5.7).

Table 5.8: Summary of the linear mixed model (LMM) analysing the effect of CSR (°C), season, and site on FBT (°C) variation in *S. serrata*, with the effect of length (mm) accounted for. The model includes season, site, and their interactions with CSR as fixed effects, and treats microhabitat as a random effect. Only predictors with estimates that have non-adjusted p-values less than 0.05 are displayed.

lmm	term	estimate	std.error	statistic	df	p.value	p.FDR
or_LMM	**Intercept1**	31.9520	3.1095	10.2755	98.7474	0.0000	< 0.0001
	CSR	2.7773	0.5964	4.6570	71.8279	0.0000	< 0.0001
	SUM	3.5957	1.1027	3.2608	94.4227	0.0015	< 0.01
	km	4.6660	1.3582	3.4355	75.8426	0.0010	< 0.01
	CSR:km	-1.6124	0.5984	-2.6948	93.1773	0.0084	< 0.05
re1_LMM	**Intercept2**	36.6181	3.4932	10.4827	104.1884	0.0000	< 0.0001
	CSR	1.1648	0.4703	2.4768	102.4450	0.0149	< 0.05
re2_LMM	**Intercept3**	35.5477	2.7554	12.9011	104.1550	0.0000	< 0.0001
	CSR	2.1763	0.5663	3.8428	72.8152	0.0003	< 0.01
re3_LMM	**Intercept4**	40.2138	3.1772	12.6569	110.7648	0.0000	< 0.0001
All	**Intercept|MH**	0.1754	NA	NA	NA	NA	NA
	Residual	11.8155	NA	NA	NA	NA	NA
	ICC|MH	0.0140	NA	NA	NA	NA	NA

FBT - final breakpoint temperature (°C); CSR - cardiac suppression range (°C); Intercept|MH – microhabitat random effect.

Model includes Benjamini-Hochberg, false discovery rate, corrected p.values (p.FDR).

The variable LMM specifies LMMs fit with different reference levels for the categorical predictors season and site.

or_LMM - Spring and Zinkwazi; re1_LMM - Spring and Kommetjie; re2_LMM - Summer and Zinkwazi; re3_LMM - Summer and Kommetjie.

5.4.3 Potential season, site and/or microhabitat driven differences in FBT

The *Siphonaria capensis* samples collected during the study exhibited FBT values ranging from 31°C to 54°C, with an overall mean of 44°C. In the factorial ANOVA evaluating FBT values across microhabitats, sites and seasons (Table 5.9), neither the three-way interaction among season, site and microhabitat ($p = 0.51$) nor the main effects of these factors on FBT were significant. The interaction between season and site, however, did significantly effect FBT ($p < 0.05$).

Table 5.9: Results from the factorial ANOVA on the effect of the three-way interaction among season, site, and microhabitat on the FBT (°C) values of *Siphonaria capensis*. All factors were treated as fixed.

Parameters	SSQ	df1	F.value	p.value
SZN	131.027	1	3.488	0.063
SITE	92.029	2	1.336	0.264
MH	38.149	1	1.021	0.313
SZN:SITE	234.293	2	3.953	< 0.05
SZN:MH	38.432	1	1.173	0.279
SITE:MH	81.994	2	0.893	0.41
SZN:SITE:MH	86.154	2	0.681	0.507
Residual	3,268.301	NA	NA	NA

SZN - season; MH - microhabitat

During spring, mean *S. capensis* FBTs were significantly higher ($p < 0.05$) in Zinkwazi than in Kommetjie. Additionally, mean FBTs in Kommetjie were significantly higher ($p < 0.01$) in summer than in spring (Figure 5.14). There were no other significant differences in mean *S. capensis* FBTs when considering the *post hoc* of the interaction between season and site. Within site differences, however, revealed significantly greater FBTs for *S. capensis* on vertical surfaces compared to crevices at Zinkwazi during summer, with no other significant differences among microhabitats for this or any other combination of site and season (Figure 5.14).

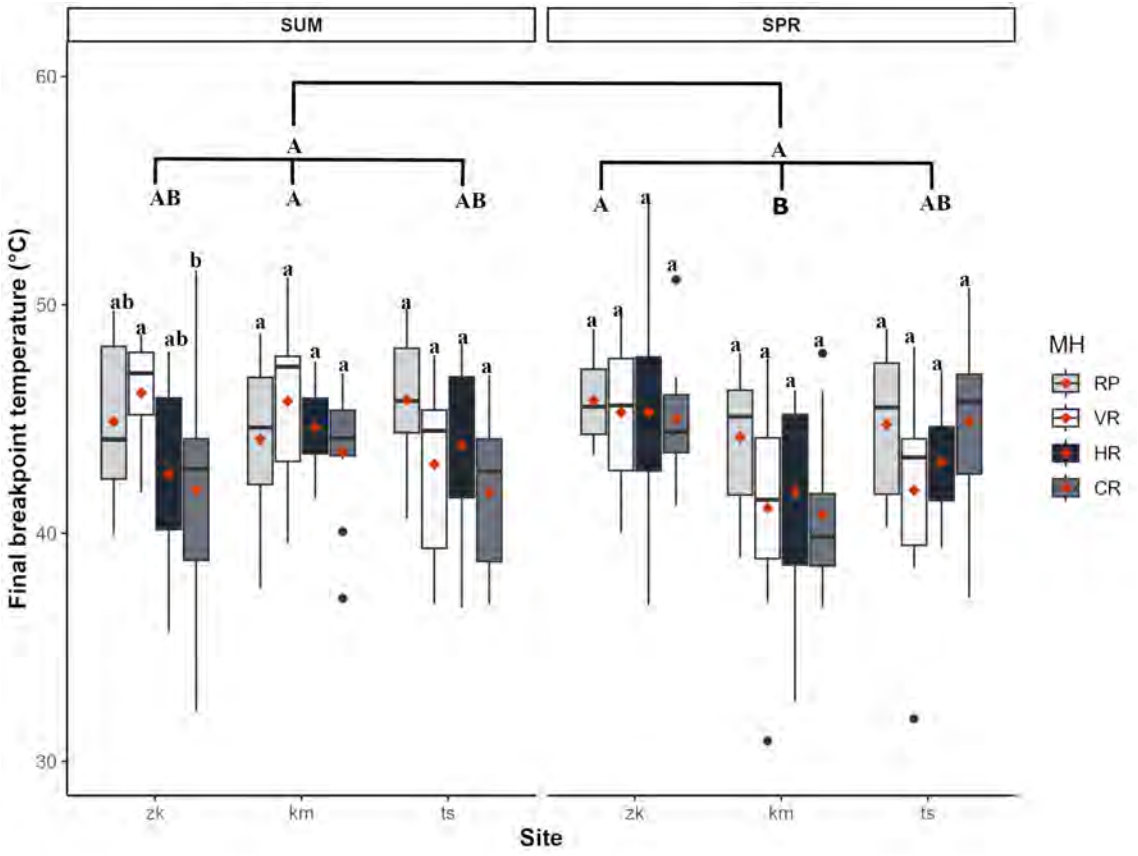

Figure 5.14: Panelled box and whisker plot illustrating the effects of season (SUM - Summer; SPR - Spring), site (zk - Zinkwazi; ts - Three Sisters; km - Kommetjie), and the interactions of microhabitat (MH) and season with site on the FBT (°C) of *Siphonaria capensis*. The plot showcases the mean (orange rhombuses), median (central horizontal line), interquartile range, as well as minimum and maximum values (whiskers). Plot colours correspond to different microhabitats (HR - Horizontal rock; VR - Vertical rock; CR - Crevice; RP - Rock pool). Homogenous groups are indicated for site and season (upper case letters) and, for microhabitat within season/site combinations (lower case letters) only.

The summary statistics for FBT in *Siphonaria serrata*, which closely mirrored those of *S. capensis*, ranged from 30°C to 52°C, with an overall mean of 43°C. In the factorial ANOVA assessing these values across various microhabitats, sites and seasons (Table 5.10), the interaction effect between season and site, and both of their main effects, were significant ($p < 0.05$ for all three). The main effect of microhabitat ($p = 0.503$) and its three-way interaction with season and site ($p = 0.210$) were not significant, however (Table 5.10).

Table 5.10: Results from the factorial ANOVA run on the effects of the three-way interaction among season, site and microhabitat on the FBT (°C) values of *Siphonaria serrata*. All factors were treated as fixed.

Parameters	SSQ	df1	F.value	p.value
SZN	167.006	1	6.002	< 0.05
SITE	208.009	1	6.616	0.01
MH	12.866	1	0.448	0.503
SZN:SITE	167.926	1	6.250	< 0.05
SZN:MH	13.526	1	0.378	0.539
SITE:MH	23.182	1	0.634	0.426
SZN:SITE:MH	51.373	1	1.573	0.21
Residual	2,280.485	NA	NA	NA

SZN - season; MH - microhabitat

Similar to *S. capensis*, the mean FBTs of *S. serrata* in Kommetjie were significantly greater in summer than in spring ($p < 0.0001$). The FBT of *S. serrata* at Kommetjie in summer were also significantly greater compared to the mean FBTs in Zinkwazi during both summer and spring (Figure 5.15). Additionally, as with *S. capensis*, there were no other significant differences in mean FBTs of *S. serrata* based on the *post hoc* analysis for the interaction between season and site.

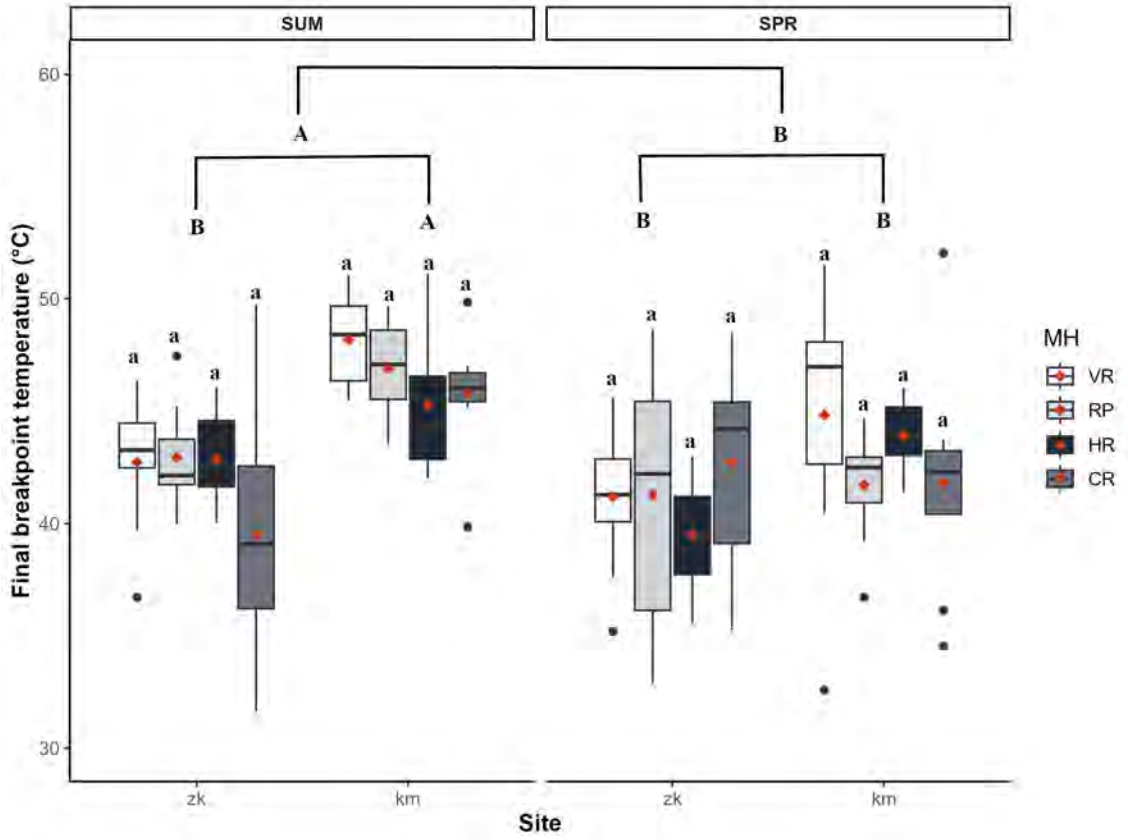

Figure 5.15: Box and whisker plot, panelled by season (SUM - Summer; SPR - Spring), site (zk - Zinkwazi; ts - Three Sisters; km - Kommetjie), and the interactions of microhabitat (MH) and season with site, depicting FBT (°C) variations in *Siphonaria serrata*. The plot highlights the mean (orange rhombuses), median (central horizontal line), interquartile range, minimum, and maximum values (whiskers). Different colours represent distinct microhabitats (HR - Horizontal rock; VR - Vertical rock; CR - Crevice; RP - Rock pool). Homogenous groups are indicated for site and season (upper case letters) and, for microhabitat within season/site combinations (lower case letters) only.

5.4.4 Animal length

Samples of *Siphonaria capensis* collected throughout the study had lengths ranging from 14.5mm - 28.1mm (Figure 5.16). There were significant effects of site ($p < 0.0001$), microhabitat ($p < 0.05$) and their interaction ($p < 0.0001$) on length (Table 5.11).

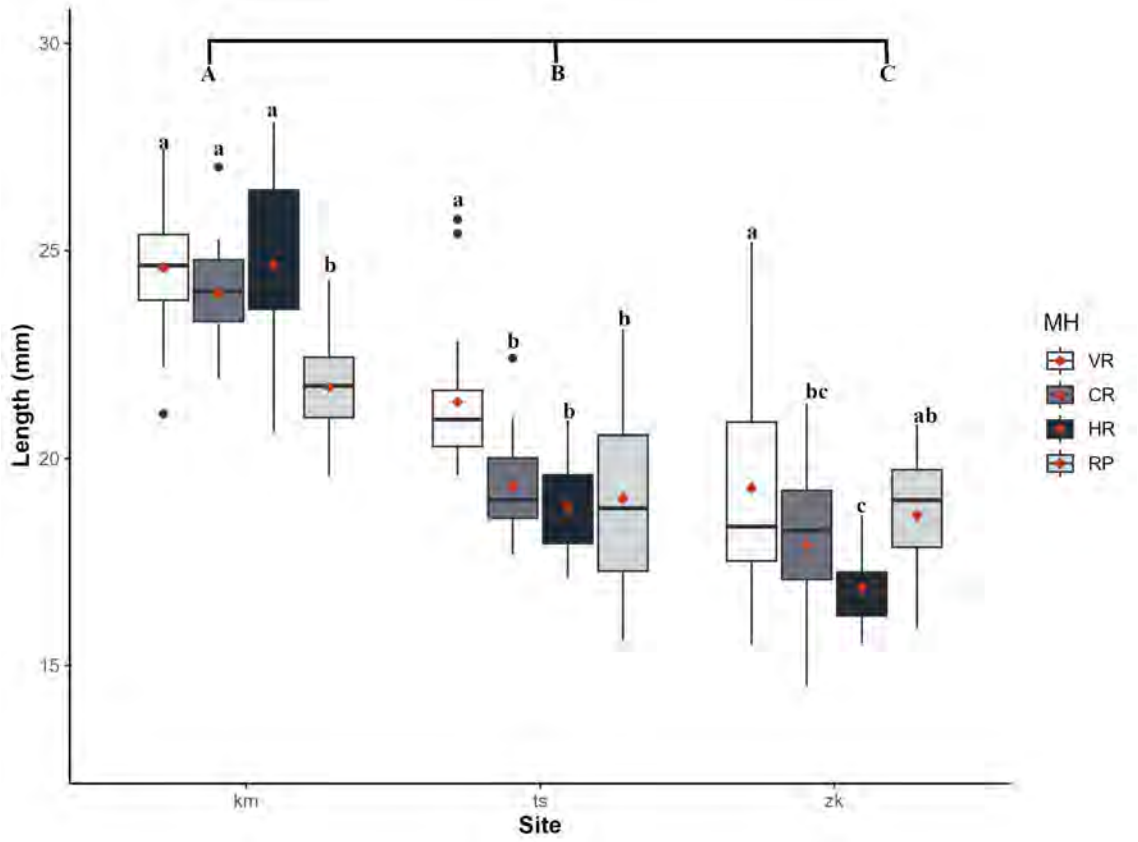

Figure 5.16: Box and whisker plot illustrating the effects of site (zk - Zinkwazi; ts - Three Sisters; km - Kommetjie) and the interaction between site and microhabitat (MH) on the shell length (mm) of *Siphonaria capensis*. The plot highlights the mean (orange rhombuses), median (central horizontal line), interquartile range, as well as minimum and maximum values (whiskers). Plot colours correspond to different microhabitats (HR - Horizontal rock; VR - Vertical rock; CR - Crevice; RP - Rock pool). Homogenous groups are indicated for site (upper case letters) and for microhabitat within each site (lower case letters) only.

The mean length of *Siphonaria capensis* at Kommetjie was significantly larger by 5.54mm than at Zinkwazi (Tukey HSD; $p < 0.0001$) and by 4.09mm than at Three Sisters (Tukey HSD; $p < 0.0001$). Additionally, individuals from Three Sisters were on average 1.46mm (Tukey HSD; $p < 0.0001$) longer than those from Zinkwazi (Figure 5.16).

Table 5.11: Results from the pooled factorial ANOVA on the effect of site and the interaction between site and microhabitat on the average (±SE) shell length (mm) of *Siphonaria capensis*. All predictors were treated as fixed factors.

Parameters	SSQ	df1	F.value	p.value
SITE	1,320.992	2	201.581	< 0.0001
MH	16.156	1	4.931	< 0.05
SITE:MH	89.159	2	13.606	< 0.0001
Residual	766.719	NA	NA	NA

MH - microhabitat

Overall, *S. capensis* collected from vertical rocks had the longest shells (Tukey HSD; $p < 0.0001$), while there were no significant differences in average lengths among the other microhabitats (Figure 5.16). Further differences in shell length among microhabitats were evident within each site. At Zinkwazi, limpets from vertical rocks and rock pools did not have significantly different shell lengths. Limpets from vertical rocks, however, were significantly longer than those from crevices and horizontal rocks, with no differences in lengths between limpets from this pair of microhabitats. Furthermore, limpets from rock pools were only longer than limpets collected from horizontal rocks (Figure 5.16). At Kommetjie, limpets from rock pools had the shortest shells, while at Three Sisters, the trend in limpet shell length among microhabitats followed the general pattern described above.

Throughout the study, *Siphonaria serrata* samples exhibited lengths between 14.62mm - 29.61mm (Figure 5.17). Notably, length was significantly influenced by site ($p < 0.0001$), microhabitat ($p < 0.001$) and their interaction ($p < 0.01$) as indicated in Table 5.12. The average length of *Siphonaria serrata* from Kommetjie exceeded that from Zinkwazi by 3.61mm, a difference that was statistically significant (Tukey HSD; $p < 0.0001$).

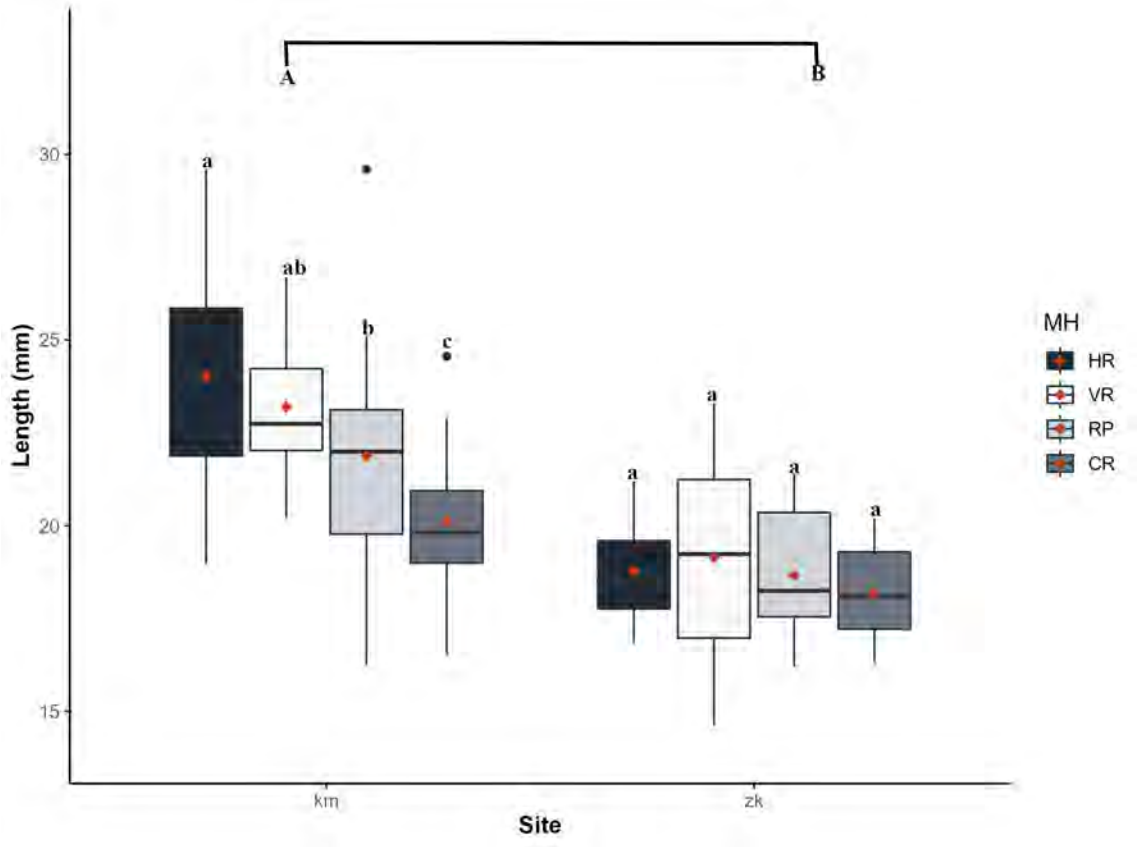

Figure 5.17: Box and whisker plot illustrating the effects of site (zk - Zinkwazi; km - Kommetjie) and the interaction between site and microhabitat (MH) on the shell length (mm) of *Siphonaria serrata*. The plot highlights the mean (orange rhombuses), median (central horizontal line), interquartile range, as well as minimum and maximum values (whiskers). Plot colours correspond to different microhabitats (HR - Horizontal rock; VR - Vertical rock; CR - Crevice; RP - Rock pool). Homogenous groups are indicated for site (upper case letters) and for microhabitat within each site (lower case letters) only.

In general, *S. serrata* collected from crevices had shorter shells (Tukey HSD; $p < 0.0001$) than those collected from horizontal and vertical surfaces, with no significant difference to those from rock pools. Additionally, there were no significant differences in average lengths among the other microhabitats. In contrast to *S. capensis*, further differences in *S. serrata* shell length among microhabitats were only observed at Kommetjie (Figure 5.17). Specifically, limpets from crevices had shorter shells than those from all the other microhabitats. Among the remaining microhabitats, the only other significant difference was that limpets from horizontal rocks were longer than

those from rock pools.

Table 5.12: Factorial ANOVA results, based on pooled data, assessing the influence of site and its' interaction with microhabitat on the mean (±SE) shell length (mm) of *Siphonaria serrata*. All predictors were treated as fixed factors.

Parameters	SSQ	df1	F.value	p.value
SITE	520.021	1	106.912	< 0.0001
MH	57.443	1	11.810	< 0.01
SITE:MH	32.858	1	6.755	< 0.01
Residual	758.784	NA	NA	NA

MH - microhabitat

5.5 Discussion

5.5.1 Overview and guiding hypotheses

This chapter investigated the physiological adaptations of two pulmonate limpets, *Siphonaria capensis* and *S. serrata*, to thermal stress across seasons and various South African coastal sites. The focus was on spring and summer at Zinkwazi, Three Sisters, and Kommetjie for *S. capensis* and at Zinkwazi and Kommetjie for *S. serrata*. The main objectives were to assess spatiotemporal variations in the links between hypometabolism and thermal tolerance, and between lethal and sub-lethal thermal limits, in these limpets. Based on MRS theory, I hypothesized that hypometabolic activity would correlate with thermal tolerance, particularly in warmer environments where heightened energy conservation mechanisms are required to mitigate thermal stress. Additionally, I predicted that, in cooler environments, lethal thermal limits would show greater co-variability with sub-lethal limits, reflecting a tighter coupling and broader potential for acclimatization of lethal limits under milder conditions. The absence of significant relationships between hypometabolic activity and thermal tolerance, or between lethal and sub-lethal thermal limits, would reject these hypotheses.

5.5.2 Summary of key findings

The results revealed significant patterns and relationships in the data. Limpet size varied significantly among sites and microhabitats, with both species attaining their largest and smallest sizes at Kommetjie and Zinkwazi, respectively. Moreover, *S. capensis* individuals from vertical surfaces were generally the largest, whereas *S. serrata* attained their largest sizes on both vertical and horizontal rocks. While no explicit hypothesis was proposed, these size differences provide valuable context for understanding potential confounding effects of variations in size across different sites or habitats on physiological performance. Both species exhibited a positive relationship between lethal and sub-lethal limits. While the relationship was significant at all sites except Kommetjie during summer for *S. capensis*, it was significant only at Kommetjie for *S. serrata*. Despite the multiple significant effects observed for *S. capensis*, this relationship between thermal limits remained consistent across seasons and sites. The markedly positive relationship between hypometabolism and thermal tolerance was context-dependent for both species. For *S. capensis*, the relationship was significant during both seasons exclusively at Three Sisters and Kommetjie, with no variation in the effect between seasons or between the two sites. In contrast, hypometabolism in *S. serrata* had a significant positive relationship with thermal tolerance at both Zinkwazi and Kommetjie during spring, but only at Zinkwazi during summer. The overall effect was stronger at Zinkwazi, though it did not vary across seasons. Both species demonstrated greater sub-lethal thermal tolerances during summer at Kommetjie, with no differences between seasons at Zinkwazi. During spring, *S. capensis* showed greater thermal tolerances in Zinkwazi, whereas *S. serrata*, interestingly, displayed higher thermal tolerances at Kommetjie during both seasons. Finally, there were generally no significant differences in thermal tolerances among microhabitats.

5.5.3 Animal size

5.5.3.1 Regional size gradients

The size range of approximately 15–30 mm recorded for both species in the current study compares favourably to the 15–25 mm size range reported by Chambers & McQuaid (1994), the only other study found that documented shell lengths for both species. Given the limited data available on size variations in the study animals sampled here, the results of this study can be compared only to findings from the scarce existing literature on general trends in marine intertidal organism sizes along the South African coast (Bustamante et al. 1995, Boland 1997). Specifically, the current study's findings of a decrease in size from the site on the West coast to the site on the East coast of South Africa are consistent with the patterns reported for the limpet *Scutellastra granularis* by Bustamante et al. (1995). Furthermore, although Boland (1997) did not examine size trends for the barnacles *Tetraclita serrata* and *Octomeris angulosa* eastward beyond the southern edge of the Cape Peninsula, both species were also found to be largest at the westernmost site. Both Bustamante et al. (1995) and Boland (1997) attribute the observed size variations in their study animals to co-occurring gradients in intertidal primary productivity. As described in Chapter 2, this trend in primary productivity corresponds to a parallel gradient in nutrient availability and an opposing trend in sea water temperatures (Bustamante et al. 1997), all of which are influenced by variable oceanographic features along the South African coast (Lutjeharms et al. 2000, Fawcett 2006, Griffiths et al. 2010).

Although species-size distributions along the South African coast in the present study cannot be definitively linked to biogeographical effects due to the sampling here being limited to one site per coast, the mechanisms underlying the intraspecific size variations described above are also highly likely to drive the observed size differences among the sites for the present study. For example, while Bosman & Hockey (1988) found that increased primary productivity leads to higher growth rates that ultimately determine maximum size (Branch 1975) in *Scutellastra granularis*, Jaramillo et al. (2017) reported

that body sizes of several intertidal crustaceans are negatively correlated with sea surface temperature. This aligns with patterns of animal size predicted by ecogeographical principles such as Bergmann's Rule (Mayr 1963), the Temperature-Size Rule (Atkinson et al. 1994), and James's Rule (Blackburn et al. 1999). Collectively, these principles suggest that changes in the size of ectothermic animals result from the dynamic interaction of intrinsic and extrinsic factors, including metabolic constraints, energy demands, and the availability of various biotic and abiotic resources (Dugan et al. 1994, Chapelle & Peck 1999, Thomas et al. 2001, Cheung et al. 2013, Weber et al. 2015).

5.5.3.2 Within-shore size gradients

Whereas more thermally benign conditions on broad geographical scales appear to encourage the occurrence of larger limpets in the current study, the opposite pattern emerges at smaller spatial scales. Several previous studies (Vermeij 1972, Branch 1975, Chambers & McQuaid 1994) align with these findings, indicating that smaller intertidal ectotherms are more frequently located in thermally favourable rocky intertidal microhabitats compared to their larger counterparts. This pattern, however, contrasts with certain inferences (Jaramillo et al. 2017, Gunderson et al. 2019, Elahi et al. 2020) and established principles (Mayr 1963, Atkinson et al. 1994, Blackburn et al. 1999) discussed earlier, which focus on broader-scale size variations in relation to environmental conditions. Specifically, across large spatial scales, larger animals tend to dominate favourable regions over smaller individuals of the same species due to a combination of interrelated factors. For instance, chronically warmer conditions across broad spatial scales elevate maintenance energy demands and accelerate reproductive development, limiting the energy available for somatic growth. This, in turn, reduces the potential for animals to achieve large body sizes (Cheung et al. 2013, Weber et al. 2015). Additionally, the greater abundance of food resources in more favourable regions amplifies this trend. Conversely, at smaller spatial scales, the inverse relationship between size and increasingly favourable environmental conditions appears to be influenced by fewer interacting factors. Larger individuals, with their lower surface

area-to-volume ratios, typically experience reduced rates of heat absorption and water loss. As a result, they are better able to withstand harsh environmental conditions expressed over short timescales and are more frequently found occupying less favourable microhabitats than smaller individuals (Vermeij 1972). These findings highlight the complex and variable mechanisms driving two opposing trends in size variation along similar thermal gradients, influenced by different environmental factors at different scales of time and space.

5.5.4 Relationship between lethal and sub-lethal limits

Observed positive correlations between sub-lethal and lethal limits, indicative of their concurrent increase under thermally stressful conditions, align with findings from similar studies, which highlight this pattern across various taxa and contexts (Wang et al. 2019, Moyen et al. 2020, 2022, Li et al. 2021, Zhang et al. 2021, Hardison et al. 2023). Notably, while Moyen et al. (2020) and Moyen et al. (2022) explicitly tested this relationship, most other studies only infer such a positive association without directly quantifying its statistical significance, as done in the current study. In their work on the high-shore mussel *Mytilus californianus*, Moyen et al. (2020) and Moyen et al. (2022) reported contrasting results regarding the relationship between critical and flatline temperatures, finding a significant positive relationship between critical and flatline temperatures only in the earlier study. The divergence in the relationship between physiological thresholds observed among these studies likely arose from methodological differences in data collection. In the current study and in Moyen et al. (2020), specimens were sampled from various intertidal zones, across several biogeographic regions or tested at consistent intervals over an extended acclimation period. These variations in sampling conditions likely introduced variability in the thermal limits of the test organisms compared to those sampled from a single rocky intertidal zone at one site on the West coast of the United States of America by Moyen et al. (2022). As noted in previous research (Anestis et al. 2007, Byrne et al. 2011, Zerebecki & Sorte 2011), environmental heterogeneity across time and space fosters more pronounced individual

and population-level differences in thermal tolerance, influencing the adaptive capacity and resilience of species.

Nevertheless, it is important to recognize that a decoupling between an organism's lethal limits and any of its sub-lethal thresholds are arguably relatively common due to differences in the regulatory mechanisms governing these threshold categories. As noted previously in this chapter, these physiological thresholds often exhibit contrasting degrees of plasticity, with lethal limits being inherently more physiologically constrained and less adaptable to environmental variability compared to sub-lethal thresholds (Stenseng et al. 2005, Pasparakis et al. 2016, Dong et al. 2017, Moyen et al. 2020, 2022, Li et al. 2021). Moreover, the limited plasticity typically associated with lethal thresholds provides insight into why significant correlations between the two limits, as well as variations in the strength of these relationships, were not consistent across all sites and seasons, for either sampled species.

5.5.5 Relationship between thermal limits and hypometabolism

5.5.5.1 Evidence that hypometabolism extends sub-lethal limits

Although studies similar to the present one, where the effect of hypometabolism on absolute thermal tolerance was empirically determined, are lacking, there is compelling evidence in support of a positive relationship between hypometabolism and sub-lethal thermal limits across a diverse array of species and ecological contexts (Storey & Storey 2004, Guppy & Withers 2007, Kelly et al. 2014, Verberk et al. 2016, Pasparakis et al. 2016, Gorr 2017, Marshall & McQuaid 2020, Hui et al. 2020, Hann 2021, Li et al. 2021, Liao et al. 2021, but see Bjelde & Todgham 2013). Studies of metabolic rate depression primarily suggest that by reducing metabolic demands as cellular processes become increasingly energy-intensive near an organism's thermal limits, hypometabolism allows these organisms to endure unfavourable conditions for longer as they approach sub-lethal thresholds (see reviews by Guppy & Withers 2007, Staples 2016, Sokolova 2021). This is achieved because metabolic depression generally facilitates energy conservation under

stressful abiotic conditions (Hui et al. 2020). For instance, during summer aestivation or winter hibernation, extended dormancy periods when energy acquisition through feeding is constrained, metabolic depression slows the depletion of endogenous energy reserves (Storey & Storey 1990, Jiang et al. 2023).

Based on the observed positive effects of hypometabolism on sub-lethal limits in both species examined here, however, it can be argued that hypometabolism not only prolongs survival but also actively extends the sub-lethal thermal limits of animals. As previously discussed, hypometabolism is a physiological adaptation that allows energy conservation in organisms from environments subject to chronically adverse conditions, such as extreme heat and desiccation stress (Newell 1969, Sokolova & Pörtner 2001, Verberk et al. 2016, Gorr 2017). Specifically, hypometabolism in *Siphonaria* species encompasses regulatory mechanisms that reduce energy expenditure through the depletion of ATP within a temperature range preceding sub-lethal thermal thresholds (see Chapter 1). By mitigating the risks of uncontrolled ATP depletion during thermal stress, hypometabolism may help extend the thermal limits of these organisms (Hand & Hardewig 1996, Abele et al. 2002). Moreover, while not empirically determined before the present study, examples of the extension of organism thermal limits by hypometabolism in warm versus cool conditions is provided in the review by Verberk et al. (2016) and the study by Liao et al. (2021), where a large proportion of species that express hypometabolism had greater thermal limits than those that do not.

5.5.5.2 Lack of context-dependent hypometabolic effects

Building on this observation that organisms in warmer environments typically exhibit greater hypometabolic activity and thermal tolerance, a stronger positive effect of hypometabolism on the sub-lethal limits of *Siphonaria serrata* at Zinkwazi, a site consistently warmer than Kommetjie during sampling (Chapter 2), was anticipated. Conversely, given that summer sampling conditions were typically warmer than those in spring (Chapter 2) and that *S. capensis* experiences similar environmental conditions to *S. serrata* at both sites, the absence of seasonal differences in the hypometabolic effect

on sub-lethal limits for either species, or site-specific differences for *S. capensis*, was unexpected. The lack of significant seasonal variation for both species may reflect the relatively mild seasonal transition in climatic conditions between spring and summer (Kwiecien et al. 2022). As highlighted in Chapter 3, the surface temperature difference of approximately 3°C recorded between these seasons in Chapter 2 may be insufficient to drive meaningful changes in the response variable of interest, especially when compared to the more substantial temperature shift of about 8°C observed between summer and winter.

Although not determined explicitly in this study, the difference between species in the effect of hypometabolism on sub-lethal limits can be attributed to inherent interspecies differences in the expression of hypometabolism. Notably, as outlined in Chapter 1, the fact that *S. capensis* is a pelagic developer while *S. serrata* is a direct developer (Chambers & McQuaid 1994), and that *S. capensis* produces greater quantities of anti-predator mucus compared to *S. serrata* (Pinchuck & Hodgson 2009), suggests a greater capacity for a risk-avoidance stress response strategy in *S. capensis*. Given that risk-avoidance strategies generally align with increased mobility, *S. capensis's* stronger inclination toward risk-avoidance, compared to *S. serrata*, may reduce its reliance on behaviours that induce hypometabolism, such as clamping, as a means of regulating body temperature (Jones & Boulding 1999, Monaco et al. 2015, Verberk et al. 2016, Marshall & McQuaid 2020). Consequently, the relatively lower expression of hypometabolism in *S. capensis* may introduce floor effects in the data, representing a clustering of observations near the lower detection limit, that typically occur when a measurable response is infrequent (Gulledge et al. 2019, Arslan & Benke 2023, Rossi et al. 2024). Therefore, the capacity to discern subtle differences in the effect of hypometabolism on sub-lethal thermal limits in *S. capensis* is diminished. Another example of this effect can be found in the study by Rossi et al. (2024), who, in their assessment of the gross motor function of children with cancer related motor impairments, found that floor effects distorted the ability to discriminate among different levels of the Gross Motor Function Measure (GMFM-88).

5.5.6 Spatiotemporal drivers of sub-lethal limit variation

5.5.6.1 Seasonal acclimatory shifts in sub-lethal limits

The overall mean sub-lethal thermal limit values of 44°C for both limpets in the current study are comparable to those determined for the limpets *Cellana toreuma* (ABT = 41.81°C) and *C. grata* (ABT = 47°C) by Dong & Williams (2011). These limpets were also sampled during summer in the mid- to high-shore zone on the rocky intertidal at a subtropical site. Apart from the study by Dong & Williams (2011), however, most similar studies report much lower sub-lethal limits for rocky intertidal limpets sampled from similar shore levels (Bjelde & Todgham 2013, Bjelde et al. 2015, Pasparakis et al. 2016, Kankondi et al. 2018). Besides species-specific thermoregulatory adaptations, the observed variation in sub-lethal thermal limits across studies is likely attributable to differences in seasonal climatic variation or site-specific climatic conditions. Specifically, in the previous research listed above (Bjelde & Todgham 2013, Bjelde et al. 2015, Pasparakis et al. 2016, Kankondi et al. 2018), all limpets were sampled either during cooler months or from sites with cooler climatic conditions.

Elevated sub-lethal thermal limits during warmer periods, as observed in summer compared to spring at Kommetjie in the current study, are likely driven by anticipatory enhancements in physiological mechanisms that boost thermal tolerance. These adaptations include the synergistic induction of hypometabolic states and the HSP response. Several researchers have shown that intertidal organisms increase baseline HSP levels as temperatures gradually rise from winter to summer (Roberts et al. 1997, Buckley et al. 2001). This primes these organisms to respond effectively to the temperature extremes typically associated with summer, thereby fostering proteome stability before the onset of harsh abiotic conditions and reducing the need for energetically expensive protein repair and synthesis. Consequently, this HSP mediated stabilization of the proteome facilitates the suppression of energy output during hypometabolic states, delaying the rapid depletion of cellular energy reserves and eventual metabolic failure (see Sokolova 2021 for review). As discussed previously in

the current chapter, when there are no observable differences in sub-lethal thermal limits between seasons, the variation in thermal profiles across seasons may not be pronounced enough to elicit significant changes in key physiological responses. Any variations in sub-lethal limits between studies, linked to site-specific climatic factors, are further supported by Broitman et al. (2021), who reported a consistent decline in the critical thermal minimum (CTmin) with decreasing temperatures along latitudinal gradients in their research on the intertidal barnacle *Jehlius cirratus*. A similar result was also recorded for *Siphonaria capensis* in the current study. This finding, however, was limited to a specific variation in thermal limits between two sites and was observed during only one of the sampled seasons.

5.5.6.2 Dispersal-mediated paradoxes in site-level tolerance

The observation that *Siphonaria capensis* exhibited a higher thermal limit at the warmer site in Zinkwazi, while *S. serrata* displayed the opposing trend by showing greater thermal limits at the cooler site, was unexpected. As discussed throughout this thesis, any enhanced thermal tolerances of limpets at sites with comparatively higher temperatures are likely a result of dynamic fluctuations between heat management strategies that prioritize endurance over risk-avoidance. These strategies typically unfold over short timescales, prompting intertidal ectotherms to adjust their behaviour and physiology in response to thermal changes during daily or tidal cycles (Crickenberger et al. 2020). This suggests quasi-continuous, environmentally and physiologically driven shifts between an inability, hesitation, and reduced need to evade increasingly unfavourable environmental conditions during day-time low tide. More specifically, for *Siphonaria spp*., which often forage on open rock surfaces during night-time low tides (Branch & Cherry 1985, McQuaid pers. comm.), low dispersal while foraging likely restricts access to cooler microhabitats before rising tides. Consequently, this leads to a greater reliance on physiological adaptations, such as hypometabolism, which extend sub-lethal limits. Without these adaptations, surviving micro-climatic conditions at warmer sites or during periods of chronically elevated temperatures would be much less

feasible on a day-to-day basis.

Given these dynamics, *S. serrata*, with its reduced dispersal rates compared to *S. capensis* (discussed in Chapter 3), was expected to exhibit the variation in thermal limits between sites observed for *S. capensis*. The finding, however, that only *S. capensis* displays greater thermal tolerance at the warmer site suggests a paradoxical operation of the underlying mechanism for each species, given their marginal differences in adult mobility and physiological strategies. Such that, rather than greater dispersal rates providing access to suitable microhabitats, *S. capensis*'s mobility can place it at greater risk of encountering suboptimal microhabitats after foraging during high tide. Conversely, *S. serrata*, which disperses less frequently and over shorter distances, may be less susceptible to exposure to such unfavourable conditions during low tide. Thus, through the dispersal-mediated variability in physiological responses described above, *S. capensis* displayed higher sub-lethal thermal limits at Zinkwazi, while *S. serrata* had greater sub-lethal limits at Kommetjie.

5.5.6.3 Regional food gradients modulate thermal limits

The contrasting trends in sub-lethal thermal limits can further be attributed to food resource availability and how it affects metabolic demands and adult dispersal. As mentioned in Chapter 2, the east-west gradient of increased nutrient availability results in greater productivity and intertidal food availability. The abundant food resources across rocky intertidal microhabitats at Kommetjie, compared to Zinkwazi, implies a heightened capacity for energy allocation, in the form of ATP, to essential maintenance and protective measures in intertidal animals at elevated temperatures (Dowd et al. 2013). Consequently, costly protective measures, such as the upregulation of antioxidant defences to manage oxidative stress, can be sustained without invoking hypometabolism (Santini et al. 2002). This increased energy synthesis also lessens the dependency of *Siphonaria capensis* on its comparatively greater potential for extended movement away from thermal refugia during foraging, further curbing hypometabolic activity. As discussed in Chapter 2, intertidal organisms often move away from thermal refugia

during foraging due to overgrazing caused by higher herbivore densities in these cooler microhabitats compared to those with warmer thermal profiles. By limiting the range and frequency of its foraging trips, *S. capensis* at Kommetjie is less likely to encounter unfavourable microhabitats after foraging than at Zinkwazi, and therefore depends less on physiological adaptations such as hypometabolism, typically associated with greater thermal tolerance.

Conversely, by benefiting from the increased food availability and the slightly milder overall thermal conditions at Kommetjie, *S. serrata* may deliberately remain in what would generally be considered less favourable microhabitats, where conditions elicit an enhanced physiological response to thermal stress. Elevated temperatures in these microhabitats therefore appear to extend thermal limits at Kommetjie through enhanced biochemical processes that reinforce oxidative defence independently of hypometabolism. These processes aid thermal tolerance primarily by neutralizing reactive oxygen species during heat stress, thereby guarding various cellular components from heat damage (Pöhlmann et al. 2011, Dowd et al. 2013).

5.5.6.4 Morphological and behavioural buffers of thermal stress

These findings suggest that the two species employ distinct short-term strategies and cost-benefit approaches to mitigate thermal stress, resulting in the divergent thermoregulatory patterns observed across sites and seasons. Several additional factors, however, not addressed in the current study, could help account for these patterns. For instance, subtle differences in morphological traits among limpet populations, such as shell shape, texture, thickness, and colouration, and ecological interactions such as aggregatory behaviour or the use of biogenic structures as shelter, may generate discrepancies between microhabitat thermal profiles and the actual body temperatures experienced by individuals (Feare 1971, Britton 1995, Soto & Bozinovic 1998, Lang et al. 1998, Sokolova & Berger 2000, Stafford & Davies 2004, Bates & Hicks 2005, Harley et al. 2009, Chapperon & Seuront 2012). These factors can consequently shape local thermal tolerance patterns in complex and sometimes unexpected ways.

For example, in their study on the limpets *Lottia gigantea*, *Patella vulgata*, and *Siphonaria gigas*, Harley et al. (2009) found that individuals with high-spired shells maintained lower body temperatures, particularly at moderate wind speeds, compared to those with low-spired shells. According to Harley et al. (2009), this difference arises because high-spired shells, projecting further into moving air, facilitate greater convective heat loss than low-spired shells, which experience higher heat conduction from contact with warm surfaces. Regarding aggregatory behaviour, Chapperon & Seuront (2012) observed that the intertidal snail *Nerita atramentosa* exhibited cooler mantle temperatures when in aggregations compared to solitary individuals, especially in the high shore zone during summer. As further proposed by Chapperon & Seuront (2012), this reduction in heat gain among aggregatory snails can be attributed to shared shading effects within the group. Ultimately, by keeping limpet body temperatures below their critical thermal thresholds these cooling effects may lessen their dependence on hypometabolic responses during heat stress (Harley 2008). Over time, this could translate into reduced thermal limits due to a weaker impetus to physiologically tolerate extreme heat beyond the thermally buffered conditions.

5.5.7 Methodological constraints and potential solutions

The methods used to quantify thermal tolerance and physiological responses in this study, while effective for rapid data acquisition, may influence the observed patterns in limpet thermoregulatory responses compared to established techniques. For example, inferring hypometabolism from plateaus or drops in heart rate before final breakpoints in thermal response curves provides valuable insights into hypometabolic responses during acute heating regimes (Bjelde & Todgham 2013). More established approaches, however, are specifically designed to explicitly determine hypometabolic states. These approaches include measuring O_2 debt repayment after re-introducing test animals to benign conditions (Marshall & McQuaid 1991, Sokolova & Pörtner 2001, Zippay & Helmuth 2012), quantifying the accumulation of anaerobic by-products like lactate or alanine (Gordon et al. 1970), assessing oxygen consumption rates (Marshall & McQuaid 1992,

Marshall & McQuaid 1993), and monitoring the downregulation of metabolic enzymes (Storey & Storey 1990, Ivanina et al. 2016). These methods leverage key properties of anaerobic respiration in animals subjected to environmental stressors. In Chapter 1, I note that anaerobic respiration provides ATP during oxygen-limited conditions but is inefficient and generates harmful by-products requiring clearance via aerobic respiration (Houlihan et al. 1981, McMahon 1988, Simpfendörfer et al. 1995, Donovan et al. 1999, Sokolova & Pörtner 2001). By reducing overall metabolic demands, however, organisms capable of hypometabolism can mitigate reliance on anaerobiosis and its associated production of harmful by-products (Grieshaber et al. 1994, Sokolova & Pörtner 2001).

Hypometabolism is characterized by the absence of what is often referred to as cardiac or respiratory overshoot, where post-stressor cardio-respiratory rates are significantly elevated compared to pre-stressor rates (Brown & Wynberg 1987, Hochachka 1988, Marshall & McQuaid 1993, Proum et al. 2017, Marshall & McQuaid 2020). To understand the relationship between heat-induced hypometabolism and organismal thermal tolerance better, future studies should adopt more integrative approaches that involve more properties of hypometabolism, as demonstrated by (Bjelde & Todgham 2013). Their investigation into how the physiological performance of the limpet *Lottia digitalis* varies between immersion and emersion during temperature increases combined measurements of oxygen consumption, cardiac activity, and glycogen content across a range of temperatures. Using this approach, they showed that in a substantial portion of the test population, heart rates, oxygen consumption, and glycogen usage were significantly suppressed despite rising temperatures until sub-lethal thresholds were reached. Therefore, their work established a connection between cardiac activity and hypometabolism, offering a framework that future studies can use and build upon.

5.5.8 Hypometabolic flux as a driver of thermal tolerance variability

The relationship between hypometabolism and environmental factors has been widely studied across various species (Newell 1969, Marshall & McQuaid 1991, Guppy & Withers 2007, Verberk et al. 2016), with some research exploring its interactions with

factors such as ontogeny and oxygen availability in relation to thermal performance (Bjelde & Todgham 2013, Kelly et al. 2014, Bjelde et al. 2015, Marshall & McQuaid 2020) and others connecting its influence on thermal performance to species distribution patterns (Hann 2021, Liao et al. 2021, Leeuwis & Gamperl 2022). While these studies deepen our understanding of the complex interactions among environmental factors and hypometabolism, and their influence on thermal tolerance, this study elucidates the nature of correlations among these variables. This chapter builds upon key inferences generated previously (Chapter 2 and 3) about the potential role of metabolic rate depression in extending the study animals' capacity to endure acute thermal stress, aligning with predictions from MRS theory discussed in Chapter 1.

In continuation, the observed lack of a pattern in the covariance between hypometabolic activity and thermal tolerance across seasons and sites, despite a significant positive correlation between the two variables, aligns with the findings of Chapter 2 and 3 for both species and those in Chapter 4 for *Siphonaria capensis*. These findings highlight how microscale distribution and thermally driven preference patterns reveal a dynamic interplay between two key heat management strategies. This subsequently underscores the capacity of individuals to adjust their metabolism flexibly in response to shifting energy demands across variable environmental conditions (Staples 2016, Sokolova 2021). For many animals inhabiting extreme environments, such as the high intertidal zone, there is evidence that hypometabolism can be reversibly triggered, "on-demand," in response to environmental stressors (Leeuwis & Gamperl 2022). There is also somewhat conflicting evidence, however, of hypometabolic activity being endogenously hardwired and synchronized with specific environmental cues. This suggests that both internal and external signals collectively drive the observed constant state of hypometabolic flux, which, in turn, influences hyper intra-specific variability in thermal tolerance (Staples 2016, Leeuwis & Gamperl 2022). Consequently, any true patterns of covariance between hypometabolism and thermal tolerance remain obscured until a broader array of potentially intersecting factors and signalling pathways is considered.

5.5.9 Conclusion

Based on the results described here, I fail to reject the hypotheses that a positive relationship exists between hypometabolism and thermal tolerance, or between sub-lethal and lethal thermal limits, despite inconclusive evidence that these relationships do not vary in magnitude with differing environmental conditions across spatial scales. In summary, while variable thermal histories likely modulate the effect of hypometabolism on thermal tolerance, the moderate differences in short-term strategies for managing heat stress displayed by the study animals, coupled with the highly dynamic and reversible characteristics of hypometabolism, preclude the identification of consistent patterns in this study.

Chapter 6

General Discussion

Climate warming poses an increasing threat to coastal ecosystems by amplifying local temperature extremes, sea-level rise and weather volatility, all of which can drive wholesale reorganisation of intertidal assemblages and their functional roles (IPCC 2018, 2021). Predicting how intertidal animals may respond to projected warming is therefore critical. Metabolic rate suppression (MRS) theory provides a mechanistic framework that can refine these predictions (Newell 1969, Marshall & McQuaid 1991, 2020, Sokolova & Pörtner 2001, Guppy & Withers 2007, Verberk et al. 2016). Unlike universal temperature dependence (UTD) models, which predict continuous increases in metabolic rates with temperature, MRS theory posits that certain organisms employ hypometabolism to limit energy consumption and survive acute stress (Storey & Storey 1990, Marshall & McQuaid 1991, Sokolova & Pörtner 2001). In the tide-driven thermal mosaics of the intertidal zone, MRS helps explain how marine species extend their thermal tolerance while maintaining ecological function (Branch 1981, Garrity 1984, Little et al. 2009).

Building on this framework, the current study assessed whether the capacity for metabolic suppression clarifies the temperature-driven distributions, preferences, and thermal tolerances of *Siphonaria capensis* and *S. serrata* along a pronounced thermal gradient on the South African coast. This involved investigating whether hypometabolism influences the resilience of intertidal limpets to thermal stress, and whether this relationship is more pronounced in those individuals predominantly exposed to warmer conditions through their distribution and habitat preferences. Thus,

by analyzing how the relationship between sub-lethal thermal limits and hypometabolic activity varies over time and across space, I examined whether hypometabolism enhances thermal tolerance in warm environmental conditions. It was therefore hypothesized that MRS theory would be supported, if, at the individual level, hypometabolism correlates positively with thermal tolerance and if this relationship is more pronounced under warmer conditions.

Chapter 5 confirms the core hypothesis of the study that limpet thermal limits were positively correlated with individual hypometabolic activity, however, this relationship did not differ between warm and cold conditions. Chapter 2 and 3 show that both limpets preferentially occupy cool refuges and, when displaced, return to them, thereby supporting the first hypothesis by demonstrating adaptive shifts in distribution and movement under thermal stress. Chapter 4 further revealed that limpets from cool microhabitats move toward cooler zones along a gradient, whereas individuals from warm microhabitats remain stationary, implying that warm-acclimated animals rely more on physiological than behavioural responses. Therefore, aligning with the expectation that those in warm conditions have enhanced physiological adaptations. Consequently, Chapters 2 - 4 document behavioural thermoregulation that complements the physiological trends measured in Chapter 5. Nevertheless, despite these adaptive behaviours and the overall benefits of hypometabolism, I did not observe a markedly stronger hypometabolic advantage in warm versus cool conditions. These findings likely reflect the highly dynamic and reversible nature of hypometabolism, which can obscure short-term contrasts in the highly variable rocky intertidal (Marshall & McQuaid 1991, Verberk et al. 2016). Furthermore, the limited variability in temperature ranges analysed, evident in the small seasonal differences in surface temperatures recorded in Chapter 2, limited the power of the study to detect population level differences. This is emphasized in Chapter 5 where a lack of significant seasonal variation in the correlation between hypometabolic activity and thermal limits was found. Finally, incomplete data for potentially relevant microhabitats, particularly rock pool edges, which were subsumed within the horizontal rock surface category (Chapter 3), may have muted physiological contrasts between benign and warmer microhabitats. Theoretically, this could explain

the reduced physiological differences observed between limpets in warmer conditions and those from more thermally favourable microhabitats.

Several methodological challenges that may have unintentionally influenced the results must be acknowledged. These include limited sampling across key explanatory variables such as site and season (Chapter 2 and 3), gaps in temperature logger data (Chapter 2) and heart rate measurements (Chapter 5), and the absence of any measurement of confounding variables such as food availability (Chapter 2). Additionally, sampling only one site on each of the East, South, and West coast (Chapter 2) likewise constrains broader biogeographic inference, highlighting the need for wider spatial replication. Furthermore, missing data reduced the robustness of meaningful statistical comparisons and introduced potential biases in some of the analysis models. Collectively, these challenges narrow the scope and precision of the findings and may obscure true patterns in limpet responses. Therefore, interpretations of temperature-driven variation should be made cautiously, with an appreciation for these methodological constraints.

Nevertheless, sufficient evidence was presented to reject the null hypothesis that hypometabolic activity has no effect on upper thermal tolerance. Therefore, I fail to reject the alternative hypothesis that hypometabolism extends thermal tolerance, with no definitive evidence to refute the possibility that this effect is particularly pronounced in warm conditions. The consistent positive correlation between hypometabolic activity and thermal limits, despite the reversible nature of hypometabolism and methodological constraints, positions MRS theory as a useful predictive framework for thermal tolerance. Comparable findings for the mussel *Mytilus galloprovincialis*, the snail *Echinolittorina malaccana*, and various other molluscs (Anestis et al. 2007, Marshall & McQuaid 2011, Liao et al. 2021) imply that hypometabolism enables survival under high-temperature stress by effectively extending thermal tolerance limits. Marshall & McQuaid (2011) and Liao et al. (2021) attribute this benefit to biochemical and molecular processes that lower energy demand, while Anestis et al. (2007) emphasise the synergistic expression of anaerobic metabolism and MRS. This synergy facilitates sustained ATP production without excessive accumulation of metabolic by-products,

helping prevent the extreme energy deficits and subsequent mortality that otherwise accompany rising temperatures.

The primary energy-saving principles of MRS theory (Chapter 1), can enhance other mechanistic frameworks that predict organismal responses to global warming. Notable examples include Dynamic Energy Budget (DEB) theory (Sousa et al. 2008, Kooijman 2010, Sarà et al. 2013), Oxygen- and Capacity-Limited Thermal Tolerance (OCLTT) theory (Pörtner 2001, Pörtner & Farrell 2008, Pörtner 2010, Verberk et al. 2011, Pörtner et al. 2017), and the Metabolic Theory of Ecology (Brown et al. 2004, Allen & Gillooly 2007). For instance, to evaluate DEB theory under highly variable climatic environments, (Monaco & McQuaid 2018) incorporated MRS as an additional parameter. Dynamic Energy Budget theory provides insights into how organisms acquire and allocate energy throughout their lifetime (Kooijman 2010). It was originally parameterised for organisms in relatively stable environments (Ross & Nisbet 1990). Therefore, to address hypometabolism in thermally variable environments, Monaco & McQuaid (2018) integrated a metabolic depression constant into the DEB framework. This integration enables more precise predictions of species fitness-related traits by simulating metabolic patterns that align more closely with observed empirical data.

Building on earlier discussions of OCLTT (Chapter 1), here I illustrate how MRS theory bolsters mechanistic frameworks of thermal tolerance. OCLTT argues that thermal tolerance is defined by aerobic scope, the balance between oxygen demand and supply, which declines as rising temperatures drive demand beyond supply (Frederich & Pörtner 2000, Pörtner 2001, Pörtner & Knust 2007, Pörtner & Farrell 2008). Subsequently, tissue hypoxia and time-limited anaerobiosis occur, ultimately defining sub-lethal thermal limits and the ensuing collapse of physiological functions (Zielinski & Pörtner 1996, Sommer et al. 1997, Pörtner 2010). Much of the support for OCLTT is derived from studies of aquatic animals inhabiting relatively stable environments (Zielinski & Pörtner 1996, Frederich & Pörtner 2000, Peck et al. 2002, Pörtner & Knust 2007), yet in more variable conditions aerobic scope alone proves an unreliable predictor of thermal tolerance (Clark et al. 2013, Norin et al. 2014, Ern et al. 2014, Gräns et al. 2014,

Neubauer & Andersen 2019). This limitation arises because non-aerobic processes, such as the synergistic expression of anaerobic metabolism and MRS (Chapter 1), can extend thermal tolerance beyond what would be predicted by a decline in aerobic scope (Ejbye-Ernst et al. 2016). In their study, Ejbye-Ernst et al. (2016) highlighted the potential overestimation of the metabolic scope available for sustainable activities in OCLTT studies that fail to consider the role of anaerobic metabolism adequately. Integrating OCLTT with MRS theory therefore promises a more holistic framework for understanding how energy-saving strategies mitigate oxygen limitation and enhance a species' ability to withstand environmental stress. In much the same way as the earlier integration of MRS with DEB, this synthesis can improve predictions of physiological resilience, ecological stability, and ecosystem dynamics in response to climate change. The integration of OCLTT with MRS would reconcile energy conservation strategies with organismal energy budgets. This in turn would provide new insights into the physiological responses of organisms capable of metabolic suppression to broad-scale environmental change under climate warming.

References

ABELE, D., HEISE, K., PÖRTNER, H. O. & PUNTARULO, S. 2002. Temperature-dependence of mitochondrial function and production of reactive oxygen species in the intertidal mud clam *Mya arenaria*. *Journal of Experimental Biology* 205:1831–1841.

AGUILERA, M. A. & NAVARRETE, S. A. 2012. Interspecific competition for shelters in territorial and gregarious intertidal grazers: consequences for individual behaviour. *PloS ONE* 7:e46205.

AHYONG, S. T. & YEO, D. C. J. 2007. Feral populations of the Australian red-claw crayfish (*Cherax quadricarinatus* von Martens) in water supply catchments of Singapore. *Biological Invasions* 9:943–946.

AKIN, J. 2011. Homeostatic processes for thermoregulation. *Nature* 3:7.

ALLANSON, B. R. 1958. On the systematics and distribution of the molluscan genus *Siphonaria* in South Africa. *Hydrobiologia* 12:149–180.

ALLEN, A. P. & GILLOOLY, J. F. 2007. The mechanistic basis of the metabolic theory of ecology. *Oikos* 116:1073–1077.

ALLOUCHE, O., TSOAR, A. & KADMON, R. 2006. Assessing the accuracy of species distribution models: prevalence, kappa and the true skill statistic (TSS). *Journal of Applied Ecology* 43:1223–1232.

ANDREWS, W. R. H. & HUTCHINGS, L. 1980. Upwelling in the southern Benguela current. *Progress in Oceanography* 9:1–81.

ANDRIDGE, R. R. 2011. Quantifying the impact of fixed effects modelling of clusters in multiple imputation for cluster randomized trials. *Biometrical Journal* 53:57–74.

ANESTIS, A., LAZOU, A., PÖRTNER, H. O. & MICHAELIDIS, B. 2007. Behavioural, metabolic, and molecular stress responses of marine bivalve *Mytilus*

galloprovincialis during long-term acclimation at increasing ambient temperature. *American Journal of Physiology-Regulatory, Integrative and Comparative Physiology* 293:R911–R921.

ANGILLETTA JR., MICHAEL J., BENNETT, ALBERT F., GUDERLEY, H., NAVAS, CARLOS A., SEEBACHER, F. & WILSON, ROBBIE S. 2006. Coadaptation a unifying principle in evolutionary thermal biology. *Physiological and Biochemical Zoology* 79:282–294.

ANGILLETTA, M. J. 2009. *Thermal adaptation: a theoretical and empirical synthesis*. Oxford University Press, Oxford, New York.

ANGILLETTA, M. J., NIEWIAROWSKI, P. H. & NAVAS, C. A. 2002. The evolution of thermal physiology in ectotherms. *Journal of Thermal Biology* 27:249–268.

ANSELL, A., GIBSON, R. N. & BARNES, M. 1999. *Oceanography and marine biology, an annual review*. CRC Press, London, England.

ARBUCKLE, J. L. 1996. *Advanced structural equation modelling: issues and techniques*. Pp. 243–278. Lawrence Erlbaum Associates, New Jersey, USA.

ARMSTRONG, J. D. 1986. Heart rate as an indicator of activity, metabolic rate, food intake and digestion in pike, *Esox lucius*. *Journal of Fish Biology* 29:207–221.

ARSLAN, J. & BENKE, K. 2023. Statistical analysis of ceiling and floor effects in medical trials. *Applied Biosciences* 2:668–681.

ATKINSON, D. L., BEGON, M. & FITTER, A. H. 1994. Temperature and organism size: A biological law for ectotherms? *Advances in Ecological Research* 25:1–58.

BABARRO, J. M. F., LABARTA, U. & REIRIZ, M. J. F. 2007. Energy metabolism and performance of *Mytilus galloprovincialis* under anaerobiosis. *Journal of the Marine Biological Association of the United Kingdom* 87:941–946.

BALADO, J., OLABARRIA, C., MARTÍNEZ-SÁNCHEZ, J., RODRÍGUEZ-PÉREZ, J. R. & PEDRO, A. 2021. Semantic segmentation of major macroalgae in coastal environments using high-resolution ground imagery and deep learning. *International Journal of Remote Sensing* 42:1785–1800.

BALLY, R., MCQUAID, C. & BROWN, A. 1984. Shores of mixed sand and rock: an unexplored marine ecosystem. *South African Journal of Science* 80:500–503.

BANDARA, K., VARPE, Ø., WIJEWARDENE, L., TVERBERG, V. & EIANE, K. 2021. Two hundred years of zooplankton vertical migration research. *Biological Reviews* 96:1547–1589.

BARBOSA, R. V., JAUD, M., BACHER, C., KERJEAN, Y., JEAN, F., AMMANN, J. & THOMAS, Y. 2022. High-resolution drone images show that the distribution of mussels depend on microhabitat features of intertidal rocky shores. *Remote Sensing* 14:5441.

BARR, D. J., LEVY, R., SCHEEPERS, C. & TILY, H. J. 2013. Random effects structure for confirmatory hypothesis testing: keep it maximal. *Journal of memory and language* 68:255–278.

BATES, D., MAECHLER, M., BOLKER, B. & WALKER, S. 2015. Fitting linear mixed-effects models using lme4. *Journal of Statistical Software* 67:1–48.

BATES, T. W. & HICKS, D. W. 2005. Locomotory behaviour and habitat selection in littoral gastropods on Caribbean limestone shores. *Journal of Shellfish Research* 24:75–84.

BEHRENS, J. W., GRÄNS, A., THERKILDSEN, N. O., NEUENFELDT, S. & AXELSSON, M. 2012. Correlations between hemoglobin type and temperature preference of juvenile Atlantic cod *Gadus morhua*. *Journal of Experimental Marine Biology and Ecology* 413:71–77.

BENINGER, P. G. & LE PENNEC, M. 2006. Structure and function in scallops. Pp. 123–227 in Shumway, S. E. & Parsons, G. J. (eds.). Elsevier, Amsterdam, Netherlands.

BERTNESS, M. D. 1989. Intraspecific competition and facilitation in a northern acorn barnacle population. *Ecology* 70:257–268.

BIRO, P. A. & DINGEMANSE, N. J. 2009. Sampling bias resulting from animal personality. *Trends in Ecology & Evolution* 24:66–67.

BJELDE, B. E., MILLER, N. A., STILLMAN, J. H. & TODGHAM, A. E. 2015. The role of oxygen in determining upper thermal limits in *Lottia digitalis* under air exposure and submersion. *Physiological and Biochemical Zoology* 88:483–493.

BJELDE, B. E. & TODGHAM, A. E. 2013. Thermal physiology of the fingered limpet

Lottia digitalis under emersion and immersion. *Journal of Experimental Biology* 216:2858–2869.

BLACKBURN, T. M., GASTON, K. J. & LODER, N. 1999. Geographic gradients in body size: a clarification of Bergmann's rule. *Diversity and Distributions* 5:165–174.

BLIESE, P. D. 2000. Within-group agreement, non-independence, and reliability: implications for data aggregation and analysis. Pp. 349–381. Jossey-Bass, San Francisco, USA.

BOLAND, J. M. 1997. Is the geographic pattern in the abundance of South African barnacles due to pre-recruitment or post-recruitment factors? *South African Journal of Marine Science* 18:63–73.

BOLBOACĂ, S. D., JÄNTSCHI, L., SESTRAŞ, A. F., SESTRAŞ, R. E. & PAMFIL, D. C. 2011. Pearson-Fisher Chi-square statistic revisited. *Information* 2:528–545.

BOLKER, B. M., BROOKS, M. E., CLARK, C. J., GEANGE, S. W., POULSEN, J. R., STEVENS, M. H. H. & WHITE, J.-S. S. 2009. Generalized linear mixed models: a practical guide for ecology and evolution. *Trends in Ecology & Evolution* 24:127–135.

BOLTON, J. J., LELIAERT, F., DE CLERCK, O., ANDERSON, R. J., STEGENGA, H., ENGLEDOW, H. E. & COPPEJANS, E. 2004. Where is the western limit of the tropical Indian Ocean seaweed flora? An analysis of intertidal seaweed biogeography on the East coast of South Africa. *Marine Biology* 144:51–59.

BONTE, D., VAN DYCK, H., BULLOCK, J. M., COULON, A., DELGADO, M., GIBBS, M., LEHOUCK, V., MATTHYSEN, E., MUSTIN, K., SAASTAMOINEN, M., SCHTICKZELLE, N., STEVENS, V. M., VANDEWOESTIJNE, S., BAGUETTE, M., BARTON, K., BENTON, T. G., CHAPUT-BARDY, A., CLOBERT, J., DYTHAM, C., HOVESTADT, T., MEIER, C. M., PALMER, S. C. F., TURLURE, C. & TRAVIS, J. M. J. 2012. Costs of dispersal. *Biological Reviews* 87:290–312.

BONTER, D. N. & BRIDGE, E. S. 2011. Applications of radio frequency identification (RFID) in ornithological research: a review. *Journal of Field Ornithology* 82:1–10.

BOONSTRA, R. 2013. Reality as the leading cause of stress: Rethinking the impact of

chronic stress in nature. *Functional Ecology* 27:11–23.

BOSMAN, A. L. & HOCKEY, P. A. R. 1988. The Influence of primary production rate on the population dynamics of *Patella granularis*, an intertidal limpet. *Marine Ecology* 9:181–198.

BOVBJERG, R. V. 1975. Dispersal and dispersion of pond snails in an experimental environment varying to three factors, singly and in combination. *Physiological Zoology* 48:203–215.

BRAHIM, A. & MARSHALL, D. J. 2020. Differences in heat tolerance plasticity between supratidal and intertidal snails indicate complex responses to microhabitat temperature variation. *Journal of Thermal Biology* 91:102620.

BRAHIM, A., MUSTAPHA, N. & MARSHALL, D. J. 2019. Non-reversible and reversible heat tolerance plasticity in tropical intertidal animals: responding to habitat temperature heterogeneity. *Frontiers in Physiology* 9:1909.

BRANCH, G. M. 1971. The ecology of *Patella* Linnaeus from the Cape Peninsula, South Africa I. Zonation, movements and feeding. *Zoologica Africana* 6:1–38.

BRANCH, G. M. 1975. Mechanisms reducing intraspecific competition in *Patella spp*.: migration, differentiation and territorial behaviour. *Journal of Animal Ecology* 44:575–600.

BRANCH, G. M. 1976. Interspecific competition experienced by South African *Patella* species. *Journal of Animal Ecology* 45:507–529.

BRANCH, G. M. 1978. The responses of South African patellid limpets to invertebrate predators. *African Zoology* 13:221–232.

BRANCH, G. M. 1981. The biology of limpets: physical factors, energy flow, and ecological interactions. *Oceanography and Marine Biology: An Annual Review* 19:235–380.

BRANCH, G. M. & CHERRY, M. I. 1985. Activity rhythms of the pulmonate limpet *Siphonaria capensis* Q. & G. as an adaptation to osmotic stress, predation and wave action. *Journal of Experimental Marine Biology and Ecology* 87:153–168.

BRANCH, G. & BRANCH, M. 1988. *The living shores of southern Africa.* Struik Publishers, Cape Town, South Africa.

BRANCH, G., BRANCH, M., GRIFFITHS, C. & BECKLEY, L. 2022. *Two oceans: a guide to the marine life of southern Africa*. Penguin Random House, South Africa.

BRANCH, G. & GRIFFITHS, C. 1994. *Two oceans: a guide to the marine life of southern Africa*. Penguin Random House, New York, USA.

BRIER, G. W. 1950. Verification of forecasts expressed in terms of probability. *Monthly Weather Review* 78:1–3.

BRITTON, J. C. 1995. The relationship between position on shore and shell ornamentation in two size-dependent morphotypes of *Littorina striata*, with an estimate of evaporative water loss in these morphotypes and in *Melarhaphe neritoides*. *Hydrobiologia* 309:129142.

BROITMAN, B. R., LAGOS, N. A., OPITZ, T., FIGUEROA, D., MALDONADO, K., RICOTE, N. & LARDIES, M. A. 2021. Phenotypic plasticity is not a cline: thermal physiology of an intertidal barnacle over 20° of latitude. *Journal of Animal Ecology* 90:1961–1972.

BROOKS, M. E., KRISTENSEN, K., BENTHEM, K. J. VAN, MAGNUSSON, A., BERG, C. W., NIELSEN, A., SKAUG, H. J., MÄCHLER, M. & BOLKER, B. M. 2017. Modelling zero-inflated count data with glmmTMB. *BioRxiv*:132753.

BROWN, A. C. & WYNBERG, R. P. 1987. Absence of an oxygen debt in the nassariid whelk *Bullia digitalis* (Dillwyn). *Journal of Molluscan Studies* 53:289–290.

BROWN, J. H., GILLOOLY, J. F., ALLEN, A. P., SAVAGE, V. M. & WEST, G. B. 2004. Toward a metabolic theory of ecology. *Ecology* 85:1771–1789.

BROWN, R. L. 1994. Efficacy of the indirect approach for estimating structural equation models with missing data: a comparison of five methods. *Structural Equation Modelling: A Multidisciplinary Journal* 1:287–316.

BROWN, V. A. 2021. An introduction to linear mixed-effects modelling in R. *Advances in Methods and Practices in Psychological Science* 4(1):2515245920960351.

BROWNIE, C., HINES, J. E., NICHOLS, J. D., POLLOCK, K. H. & HESTBECK, J. B. 1993. Capture-recapture studies for multiple strata including non-Markovian transitions. *Biometrics*:1173–1187.

BRUMLEY, D. R., CARRARA, F., HEIN, A. M., HAGSTROM, G. I., LEVIN, S. A. &

STOCKER, R. 2020. Cutting through the noise: bacterial chemotaxis in marine microenvironments. *Frontiers in Marine Science* 7:527.

BUASAKAEW, N., CHAN, B. K. K. & WANGKULANGKUL, K. 2021. Why are barnacles common on intertidal rocks but rare in rock pools? Effect of water temperature, salinity, and continuous submergence on barnacle survival in Indian Ocean rock pools. *Frontiers in Marine Science* 8:688894.

BUCKLEY, B. A., OWEN, M.-E. & HOFMANN, G. E. 2001. Adjusting the thermostat: the threshold induction temperature for the heat shock response in intertidal mussels (genus *Mytilus*) changes as a function of thermal history. *Journal of Experimental Biology* 204:3571–3579.

BURNETT, N. P., SEABRA, R., PIRRO, M. DE, WETHEY, D. S., WOODIN, S. A., HELMUTH, B., ZIPPAY, M. L., SARÀ, G., MONACO, C. & LIMA, F. P. 2013. An improved non-invasive method for measuring heartbeat of intertidal animals. *Limnology and Oceanography: Methods* 11:91–100.

BURNHAM, K. P. & ANDERSON, D. R. 2002. *Model selection and multimodel inference: a practical information-theoretic approach*. Springer Science & Business Media, Berlin, Germany.

BUSTAMANTE, R. H., BRANCH, G. M. & EEKHOUT, S. 1997. The influences of physical factors on the distribution and zonation patterns of South African rocky-shore communities. *South African Journal of Marine Science* 18:119–136.

BUSTAMANTE, R. H., BRANCH, G. M., EEKHOUT, S., ROBERTSON, B., ZOUTENDYK, P., SCHLEYER, M., DYE, A., HANEKOM, N., KEATS, D., JURD, M. & MCQUAID, C. 1995. Gradients of intertidal primary productivity around the coast of South Africa and their relationships with consumer biomass. *Oecologia* 102:189–201.

BUSTAMANTE, R. & BRANCH, G. 1996. Large scale patterns and trophic structure of southern African rocky shores: the roles of geographic variation and wave exposure. *Journal of Biogeography* 23:339–351.

BUUREN, STEF. VAN. 2018. *Flexible imputation of missing data* (2nd edition). Chapman & Hall/CRC, Florida, USA.

BUUREN, STEF. VAN & GROOTHUIS-OUDSHOORN, K. 2011. mice: Multivariate imputation by chained equations in R. *Journal of Statistical Software* 45:1–67.

BYRNE, M., SELVAKUMARASWAMY, P., HO, M. A., WOOLSEY, E. & NGUYEN, H. D. 2011. Sea urchin development in a global change hotspot, potential for southerly migration of thermotolerant propagules. *Deep Sea Research Part II: Topical Studies in Oceanography* 58:712–719.

CAMACHO, F. A. & THACKER, R. W. 2013. Predator cues alter habitat use by the amphipod *Hyalella azteca* (Saussure). *Freshwater Science* 32:1148–1154.

CAMPOS, D. F., AMANAJÁS, R. D., ALMEIDA-VAL, V. M. & VAL, A. L. 2021. Climate vulnerability of south American freshwater fish: thermal tolerance and acclimation. *Journal of Experimental Zoology Part A: Ecological and Integrative Physiology* 335:723–734.

CANTY, A., RIPLEY, B. & OTHERS. 2017. *Boot: Bootstrap r (s-plus) functions*. Pp. 3–20 *CRAN: Contributed Packages*. The R Foundation.

CARLSON, A. J. 1905. Comparative physiology of the invertebrate heart. *Biological Bulletin* 8:123–168.

CARPENTER, J. & KENWARD, M. 2012. *Multiple imputation and its application*. John Wiley & Sons, New Jersey, USA.

CARTWRIGHT, S. R. & WILLIAMS, G. A. 2012. Seasonal variation in utilization of biogenic microhabitats by littorinid snails on tropical rocky shores. *Marine Biology* 159:2323–2332.

CASAL, G., KUTSER, T., DOMÍNGUEZ-GÓMEZ, J. A., SÁNCHEZ-CARNERO, N. & FREIRE, J. 2013. Assessment of the hyperspectral sensor CASI-2 for macroalgal discrimination on the Ría de Vigo coast (NW Spain) using field spectroscopy and modelled spectral libraries. *Continental Shelf Research* 55:129–140.

CASTEJÓN, D., GARCÍA, L., CAÑIZARES, J. M., DE GIROLAMO, M., NUNES, C., ISIDRO, E., COURTOIS DE VIÇOSE, G., NOGUEIRA, N. & ANDRADE, C. A. P. 2022. Methodologies for patellid *limpets*' aquaculture: from broodstock management to juveniles. *Frontiers in Marine Science* 9:884262.

CASTILLA, J. C., LAGOS, N. A. & CERDA, M. 2004. Marine ecosystem engineering

by the alien ascidian *Pyura praeputialis* on a mid-intertidal rocky shore. *Marine Ecology Progress Series* 268:119–130.

CHAMBERS, R. J. 1995. The conflict between adaptation and constraint: the case of the siphonariid limpets. PhD thesis, Rhodes University, South Africa.

CHAMBERS, R. J. & MCQUAID, C. D. 1994. Notes on the taxonomy, spawn and larval development of South African species of the intertidal limpet *Siphonaria* (Gastropoda: Pulmonata). *Journal of Molluscan Studies* 60:263–275.

CHAPELLE, G. & PECK, L. S. 1999. Polar gigantism dictated by oxygen availability. *Nature* 399:114–115.

CHAPMAN, M. G. 1986. Assessment of some controls in experimental transplants of intertidal gastropods. *Journal of Experimental Marine Biology and Ecology* 103:181–201.

CHAPMAN, M. G. 2000. A comparative study of differences among species and patches of habitat on movements of three species of intertidal gastropods. *Journal of Experimental Marine Biology and Ecology* 244:181–201.

CHAPPERON, C. & SEURONT, L. 2009. Cue synergy in *Littorina littorea* navigation following wave dislodgement. *Journal of the Marine Biological Association of the United Kingdom* 89:1133–1136.

CHAPPERON, C. & SEURONT, L. 2011. Variability in the motion behaviour of intertidal gastropods: ecological and evolutionary perspectives. *Journal of the Marine Biological Association of the United Kingdom* 91:237–244.

CHAPPERON, C. & SEURONT, L. 2012. Keeping warm in the cold: on the thermal benefits of aggregation behaviour in an intertidal ectotherm. *Journal of Thermal Biology* 37:640–647.

CHAPPERON, C., STUDERUS, K. & CLAVIER, J. 2017. Mitigating thermal effect of behaviour and microhabitat on the intertidal snail *Littorina saxatilis* (Olivi) over summer. *Journal of Thermal Biology* 67:40–48.

CHAPPERON, C., VOLKENBORN, N., CLAVIER, J., SÉITÉ, S., SEABRA, R. & LIMA, F. P. 2016. Exposure to solar radiation drives organismal vulnerability to climate: evidence from an intertidal limpet. *Journal of Thermal Biology* 57:92–100.

CHEN, I. CHING., HILL, J. K., OHLEMÜLLER, R., ROY, D. B. & THOMAS, C. D. 2011. Rapid range shifts of species associated with high levels of climate warming. *Science* 333:1024–1026.

CHESTER, E. T., MILLER, A. D., VALENZUELA, I., WICKSON, S. J. & ROBSON, B. J. 2015. Drought survival strategies, dispersal potential and persistence of invertebrate species in an intermittent stream landscape. *Freshwater Biology* 60:2066–2083.

CHEUNG, W. W. L., SARMIENTO, J. L., DUNNE, J., FRÖLICHER, T. L., LAM, V. W. Y., DENG PALOMARES, M. L., WATSON, R. & PAULY, D. 2013. Shrinking of fishes exacerbate impacts of global ocean changes on marine ecosystems. *Nature Climate Change* 3:254–258.

CHOI, F., GOUHIER, T., LIMA, F., RILOV, G., SEABRA, R. & HELMUTH, B. 2019. Mapping physiology: biophysical mechanisms define scales of climate change impacts. *Conservation Physiology* 7:coz028.

CLARK, T. D., SANDBLOM, E. & JUTFELT, F. 2013. Aerobic scope measurements of fishes in an era of climate change: respirometry, relevance and recommendations. *The Journal of Experimental Biology* 216:2771–2782.

CLENCH, H. K. 1966. Behavioral thermoregulation in butterflies. *Ecology* 47:1021–1034.

CLUSELLA-TRULLAS, S., BLACKBURN, T. M. & CHOWN, S. L. 2011. Climatic predictors of temperature performance curve parameters in ectotherms imply complex responses to climate change. *The American Naturalist* 177:738–751.

COLLINS, L. M., SCHAFER, J. L. & KAM, C. M. 2001. A comparison of inclusive and restrictive strategies in modern missing data procedures. *Psychological Methods* 6:330–351.

COLOSIMO, I., VET, P. L. M. DE, MAREN, D. S. VAN, RENIERS, A. J. H. M., WINTERWERP, J. C. & PROOIJEN, B. C. VAN. 2020. The impact of wind on flow and sediment transport over intertidal flats. *Journal of Marine Science and Engineering* 8:910.

COMPAIRE, J. C., MONTES, J., GONÇALVES, J. M. S., SORIGUER, M. C. &

ERZINI, K. 2022. Site fidelity of fish on a rocky intertidal in the south of Portugal. *Journal of Sea Research* 183:102202.

CONNELL, L. J., BEINE, K. & GREENFIELD, R. 2025. Reaching a breaking point: upper thermal limit of the limpets, *Scutellastra granularis* and *Siphonaria capensis*, along the southern and west coasts of South Africa. *Journal of Thermal Biology* 24:104148.

CONNOR, K. M. & GRACEY, A. Y. 2012. High-resolution analysis of metabolic cycles in the intertidal mussel *Mytilus californianus*. *American Journal of Physiology. Regulatory, Integrative and Comparative Physiology* 302:R103–111.

COOK, R. D. 1977. Detection of influential observation in linear regression. *Technometrics* 19:15–18.

COSSINS, A. R. & BOWLER, K. 1987. *Temperature biology of animals.* Springer Science & Business Media, Berlin, Germany.

COWLES, R. B. & BOGERT, C. M. 2006. Preliminary study of the thermal requirements of desert reptiles. *Iguana* 13:53–60.

COX, D. K., GIBBONS, J. & SHARITZ, R. 1974. Effects of three heating rates on the critical thermal maximum of bluegill. *Thermal ecology*.

CREESE, R. G. & UNDERWOOD, A. J. 1982. Analysis of inter- and intra-specific competition amongst intertidal limpets with different methods of feeding. *Oecologia* 53:337–346.

CRICKENBERGER, S., HUI, T., YUAN, F. L., BONEBRAKE, T. & WILLIAMS, G. 2020. Preferred temperature of intertidal ectotherms: broad patterns and methodological approaches. *Journal of Thermal Biology* 87:102468.

CROWE, T. P. & UNDERWOOD, A. 1998. Testing behavioural 'preference' for suitable microhabitat. *Journal of Experimental Marine Biology and Ecology* 225:1–11.

CURTIS, T., WILLIAMSON, R. & DEPLEDGE, M. 2000. Simultaneous, long-term monitoring of valve and cardiac activity in the blue mussel *Mytilus edulis* exposed to copper. *Marine Biology* 136:837–846.

D'URBAN JACKSON, T., WILLIAMS, G. J., WALKER-SPRINGETT, G. & DAVIES, A. J. 2020. Three-dimensional digital mapping of ecosystems: a new era in spatial

ecology. *Proceedings of the Royal Society B: Biological Sciences* 287:2019–2383.

DALGAARD, P. 2002. *Introductory statistics with R* (1st edition). Springer, New York, USA.

DARIAS, J., CUETO, M. & DIAZ-MARRERO, A. 2006. The chemistry of marine pulmonate gastropods. *Progress in Molecular and Subcellular Biology* 43:105–31.

DAVIES, A., JOHNSON, M. & MAGGS, C. 2007. Limpet grazing and loss of *Ascophyllum nodosum* canopies on decadal time scales. *Marine Ecology Progress Series* 339:131–141.

DAVIES, M. & BECKWITH, P. 1999. Role of mucus trails and trail-following in the behaviour and nutrition of the periwinkle *Littorina littorea*. *Marine Ecology Progress Series* 179:247–257.

DAVIES-COLEMAN, M. T. 2006. Secondary metabolites from the marine gastropod molluscs of Antarctica, southern Africa and South America. *Progress in Molecular and Subcellular Biology* 43:133–157.

DEACON, H., JURY, M. & ELLIS, F. 1992. Selective regime and time. Pp. 6–22 in Cowling, R. M. (ed.). *The ecology of fynbos: Nutrients, fire and diversity*. Oxford University Press, Oxford, England.

DEBRUINE, L. 2021. *faux: Simulation for factorial designs*. *CRAN: Contributed Packages*. The R Foundation.

DELDICQ, N., LANGLET, D., DELAETER, C., BEAUGRAND, G., SEURONT, L. & BOUCHET, V. M. P. 2021. Effects of temperature on the behaviour and metabolism of an intertidal foraminifera and consequences for benthic ecosystem functioning. *Scientific Reports* 11:4013.

DELORME, N. J., KING, N., CERVANTES-LORETO, A., SOUTH, P. M., BAETTIG, C. G., ZAMORA, L. N., KNIGHT, B. R., ERICSON, J. A., SMITH, K. F. & RAGG, N. L. C. 2024. Genetics and ontogeny are key factors influencing thermal resilience in a culturally and economically important bivalve. *Scientific Reports* 14:19130.

DEMPSTER, Y. & BRANCH, G. M. 1999. A review of the genus *Burnupena iredale*, 1918 (Gastropoda: Buccinidae), with descriptions of two new species. *Annals of the Natal Museum* 40:173–204.

DENNY, M. W. & HARLEY, C. D. G. 2006. Hot limpets: predicting body temperature in a conductance-mediated thermal system. *Journal of Experimental Biology* 209:2409–2419.

DENNY, M. & DOWD, W. 2012. Biophysics, environmental stochasticity, and the evolution of thermal safety margins in intertidal limpets. *Journal of Experimental Biology* 215:934–947.

DENNY, M., DOWD, W., BILIR, L. & MACH, K. 2011. Spreading the risk: small-scale body temperature variation among intertidal organisms and its implications for species persistence. *Journal of Experimental Marine Biology and Ecology* 400:175–190.

DEPLEDGE, M. H. & ANDERSEN, B. B. 1990. A computer-aided physiological monitoring system for continuous, long-term recording of cardiac activity in selected invertebrates. *Comparative Biochemistry and Physiology Part A: Physiology* 96:473–477.

DEUTSCH, C. A., TEWKSBURY, J. J., HUEY, R. B., SHELDON, K. S., GHALAMBOR, C. K., HAAK, D. C. & MARTIN, P. R. 2008. Impacts of climate warming on terrestrial ectotherms across latitude. *Proceedings of the National Academy of Sciences* 105:6668–6672.

DIAZ, F., RE, A. D., MEDINA, Z., RE, G., VALDEZ, G. & VALENZUELA, F. 2006. Thermal preference and tolerance of green abalone *Haliotis fulgens* (Philippi, 1845) and pink abalone *Haliotis corrugata* (Gray, 1828). *Aquaculture Research* 37:877–884.

DIAZ, F., SALAS, A., RE, A., GONZÁLEZ, M. & REYES, I. 2011. Thermal preference and tolerance of *Megastrea* (*ithopoma*) *undosa* (Wood, 1828; Gastropoda: Turbinidae). *Journal of Thermal Biology* 36:34–37.

DIEDERICH, C. & PECHENIK, J. 2013. Thermal tolerance of *Crepidula fornicata* (Gastropoda) life history stages from intertidal and subtidal subpopulations. *Marine Ecology Progress Series* 486:173–187.

DILLON, M. E., LIU, R., WANG, G. & HUEY, R. B. 2012. Disentangling thermal preference and the thermal dependence of movement in ectotherms. *Journal of*

Thermal Biology 37:631–639.

DILLON, M. E., WANG, G., GARRITY, P. A. & HUEY, R. B. 2009. Thermal preference in *Drosophila*. *Journal of Thermal Biology* 34:109–119.

DOERING, P. H. & PHILLIPS, D. W. 1983. Maintenance of the shore-level size gradient in the marine snail *Tegula funebralis* (A. Adams): importance of behavioural responses to light and sea star predators. *Journal of Experimental Marine Biology and Ecology* 67:159–173.

DONG, Y., LI, X., CHOI, F. M. P., WILLIAMS, G. A., SOMERO, G. N. & HELMUTH, B. 2017. Untangling the roles of microclimate, behaviour and physiological polymorphism in governing vulnerability of intertidal snails to heat stress. *Proceedings of the Royal Society B: Biological Sciences* 284:20162367.

DONG, Y., LIAO, M., HAN, G. & SOMERO, G. N. 2021. An integrated, multi-level analysis of thermal effects on intertidal molluscs for understanding species distribution patterns. *Biological Reviews* 97:554–581.

DONG, Y. & WILLIAMS, G. A. 2011. Variations in cardiac performance and heat shock protein expression to thermal stress in two differently zoned limpets on a tropical rocky shore. *Marine biology* 158:1223–1231.

DONOVAN, D., BALDWIN, J. & CAREFOOT, T. 1999. The contribution of anaerobic energy to gastropod crawling and a re-estimation of minimum cost of transport in the abalone, *Haliotis kamtschatkana* (Jonas). *Journal of Experimental Marine Biology and Ecology* 235:273–284.

DOUTHWAITE, R., JONES, E., TYSER, A. & VRDOLJAK, S. 2018. The introduction, spread and ecology of redclaw crayfish *Cherax quadricarinatus* in the Zambezi catchment. *African Journal of Aquatic Science* 43:353–366.

DOWD, W. W., FELTON, C. A., HEYMANN, H. M., KOST, L. E. & SOMERO, G. N. 2013. Food availability, more than body temperature, drives correlated shifts in ATP-generating and antioxidant enzyme capacities in a population of intertidal mussels (*Mytilus californianus*). *Journal of Experimental Marine Biology and Ecology* 449:171–185.

DOWER, K. M. 1989. Sand inundanon on rocky shores: its effects on species richness

and the structure of species assemblages. PhD thesis, Rhodes University, South Africa.

DRAKE, M. J., MILLER, N. A. & TODGHAM, A. E. 2017. The role of stochastic thermal environments in modulating the thermal physiology of an intertidal limpet, *Lottia digitalis*. *Journal of Experimental Biology* 220:3072–3083.

DRECHSLER, J. 2015. Multiple imputation of multilevel missing data—rigor versus simplicity. *Journal of Educational and Behavioural Statistics* 40:69–95.

DUGAN, J. E., HUBBARD, D. M. & WENNER, A. M. 1994. Geographic variation in life history of the sand crab, *Emerita analoga* (Stimpson) on the California coast: relationships to environmental variables. *Journal of Experimental Marine Biology and Ecology* 181:255–278.

DUNN, P. K. & SMYTH, G. K. 2018. *Generalized linear models with examples in R*. Springer, New York, USA.

EASTERLING, D., MEEHL, G., PARMESAN, C., CHANGNON, S., KARL, T. R. & MEARNS, L. 2000. Climate extremes: observations, modelling, and impacts. *Science* 289:2068–74.

EDWARDS & DAVIES, M. 2002. Functional and ecological aspects of the mucus trails of the intertidal prosobranch gastropod *Littorina littorea* (L.). *Marine Ecology Progress Series* 239:129–137.

EEKHOUT, I., BOER, R. M. DE, TWISK, J. W. R., VET, H. C. W. DE & HEYMANS, M. W. 2012. Missing data a systematic review of how they are reported and handled. *Epidemiology* 23:729732.

EJBYE-ERNST, R., MICHAELSEN, T. Y., TIRSGAARD, B., WILSON, J. M., JENSEN, L. F., STEFFENSEN, J. F., PERTOLDI, C., AARESTRUP, K. & SVENDSEN, J. C. 2016. Partitioning the metabolic scope: the importance of anaerobic metabolism and implications for the oxygen- and capacity-limited thermal tolerance (OCLTT) hypothesis. *Conservation Physiology* 4:cow019.

ELAHI, R., MILLER, L. P. & LITVIN, S. Y. 2020. Historical comparisons of body size are sensitive to data availability and ecological context. *Ecology* 101:e03101.

ELLEM, G. K., FURST, J. E. & ZIMMERMAN, K. D. 2002. Shell clamping behaviour

in the limpet *Cellana tramoserica*. *Journal of Experimental Biology* 205:539–547.

ELLINGTON, E. H., BASTILLE-ROUSSEAU, G., AUSTIN, C., LANDOLT, K. N., POND, B. A., REES, E. E., ROBAR, N. & MURRAY, D. L. 2015. Using multiple imputation to estimate missing data in meta-regression. *Methods in Ecology and Evolution* 6:153–163.

ENDERS, C. K. 2001. A primer on maximum likelihood algorithms available for use with missing data. *Structural Equation Modelling: A Multidisciplinary Journal* 8:128–141.

ENDERS, C. K. 2010. *Applied missing data analysis*. Guilford Press, New York, USA.

ENDERS, C. K., MISTLER, S. A. & KELLER, B. T. 2016. Multilevel multiple imputation: a review and evaluation of joint modelling and chained equations imputation. *Psychological Methods* 21:222–240.

ERN, R., HUONG, D. T. T., PHUONG, N. T., WANG, T. & BAYLEY, M. 2014. Oxygen delivery does not limit thermal tolerance in a tropical eurythermal crustacean. *Journal of Experimental Biology* 217:809–814.

ESTES, L., ELSEN, P. R., TREUER, T., AHMED, L., CAYLOR, K., CHANG, J., CHOI, J. J. & ELLIS, E. C. 2018. The spatial and temporal domains of modern ecology. *Nature Ecology & Evolution* 2:819–826.

FANGUE, N. A., MANDIC, M., RICHARDS, J. G. & SCHULTE, P. M. 2008. Swimming performance and energetics as a function of temperature in killifish *Fundulus heteroclitus*. *Physiological and Biochemical Zoology* 81:389–401.

FANGUE, NANN A., PODRABSKY, JASON E., CRAWSHAW, LARRY I. & SCHULTE, PATRICIA M. 2009. Countergradient variation in temperature preference in populations of killifish *Fundulus heteroclitus*. *Physiological and Biochemical Zoology* 82:776–786.

FAULKNER, K. T., CLUSELLA-TRULLAS, S., PECK, L. S. & CHOWN, S. L. 2014. Lack of coherence in the warming responses of marine crustaceans. *Functional Ecology* 28:895–903.

FAWCETT, T. 2006. Introduction to ROC analysis. *Pattern Recognition Letters* 27:861–874.

FEARE, C. J. 1971. The adaptive significance of aggregation behaviour in the dogwhelk *Nucella lapillus* (L.). *Oecologia* 7:117–126.

FEDER, M. E. & HOFMANN, G. E. 1999. Heat shock proteins, molecular chaperones, and the stress response: evolutionary and ecological physiology. *Annual Review of Physiology* 61:243–282.

FEMINO, R. J. & MATHIESON, A. C. 1980. Investigations of New England marine algae IV. The ecology and seasonal succession of tide pool algae at Bald Head Cliff, York, Maine, USA. *Botanica Marina* 23:319–332.

FINKE, G. R., NAVARRETE, S. A. & BOZINOVIC, F. 2007. Tidal regimes of temperate coasts and their influences on aerial exposure for intertidal organisms. *Marine Ecology Progress Series* 343:57–62.

FIRTH, L. B. & WILLIAMS, GRAY. A. 2009. The influence of multiple environmental stressors on the limpet *Cellana toreuma* during the summer monsoon season in Hong Kong. *Journal of Experimental Marine Biology and Ecology* 375:70–75.

FOLK, A. & MENNERAT, A. 2024. Methods for tagging an ectoparasite, the salmon louse *Lepeophtheirus salmonis*. *Peer Community Journal* 4.

FOX, J. & MONETTE, G. 2002. *R and s-plus companion to applied regression*. Sage Publications, Inc., New York, USA.

FRASER, C. M. L., SEEBACHER, F., LATHLEAN, J. & COLEMAN, R. A. 2016. Facing the heat: does desiccation and thermal stress explain patterns of orientation in an intertidal invertebrate? *PloS ONE* 11:e0150200.

FREDERICH, M. & PÖRTNER, H. O. 2000. Oxygen limitation of thermal tolerance defined by cardiac and ventilatory performance in spider crab, *Maja squinado*. *American Journal of Physiology - Regulatory, Integrative and Comparative Physiology* 279:R1531–R1538.

FRY, F. E. J. 1947. *Effects of the environment on animal activity*. The University of Toronto Press, Toronto, Canada.

GÄDE, G. 1983. Energy metabolism of arthropods and molluscs during environmental and functional anaerobiosis. *Journal of Experimental Zoology* 228:415–429.

GANSER, A. M., NEWTON, T. J. & HARO, R. J. 2015. Effects of elevated water

temperature on physiological responses in adult freshwater mussels. *Freshwater Biology* 60:1705–1716.

GARCÍA-GUERRERO, M. U., HERNÁNDEZ-SANDOVAL, P., ORDUÑA-ROJAS, J. & CORTÉS-JACINTO, E. 2013. Effect of temperature on weight increase, survival, and thermal preference of juvenile redclaw crayfish *Cherax quadricarinatus*. *Hidrobiologica* 23:73–81.

GARNER, C. J. 2013. Characterisation and biotic classification of eastern Cape mixed substrate shores. PhD thesis, Nelson Mandela Metropolitan University, South Africa.

GARRITY, S. D. 1984. Some adaptations of gastropods to physical stress on a tropical rocky shore. *Ecology* 65:559–574.

GENDRON, R. P. 1977. Habitat selection and migratory behaviour of the intertidal gastropod *Littorina littorea* (L.). *Journal of Animal Ecology* 46:79–92.

GERALD, B. & PATSON, T. F. 2021. Parametric and nonparametric tests: a brief review. *International Journal of Statistical Distributions and Applications* 7:78–82.

GIBBONS, W. J. & ANDREWS, K. M. 2004. PIT tagging: simple technology at its best. *BioScience* 54:447–454.

GINKEL, J. R. VAN, SIJTSMA, K., ARK, L. A. VAN DER & VERMUNT, J. K. 2010. Incidence of missing item scores in personality measurement, and simple item score imputation. *Methodology* 6:17–30.

GIOMI, F., BARAUSSE, A., DUARTE, C. M., BOOTH, J., AGUSTI, S., SADERNE, V., ANTON, A., DAFFONCHIO, D. & FUSI, M. 2019. Oxygen supersaturation protects coastal marine fauna from ocean warming. *Science Advances* 5:eaax1814.

GLEASON, L. U. & BURTON, R. S. 2015. RNA-seq reveals regional differences in transcriptome response to heat stress in the marine snail *Chlorostoma funebralis*. *Molecular Ecology* 24:610–627.

GODET, L., FOURNIER, J., TOUPOINT, N. & OLIVIER, F. 2009. Mapping and monitoring intertidal benthic habitats: a review of techniques and a proposal for a new visual methodology for the European coasts. *Progress in Physical Geography: Earth and Environment* 33:378–402.

GOLDSTEIN, H. 2011. *Multilevel statistical models*. John Wiley & Sons, New Jersey,

USA.

GOMES, D. G. 2022. Should I use fixed effects or random effects when I have fewer than five levels of a grouping factor in a mixed-effects model? *PeerJ* 10:e12794.

GONZÁLEZ, R. A., DÍAZ, F., LICEA, A., DENISSE RE, A., NOEMÍ SÁNCHEZ, L. & GARCÍA-ESQUIVEL, Z. 2010. Thermal preference, tolerance and oxygen consumption of adult white shrimp *Litopenaeus vannamei* (Boone) exposed to different acclimation temperatures. *Journal of Thermal Biology* 35:218–224.

GORDON, M. S., FISCHER, S. & TARIFEÑO S., E. 1970. Aspects of the physiology of terrestrial life in amphibious fishes: II. The Chilean clingfish, *Sicyases sanguineus*. *Journal of Experimental Biology* 53:559–572.

GORR, T. A. 2017. Hypometabolism as the ultimate defence in stress response: how the comparative approach helps understanding of medically relevant questions. *Acta Physiologica* 219:409–440.

GRACEY, A. Y., CHANEY, M. L., BOOMHOWER, J. P., TYBURCZY, W. R., CONNOR, K. & SOMERO, G. N. 2008. Rhythms of gene expression in a fluctuating intertidal environment. *Current biology: CB* 18:1501–1507.

GRAHAM, J. W. 2003. Adding missing-data-relevant variables to fiml-based structural equation models. *Structural Equation Modelling: A Multidisciplinary Journal* 10:80–100.

GRAHAM, J. W. 2009. Missing data analysis: making it work in the real world. *Annual review of psychology* 60:549–576.

GRAHAM, J. W., HOFER, S. M. & MACKINNON, D. P. 1996. Maximizing the usefulness of data obtained with planned missing value patterns: an application of maximum likelihood procedures. *Multivariate Behavioural Research* 31:197–218.

GRAHAM, J. W., TAYLOR, B. J., OLCHOWSKI, A. E. & CUMSILLE, P. E. 2006. Planned missing data designs in psychological research. *Psychological Methods* 11:323–343.

GRANCHI, C., BERTINI, S., MACCHIA, M. & MINUTOLO, F. 2010. Inhibitors of lactate dehydrogenase isoforms and their therapeutic potentials. *Current Medicinal Chemistry* 17:672–697.

GRÄNS, A., JUTFELT, F., SANDBLOM, E., JÖNSSON, E., WIKLANDER, K., SETH, H., OLSSON, C., DUPONT, S., ORTEGA-MARTINEZ, O., EINARSDOTTIR, I., BJÖRNSSON, B. T., SUNDELL, K. & AXELSSON, M. 2014. Aerobic scope fails to explain the detrimental effects on growth resulting from warming and elevated CO2 in Atlantic halibut. *The Journal of Experimental Biology* 217:711–717.

GRAY, D. R. & HODGSON, A. N. 1998. Foraging and homing behaviour in the high-shore, crevice-dwelling limpet *Helcion pectunculus* (Prosobranchia: Patellidae). *Marine Biology* 132:283–294.

GREEN, J. A. 2011. The heart rate method for estimating metabolic rate: review and recommendations. *Comparative Biochemistry and Physiology. Part A, Molecular & Integrative Physiology* 158:287–304.

GRIESHABER, M. K., HARDEWIG, I., KREUTZER, U. & PÖRTNER, H. O. 1994. Physiological and metabolic responses to hypoxia in invertebrates. Pp. 43–147. Springer, Berlin, Germany.

GRIFFITHS, C. L., ROBINSON, T. B., LANGE, L. & MEAD, A. 2010. Marine biodiversity in South Africa: an evaluation of current states of knowledge. *PloS ONE* 5:e12008.

GRUND, S., LÜDTKE, O. & ROBITZSCH, A. 2016. Multiple imputation of multilevel missing data: an introduction to the R package pan. *SAGE Open* 6:2158244016668220.

GRUND, S., LÜDTKE, O. & ROBITZSCH, A. 2018. Multiple imputation of missing data for multilevel models: simulations and recommendations. *Organizational Research Methods* 21:111–149.

GRÜNDLINGH, M. L. 1983. On the course of the Agulhas current. *South African Geographical Journal* 65:49–57.

GULLEDGE, C. M., SMITH, D. G., ZIEDAS, A., MUH, S. J., MOUTZOUROS, V. & MAKHNI, E. C. 2019. Floor and ceiling effects, time to completion, and question burden of PROMIS CAT domains among shoulder and knee patients undergoing nonoperative and operative treatment. *JBJS Open Access* 4:e0015.

GUNDERSON, A. R., ABEGAZ, M., CEJA, A. Y., LAM, E., SOUTHER, B. F.,

BOYER, K., KING, E., YOU MAK, K. T., TSUKIMURA, B. & STILLMAN, J. H. 2019. Hot rocks and not-so-hot rocks on the seashore: patterns and body-size dependent consequences of microclimatic variation in intertidal zone boulder habitat. *Integrative Organismal Biology* 1:obz024.

GUPPY, M. & WITHERS, P. 2007. Metabolic depression in animals: physiological perspectives and biochemical generalizations. *Biological Reviews* 74:1–40.

HAMILTON, P. V. 1978. Adaptive visually-mediated movements of *Littorina irrorata* (Mollusca: Gastropoda) when displaced from their natural habitat. *Marine Behaviour and Physiology* 5:255–271.

HAN, G., WANG, W. & DONG, Y. 2020. Effects of balancing selection and microhabitat temperature variations on heat tolerance of the intertidal black mussel *Septifer virgatus*. *Integrative Zoology* 15:416–427.

HAN, G., ZHANG, S., MARSHALL, D. J., KE, C. & DONG, Y. 2013. Metabolic energy sensors (AMPK and SIRT1), protein carbonylation and cardiac failure as biomarkers of thermal stress in an intertidal limpet: linking energetic allocation with environmental temperature during aerial emersion. *The Journal of Experimental Biology* 216:3273–3282.

HAND, S. C. & HARDEWIG, I. 1996. Downregulation of cellular metabolism during environmental stress: mechanisms and implications. *Annual Review of Physiology* 58:539–563.

HANN, I. 2021. Variations in thermal performance of cardiac function of pure and hybrid *Mytilus spp*. as a factor influencing hybrid zone dynamics. *The Plymouth Student Scientist* 14:91–106.

HARADA, A. E. & BURTON, R. S. 2019. Ecologically relevant temperature ramping rates enhance the protective heat shock response in an intertidal ectotherm. *Physiological and Biochemical Zoology* 92:152–162.

HARDISON, E. A., SCHWIETERMAN, G. D. & ELIASON, E. J. 2023. Diet changes thermal acclimation capacity, but not acclimation rate, in a marine ectotherm (*Girella nigricans*) during warming. *Proceedings of the Royal Society B: Biological Sciences* 290:20222505.

HARLEY, C. 2008. Tidal dynamics, topographic orientation, and temperature-mediated mass mortalities on rocky shores. *Marine Ecology Progress Series* 371:37–46.

HARLEY, C. D. G. & HELMUTH, B. S. T. 2003. Local- and regional-scale effects of wave exposure, thermal stress, and absolute versus effective shore level on patterns of intertidal zonation. *Limnology and Oceanography* 48:1498–1508.

HARLEY, C. D., DENNY, M. W., MACH, K. J. & MILLER, L. P. 2009. Thermal stress and morphological adaptations in limpets. *Functional ecology* 23:292301.

HARPER, K. D. & WILLIAMS, G. A. 2001. Variation in abundance and distribution of the chiton *Acanthopleura japonica* and associated molluscs on a seasonal, tropical, rocky shore. *Journal of Zoology* 253:293–300.

HARRISON, X. A. 2014. Using observation-level random effects to model overdispersion in count data in ecology and evolution. *PeerJ* 2:e616.

HARRISON, X. A., DONALDSON, L., CORREA-CANO, M. E., EVANS, J., FISHER, D. N., GOODWIN, C. E. D., ROBINSON, B. S., HODGSON, D. J. & INGER, R. 2018. A brief introduction to mixed effects modelling and multi-model inference in ecology. *PeerJ* 6:e4794.

HASTIE, T. J. & TIBSHIRANI, R. J. 2017. *Generalized additive models*. Routledge, New York.

HAYES, L., LUKIĆ, I., MOY, S. R., FAGERLI, C. W., RINDE, E., CHRISTIE, H. & BEKKBY, T. 2024. Effects of wave exposure and habitat fragmentation on growth and grazing of rocky shore seaweeds: a mesocosm experiment. *Marine Biology* 171:145.

HAYFORD, H. A., GILMAN, S. E. & CARRINGTON, E. 2015. Foraging behaviour minimizes heat exposure in a complex thermal landscape. *Marine Ecology Progress Series* 518:165–175.

HAYFORD, H. A., GILMAN, S. E. & CARRINGTON, E. 2021. Tidal cues reduce thermal risk of climate change in a foraging marine snail. *Climate Change Ecology* 1:100003.

HAYFORD, H. A., O'DONNELL, M. J. & CARRINGTON, E. 2018. Radio tracking detects behavioural thermoregulation at a snail's pace. *Journal of Experimental*

Marine Biology and Ecology 499:17–25.

HELMOND, E., FINLAY, K., SHEFFIELD, C., HART, M. & HERON, J. 2023. Ascertaining the life history and thermal preferences and tolerances of the hot spring snail *Physella wrighti* (Gastropoda: Physidae). *Canadian Journal of Zoology* 101:672–685.

HELMUTH, B. 2002. How do we measure the environment? Linking intertidal thermal physiology and ecology through biophysics. *Integrative and comparative biology* 42:837–845.

HELMUTH, B. S. T. 1998. Intertidal mussel microclimates: predicting the body temperature of a sessile invertebrate. *Ecological Monographs* 68:51–74.

HELMUTH, B. S. & HOFMANN, G. E. 2001. Microhabitats, thermal heterogeneity, and patterns of physiological stress in the rocky intertidal zone. *The Biological Bulletin* 201:374–384.

HELMUTH, B., BROITMAN, B. R., BLANCHETTE, C. A., GILMAN, S., HALPIN, P., HARLEY, C. D. G., O'DONNELL, M. J., HOFMANN, G. E., MENGE, B. & STRICKLAND, D. 2006. Mosaic patterns of thermal stress in the rocky intertidal zone: implications for climate change. *Ecological Monographs* 76:461–479.

HELMUTH, B., CHOI, F., MATZELLE, A., TOROSSIAN, J. L., MORELLO, S. L., MISLAN, K. A. S., YAMANE, L., STRICKLAND, D., SZATHMARY, P. L., GILMAN, S. E., TOCKSTEIN, A., HILBISH, T. J., BURROWS, M. T., POWER, A. M., GOSLING, E., MIESZKOWSKA, N., HARLEY, C. D. G., NISHIZAKI, M., CARRINGTON, E., MENGE, B., PETES, L., FOLEY, M. M., JOHNSON, A., POOLE, M., NOBLE, M. M., RICHMOND, E. L., ROBART, M., ROBINSON, J., SAPP, J., SONES, J., BROITMAN, B. R., DENNY, M. W., MACH, K. J., MILLER, M., ROSS, P., HOFMANN, G. E., ZIPPAY, M., BLANCHETTE, C., MACFARLAN, J. A., CARPIZO-ITUARTE, E., RUTTENBERG, B., PEÑA MEJÍA, C. E., MCQUAID, C. D., LATHLEAN, J., MONACO, C. J., NICASTRO, K. R. & ZARDI, G. 2016. Long-term, high frequency in situ measurements of intertidal mussel bed temperatures using biomimetic sensors. *Scientific Data* 3:160087.

HELMUTH, B., RUSSELL, B., CONNELL, S., DONG, Y., HARLEY, C., LIMA, F.,

SARÀ, G., WILLIAMS, G. & MIESZKOWSKA, N. 2014. Beyond long-term averages: making biological sense of a rapidly changing world. *Climate Change Responses* 1:6.

HELMUTH, B., YAMANE, L., LALWANI, S., MATZELLE, A., TOCKSTEIN, A. & GAO, N. 2011. Hidden signals of climate change in intertidal ecosystems: what (not) to expect when you are expecting. *Journal of Experimental Marine Biology and Ecology* 400:191–199.

HENRY, J., BAI, Y., KREUDER, F., SAARISTO, M., KASLIN, J. & WLODKOWIC, D. 2022. A miniaturized electrothermal array for rapid analysis of temperature preference behaviours in ecology and ecotoxicology. *Environmental Pollution* 314:120202.

HENRY, P.-Y. & JARNE, P. 2007. Marking hard-shelled gastropods: tag loss, impact on life-history traits, and perspectives in biology. *Invertebrate Biology* 126:138–153.

HEO, J.-M., KIM, S.-S., KIM, D.-Y., LEE, S. W., LEE, J. S., KANG, M. H. & KIM, S. E. 2023. Impact of exposure temperature rise on mass mortality of tidal flat pacific oysters. *Frontiers in Marine Science* 10:1275521.

HERRENDÖRFER, G. 1993. Resource selection by animals-statistical design and analysis for field studies. Wiley Online Library, New Jersey, USA.

HERRERA, F. D., RAMIREZ, F. B., SEVILLA, B. B. & FARFÁN, C. 1996. Behavioural thermoregulation of *Bulla gouldiana* (Gastropoda: Opisthobranchia: Cephalaspidea). *Journal of Thermal Biology* 21:319–322.

HERTZ, P. E., HUEY, R. B. & STEVENSON, R. D. 1993. Evaluating temperature regulation by field-active ectotherms: the fallacy of the inappropriate question. *The American Naturalist* 142:796–818.

HEYMANS, M. W. & EEKHOUT, I. 2019. *Applied missing data analysis with SPSS and (R) studio*. [Internet], Amsterdam.

HILL, J. & WILKINSON, C. 2004. Methods for ecological monitoring of coral reefs. *Australian Institute of Marine Science, Townsville* 117.

HIPPEL, P. T. VON. 2009. How to impute interactions, squares, and other transformed variables. *Sociological Methodology* 39:265–291.

HOBBS, L., BANAS, N. S., COHEN, J. H., COTTIER, F. R., BERGE, J. & VARPE, Ø. 2021. A marine zooplankton community vertically structured by light across diel to interannual timescales. *Biology Letters* 17:20200810.

HOCHACHKA, P. W. 1988. Metabolic suppression and oxygen availability. *Canadian Journal of Zoology* 66:152–158.

HODGSON, A. N. 1999. The biology of siphonariid limpets (Gastropoda: Pulmonata). Pp. 253–322 *Oceanography and marine biology*. CRC Press, Florida, USA.

HOLMER, B., POSTGÅRD, U. & ERIKSSON, M. 2001. Sky view factors in forest canopies calculated with IDRISI. *Theoretical and Applied Climatology* 68:33–40.

HOPKINS, S., DETTORI, J. R. & CHAPMAN, J. R. 2018. Parametric and nonparametric tests in spine research: why do they matter? *Global Spine Journal* 8:652–654.

HOSMER, D. 2000. Applied logistic regression. John Wiley & Sons, New Jersey, USA.

HOSSIE, T. J., GOBIN, J. & MURRAY, D. L. 2021. Confronting missing ecological data in the age of pandemic lockdown. *Frontiers in Ecology and Evolution* 9:542.

HOULIHAN, D. F., INNES, A. J. & DEY, D. G. 1981. The influence of mantle cavity fluid on the aerial oxygen consumption of some intertidal gastropods. *Journal of Experimental Marine Biology and Ecology* 49:57–68.

HOYLMAN, Z. H., JENCSO, K. G., HU, J., MARTIN, J. T., HOLDEN, Z. A., SEIELSTAD, C. A. & ROWELL, E. M. 2018. Hillslope topography mediates spatial patterns of ecosystem sensitivity to climate. *Journal of Geophysical Research: Biogeosciences* 123:353–371.

HUANG, X., WANG, T., YE, Z., HAN, G. & DONG, Y. 2015. Temperature relations of aerial and aquatic physiological performance in a mid-intertidal limpet *Cellana toreuma*: adaptation to rapid changes in thermal stress during emersion. *Integrative Zoology* 10:159–170.

HUEY, R. B. & KINGSOLVER, J. G. 1989. Evolution of thermal sensitivity of ectotherm performance. *Trends in Ecology & Evolution* 4:131–135.

HUI, T. Y., CRICKENBERGER, S., LAU, J. W. T. & WILLIAMS, G. A. 2022. Why are 'suboptimal' temperatures preferred in a tropical intertidal ectotherm? *Journal of*

Animal Ecology 91:1400–1415.

HUI, T. Y., DONG, Y., HAN, G., LAU, S. L. Y., CHENG, M. C. F., MEEPOKA, C., GANMANEE, M. & WILLIAMS, G. A. 2020. Timing metabolic depression: predicting thermal stress in extreme intertidal environments. *The American Naturalist* 196:501–511.

IPCC. 2018. Global warming of 1.5°C. An IPCC special report on the impacts of global warming of 1.5°C above pre-industrial levels and related global greenhouse gas emission pathways, in the context of strengthening the global response to the threat of climate change. P. 32 in Masson-Delmotte, V., Zhai, P., Pörtner, H. O., Roberts, D., Skea, J., Shukla, P., Pirani, A., Moufouma-Okia, W., Péan, C., Pidcock, R., Connors, S., Matthews, R., Chen, Y., Zhou, X., Gomis, M., Lonnoy, E., Maycock, T., Tignor, M. & Tabatabaei, M. (eds.). *Sustainable development, and efforts to eradicate poverty*. Florida, USA.

IPCC. 2021. Summary for policymakers. Climate change 2021: the physical science basis. P. 2391 in Masson-Delmotte, V. P., Zhai, P., Pirani, S. L., Connors, C., Péan, S., Berger, N., Caud, Y., Chen, L., Goldfarb, M. I. & Scheel Monteiro, P. M. (eds.). *Contribution of Working Group I to the sixth assessment report of the intergovernmental panel on climate change.* Cambridge University Press, Cambridge, United Kingdom.

IVANINA, A. V., NESMELOVA, I., LEAMY, L., SOKOLOV, E. P. & SOKOLOVA, I. M. 2016. Intermittent hypoxia leads to functional reorganization of mitochondria and affects cellular bioenergetics in marine molluscs. *The Journal of Experimental Biology* 219:1659–1674.

IWASAKI, K. 1992. Factors affecting individual variation in resting site fidelity in the patellid limpet, *Cellana toreuma* (Reeve). *Ecological Research* 7:305–331.

IWASAKI, K. 1993. Analyses of limpet defence and predator offense in the field. *Marine Biology* 116:277–289.

IWASAKI, K. 1995. Comparison of mussel bed community between two intertidal mytilids *Septifer virgatus* and *Hormomya mutabilis*. *Marine Biology* 123:109–119.

JACKSON, A. C., MURPHY, R. J. & UNDERWOOD, A. J. 2013. Biofilms on rocky

shores: influences of rockpools, local moisture and temperature. *Journal of Experimental Marine Biology and Ecology* 443:46–55.

JAKOB, E. M., PORTER, A. H. & UETZ, G. W. 2001. Site fidelity and the costs of movement among territories: an example from colonial web-building spiders. *Canadian Journal of Zoology* 79:2094–2100.

JANETZKI, N., BENKENDORFF, K. & FAIRWEATHER, P. G. 2021. Where three snail species attach while emersed in relation to heterogenous substrate temperatures underneath intertidal boulders. *PeerJ* 9:e11675.

JARAMILLO, E., DUGAN, J. E., HUBBARD, D. M., CONTRERAS, H., DUARTE, C., ACUÑA, E. & SCHOEMAN, D. S. 2017. Macroscale patterns in body size of intertidal crustaceans provide insights on climate change effects. *PloS ONE* 12:e0177116.

JENKINS, S. R. & HARTNOLL, R. G. 2001. Food supply, grazing activity and growth rate in the limpet *Patella vulgata* L.: a comparison between exposed and sheltered shores. *Journal of Experimental Marine Biology and Ecology* 258:123–139.

JIANG, C., STOREY, K. B., YANG, H. & SUN, L. 2023. Aestivation in nature: physiological strategies and evolutionary adaptations in hypometabolic states. *International Journal of Molecular Sciences* 24:14093.

JOHANSSON, M. 2015. Adjusting to the extreme: thermal adaptation in a freshwater gastropod. PhD thesis, Acta Universitatis Upsaliensis, Sweden.

JONES, K. M. M. & BOULDING, E. G. 1999. State-dependent habitat selection by an intertidal snail: the costs of selecting a physically stressful microhabitat. *Journal of Experimental Marine Biology and Ecology* 242:149–177.

JUDGE, R., CHOI, F. & HELMUTH, B. 2018. Recent advances in data logging for intertidal ecology. *Frontiers in Ecology and Evolution* 6:213.

JURY, M. R. 2013. Climate trends in southern Africa: research article. *South African Journal of Science* 109:1–11.

KANIEWSKA, P., ALON, S., KARAKO-LAMPERT, S., HOEGH-GULDBERG, O. & LEVY, O. 2015. Signalling cascades and the importance of moonlight in coral broadcast mass spawning. *eLife* 4:e09991.

KANKONDI, S. L., MCQUAID, C. D. & TAGLIAROLO, M. 2018. Influence of respiratory mode on the thermal tolerance of intertidal limpets. *PloS ONE* 13:e0203555.

KEARNEY, M., SHINE, R. & PORTER, W. P. 2009. The potential for behavioural thermoregulation to buffer 'cold-blooded' animals against climate warming. *Proceedings of the National Academy of Sciences* 106:3835–3840.

KELLY, N. I., ALZAID, A., NASH, G. W. & GAMPERL, A. K. 2014. Metabolic depression in cunner (*Tautogolabrus adspersus*) is influenced by ontogeny, and enhances thermal tolerance. *PloS ONE* 9:e114765.

KLEPSATEL, P., GÁLIKOVÁ, M., XU, Y. & KÜHNLEIN, R. P. 2016. Thermal stress depletes energy reserves in *Drosophila*. *Scientific reports* 6:33667.

KOOIJMAN, S. A. L. M. 2010. *Dynamic energy budget theory for metabolic organisation*. Cambridge University Press, Cambridge, United Kingdom.

KOVACH, R. P. & TALLMON, D. A. 2010. Strong influence of microhabitat on survival for an intertidal snail, *Nucella lima*. *Hydrobiologia* 652:49–56.

KREBS, J. R. & DAVIES, N. 1987. An introduction to behavioural ecology. Sinauer Associates, Sunderland, USA.

KRULL, M. & NEWMAN, M. C. 2022. Joint effects of fragmentation and mercury contamination on marsh periwinkle (*Littoraria irrorata*) movement. *Environmental Toxicology and Chemistry* 41:1742–1753.

KUHN, M., WICKHAM, H. & HVITFELDT, E. 2024. recipes: Preprocessing and feature engineering steps for modelling. *CRAN: Contributed Packages*. The R Foundation.

KULTZ, D. 2005. Molecular and evolutionary basis of the cellular stress response. *Annual Review of Physiology* 67:225–257.

KULTZ, D. 2020. Evolution of cellular stress response mechanisms. *Journal of Experimental Zoology Part A: Ecological and Integrative Physiology* 333:359–378.

KWIECIEN, O., BRAUN, T., BRUNELLO, C. F., FAULKNER, P., HAUSMANN, N., HELLE, G., HOGGARTH, J. A., IONITA, M., JAZWA, C. S., KELMELIS, S., MARWAN, N., NAVA-FERNANDEZ, C., NEHME, C., OPEL, T., OSTER, J. L.,

PERŞOIU, A., PETRIE, C., PRUFER, K., SAARNI, S. M., WOLF, A. & BREITENBACH, S. F. M. 2022. What we talk about when we talk about seasonality – a transdisciplinary review. *Earth-Science Reviews* 225:103843.

LAGERSPETZ, K. & VAINIO, L. 2006. Thermal behaviour of crustaceans. *Biological reviews of the Cambridge Philosophical Society* 81:237–58.

LAHOZ-MONFORT, J. J. & MAGRATH, M. J. L. 2021. A comprehensive overview of technologies for species and habitat monitoring and conservation. *BioScience* 71:1038–1062.

LAI, J. H., ALAMO, J. C. DEL, RODRÍGUEZ-RODRÍGUEZ, J. & LASHERAS, J. C. 2010. The mechanics of the adhesive locomotion of terrestrial gastropods. *Journal of Experimental Biology* 213:3920–3933.

LAM, E. K., ABEGAZ, M., GUNDERSON, A. R., TSUKIMURA, B. & STILLMAN, J. H. 2022. Interactions between temperature variability and reproductive physiology across traits in an intertidal crab. *Frontiers in Physiology*:326.

LANG, R. C., BRITTON, J. C. & METZ, T. 1998. What to do when there is nothing to do: the ecology of Jamaican intertidal *Littorinidae* (Gastropoda: Prosobranchia) in repose. *Hydrobiologia* 378:161–185.

LATHLEAN, J. A., AYRE, D. J., COLEMAN, R. A. & MINCHINTON, T. E. 2015. Using biomimetic loggers to measure interspecific and microhabitat variation in body temperatures of rocky intertidal invertebrates. *Marine and Freshwater Research* 66:86.

LATHLEAN, J. A., AYRE, D. J. & MINCHINTON, T. E. 2011. Rocky intertidal temperature variability along the southeast coast of Australia: comparing data from in situ loggers, satellite-derived SST and terrestrial weather stations. *Marine Ecology Progress Series* 439:83–95.

LATHLEAN, J. A., SEURONT, L. & NG, T. P. 2017. On the edge: the use of infrared thermography in monitoring responses of intertidal organisms to heat stress. *Ecological Indicators* 81:567–577.

LATHLEAN, J. & MINCHINTON, T. 2012. Manipulating thermal stress on rocky shores to predict patterns of recruitment of marine invertebrates under a changing

climate. *Marine Ecology Progress Series* 467:121–136.

LEBRETON, J.-D., BURNHAM, K. P., CLOBERT, J. & ANDERSON, D. R. 1992. Modelling survival and testing biological hypotheses using marked animals: a unified approach with case studies. *Ecological monographs* 62:67–118. New Jersey, USA.

LEE, K. J. & CARLIN, J. B. 2010. Multiple imputation for missing data: fully conditional specification versus multivariate normal imputation. *American Journal of Epidemiology* 171:624–632.

LEEUWIS, R. & GAMPERL, A. 2022. *Adaptations and plastic phenotypic responses of marine animals to the environmental challenges of the high intertidal zone*. Pp. 625–679. CRC press, London, England.

LEGRAND, E., RIERA, P., POULIQUEN, L., BOHNER, O., CARIOU, T. & MARTIN, S. 2018. Ecological characterization of intertidal rockpools: seasonal and diurnal monitoring of physico-chemical parameters. *Regional Studies in Marine Science* 17:1–10.

LENOIR, J. & SVENNING, J.-C. 2015. Climate-related range shifts–a global multidimensional synthesis and new research directions. *Ecography* 38:15–28.

LENTH, R. V. 2023. *Emmeans: Estimated marginal means, aka least-squares means*. *CRAN: Contributed Packages*. The R Foundation.

LETENDRE, F., TWARDOWSKI, M., BLACKBURN, A., POULIN, C. & LATZ, M. I. 2024. A review of mechanically stimulated bioluminescence of marine plankton and its applications. *Frontiers in Marine Science* 10:1299602.

LEVINS, R. 1968. *Evolution in changing environments: some theoretical explorations*. Princeton University Press, New Jersey, USA.

LEWIS, L. & AYERS, J. 2014. Temperature preference and acclimation in the Jonah crab, *Cancer borealis*. *Journal of Experimental Marine Biology and Ecology* 455:7–13.

LI, X., TAN, Y., SUN, Y., WANG, J. & DONG, Y. 2021. Microhabitat temperature variation combines with physiological variation to enhance thermal resilience of the intertidal mussel *Mytilisepta virgata*. *Functional Ecology* 35:2497–2507.

LIAO, M., LI, G., WANG, J., MARSHALL, D. J., HUI, T. Y., MA, S., ZHANG, Y., HELMUTH, B. & DONG, Y. 2021. Physiological determinants of biogeography: the importance of metabolic depression to heat tolerance. *Global Change Biology* 27:2561–2579.

LICHT, P. 1965. The relation between preferred body temperatures and testicular heat sensitivity in lizards. *Copeia* 1965:428.

LIMA, F. P. & WETHEY, D. S. 2009. Robolimpets: measuring intertidal body temperatures using biomimetic loggers. *Limnology and Oceanography: Methods* 7:347–353.

LINDQUIST, S. 1986. The heat shock response. *Annual Review of Biochemistry* 55:1151–1191.

LITTLE, C., WILLIAMS, G. A. & TROWBRIDGE, C. D. 2009. *The biology of rocky shores* (Second Edition). Oxford University Press, New York, USA.

LITTLE, R. 2008. Selection and pattern-mixture models. Chapman; Hall/CRC.

LITTLE, R. J. A. 1988. A test of missing completely at random for multivariate data with missing values. *Journal of the American Statistical Association* 83:1198–1202.

LITTLE, T. D., JORGENSEN, T. D., LANG, K. M. & MOORE, E. W. G. 2014. On the joys of missing data. *Journal of Pediatric Psychology* 39:151–162.

LIU, L., SHIH, Y.-C. T., STRAWDERMAN, R. L., ZHANG, D., JOHNSON, B. A. & CHAI, H. 2019. Statistical analysis of zero-inflated nonnegative continuous data: a review. *Statistical Science* 34.

LIU, Z., ZHENG, J., LI, H., FANG, K., WANG, S., HE, J., ZHOU, D., WENG, S., CHI, M., GU, Z., HE, J., LI, F. & WANG, M. 2024. Genome assembly of redclaw crayfish (*Cherax quadricarinatus*) provides insights into its immune adaptation and hypoxia tolerance. *BMC Genomics* 25:746.

LLOYD, C. J. & FROMMER, D. J. 2008. An application of multinomial logistic regression to estimating performance of a multiple-screening test with incomplete verification. *Journal of the Royal Statistical Society Series C: Applied Statistics* 57:89–102.

LO, N., MACEWICZ, B. & GRIFFITH, D. 2011. Migration of pacific sardine

(*Sardinops sagax*) off the West coast of United States in 2003–2005. *Bulletin of Marine Science* 87.

LORD, J. P., LYCZKOWSKI, E. R. & WILSON, W. H. 2011. Behaviour and microhabitat selection of the tortoiseshell limpet *Testudinalia testudinalis* in the northwest Atlantic intertidal zone. *Journal of Experimental Marine Biology and Ecology* 407:234–240.

LUDTKE, O., ROBITZSCH, A. & GRUND, S. 2017. Multiple imputation of missing data in multilevel designs: a comparison of different strategies. *Psychological Methods* 22:141–165.

LUTJEHARMS, J. 2006. The coastal oceans of south-eastern Africa 14:783–834. Harvard University Press, Cambridge, United Kingdom.

LUTJEHARMS, J. R. E. 2007. Three decades of research on the greater Agulhas current. *Ocean Science* 3:129–147.

LUTJEHARMS, J. R. E., COOPER, J. & ROBERTS, M. 2000. Upwelling at the inshore edge of the Agulhas current. *Continental Shelf Research* 20:737–761.

MACDONALD, I. A. W. & SIMMONS, M. 1996. The Cape Peninsula, South Africa: physiographical, biological and historical background to an extraordinary hot-spot of biodiversity. *Biodiversity and Conservation* 5:527–550.

MACE, M., KIMBALL, M. & HAFFEY, E. 2018. Recruitment and habitat use of early life stage tarpon (*Megalops atlanticus*) in South Carolina estuaries. *Estuaries and Coasts* 41:841854.

MACKAY, D. & UNDERWOOD, A. 1977. Experimental studies on homing in the intertidal patellid limpet *Cellana tramoserica* (Sowerby). *Oecologia* 30:215–237.

MACKAY, F., SHEPPARD, J. & GOBLE, B. 2012. Biophysical assessments of the Zinkwazi and Nonoti estuaries: high and low flow surveys. Unpublished Report.

MACNEIL-VROOMEN, J., EEKHOUT, I., DIJKGRAAF, M. G., HOUT, H. VAN, ROOIJ, S. E. DE, HEYMANS, M. W. & BOSMANS, J. E. 2016. Multiple imputation strategies for zero-inflated cost data in economic evaluations: which method works best? *The European Journal of Health Economics* 17:939–950.

MANEL, S., WILLIAMS, H. C. & ORMEROD, S. J. 2001. Evaluating

presence–absence models in ecology: the need to account for prevalence. *Journal of Applied Ecology* 38:921–931.

MARSHALL, A., ALTMAN, D. G., ROYSTON, P. & HOLDER, R. L. 2010. Comparison of techniques for handling missing covariate data within prognostic modelling studies: a simulation study. *BMC Medical Research Methodology* 10:7.

MARSHALL, D. J., BRAHIM, A., MUSTAPHA, N., DONG, Y. & SINCLAIR, B. J. 2018. Substantial heat tolerance acclimation capacity in tropical thermophilic snails, but to what benefit? *Journal of Experimental Biology* 221:jeb187476.

MARSHALL, D. J. & MCQUAID, C. D. 1991. Metabolic rate depression in a marine pulmonate snail: pre-adaptation for a terrestrial existence? *Oecologia* 88:274–276.

MARSHALL, D. J. & MCQUAID, C. D. 1992. Comparative aerial metabolism and water relations of the intertidal limpets *Patella granularis* L. (Mollusca: Prosobranchia) and *Siphonaria oculus* KR. (Mollusca: Pulmonata). *Physiological Zoology* 65:1040–1056.

MARSHALL, D. J. & MCQUAID, C. D. 1993. Effects of hypoxia and hyposalinity on the heartbeat of the intertidal limpets *Patella granularis* (Prosobranchia) and *Siphonaria capensis* (Pulmonata). *Comparative Biochemistry and Physiology Part A: Physiology* 106:65–68.

MARSHALL, D. J. & MCQUAID, C. D. 2011. Warming reduces metabolic rate in marine snails: adaptation to fluctuating high temperatures challenges the metabolic theory of ecology. *Proceedings of the Royal Society B: Biological Sciences* 278:281–288.

MARSHALL, D. J. & MCQUAID, C. D. 2020. Metabolic regulation, oxygen limitation and heat tolerance in a subtidal marine gastropod reveal the complexity of predicting climate change vulnerability. *Frontiers in Physiology* 11:1106.

MARSHALL, D. J., REZENDE, E. L., BAHARUDDIN, N., CHOI, F. & HELMUTH, B. 2015. Thermal tolerance and climate warming sensitivity in tropical snails. *Ecology and evolution* 5:5905–5919.

MARTÍNEZ-LAIZ, G., ROS, M., NAVARRO-BARRANCO, C. & GUERRA-GARCÍA, J. 2018. Habitat selection of intertidal caprellid amphipods in a changing scenario.

Behavioural processes 153:16–24.

MARTINS, G., HAWKINS, S., THOMPSON, R. & JENKINS, S. 2007. Community structure and functioning in intertidal rock pools: effects of pool size and shore height at different successional stages. *Marine Ecology Progress Series* 329:43–55.

MASHAO, F. M., MOTHAPO, M. C., MUNYAI, R. B., LETSOALO, J. M., MBOKODO, I. L., MUOFHE, T. P., MATSANE, W. & CHIKOORE, H. 2023. Extreme rainfall and flood risk prediction over the East coast of South Africa. *Water* 15:50.

MAYR, E. 1963. *Animal species and evolution*. Harvard University Press, Cambridge, USA.

MCALISTER, R. O. & FISHER, F. M. 1968. Responses of the false limpet, *Siphonaria pectinata linnaeus* (Gastropoda, Pulmonata) to osmotic stress. *Biological Bulletin* 134:96–117.

MCCORMACK, R. B. 2012. Basic anatomy. P. 31. CSIRO Publishing, Clayton, Australia.

MCDOWELL, W. G. & SOUSA, R. 2019. Mass mortality events of invasive freshwater bivalves: current understanding and potential directions for future research. *Frontiers in Ecology and Evolution* 7:331.

MCGAW, I. J. 2003. Behavioural thermoregulation in *Hemigrapsus nudus*, the amphibious purple shore crab. *The Biological Bulletin* 204:38–49.

MCHUGH, M. L. 2013. The chi-square test of independence. *Biochemia Medica* 23:143–149.

MCMAHON, B. R. 1988. Physiological responses to oxygen depletion in intertidal animals. *American Zoologist* 28:39–53.

MCMAHON, R. F. 1990. Thermal tolerance, evaporative water loss, air-water oxygen consumption and zonation of intertidal prosobranchs: a new synthesis. *Hydrobiologia* 193:241–260.

MCMAHON, R. F. & RUSSELL-HUNTER, W. D. 1977. Temperature relations of aerial and aquatic respiration in six littoral snails in relation to their vertical zonation. *The Biological Bulletin* 152:182–198.

MCQUAID, C. D. & BRANCH, G. M. 1984. Influence of sea temperature, substratum and wave exposure on rocky intertidal communities: an analysis of faunal and floral biomass. *Marine Ecology Progress Series* 19:145–151.

MCQUAID, C. D., CRETCHLEY, R. & RAYNER, J. L. 1999. Chemical defence of the intertidal pulmonate limpet *Siphonaria capensis* (Quoy & Gaimard) against natural predators. *Journal of Experimental Marine Biology and Ecology* 237:141–154.

MENGE, B. A. 1976. Organization of the New England rocky intertidal community: role of predation, competition, and environmental heterogeneity. *Ecological Monographs* 46:355–393.

MENGE, B. A., GRAVEM, S. A., JOHNSON, A., ROBINSON, J. W. & POIRSON, B. N. 2022. Increasing instability of a rocky intertidal meta-ecosystem. *Proceedings of the National Academy of Sciences* 119:e2114257119.

MIESZKOWSKA, N., BURROWS, M. T., HAWKINS, S. J. & SUGDEN, H. 2021. Impacts of pervasive climate change and extreme events on rocky intertidal communities: evidence from long-term data. *Frontiers in Marine Science* 8:642764.

MIESZKOWSKA, N., KENDALL, M., HAWKINS, S., LEAPER, R., WILLIAMSON, P., HARDMAN-MOUNTFORD, N. & SOUTHWARD, A. 2006. Changes in the range of some common rocky shore species in Britain: a response to climate change? *Marine Biodiversity: Patterns and Processes, Assessment, Threats, Management and Conservation* 555:241–251.

MILLER, A. W. & AMBROSE, R. F. 2000. Sampling patchy distributions: comparison of sampling designs in rocky intertidal habitats. *Marine Ecology Progress Series* 19:1–14.

MILLER, L. P., HARLEY, C. D. & DENNY, M. W. 2009. The role of temperature and desiccation stress in limiting the local-scale distribution of the owl limpet, *Lottia gigantea*. *Functional Ecology* 23:756–767. New Jersey, USA.

MILLER, S. L. 1974. Adaptive design of locomotion and foot form in prosobranch gastropods. *Journal of Experimental Marine Biology and Ecology* 14:99–156.

MOISEZ, E., SPILMONT, N. & SEURONT, L. 2020. Microhabitats choice in intertidal gastropods is species-, temperature- and habitat-specific. *Journal of Thermal Biology*

94:102785.

MONACO, C. J. & MCQUAID, C. D. 2018. Applicability of dynamic energy budget (DEB) models across steep environmental gradients. *Scientific Reports* 8:16384.

MONACO, C. J., MCQUAID, C. D. & MARSHALL, D. J. 2017. Decoupling of behavioural and physiological thermal performance curves in ectothermic animals: a critical adaptive trait. *Oecologia* 185:583–593.

MONACO, C. J., WETHEY, D. S., GULLEDGE, S. & HELMUTH, B. 2015. Shore-level size gradients and thermal refuge use in the predatory sea star *Pisaster ochraceus*: the role of environmental stressors. *Marine Ecology Progress Series* 539:191–205.

MONACO, C. J., WETHEY, D. S. & HELMUTH, B. 2016. Thermal sensitivity and the role of behaviour in driving an intertidal predator–prey interaction. *Ecological Monographs* 86:429–447.

MONTECINOS, C., RIERA, R. & BRANTE, A. 2020. Site fidelity and homing behaviour in the intertidal species *Chiton granosus* (Polyplacophora) (Frembly 1889). *Journal of Sea Research* 164:101932.

MORLEY, S. A., CHU, J. W. F., PECK, L. S. & BATES, A. E. 2022. Temperatures leading to heat escape responses in Antarctic marine ectotherms match acute thermal limits. *Frontiers in Physiology* 13:1077376.

MORRIS, D. W. 1987. Ecological scale and habitat use. *Ecology* 68:362–369.

MORRIS, S. & TAYLOR, A. C. 1983. Diurnal and seasonal variation in physico-chemical conditions within intertidal rock pools. *Estuarine, Coastal and Shelf Science* 17:339–355.

MOURA, P. A., CORSO, G., MONTGOMERY, S. H. & CARDOSO, M. Z. 2022. True site fidelity in pollen-feeding butterflies. *Functional Ecology* 36:572–582.

MOYEN, N. E., SOMERO, G. N. & DENNY, M. W. 2020. Mussel acclimatization to high, variable temperatures is lost slowly upon transfer to benign conditions. *Journal of Experimental Biology* 223:jeb222893.

MOYEN, N. E., SOMERO, G. N. & DENNY, M. W. 2022. Effects of heat acclimation on cardiac function in the intertidal mussel *Mytilus californianus*: can

laboratory-based indices predict survival in the field? *The Journal of Experimental Biology* 225:jeb243050.

MUGGEO, V. 2020. Selecting number of breakpoints in segmented regression: implementation in the R package segmented. *Technical report*. University of Palermo, Italy.

MUGGEO, V. M. R. 2008. segmented: An R package to fit regression models with broken-line relationships. *R news* 8:20–25.

MÜLLER, M., MENTEL, M., HELLEMOND, J. J. VAN, HENZE, K., WOEHLE, C., GOULD, S. B., YU, R.-Y., GIEZEN, M. VAN DER, TIELENS, A. G. M. & MARTIN, W. F. 2012. Biochemistry and evolution of anaerobic energy metabolism in eukaryotes. *Microbiology and Molecular Biology Reviews* 76:444–495.

MURRAY, J. A., HEWES, R. S. & WILLOWS, A. O. D. 1992. Water-flow sensitive pedal neurons in *Tritonia*: role in rheotaxis. *Journal of Comparative Physiology A* 171:373–385.

MYRICK, C., FOLGNER, D. & JR, J. 2004. An annular chamber for aquatic animal preference studies. *Transactions of The American Fisheries Society* 133:427–433.

NAKAGAWA, S. 2015. Missing data: mechanisms, methods, and messages. Oxford University Press, Oxford, England.

NAKAGAWA, S. & FRECKLETON, R. P. 2008. Missing inaction: the dangers of ignoring missing data. *Trends in Ecology & Evolution* 23:592–596.

NAVAS, C. & CARVALHO, J. 2010. *Energy and water in aestivating amphibians*. Pp. 141–169. Springer, New Jersey, USA.

NEUBAUER, P. & ANDERSEN, K. H. 2019. Thermal performance of fish is explained by an interplay between physiology, behaviour and ecology. *Conservation Physiology* 7:coz025.

NEWELL, R. C. 1969. Effect of fluctuations in temperature on the metabolism of intertidal invertebrates. *American Zoologist* 9:293–307.

NEWELL, R. C. 1979. *Biology of intertidal animals* (3rd Revised edition). Marine Ecological Surveys, London, England.

NG, T. P. T., SALTIN, S. H., DAVIES, M. S., JOHANNESSON, K., STAFFORD, R. &

WILLIAMS, G. A. 2013. Snails and their trails: the multiple functions of trail-following in gastropods. *Biological Reviews* 88:683–700.

NGUYEN, K. D. T., MORLEY, S. A., LAI, C.-H., CLARK, M. S., TAN, K. S., BATES, A. E. & PECK, L. S. 2011. Upper temperature limits of tropical marine ectotherms: global warming implications. *PloS ONE* 6:e29340.

NICHOLS, J. D. & KENDALL, W. L. 1995. The use of multi-state capture-recapture models to address questions in evolutionary ecology. *Journal of Applied Statistics* 22:835–846.

NILSSON, D.-E. 2009. The evolution of eyes and visually guided behaviour. *Philosophical Transactions of the Royal Society B: Biological Sciences* 364:2833–2847.

NOBLE, D. W. A. & NAKAGAWA, S. 2018. Planned missing data design: stronger inferences, increased research efficiency and improved animal welfare in ecology and evolution. *BioRxiv*:247064.

NOBLE, D. & NAKAGAWA, S. 2021. Planned missing data designs and methods: options for strengthening inference, increasing research efficiency and improving animal welfare in ecological and evolutionary research. *Evolutionary Applications* 14:1958–1968.

NOËL, L. M.-L. J., HAWKINS, S. J., JENKINS, S. R. & THOMPSON, R. C. 2009. Grazing dynamics in intertidal rockpools: connectivity of microhabitats. *Journal of Experimental Marine Biology and Ecology* 370:9–17.

NORIN, T., MALTE, H. & CLARK, T. D. 2014. Aerobic scope does not predict the performance of a tropical eurythermal fish at elevated temperatures. *Journal of Experimental Biology* 217:244–251.

NUÑEZ, J. D., OCAMPO, E. H. & CLEDÓN, M. 2014. A geographic comparison of the resting site fidelity behaviour in an intertidal limpet: correlation with biological and physical factors. *Journal of Sea Research* 89:23–29.

NUÑEZ, J. D., RIBEIRO, P. D., OCAMPO, E. H. & LUPPI, T. A. 2018. *Neohelice granulata* burrow fidelity behaviour related to landscape heterogeneity. *Helgoland Marine Research* 72:17.

O'DWYER, K., KAMIYA, T. & POULIN, R. 2014. Altered microhabitat use and movement of littorinid gastropods: the effects of parasites. *Marine Biology* 161:437–445.

O'HARA, R. B. & KOTZE, D. J. 2010. Do not log-transform count data. *Methods in Ecology and Evolution* 1:118–122.

OLABARRIA, C., UNDERWOOD, A. & CHAPMAN, M. 2002. Appropriate experimental design to evaluate preferences for microhabitat: an example of preferences by species of microgastropods. *Oecologia* 132:159–166.

PADILLA-RAMÍREZ, S., DÍAZ, F., RE, A. D., GALINDO-SANCHEZ, C. E., SANCHEZ-LIZARRAGA, A. L., NUÑEZ-MORENO, L. A., MORENO-SIERRA, D., PASCHKE, K. & ROSAS, C. 2015. The effects of thermal acclimation on the behaviour, thermal tolerance, and respiratory metabolism in a crab inhabiting a wide range of thermal habitats (*Cancer antennarius* Stimpson, 1856, the red shore crab). *Marine and Freshwater Behaviour and Physiology* 48:89–101.

PANKHURST, N. W. & MUNDAY, P. L. 2011. Effects of climate change on fish reproduction and early life history stages. *Marine and Freshwater Research* 62:1015–1026.

PARMESAN, C. 2006. Ecological and evolutionary responses to recent climate change. *Annual Review of Ecology, Evolution, and Systematics* 37:637–669.

PASPARAKIS, C., DAVIS, B. E. & TODGHAM, A. E. 2016. Role of sequential low-tide-period conditions on the thermal physiology of summer and winter laboratory-acclimated fingered limpets, *Lottia digitalis*. *Marine Biology* 163:1–17.

PATIL, I. 2021. statsExpressions: R package for tidy dataframes and expressions with statistical details. *Journal of Open Source Software* 6:3236.

PATOKA, J., WARDIATNO, Y., KUŘÍKOVÁ, P., PETRTÝL, M. & KALOUS, L. 2016. *Cherax quadricarinatus* (von Martens) has invaded Indonesian territory west of the Wallace Line: evidence from Java. *Knowledge & Management of Aquatic Ecosystems*:39.

PAXTON, C. W., BARIA, M. V. B., WEIS, V. M. & HARII, S. 2016. Effect of elevated temperature on fecundity and reproductive timing in the coral *Acropora digitifera*.

Zygote 24:511–516.

PECK, L. S., &. & HARDEWIG, I. 2002. Metabolic demand, oxygen supply, and critical temperatures in the Antarctic bivalve *Laternula elliptica*. *Physiological and Biochemical Zoology* 75:123–133.

PENG, C.-Y. J., LEE, K. L. & INGERSOLL, G. M. 2002. An introduction to logistic regression analysis and reporting. *The journal of educational research* 96:3–14.

PEREA, J., GARCIA, A., GÓMEZ, G., ACERO, R., PEÑA, F. & GÓMEZ, S. 2007. Effect of light and substratum structural complexity on microhabitat selection by the snail *Helix aspersa* Müller. *Journal of Molluscan Studies* 73:39–43.

PÉREZ-ESCUDERO, A., VICENTE-PAGE, J., HINZ, R. C., ARGANDA, S. & POLAVIEJA, G. G. DE. 2014. idTracker: tracking individuals in a group by automatic identification of unmarked animals. *Nature Methods* 11:743–748.

PERRY, A. L., LOW, P. J., ELLIS, J. R. & REYNOLDS, J. D. 2005. Climate change and distribution shifts in marine fishes. *Science* 308:1912–1915.

PETRAITIS, P. S. 1982. Occurrence of random and directional movements in the periwinkle, *Littorina littorea* (l.). *Journal of Experimental Marine Biology and Ecology* 59:207–217.

PETROV, A. I. & RAZUVAEVA, M. V. 2018. Effect of temperature on metabolism and lifespan in several homeothermic animals. *Technical Physics* 63:1410–1414.

PEUGH, J. L. & ENDERS, C. K. 2004. Missing data in educational research: a review of reporting practices and suggestions for improvement. *Review of Educational Research* 74:525–556.

PINCHUCK, S. C. & HODGSON, A. N. 2009. Comparative structure of the lateral pedal defensive glands of three species of *Siphonaria* (Gastropoda: Basommatophora). *Journal of Molluscan Studies* 75:371–380.

PINCHUK, A. I., COYLE, K. O. & HOPCROFT, R. R. 2008. Climate-related variability in abundance and reproduction of euphausiids in the northern Gulf of Alaska in 1998–2003. *Progress in Oceanography* 77:203–216.

PINNA, S., PAIS, A., CAMPUS, P., SECHI, N. & CECCHERELLI, G. 2012. Habitat preferences of the sea urchin *Paracentrotus lividus*. *Marine Ecology Progress Series*

445:173–180.

PÖHLMANN, K., KOENIGSTEIN, S., ALTER, K., ABELE, D. & HELD, C. 2011. Heat shock response and antioxidant defence during air exposure in Patagonian shallow-water limpets from different climatic habitats. *Cell Stress & Chaperones* 16:621–632.

PONDER, W. & LINDBERG, D. R. R. (Eds.). 2008. *Phylogeny and evolution of the Mollusca* (First Edition). University of California Press, Berkeley, USA.

PÖRTNER, H. O. 2001. Climate change and temperature-dependent biogeography: oxygen limitation of thermal tolerance in animals. *Naturwissenschaften* 88:137–146.

PÖRTNER, H. O. 2010. Oxygen- and capacity-limitation of thermal tolerance: a matrix for integrating climate-related stressor effects in marine ecosystems. *Journal of Experimental Biology* 213:881–893.

PÖRTNER, H. O., BOCK, C. & MARK, F. C. 2017. Oxygen- and capacity-limited thermal tolerance: bridging ecology and physiology. *Journal of Experimental Biology* 220:2685–2696.

PÖRTNER, H. O. & FARRELL, A. P. 2008. Physiology and climate change. *Science* 322:690–692.

PÖRTNER, H. O. & KNUST, R. 2007. Climate change affects marine fishes through the oxygen limitation of thermal tolerance. *Science* 315:95–97.

POUND, R. J., MILLER, L. P., KING, F. A. & BURNAFORD, J. L. 2020. Temperature affects susceptibility of intertidal limpets to bird predation. *Journal of Experimental Biology* 223:jeb213595.

PROUM, S., HARLEY, C. D., STEELE, M. & MARSHALL, D. J. 2017. Aerobic and behavioural flexibility allows estuarine gastropods to flourish in rapidly changing and extreme pH conditions. *Marine Biology* 164:97.

PUTRA, I. D., NIMIYA, H., KUBOTA, T., LEE, H. S., IKETANI, F., TRIHAMDANI, A., SOPAHELUWAKAN, A., ALFATA, M., PERMANA, D. & SUGIHARTO, R. 2023. Study of vertical solar irradiance and local scale climate to assess passive cooling potential in Tangerang of Indonesia. *E3S Web of Conferences* 396:05002.

R CORE TEAM. 2021. *R: A language and environment for statistical computing*. R

Foundation for Statistical Computing, Vienna, Austria.

RAIMONDI, P. T. 1990. Patterns, mechanisms, consequences of variability in settlement and recruitment of an intertidal barnacle. *Ecological Monographs* 60:283–309.

RAINA, J.-B., LAMBERT, B. S., PARKS, D. H., RINKE, C., SIBONI, N., BRAMUCCI, A., OSTROWSKI, M., SIGNAL, B., LUTZ, A., MENDIS, H., RUBINO, F., FERNANDEZ, V. I., STOCKER, R., HUGENHOLTZ, P., TYSON, G. W. & SEYMOUR, J. R. 2022. Chemotaxis shapes the microscale organization of the ocean's microbiome. *Nature* 605:132–138.

RAVAUX, J., LÉGER, N., RABET, N., FOURGOUS, C., VOLAND, G., ZBINDEN, M. & SHILLITO, B. 2016. Plasticity and acquisition of the thermal tolerance (upper thermal limit and heat shock response) in the intertidal species *Palaemon elegans*. *Journal of Experimental Marine Biology and Ecology* 484:39–45.

RAW, J., MIRANDA, N. & PERISSINOTTO, R. 2013. Chemical cues released by an alien invasive aquatic gastropod drive its invasion success. *PloS ONE* 8:e64071.

REASON, C. J. C., LANDMAN, W. & TENNANT, W. 2006. Seasonal to decadal prediction of southern African climate and its links with variability of the Atlantic ocean. *Bulletin of the American Meteorological Society* 87:941–956.

REISER, S., TEMMING, A., ECKHARDT, A. & HERRMANN, J.-P. 2013. Automation and critical evaluation of an annular chamber for aquatic ectotherm temperature preference experiments. *Methods in Ecology and Evolution* 4:531–541.

RENSBURG, C. VAN, ROBBINS, A. & GRIFFITHS, C. 2021. Temperature cycles beneath, and adjacent to, intertidal boulders and associated differences in biotic composition. *African Journal of Marine Science* 43:435–441.

REYNOLDS, W. W. & CASTERLIN, M. E. 1979. Behavioural thermoregulation and the "final preferendum" paradigm. *American Zoologist* 19:211–224.

RHODES, C. J., HENRYS, P., SIRIWARDENA, G. M., WHITTINGHAM, M. J. & NORTON, L. R. 2015. The relative value of field survey and remote sensing for biodiversity assessment. *Methods in Ecology and Evolution* 6:772–781.

RICHARDS, J. G. 2010. Metabolic rate suppression as a mechanism for surviving environmental challenge in fish. Pp. 113–139 in Arturo Navas, C. & Carvalho, J. E.

(eds.). Springer, Berlin, Germany.

RICHTER, K., HASLBECK, M. & BUCHNER, J. 2010. The heat shock response: life on the verge of death. *Molecular Cell* 40:253–266.

RIDOUT, M. S. & DIGGLE, P. J. 1991. Testing for random dropouts in repeated measurement data. *Biometrics* 47:1617–1621.

RIESGO, A. & MALDONADO, M. 2008. Differences in reproductive timing among sponges sharing habitat and thermal regime. *Invertebrate Biology* 127:357–367.

RILOV, G., MAZARIS, A. D., STELZENMÜLLER, V., HELMUTH, B., WAHL, M., GUY-HAIM, T., MIESZKOWSKA, N., LEDOUX, J.-B. & KATSANEVAKIS, S. 2019. Adaptive marine conservation planning in the face of climate change: what can we learn from physiological, ecological and genetic studies? *Global Ecology and Conservation* 17:e00566.

RIPLEY, D. M., QUINN, F. A., DICKSON, J., ARTHUR, J. & SHIELS, H. A. 2022. Thermal preference does not align with optimal temperature for aerobic scope in zebrafish (*Danio rerio*). *The Journal of Experimental Biology* 225:jeb243774.

ROBERTS, D. A., HOFMANN, G. E. & SOMERO, G. N. 1997. Heat shock protein expression in *Mytilus californianus*: acclimatization (seasonal and tidal-height comparisons) and acclimation effects. *The Biological Bulletin* 192:309–320.

ROBINSON, E. J. H., RICHARDSON, T. O., SENDOVA-FRANKS, A. B., FEINERMAN, O. & FRANKS, N. R. 2009. Radio tagging reveals the roles of corpulence, experience and social information in ant decision making. *Behavioural Ecology and Sociobiology* 63:627–636.

ROBITZSCH, A. & GRUND, S. 2022. *Miceadds: Some additional multiple imputation functions, especially for 'mice'. CRAN: Contributed Packages*. The R Foundation.

ROBLES, C. D., DESHARNAIS, R. A., GARZA, C., DONAHUE, M. J. & MARTINEZ, C. A. 2009. Complex equilibria in the maintenance of boundaries: experiments with mussel beds. *Ecology* 90:985–995.

ROCHETTE, R. & DILL, L. M. 2000. Mortality, behaviour and the effects of predators on the intertidal distribution of littorinid gastropods. *Journal of Experimental Marine Biology and Ecology* 253:165–191.

ROCHETTE, R., DUNMALL, K. & DILL, L. M. 2003. The effect of life-history variation on the population size structure of a rocky intertidal snail (*Littorina sitkana*). *Journal of Sea Research* 49:119–132.

ROCKEL, T. 2022. *missMethods: Methods for missing data*. *CRAN: Contributed Packages*. The R Foundation.

RODA, A., CONG, M. Y., DONNER, B., DICKENS, K., HOWE, A., SHARMA, S. & SMITH, T. 2018. Designing a trapping strategy to aid Giant African snail (*Lissachatina fulica*) eradication programs. *PloS ONE* 13:e0203572.

ROSS, A. H. & NISBET, R. M. 1990. Dynamic models of growth and reproduction of the mussel *Mytilus edulis* L. *Functional Ecology* 4:777–787.

ROSSI, F., VALLE, M., GALEOTO, G., TOFANI, M., BERCHIALLA, P., SCIANNAMEO, V., BERTIN, D., CALCAGNO, A., CASALAZ, R., CERBONESCHI, M., CERVO, M., CORNELLI, A., DI PEDE, C., ESPOSITO, M., FERRARESE, M., IMAZIO, P., LORENZON, M., LONGO, L., MARTINUZZI, A., NARETTO, G., ORSINI, N., PANZERI, D., PELLEGRINI, C., PERANZONI, M., PICONE, F., RABUSIN, M., RICCI, F., ZIGRINO, C., ZUCCHETTI, G. & FAGIOLI, F. 2024. Internal consistency and floor/ceiling effects of the gross motor function measure for use with children affected by cancer: a cross-sectional study. *Current Oncology* 31:5291–5306.

ROYSTON, P. 2004. Multiple imputation of missing values. *The Stata Journal* 4:227–241.

RUBIN, D. B. 1976. Inference and missing data. *Biometrika* 63:581–592.

RUBIN, D. B. 1987. *Multiple imputation for survey nonresponse*. John Wiley & Sons, New York, USA.

RUIZ SEBASTIÁN, C., STEFFANI, C. & BRANCH, G. 2002. Homing and movement patterns of a South African limpet *Scutellastra argenvillei* in an area invaded by an alien mussel *Mytilus galloprovincialis*. *Marine Ecology Progress Series* 243:111–122.

RUSSO, A. R. 1987. Role of habitat complexity in mediating predation by the gray damselfish *Abudefduf sordidus* on epiphytal amphipods. *Marine Ecology Progress*

Series 36:101–105.

SALAS, A., DIAZ, F., RE, A. D., GONZALEZ, M. & GALINDO, C. 2012. Thermoregulatory behaviour of red sea urchin *Strongylocentrotus franciscanus* (Agassiz, 1863) and purple sea urchin *Strongylocentrotus purpuratus* (Stimpson, 1857) (Echinodermata: Echinoidea). *The Open Zoology Journal* 5.

SANGPHUEAK, S., TIN, Y., TIN YAN, H., LAU, S. L. Y., WILLIAMS, G., WANGKULANGKUL, K. & CHAN, B. 2024. Habitat partitioning in two intertidal limpets, *Siphonaria guamensis* (Heterobranchia) and *Patelloida saccharina* (Patellogastropoda), from southern Thailand. *Zoological Studies* 63:11.

SANTINA, P. D. 1994. Homing pattern, activity area and trail following of the high shore Mediterranean limpet *Patella rustica* L. (Mollusca Gastropoda). *Ethology Ecology & Evolution* 6:65–73.

SANTINI, G., BIANCHI, T. & CHELAZZI, G. 2002. Metabolic responses to food deprivation in two limpets with different foraging regimes, revealed by recording of cardiac activity. *Journal of Zoology* 256:11–15.

SANTINI, G., NGAN, A., BURROWS, M. T., CHELAZZI, G. & WILLIAMS, G. A. 2014. What drives foraging behaviour of the intertidal limpet *Cellana grata*? A quantitative test of a dynamic optimization model. *Functional Ecology* 28:963–972.

SARÀ, G., PALMERI, V., MONTALTO, V., RINALDI, A. & WIDDOWS, J. 2013. Parameterisation of bivalve functional traits for mechanistic eco-physiological dynamic energy budget (DEB) models. *Marine Ecology Progress Series* 480:99–117.

SCHAFER, J. L. 2003. Multiple Imputation in multivariate problems when the imputation and analysis models differ. *Statistica Neerlandica* 57:19–35.

SCHAFER, J. L. & GRAHAM, J. W. 2002. Missing data: our view of the state of the art. *Psychological Methods* 7:147–177.

SCHAFER, J. L. & OLSEN, M. K. 1998. Multiple imputation for multivariate missing-data problems: a data analyst's perspective. *Multivariate Behavioural Research* 33:545–571.

SCHAKMANN, M., CHRISTENSEN, E. A. F., STEFFENSEN, J. F. & SVENDSEN, M. B. S. 2023. The influence of body size on behavioural thermal preference in

Atlantic cod (*Gadus morhua*): larger fish favour colder waters. *Fishes* 8:596.

SCHIELZETH, H., DINGEMANSE, N. J., NAKAGAWA, S., WESTNEAT, D. F., ALLEGUE, H., TEPLITSKY, C., RÉALE, D., DOCHTERMANN, N. A., GARAMSZEGI, L. Z. & ARAYA-AJOY, Y. G. 2020. Robustness of linear mixed-effects models to violations of distributional assumptions. *Methods in Ecology and Evolution* 11:1141–1152.

SCHMIDT-NIELSEN, K. 1997. *Animal physiology: adaptation and environment*. Cambridge University Press, Cambridge, United Kingdom.

SCHNIEBS, K., GLER, P., VINARSKI, M. & HUNDSDOERFER, A. 2011. Intraspecific morphological and genetic variability in *Radix balthica* (Linnaeus 1758) (Gastropoda: Basommatophora: Lymnaeidae) with morphological comparison to other European *Radix* species. *Journal of Conchology* 40:657.

SCHTICKZELLE, N. 2024. Marking invertebrates using RFID tags. *Peer Community in Ecology* 1:100585.

SCHÜDER, I., PORT, G. & BENNISON, J. 2003. Barriers, repellents and antifeedants for slug and snail control. *Crop Protection* 22:1033–1038.

SCHULTE, P. M. 2015. The effects of temperature on aerobic metabolism: towards a mechanistic understanding of the responses of ectotherms to a changing environment. *Journal of Experimental Biology* 218:1856–1866.

SCHUMANN, E. H. & BEEKMAN, L. J. 1984. Ocean temperature structures on the Agulhas bank. *Transactions of the Royal Society of South Africa* 45:191–203.

SEABRA, M. I., PENTEADO, N., CRUZ, T. & HAWKINS, S. J. 2023. Variability and connectivity in populations of different limpet species across rockpool-generated mosaic landscapes. *Frontiers in Marine Science* 10:1206159.

SEABRA, R., WETHEY, D. S., SANTOS, A. M. & LIMA, F. P. 2011. Side matters: microhabitat influence on intertidal heat stress over a large geographical scale. *Journal of Experimental Marine Biology and Ecology* 1-2:200–208.

SEABRA, R., WETHEY, D. S., SANTOS, A. M. & LIMA, F. P. 2015. Understanding complex biogeographic responses to climate change. *Scientific reports* 5:1–6.

SEURONT, L., MOISEZ, E., HENNION, C., SEURONT-SCHEFFBUCH, D. &

SEURONT, L. M. Y. 2018. *Littorina littorea* show small-scale persistent tidal height and habitat partitioning that is resilient to dislodgement through specific movement rates. *Journal of Experimental Marine Biology and Ecology* 509:24–35.

SEURONT, L. & SPILMONT, N. 2015. The smell of sex: water-borne and air-borne sex pheromones in the intertidal gastropod *Littorina littorea*. *Journal of Molluscan Studies* 81:96–103.

SEYER, J.-O., NILSSON, D.-E. & WARRANT, E. J. 1998. Spatial vision in the prosobranch gastropod *Ampularia sp*. *Journal of Experimental Biology* 201:1673–1679.

SHANKS, A. L. 2002. Previous agonistic experience determines both foraging behaviour and territoriality in the limpet *Lottia gigantea* (Sowerby). *Behavioural Ecology* 13:467–471.

SHANNON, L. V. 1985. The Benguela ecosystem I: evolution of the Benguela, physical features and processes. *Oceanography and Marine Biology - An Annual Review* 23:105–182.

SHANNON, L. V. & NELSON, G. 1996. The Benguela: large scale features and processes and system variability. *The South Atlantic*:163–210.

SHAW, R. G. & MITCHELL-OLDS, T. 1993. Anova for unbalanced data: an overview. *Ecology* 74:1638–1645.

SHILLINGTON, F. A. & WYNDHAM HARRIS, T. F. 1978. Surface waves near Cape Town and their associated atmospheric pressure distributions over the South Atlantic. *Deutsche Hydrografische Zeitschrift* 31:67–82.

SILVA, A. C. F., BOAVENTURA, D. M., THOMPSON, R. C. & HAWKINS, S. J. 2014. Spatial and temporal patterns of subtidal and intertidal crabs excursions. *Journal of Sea Research* 85:343–348.

SIMPFENDÖRFER, R. W., VIAL, M. V., LÓPEZ, D. A., VERDALA, M. & GONZÁLEZ, M. L. 1995. Relationship between the aerobic and anaerobic metabolic capacities and the vertical distribution of three intertidal sessile invertebrates: *Jehlius cirratus* (Darwin) (Cirripedia), *Perumytilus purpuratus* (Lamarck) (Bivalvia) and *Mytilus chilensis* (Hupé) (Bivalvia). *Comparative Biochemistry and Physiology Part*

B: Biochemistry and Molecular Biology 111:615–623.

SINGHAL, R. & RANA, R. 2015. Chi-square test and its application in hypothesis testing. *Journal of the Practice of Cardiovascular Sciences* 1:69–71.

SMIT, A. J., ROBERTS, M., ANDERSON, R. J., DUFOIS, F., DUDLEY, S. F. J., BORNMAN, T. G., OLBERS, J. & BOLTON, J. J. 2013. A coastal seawater temperature dataset for biogeographical studies: large biases between *in situ* and remotely-sensed data sets around the coast of South Africa. *PloS ONE* 8:e81944.

SNIJDERS, T. A. & BOSKER, R. J. 2011. *Multilevel analysis: An introduction to basic and advanced multilevel modelling*. Pp. 1–368. sage, Newcastle Upon Tyne, United Kingdom.

SOKOLOVA, I. 2021. Bioenergetics in environmental adaptation and stress tolerance of aquatic ectotherms: linking physiology and ecology in a multi-stressor landscape. *Journal of Experimental Biology* 224:jeb236802.

SOKOLOVA, I. M. & BERGER, V. J. 2000. Physiological variation related to shell colour polymorphism in White sea *Littorina saxatilis*. *Journal of Experimental Marine Biology and Ecology* 245:1–23.

SOKOLOVA, I. M. & PÖRTNER, H. O. 2001. Physiological adaptations to high intertidal life involve improved water conservation abilities and metabolic rate depression in *Littorina saxatilis*. *Marine Ecology Progress Series* 224:171–186.

SOMERO, G. 2010. The physiology of climate change: how potentials for acclimatization and genetic adaptation will determine 'winners' and 'losers'. *Journal of Experimental Biology* 213:912–920.

SOMERO, G. N. 2002. Thermal physiology and vertical zonation of intertidal animals: optima, limits, and costs of living. *Integrative and Comparative Biology* 42:780–789.

SOMERO, G. N. 2020. The cellular stress response and temperature: function, regulation, and evolution. *Journal of Experimental Zoology Part A: Ecological and Integrative Physiology* 333:379–397.

SOMMER, A., KLEIN, B. & PÖRTNER, H. O. 1997. Temperature induced anaerobiosis in two populations of the polychaete worm *Arenicola marina* (L.). *Journal of Comparative Physiology B* 167:25–35.

SOON, T. K. & RANSANGAN, J. 2019. Extrinsic factors and marine bivalve mass mortalities: an overview. *Journal of Shellfish Research* 38:223–232.

SOTO, R. E. & BOZINOVIC, F. 1998. Behavioural thermoregulation of the periwinkle *Nodilittorina peruviana* inhabiting the rocky intertidal of central Chile: a laboratory and field study. Pp. 375–382 *Revista Chilena de Historia Natural*.

SOUSA, T., DOMINGOS, T. & KOOIJMAN, S. A. L. M. 2008. From empirical patterns to theory: a formal metabolic theory of life. *Philosophical Transactions of the Royal Society B: Biological Sciences* 363:2453–2464.

STAFFORD, R. & DAVIES, M. S. 2004. Temperature and desiccation do not affect aggregation behaviour in high shore littorinids in North-East England. *Journal of Negative Results* 1:16–20.

STAPLES, J. F. 2016. Metabolic flexibility: hibernation, torpor, and estivation. *Comprehensive Physiology* 6:737–771.

STEGENGA, H. & BOLTON, J. J. 1992. Ceramiaceae (Rhodophyta) of the Cape province, South Africa: distribution in relation to concepts of marine provinces. *Botanica Marina* 35:99–108.

STENSENG, E., BRABY, C. E. & SOMERO, G. N. 2005. Evolutionary and acclimation-induced variation in the thermal limits of heart function in congeneric marine snails (genus *Tegula*): implications for vertical zonation. *The Biological Bulletin* 208:138–144.

STEPHENSON, T. A. & STEPHENSON, A. 1972. Life between tidemarks on rocky shores. WH Freeman, San Francisco, USA.

STEYERBERG, E. W., VICKERS, A. J., COOK, N. R., GERDS, T., GONEN, M., OBUCHOWSKI, N., PENCINA, M. J. & KATTAN, M. W. 2010. Assessing the performance of prediction models: a framework for traditional and novel measures. *Epidemiology* 21:128–138.

STILLMAN, J. & SOMERO, G. 1996. Adaptation to temperature stress and aerial exposure in congeneric species of intertidal porcelain crabs (genus *Petrolisthes*): correlation of physiology, biochemistry and morphology with vertical distribution. *Journal of Experimental Biology* 199:1845–1855.

STOREY, K. B. 1998. Survival under stress: molecular mechanisms of metabolic rate depression in animals. *African Zoology* 33:55–64.

STOREY, K. B. 2015. Regulation of hypometabolism: insights into epigenetic controls. *Journal of Experimental Biology* 218:150–159.

STOREY, K. B. & STOREY, J. M. 1990. Metabolic rate depression and biochemical adaptation in anaerobiosis, hibernation and estivation. *The Quarterly Review of Biology* 65:145–174.

STOREY, K. B. & STOREY, J. M. 2004. Metabolic rate depression in animals: transcriptional and translational controls. *Biological Reviews* 79:207–233.

STOREY, K. B. & STOREY, J. M. 2012. Aestivation: signalling and hypometabolism. *Journal of Experimental Biology* 215:1425–1433.

STOW, C. A. 2011. Spatial and temporal variations in macrozoobenthic communities in Kwazulu-Natal temporarily open/closed estuaries. PhD thesis, University of KwaZulu-Natal, South Africa.

STRINGER, I. A. N., PARRISH, G. R. & SHERLEY, G. H. 2018. Homing, dispersal and mortality after translocation of long-lived land snails *Placostylus ambagiosus* and *P. Hongii* (Gastropoda: Bothriembryontidae) in New Zealand. *Molluscan Research* 38:56–76.

STRUNOV, A., SCHOENHERR, C. & KAPUN, M. 2023. Wolbachia has subtle effects on thermal preference in highly inbred *Drosophila melanogaster* which vary with life stage and environmental conditions. *Scientific Reports* 13:13792.

SUNDAY, J. M., BATES, A. E. & DULVY, N. K. 2011. Global analysis of thermal tolerance and latitude in ectotherms. *Proceedings. Biological Sciences* 278:1823–1830.

SUNDAY, J., BENNETT, J. M., CALOSI, P., CLUSELLA-TRULLAS, S., GRAVEL, S., HARGREAVES, A. L., LEIVA, F. P., VERBERK, W. C., OLALLA-TÁRRAGA, M. Á. & MORALES-CASTILLA, I. 2019. Thermal tolerance patterns across latitude and elevation. *Philosophical Transactions of the Royal Society B* 374:20190036.

TAGLIAROLO, M. & MCQUAID, C. 2015. Sub-lethal and sub-specific temperature effects are better predictors of mussel distribution than thermal tolerance. *Marine*

Ecology Progress Series 535:145–159.

TAGLIAROLO, M., MONTALTO, V., SARÀ, G., LATHLEAN, J. A. & MCQUAID, C. D. 2016. Low temperature trumps high food availability to determine the distribution of intertidal mussels *Perna perna* in South Africa. *Marine Ecology Progress Series* 558:51–63.

TAGLIAROLO, M., PORRI, F. & SCHARLER, U. 2018. Temperature-induced variability in metabolic activity of ecologically important estuarine macrobenthos. *Marine Biology* 165:23.

TALLAM, K., NGUYEN, N., VENTURA, J., FRICKER, A., CALHOUN, S., O'LEARY, J., FITZGIBBONS, M., ROBBINS, I. & WALTER, R. K. 2023. Application of deep learning for classification of intertidal eelgrass from drone-acquired imagery. *Remote Sensing* 15:2321.

TÂMEGA, F. T. S. & FIGUEIREDO, M. A. O. 2019. Colonization, growth and productivity of crustose coralline algae in sunlit reefs in the Atlantic southernmost coral reef. *Frontiers in Marine Science* 6.

TEPLER, S., MACH, K. & DENNY, M. 2011. Preference *versus* performance: body temperature of the intertidal snail *Chlorostoma funebralis*. *The Biological Bulletin* 220:107–117.

TERRIEN, J., PERRET, M. & AUJARD, F. 2011. Behavioral thermoregulation in mammals: a review. *Frontiers in bioscience* 16:1428–1444.

TESKE, P. R., EMAMI-KHOYI, A., GOLLA, T. R., SANDOVAL-CASTILLO, J., LAMONT, T., CHIAZZARI, B., MCQUAID, C. D., BEHEREGARAY, L. B. & LINGEN, C. D. VAN DER. 2021. The sardine run in southeastern Africa is a mass migration into an ecological trap. *Science Advances* 7:eabf4514.

THAIN, V. M., THAIN, J. F. & KITCHING, J. A. 1985. Return of the prosobranch *Gibbula umbilicalis* (Da Costa) to the littoral region after displacement to the shallow sublittoral. *Journal of Molluscan Studies* 51:205–210.

THOMAS, A. C., CARR, M.-E. & STRUB, P. T. 2001. Chlorophyll variability in eastern boundary currents. *Geophysical Research Letters* 28:3421–3424.

THOMPSON, R. C., JENKINS, S. & BUSSELL, J. A. 2000. A method for recording

predator–prey encounters between crabs and limpets using wax replicas. *Journal of the Marine Biological Association of the UK* 80:633–638.

TIERNEY, N., COOK, D., MCBAIN, M. & FAY, C. 2021. *Naniar: Data structures, summaries, and visualisations for missing data*. P. 1 *CRAN: Contributed Packages*. The R foundation.

TIM, N., ZORITA, E., HÜNICKE, B. & IVANCIU, I. 2023. The impact of the Agulhas current system on precipitation in southern Africa in regional climate simulations covering the recent past and future. *Weather and Climate Dynamics* 4:381–397.

TOMANEK, L. 2010. Variation in the heat shock response and its implication for predicting the effect of global climate change on species' biogeographical distribution ranges and metabolic costs. *The Journal of experimental biology* 213:971–9.

TOUSKA, F., WINTER, Z., MUELLER, A., VLACHOVA, V., LARSEN, J. & ZIMMERMANN, K. 2016. Comprehensive thermal preference phenotyping in mice using a novel automated circular gradient assay. *Temperature* 3:77–91.

TROPEA, C., STUMPF, L. & LÓPEZ GRECO, L. S. 2015. Effect of temperature on biochemical composition, growth and reproduction of the ornamental red cherry shrimp *Neocaridina heteropoda* (Decapoda, Caridea). *PloS ONE* 10:e0119468.

TRUEBANO, M., FENNER, P., TILLS, O., RUNDLE, S. D. & REZENDE, E. L. 2018. Thermal strategies vary with life history stage. *Journal of Experimental Biology* 221:jeb171629.

TRUITT, A. M., KAPUN, M., KAUR, R. & MILLER, W. J. 2018. *Wolbachia* modifies thermal preference in *Drosophila melanogaster*. *Environmental Microbiology* 21:3259.

TUCKER, L., GRIFFITHS, C., SCHROETER, F. & VETTER, H. 2017. Boulder shores in South Africa – a distinct but poorly documented coastal habitat type. *African Journal of Marine Science* 39:193–202.

TURPIE, J. K., BECKLEY, L. E. & KATUA, S. M. 2000. Biogeography and the selection of priority areas for conservation of South African coastal fishes. *Biological Conservation* 92:59–72.

TYRAKOWSKI, T., KACZOROWSKI, P., PAWŁOWICZ, W., ZIÓŁKOWSKI, M., SMUSZKIEWICZ, P., TROJANOWSKA, I., MARSZAEK, A., ŻEBROWSKA, M., LUTOWSKA, M., KOPCZYŃSKA, E., LAMPKA, M., HOYŁŃSKA-IWAN, I. & PISKORSKA, E. 2012. Discrete movements of foot epithelium during adhesive locomotion of a land snail. *Folia Biologica* 60:99–106.

UNDERWOOD, A. J. & SKILLETER, G. A. 1996. Effects of patch-size on the structure of assemblages in rock pools. *Journal of Experimental Marine Biology and Ecology* 197:63–90.

URBAN, D. L., O'NEILL, R. V. & SHUGART, H. H. 1987. Landscape ecology. *BioScience* 37:119–127.

VAN HOORDE, K., VERGOUWE, Y., TIMMERMAN, D., VAN HUFFEL, S., STEYERBERG, E. W. & VAN CALSTER, B. 2014. Assessing calibration of multinomial risk prediction models. *Statistics in Medicine* 33:2585–2596.

VAT, L. 2000. The growth and reproduction of *Patella granularis* (Mollusca : Patellogastropoda) on the South-East coast of South Africa. PhD thesis, Rhodes University, South Africa.

VERBEKE, G. & DAVIDIAN, M. 2009. Joint models for longitudinal data: introduction and overview. Chapman; Hal/CRC, London, England.

VERBERK, W. C. E. P., BARTOLINI, F., MARSHALL, D. J., PÖRTNER, H. O., TERBLANCHE, J. S., WHITE, C. R. & GIOMI, F. 2016. Can respiratory physiology predict thermal niches? *Annals of the New York Academy of Sciences* 1365:73–88.

VERBERK, W. C. E. P., BILTON, D. T., CALOSI, P. & SPICER, J. I. 2011. Oxygen supply in aquatic ectotherms: partial pressure and solubility together explain biodiversity and size patterns. *Ecology* 92:1565–1572.

VERDERBER, G., SB, C. & CB, C. 1983. The role of the home scar in reducing water loss during aerial exposure of the pulmonate limpet, *Siphonaria alternata* (SAY). *Veliger* 25:235–243.

VERMEIJ, G. 1972. Intraspecific shore-level size gradients in intertidal molluscs. *Ecology* 53:693–700.

VICKERS, A. J. 2005. Parametric versus non-parametric statistics in the analysis of

randomized trials with non-normally distributed data. *BMC Medical Research Methodology* 5:35.

VINAGRE, C., DIAS, M., CEREJA, R., ABREU-AFONSO, F., FLORES, A. A. & MENDONÇA, V. 2019. Upper thermal limits and warming safety margins of coastal marine species: indicator baseline for future reference. *Ecological Indicators* 102:644–649.

VIRGIN, S. D. S. & SCHIEL, D. R. 2023. Behavioural thermoregulation and food availability drive fine-scale seasonal habitat partitioning in limpets. *Functional Ecology* 37:2687–2702.

WÄLDCHEN, J. & MÄDER, P. 2018. Machine learning for image based species identification. *Methods in Ecology and Evolution* 9:2216–2225.

WANG, J., MA, L.-X. & DONG, Y.-W. 2023. Coping with harsh heat environments: molecular adaptation of metabolic depression in the intertidal snail *Echinolittorina radiata*. *Cell Stress and Chaperones* 28:477–491. Elsevier.

WANG, J., PENG, X. & DONG, Y. 2020. High abundance and reproductive output of an intertidal limpet (*Siphonaria japonica*) in environments with high thermal predictability. *Marine Life Science & Technology* 2:324–333.

WANG, S. & TSODIKOV, A. 2010. A self-consistency approach to multinomial logit model with random effects. *Journal of statistical planning and inference* 140:1939–1947.

WANG, T., TANNER, R. L., ARMSTRONG, E. J., LINDBERG, D. R. & STILLMAN, J. H. 2019. Plasticity of foot muscle and cardiac thermal limits in the limpet *Lottia limatula* from locations with differing temperatures. *Aquatic Biology* 28:113–125.

WEBER, M. J., BROWN, M. L., WAHL, D. H. & SHOUP, D. E. 2015. Metabolic theory explains latitudinal variation in common carp populations and predicts responses to climate change. *Ecosphere* 6:1–16.

WEINSTEIN, B. G. 2018. A computer vision for animal ecology. *Journal of Animal Ecology* 87:533–545.

WETHEY, D. S. 1983. Geographic limits and local zonation: the barnacles *Semibalanus* (*balanus*) and *Chthamalus* in New England. *The Biological Bulletin* 165:330–341.

WETHEY, D. S. 2002. Biogeography, competition, and microclimate: the barnacle *Chthamalus fragilis* in New England. *Integrative and Comparative Biology* 42:872–880.

WETHEY, D. S. & WOODIN, S. A. 2008. Ecological hindcasting of biogeographic responses to climate change in the European intertidal zone. Pp. 139–151 *Challenges to marine ecosystems: proceedings of the 41st European marine biology symposium*. Springer, New Jersey, USA.

WHITE, G. E., HOSE, G. C. & BROWN, C. 2015. Influence of rockpool characteristics on the distribution and abundance of intertidal fishes. *Marine Ecology* 36:1332–1344.

WHITE, I. R., ROYSTON, P. & WOOD, A. M. 2011. Multiple imputation using chained equations: issues and guidance for practice. *Statistics in Medicine* 30:377–399.

WHITE, R. L. 1983. Effects of acute temperature change and acclimation temperature on neuromuscular function and lethality in crayfish. *Physiological Zoology* 56:174–194.

WICKHAM, H. 2016. *ggplot2: Elegant graphics for data analysis*. Springer, New York, USA.

WILLIAMS, G. A., DE PIRRO, M., CARTWRIGHT, S., KHANGURA, K., NG, W.-C., LEUNG, P. T. Y. & MORRITT, D. 2011. Come rain or shine: the combined effects of physical stresses on physiological and protein-level responses of an intertidal limpet in the monsoonal tropics. *Functional Ecology* 25:101–110.

WILLIAMS, G. & MORRITT, D. 1995. Habitat partitioning and thermal tolerance in a tropical limpet, *Cellana grata*. *Marine Ecology Progress Series* 124:89–103.

WILSON, G., BRANCH, G. & COITO, P. DE. 2009. Comparative salinity tolerances of four siphonariid limpets in relation to habitat restriction of the rare and endangered *Siphonaria compressa*. *African Journal of Marine Science* 31:311–318.

WOLCOTT, T. G. 1973. Physiological ecology and intertidal zonation in limpets *Acmaea*: a critical look at ”limiting factors”. *The Biological Bulletin* 145:389–422.

WOODS, A., KINGSOLVER, J., FEY, S. & VASSEUR, D. 2018. Uncertainty in geographical estimates of performance and fitness. *Methods in Ecology and Evolution* 9:1996–2008.

WOTHKE, W. 2000. Longitudinal and multigroup modelling with missing data. Lawrence Erlbaum Associates Publishers, New Jersey, USA.

WRIGHT, P. J., ORPWOOD, J. E. & SCOTT, B. E. 2017. Impact of rising temperature on reproductive investment in a capital breeder: the lesser sand eel. *Journal of Experimental Marine Biology and Ecology* 486:52–58.

XING, Q., LI, Y., GUO, H., YU, Q., HUANG, X., WANG, S., HU, X., ZHANG, L. & BAO, Z. 2016. Cardiac performance: a thermal tolerance indicator in scallops. *Marine Biology* 163:244.

YONGE, C. M. 1952. The mantle cavity in *Siphonaria alternata* say. *Journal of Molluscan Studies* 29:190–199.

ZEREBECKI, R. A. & SORTE, C. J. B. 2011. Temperature tolerance and stress proteins as mechanisms of invasive species success. *PloS ONE* 6:e14806.

ZHANG, S., HAN, G. & DONG, Y. 2014. Temporal patterns of cardiac performance and genes encoding heat shock proteins and metabolic sensors of an intertidal limpet *Cellana toreuma* during sublethal heat stress. *Journal of Thermal Biology* 41:31–37.

ZHANG, Z., XU, S., ZHANG, S., QIAO, T. & CAO, S. 2021. Attention based convolutional recurrent neural network for environmental sound classification. *Neurocomputing* 453:896–903.

ZHAO, Q., MYINT, S. W., WENTZ, E. A. & FAN, C. 2015. Rooftop surface temperature analysis in an urban residential environment. *Remote Sensing* 7:12135–12159.

ZHURAVLEV, V. L. & SAFONOVA, T. A. 1984. Regulation of snail heart contractions by neurons of the visceral ganglion. *Fiziologicheskii zhurnal SSSR imeni I M. Sechenova* 70:425–429.

ZIELINSKI, S. & PÖRTNER, H. O. 1996. Energy metabolism and ATP free-energy change of the intertidal worm *Sipunculus nudus* below a critical temperature. *Journal of Comparative Physiology B* 166:492–500.

ZIPPAY, M. & HELMUTH, B. 2012. Effects of temperature change on mussel, *Mytilus*. *Integrative zoology* 7:312–27.

ZOCCOLA, D. & TAMBUTTÉ, S. 2015. Sex under the moon. *eLife* 4:e12936.

ZUUR, A. F. 2007. *Analysing ecological data*. Springer, New York, USA.

ZUUR, A. F. & IENO, E. N. 2016. *Beginner´s guide to zero-inflated models with R*. Highland Statistics Ltd, Newburgh, USA.

ZUUR, A. F., IENO, E. N., WALKER, N., SAVELIEV, A. A. & SMITH, G. M. 2009. *Mixed effects models and extensions in ecology with R*. Springer, New York, USA.

Chapter 7

Appendix

This appendix provides supplementary material, primarily detailing the validation and diagnostic procedures for the statistical methods and models used in data Chapters 2, 3, 4 and 5 of the current thesis.

A1 Microhabitat use analysis

The diagnostic assessments in Figure A1 confirmed that the residuals of the Tweedie GLMM (Equation 2.1) used in (Chapter 2) were normally distributed, with no significant evidence of zero-inflation, overdispersion, or outliers. For the variance homogeneity tests, no significant deviations were detected overall, however, a significant within-group deviation from uniformity for horizontal rocks was identified (Figure A2). Although the uniformity issue for horizontal surfaces suggests a need for caution when interpreting the model estimates, this does not invalidate the model (Burnham & Anderson 2002). This localized deviation likely reflects the much larger average area of horizontal rocks across sites compared to other microhabitats (Figure 2.7), which may have introduced residual bias for this category (Bolker et al. 2009). Nonetheless, the diagnostics collectively indicate that the chosen model is suitable for understanding broad differences in microhabitat area using the available data from each site. Additionally, attempts to include an interaction term between microhabitat and site resulted in model convergence issues, further supporting the decision to exclude this term given that specific site-level

differences in microhabitat cover patterns were not a primary interest of this study (Section 2.3.5).

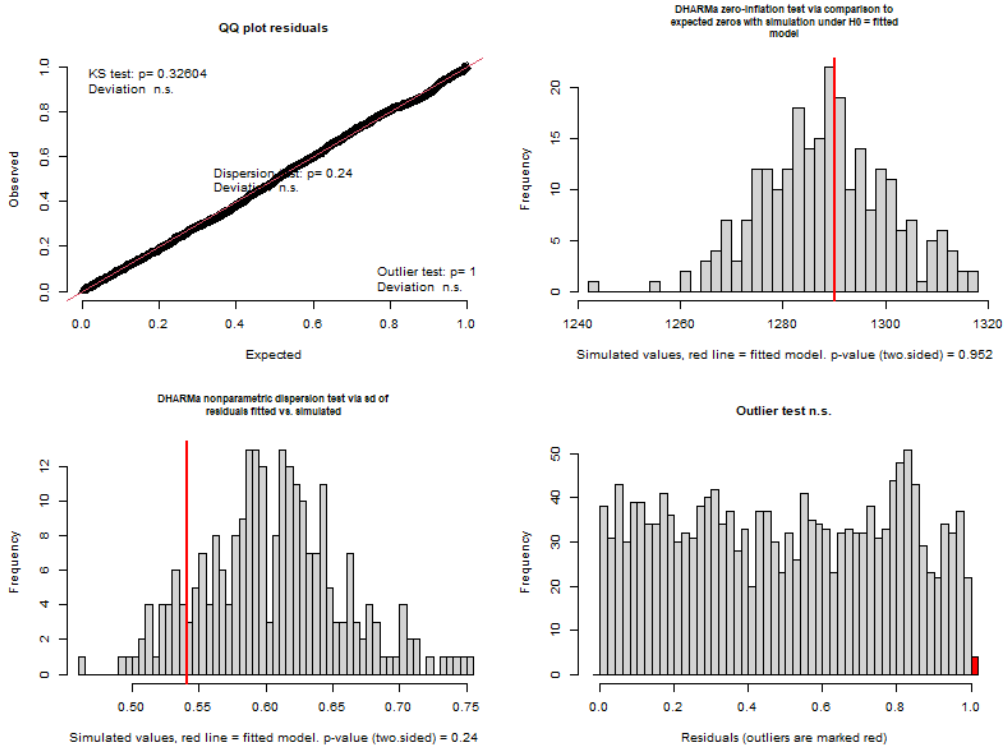

Figure A1: Diagnostic plots for the zero-inflated Tweedie GLMM analyzing variations in area (cm²) among microhabitats (CR - crevices, HR - horizontal rocks, RP - rock pools, VRE - east-facing vertical rocks, VRN - north-facing vertical rocks, VRS - south-facing vertical rocks, VRW - west-facing vertical rocks) irrespective of site.

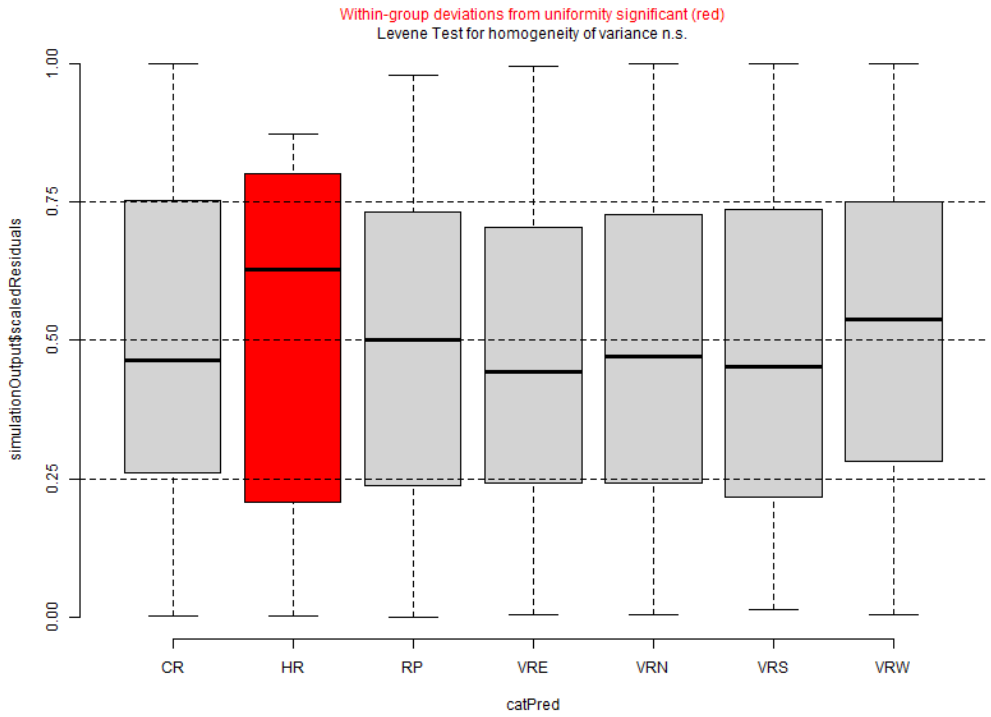

Figure A2: Diagnostic tests of within-group uniformity and variance homogeneity for the zero-inflated Tweedie GLMM analyzing variations in area (cm^2) among microhabitats (CR - crevices, HR - horizontal rocks, RP - rock pools, VRE - east-facing vertical rocks, VRN - north-facing vertical rocks, VRS - south-facing vertical rocks, VRW - west-facing vertical rocks) irrespective of site.

For the Poisson GLMMs analyzing variation in occurrence rates for both species (Equation 2.2), neither the microhabitat groups nor the site groups exhibited any significant within-group deviation from uniformity or variance heterogeneity (Figure A3 and A4). This indicated stable residual distributions across those factors in these models.

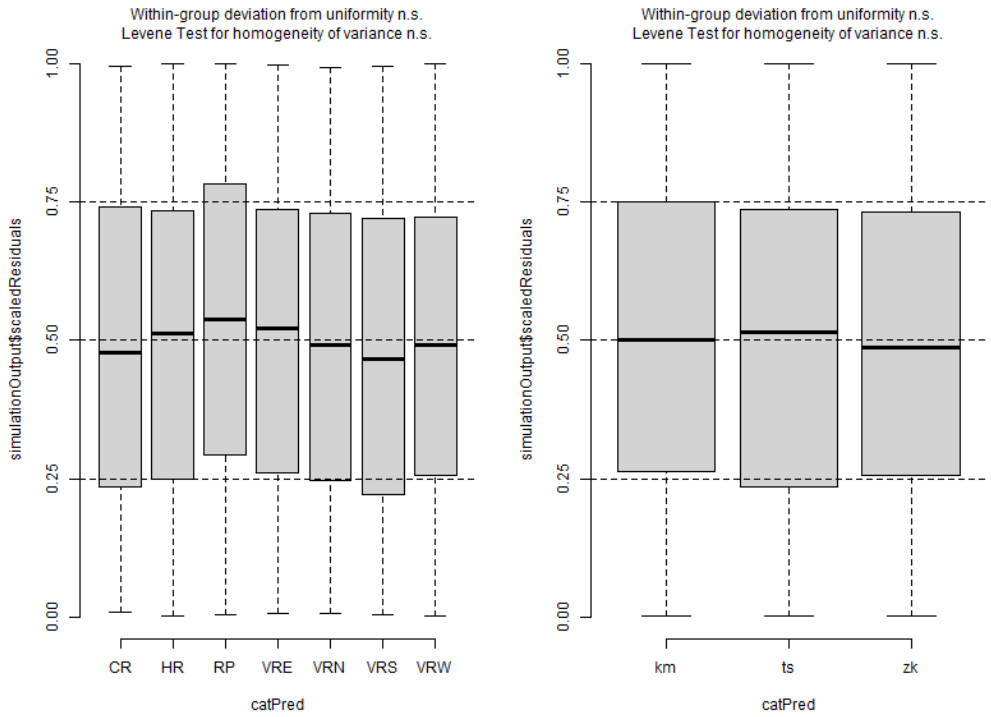

Figure A3: Diagnostic tests of within-group uniformity and variance homogeneity for the zero-inflated Poisson GLMM assessing variations in *Siphonaria capensis* occurrences (counts/cm^2) among microhabitats (CR - crevices, HR - horizontal rocks, RP - rock pools, VRE - east-facing vertical rocks, VRN - north-facing vertical rocks, VRS - south-facing vertical rocks, VRW - west-facing vertical rocks) and sites (km - Kommetjie, ts - Three Sisters, zk - Zinkwazi).

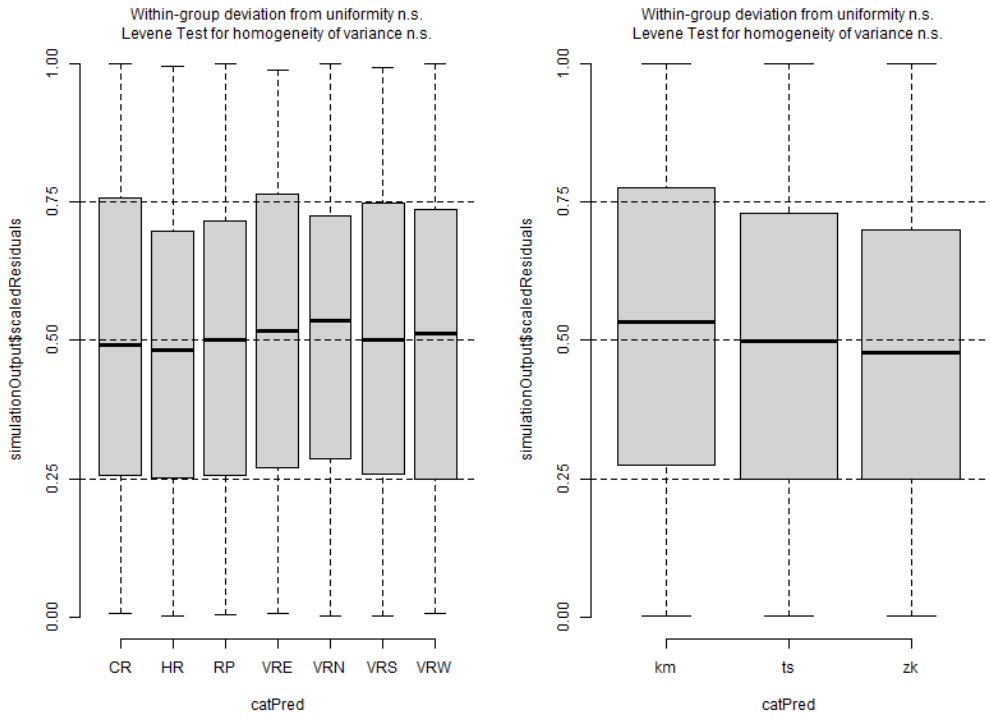

Figure A4: Diagnostic tests of within-group uniformity and variance homogeneity for the zero-inflated Poisson GLMM assessing variations in *Siphonaria serrata* occurrences (counts/cm^2) among microhabitats (CR - crevices, HR - horizontal rocks, RP - rock pools, VRE - east-facing vertical rocks, VRN - north-facing vertical rocks, VRS - south-facing vertical rocks, VRW - west-facing vertical rocks) and sites (km - Kommetjie, ts - Three Sisters, zk - Zinkwazi).

The remaining diagnostic tests (Figure A5 and A6) indicate that the model residuals were normally distributed, showing no significant signs of zero-inflation or overdispersion for both study species. Additionally, while no significant outliers were detected for *Siphonaria serrata*, the outlier issue for *S. capensis* was statistically significant. This suggests that a small number of observations in the affected dataset exert high leverage on model estimates, potentially reflecting genuine ecological extremes, data errors, or unresolved overdispersion (Bolker et al. 2009). Only a minor proportion (≈ 1.3%) of the 1701 observations were flagged as outliers, however. Moreover, most outliers (≈ 55%) were linked to Zinkwazi, where the unusually low occurrence rates of *S. capensis* (see Section 2.4.3.1) may have contributed substantially to the outlier issue. Thus, while the

presence of outliers was significant, its limited magnitude and probable association with a documented ecological extreme suggest it likely has minimal impact on model fit (Bolker et al. 2009) and can be retained in the current model specification. Furthermore, as with the Tweedie GLMM (Equation 2.1), including an interaction term caused model convergence issues in the Poisson GLMMs fitted to both species' data (Equation 2.2). Nonetheless, examining broad site- and microhabitat-level differences in occurrence rates was deemed sufficient to address the primary research question of this chapter.

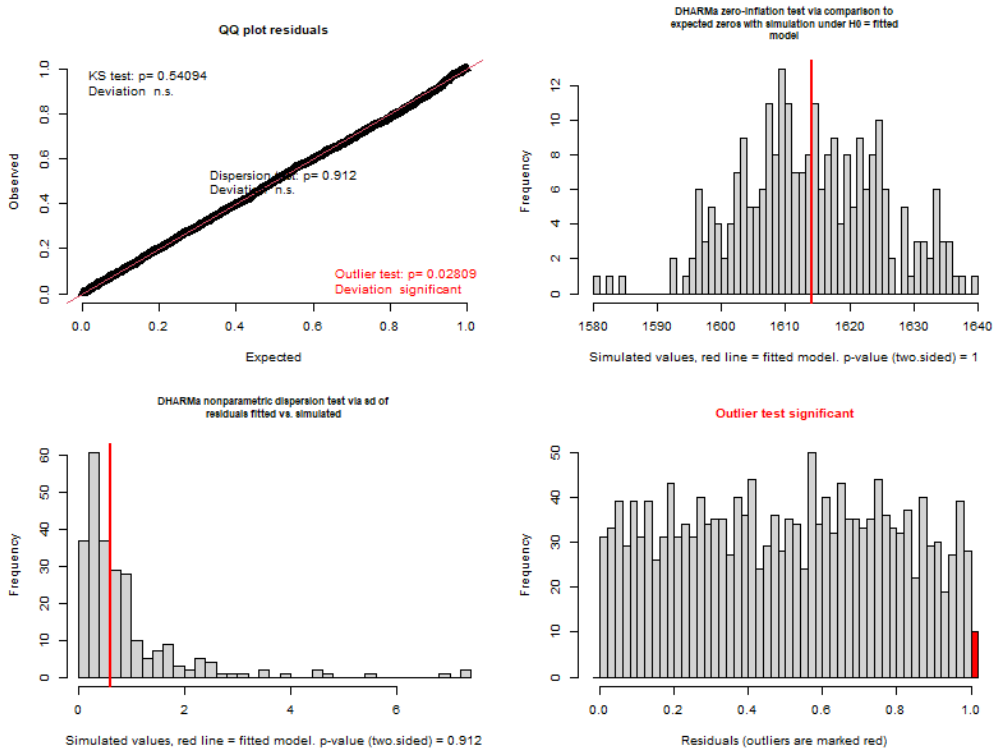

Figure A5: Diagnostic plots for the zero-inflated Poisson GLMM assessing variations in *Siphonaria capensis* occurrences (counts/cm^2) among microhabitats and sites.

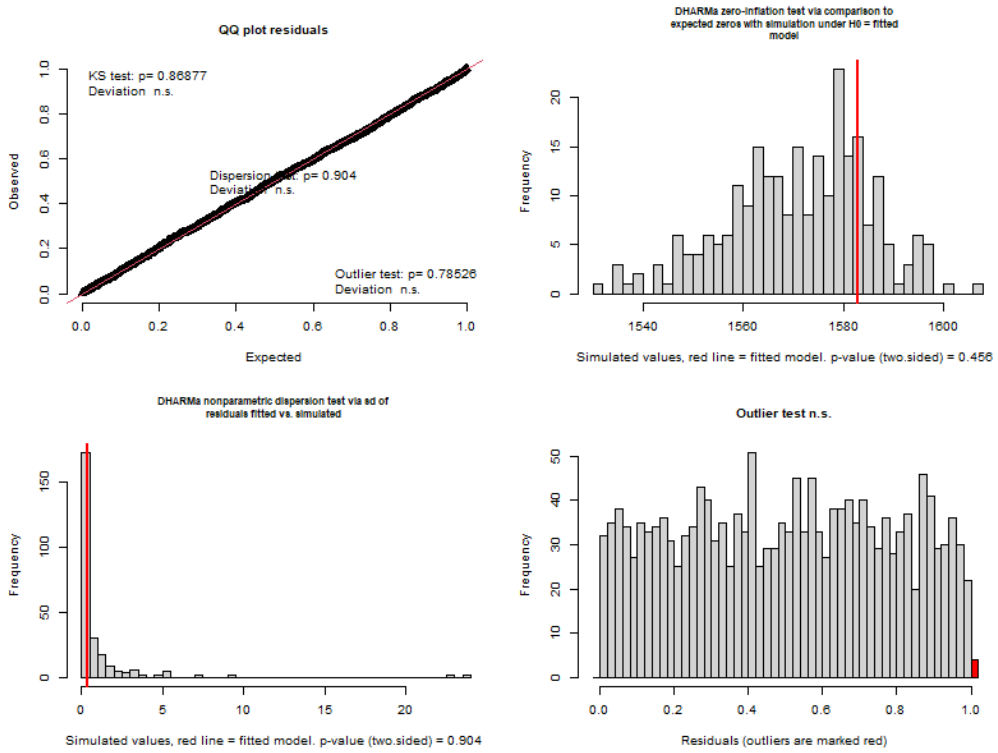

Figure A6: Diagnostic plots for the zero-inflated Poisson GLMM assessing variations in *Siphonaria serrata* occurrences (counts/cm^2) among microhabitats and sites.

For the diagnostic tests performed on the Poisson GLMMs fitted to assess within-site variation in microhabitat-specific species distributions, any flagged outlier (Figures A8, A10, A14 and A16) or overdispersion (Figure A12) issues exhibited similar severity and characteristics to those described above for the Tweedie and Poisson GLMMs in this appendix section. These issues were subsequently addressed in a similar fashion.

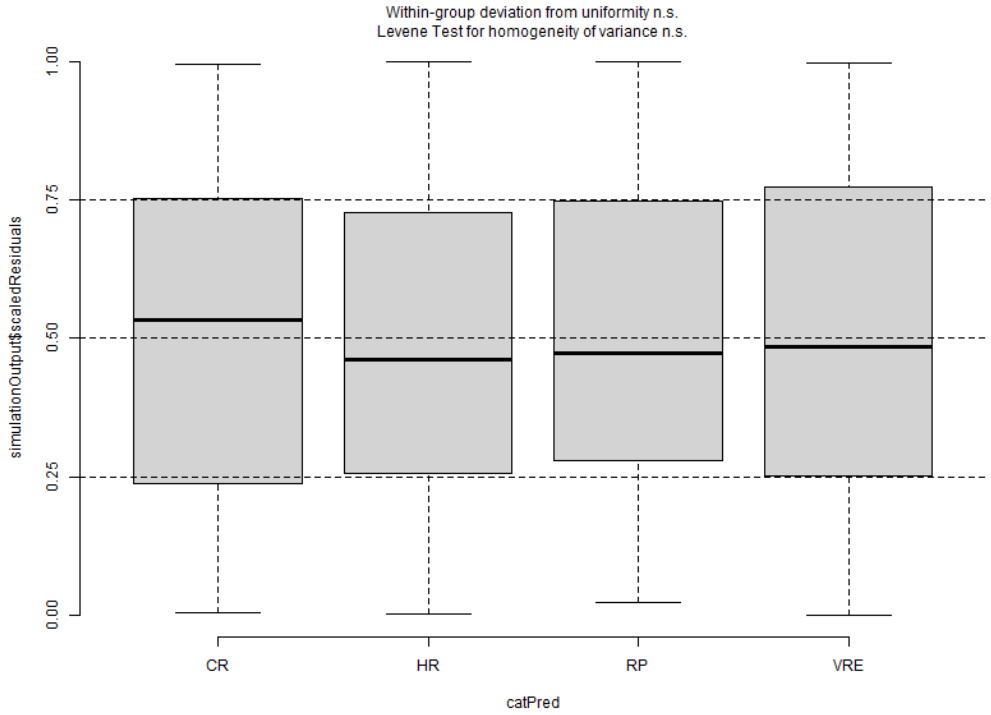

Figure A7: Diagnostic tests of within-group uniformity and variance homogeneity for the zero-inflated Poisson GLMM assessing variations in *Siphonaria capensis* occurrences (counts/cm^2) among microhabitats (CR - crevices, HR - horizontal rocks, RP - rock pools, VRE - east-facing vertical rocks) at Kommetjie.

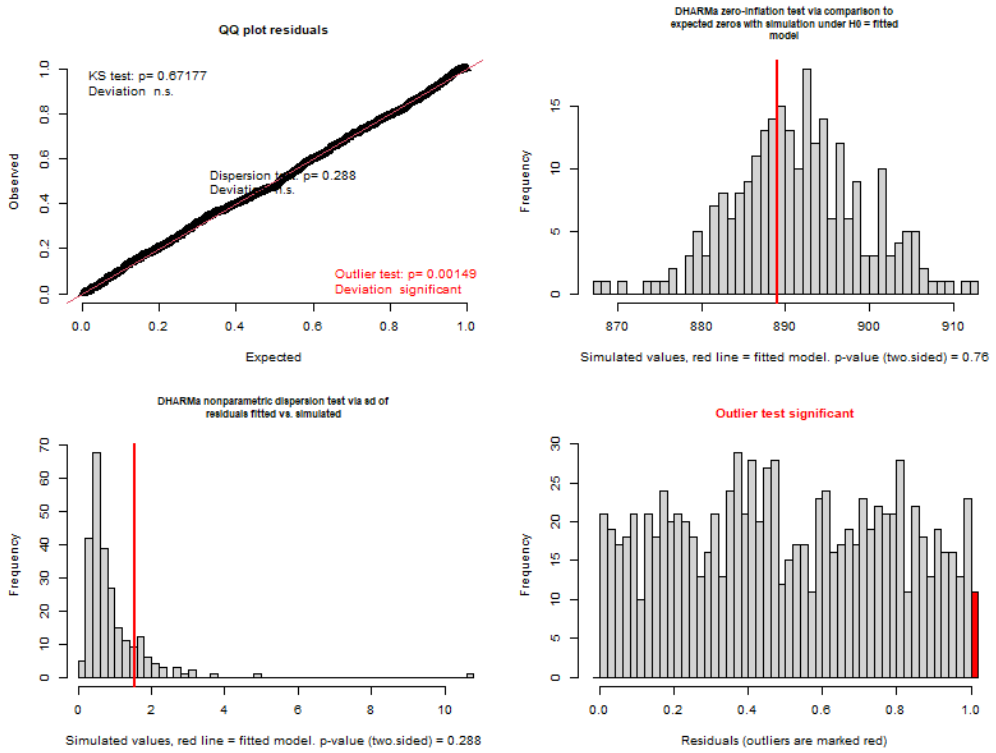

Figure A8: Diagnostic plots for the zero-inflated Poisson GLMM assessing variations in *Siphonaria capensis* occurrences (counts/cm^2) among microhabitats at Kommetjie.

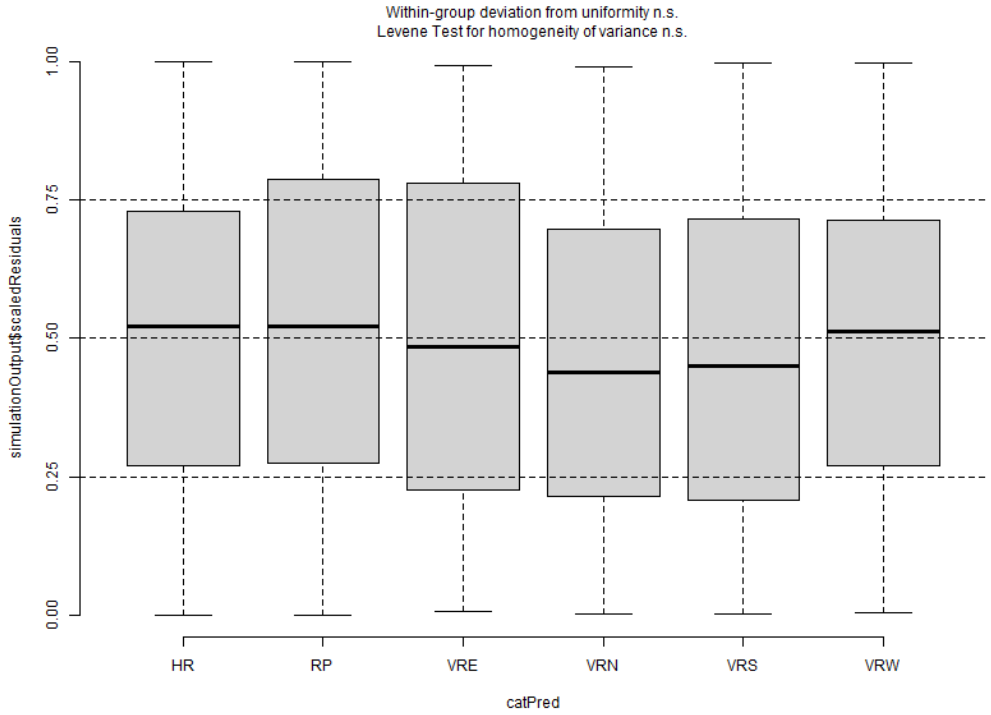

Figure A9: Diagnostic tests of within-group uniformity and variance homogeneity for the zero-inflated Poisson GLMM assessing variations in *Siphonaria capensis* occurrences (counts/cm^2) among microhabitats (HR - horizontal rocks, RP - rock pools, VRE - east-facing vertical rocks, RP - rock pools, VRE - east-facing vertical rocks, VRN - north-facing vertical rocks, VRS - south-facing vertical rocks, VRW - west-facing vertical rocks) at Three Sisters.

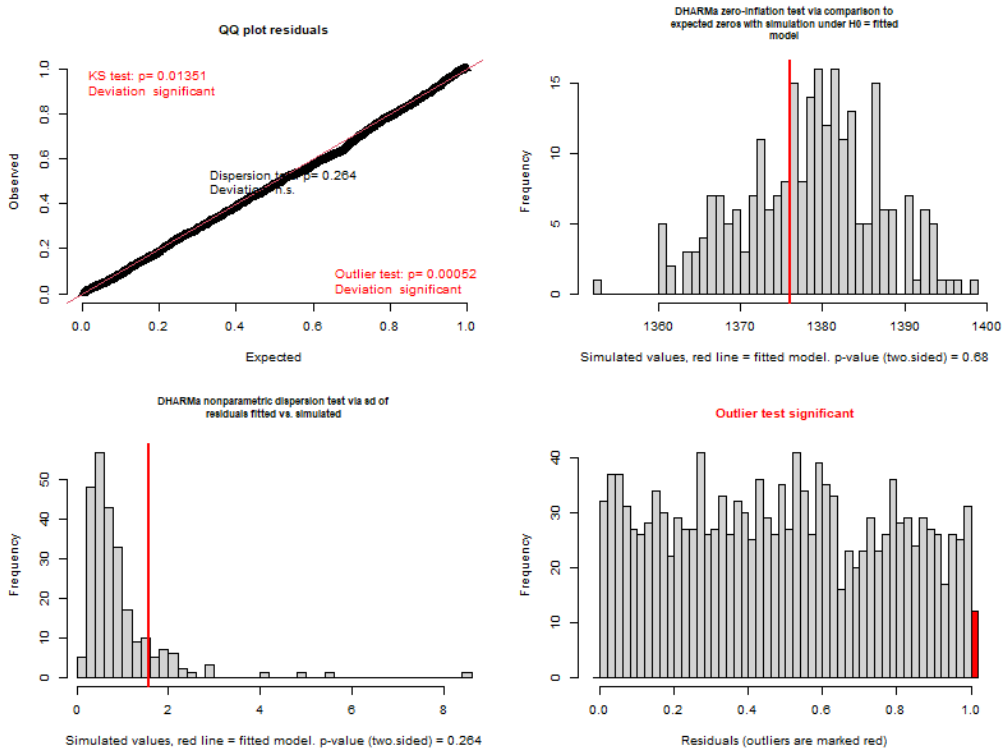

Figure A10: Diagnostic plots for the zero-inflated Poisson GLMM assessing variations in *Siphonaria capensis* occurrences (counts/cm^2) among microhabitats at Three Sisters.

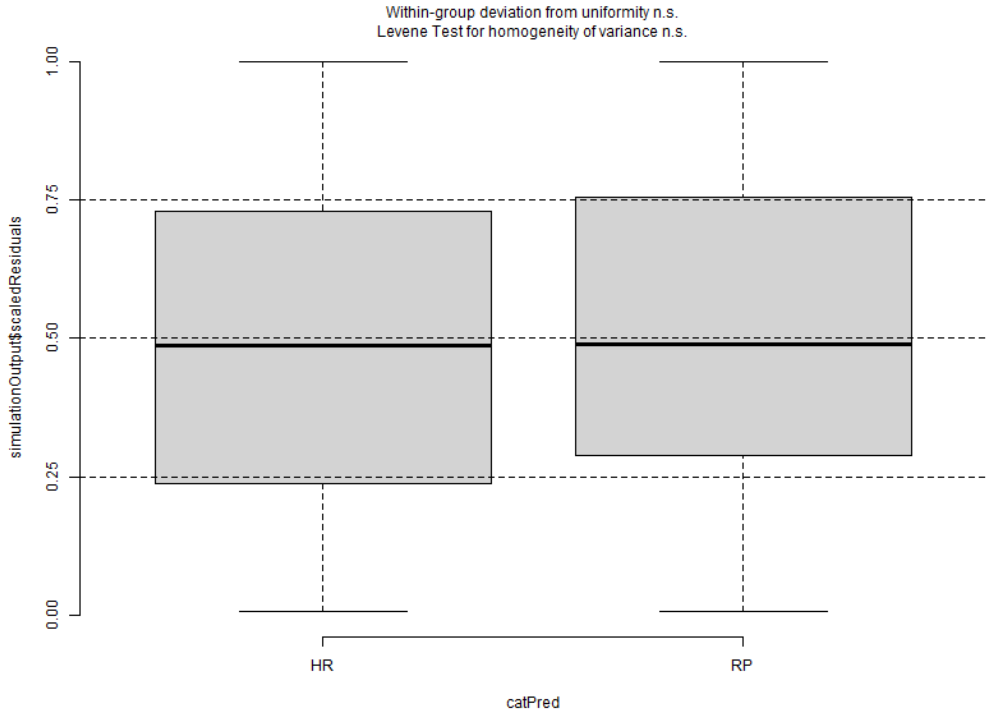

Figure A11: Diagnostic tests of within-group uniformity and variance homogeneity for the zero-inflated Poisson GLMM assessing variations in *Siphonaria capensis* occurrences (counts/cm^2) between microhabitats (HR - horizontal rocks, RP - rock pools) at Zinkwazi.

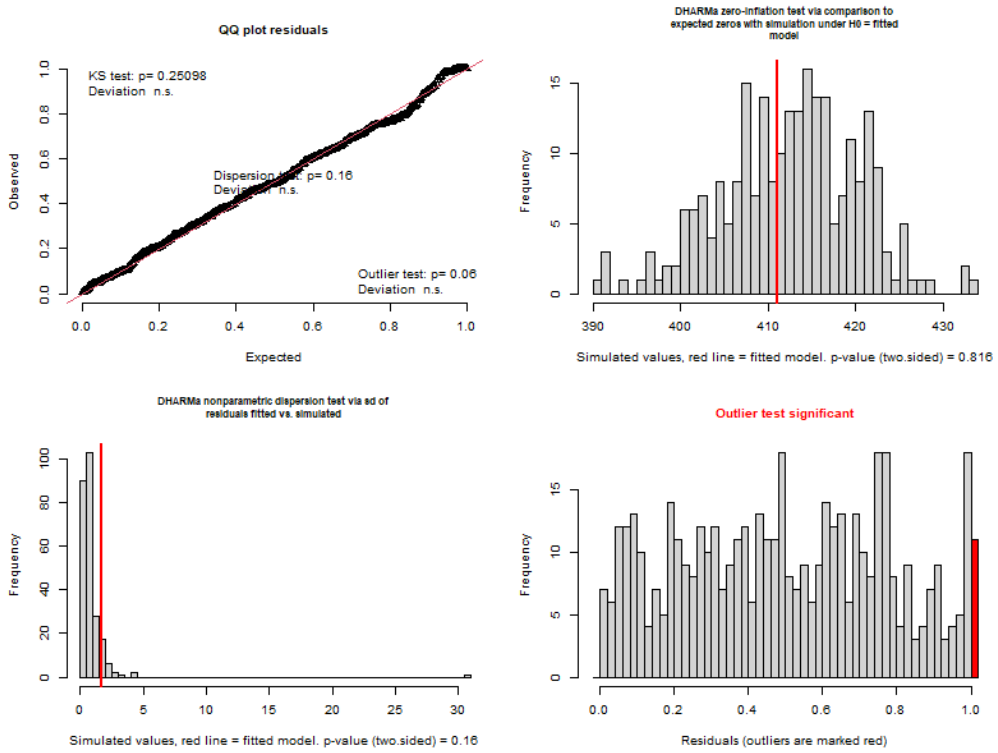

Figure A12: Diagnostic plots for the zero-inflated Poisson GLMM assessing variations in *Siphonaria capensis* occurrences (counts/cm^2) between microhabitats at Zinkwazi.

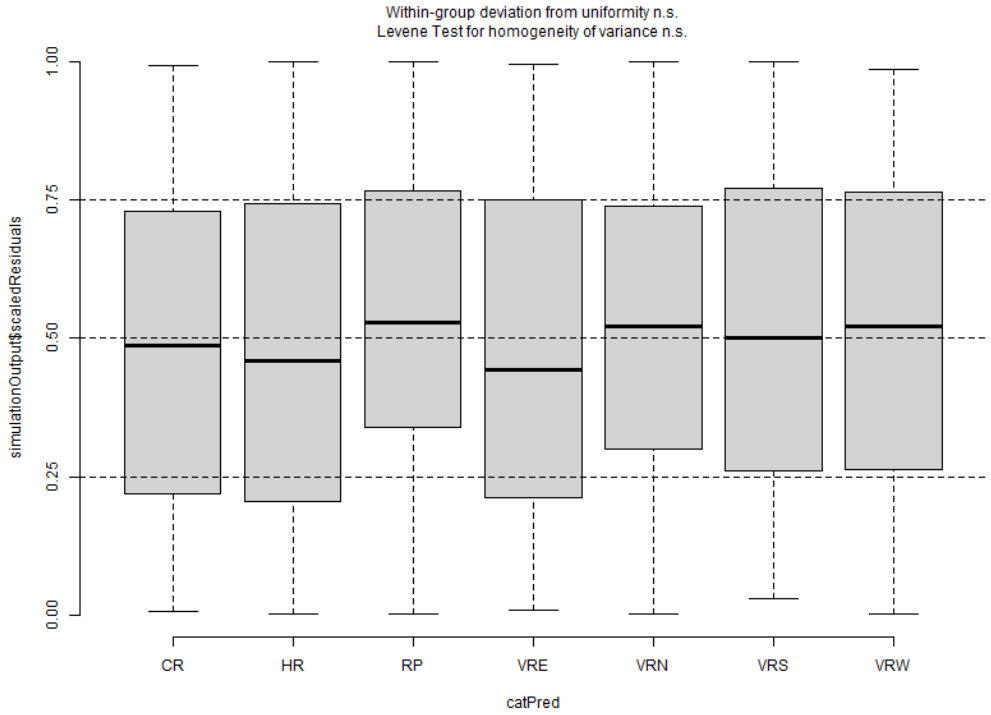

Figure A13: Diagnostic tests of within-group uniformity and variance homogeneity for the zero-inflated Poisson GLMM assessing variations in *Siphonaria serrata* occurrences (counts/cm^2) among microhabitats (CR - crevices, HR - horizontal rocks, RP - rock pools, VRE - east-facing vertical rocks, VRN - north-facing vertical rocks, VRS - south-facing vertical rocks, VRW - west-facing vertical rocks) at Kommetjie.

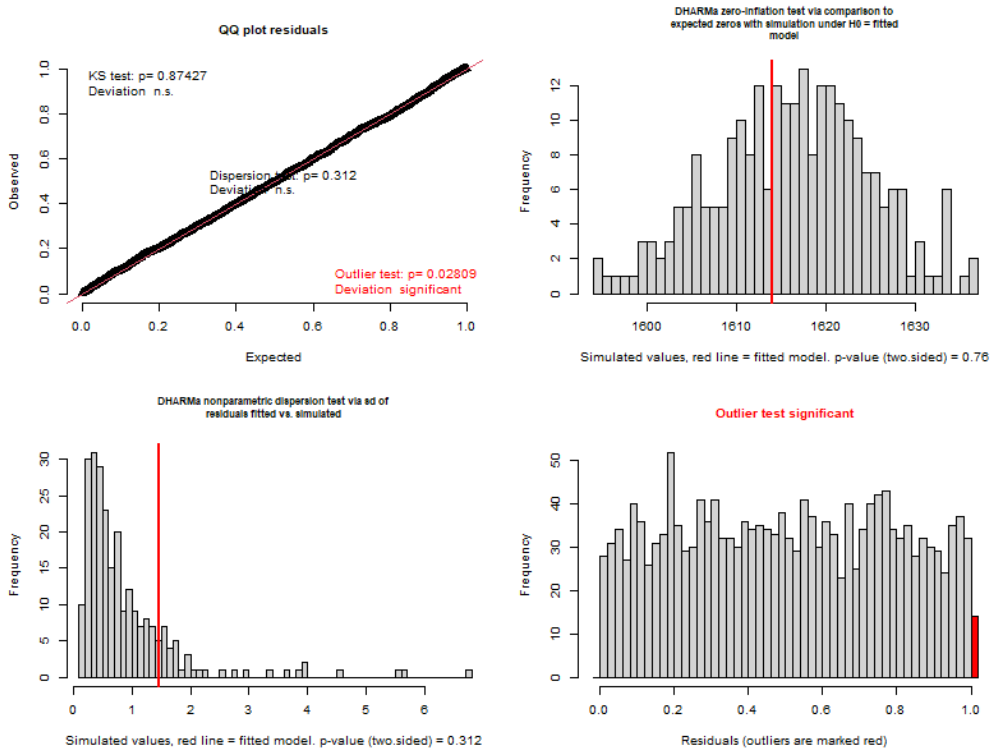

Figure A14: Diagnostic plots for the zero-inflated Poisson GLMM assessing variations in *Siphonaria serrata* occurrences (counts/cm^2) among microhabitats at Kommetjie.

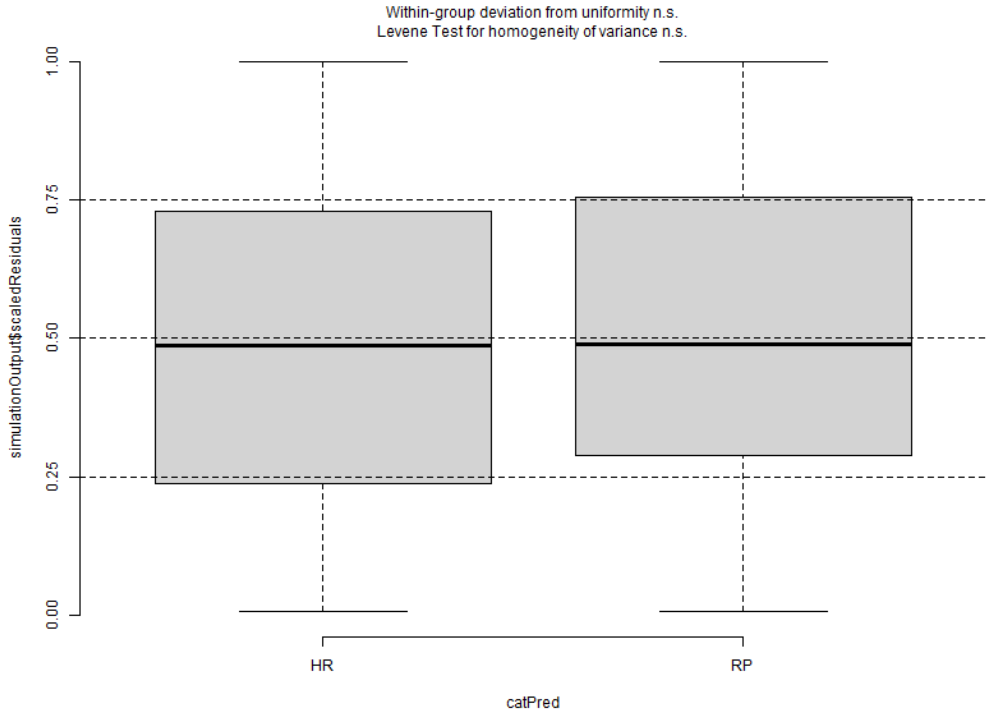

Figure A15: Diagnostic tests of within-group uniformity and variance homogeneity for the zero-inflated Poisson GLMM assessing variations in *Siphonaria serrata* occurrences (counts/cm^2) between microhabitats (HR - horizontal rocks, RP - rock pools) at Zinkwazi.

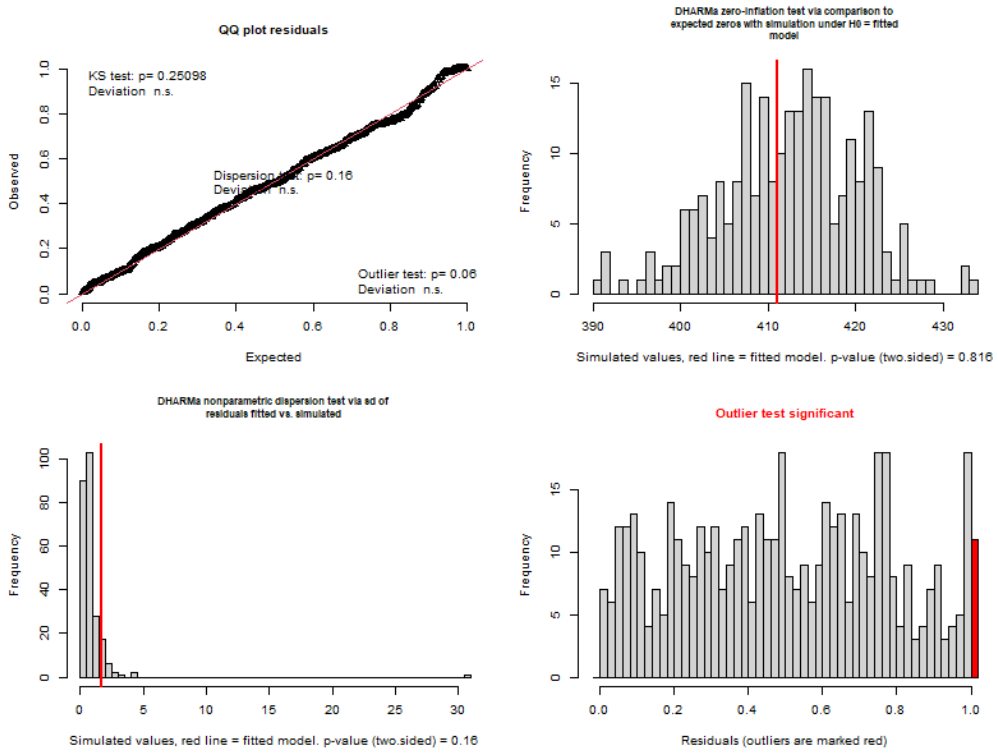

Figure A16: Diagnostic plots for the zero-inflated Poisson GLMM assessing variations in *Siphonaria serrata* occurrences (counts/cm^2) between microhabitats at Zinkwazi.

Table A1: Random effect (quadrat) output from the detailed model summary of the zero-inflated Tweedie GLMM used to analyze the variation in area (cm^2) as a function of microhabitat irrespective of site.

group	variance	st_dev
Quadrat	< 0.0001	< 0.0001

Table A2: Random effect (quadrat) output from the detailed model summary of the zero-inflated Poisson GLMM used to evaluate the occurrence (counts/cm^2) of *Siphonaria capensis* across sites and microhabitats.

group	variance	st_dev
Quadrat	0.7809	0.8837

Table A3: Random effect (quadrat) output from the detailed model summary of the zero-inflated Poisson GLMM used to evaluate the occurrence (counts/cm^2) of *Siphonaria serrata* across sites and microhabitats.

group	variance	st_dev
Quadrat	1.2117	1.1008

A2 Microhabitat preference analysis

The diagnostic evaluations presented in Figure A17 and A18, revealed no significant within-group deviations from uniformity or variance heterogeneity in the models assessing variation in the proportion of recaptured individuals of both species (Equation 3.1). Furthermore, Figure A19 and A20 displayed no evidence of non-normality, zero-inflation, overdispersion, or influential outliers in the model residuals.

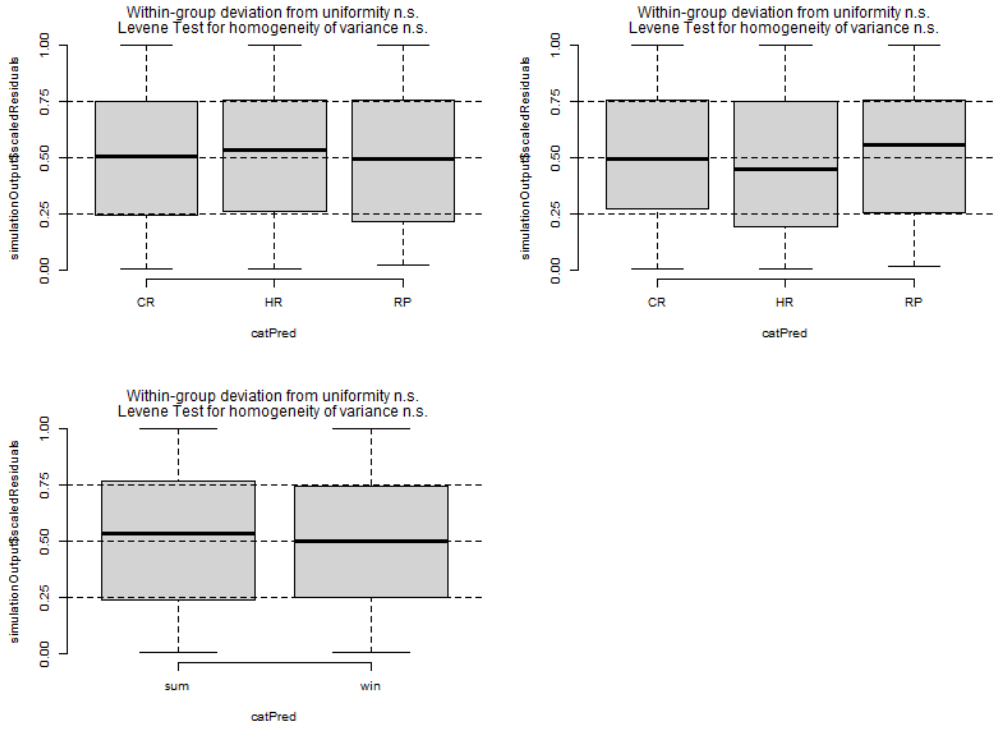

Figure A17: Diagnostic tests of within-group uniformity and variance homogeneity for the zero-inflated Beta-binomial GLMM assessing variation in the proportion of recaptured *Siphonaria capensis* between seasons (sum - summer, win - winter), and among original and new microhabitats (CR - crevices, HR - horizontal rocks, RP - rock pools) irrespective of site.

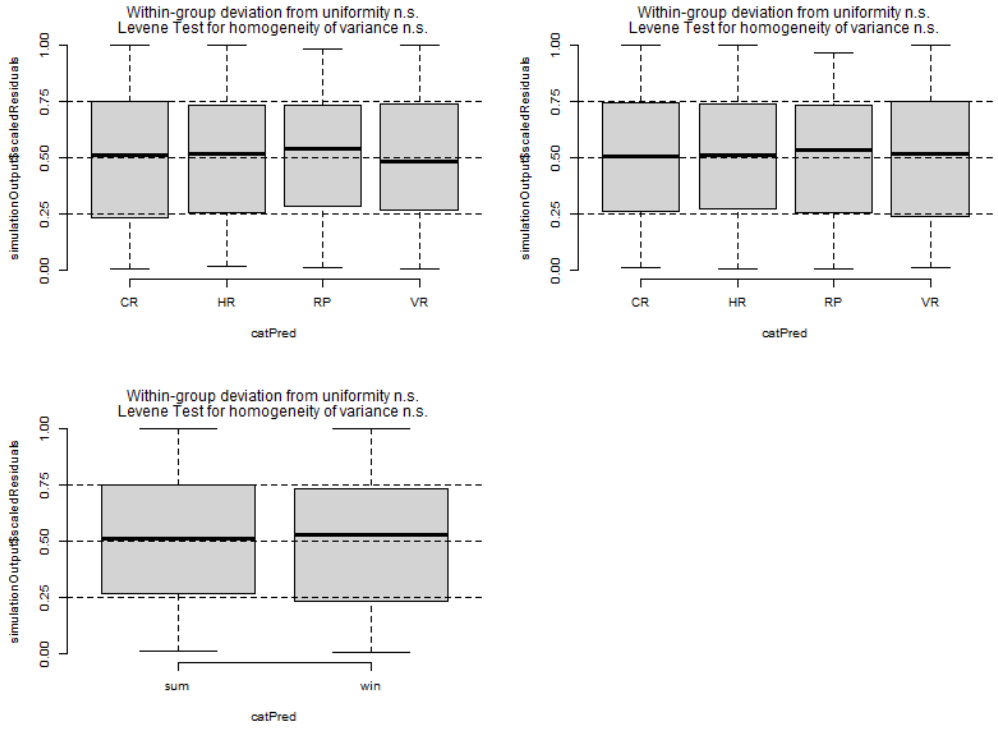

Figure A18: Diagnostic tests of within-group uniformity and variance homogeneity for the zero-inflated Beta-binomial GLMM assessing variation in the proportion of recaptured *Siphonaria serrata* between seasons (sum - summer, win - winter), and among original and new microhabitats (CR - crevices, HR - horizontal rocks, RP - rock pools, VR - vertical rocks) irrespective of site.

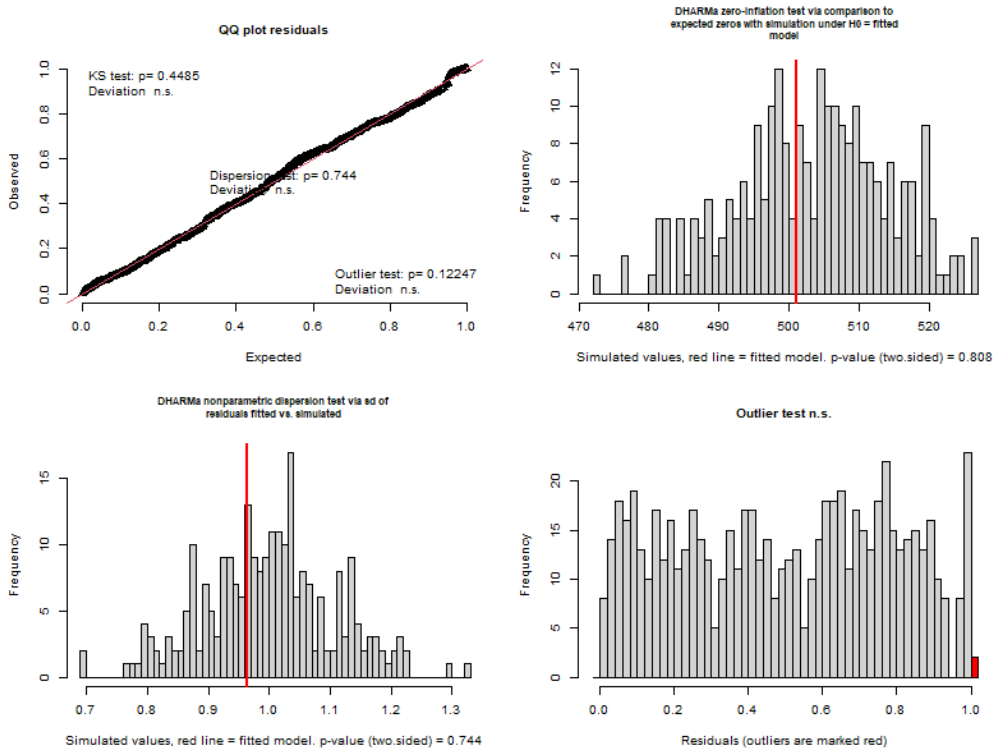

Figure A19: Diagnostic plots for the zero-inflated Beta-binomial GLMM assessing variation in the proportion of recaptured *Siphonaria capensis* between seasons, and among original and new microhabitats irrespective of site.

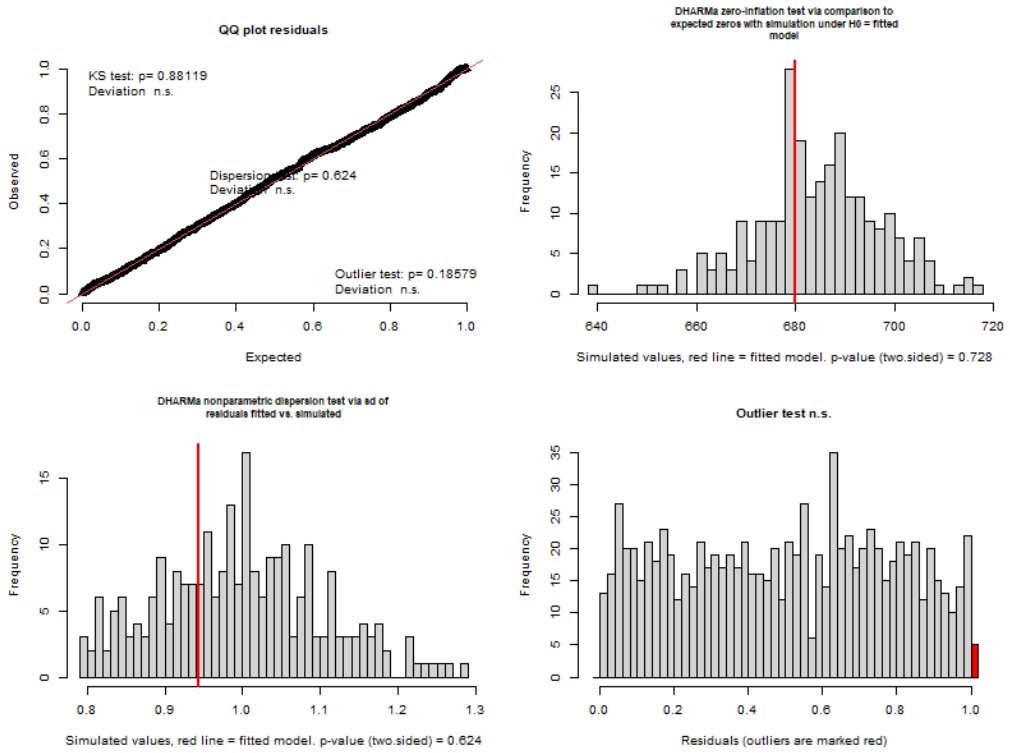

Figure A20: Diagnostic plots for the zero-inflated Beta-binomial GLMM assessing variation in the proportion of recaptured *Siphonaria serrata* between seasons, and among original and new microhabitats irrespective of site.

The likelihood ratio tests comparing different Beta-binomial models for the proportion of recaptured *Siphonaria capensis* and *S. serrata* yield contrasting findings regarding the decision on whether to include interaction terms versus no interaction terms (Table A4 and A5). For *Siphonaria capensis*, models excluding interaction terms demonstrated superior fit, while for *S. serrata*, models incorporating multiple interaction terms performed best (Table A5). I chose, however, to supersede the likelihood ratio test results and selected models for analyzing limpet recapture proportions that retained only the interaction term between new and original microhabitat. This specification was adopted for *S. serrata* because interactions between season and each of original and new microhabitat generated significantly overdispersed residuals and deviations from the expected residual distribution. For *S. capensis*, although likelihood ratio tests favoured the interaction-free model, the selected model exhibited lower AIC and deviance scores (Table A4). This indicates that the interaction-free model offers only a marginal

improvement, as it outperformed the selected model in just two of three fit criteria. Finally, choosing this interaction-based model for *S. capensis* achieves consistency in how I specified models for both species' recapture proportions (Equation 3.1), while still maintaining acceptable model performance.

Table A4: Model selection results for the zero-inflated Beta-binomial GLMM assessing variation in the proportion of recaptured *Siphonaria capensis* between seasons, and among original and new microhabitats irrespective of site.

model	Df	AIC	BIC	logLik	deviance	Chisq	Chi Df	p.value
model1	9	1,692.4	1,733.0	-837.2	1,674.4	NA	NA	NA
model2	13	1,691.3	1,750.0	-832.7	1,665.3	9.1	4	0.1
model3	17	1,693.0	1,769.6	-829.5	1,659.0	6.4	4	0.2

model1 - no interaction between variables, model2 - two-way interaction between original (omh) and new microhabitat (nmh), model3 - two-way interaction of season with original microhabitat and with new microhabitat.

Table A5: Model selection results for the zero-inflated Beta-binomial GLMM assessing variation in the proportion of recaptured *Siphonaria serrata* between seasons, and among original and new microhabitats irrespective of site.

model	Df	AIC	BIC	logLik	deviance	Chisq	Chi Df	p.value
model1	11	2,283.4	2,336.4	-1,130.7	2,261.4	NA	NA	NA
model2	20	2,282.4	2,378.7	-1,121.2	2,242.4	19.0	9	< 0.0001
model3	26	2,279.8	2,405.0	-1,113.9	2,227.8	14.6	6	< 0.0001

model1 - no interaction between variables, model2 - two-way interaction between original (omh) and new microhabitat (nmh), model3 - two-way interaction of season with original microhabitat and with new microhabitat.

Table A6: Random effect (mark event) output from the detailed model summary of the zero-inflated Beta-binomial GLMM assessing variation in the proportion of recaptured *Siphonaria capensis* between seasons, and among original and new microhabitats irrespective of site.

group	variance	st_dev
m_i	< 0.0001	< 0.0001

m_i - mark event

Table A7: Random effect (mark event) output from the detailed model summary of the zero-inflated Beta-binomial GLMM assessing variation in the proportion of recaptured *Siphonaria serrata* between seasons, and among original and new microhabitats irrespective of site.

group	variance	st_dev
m_i	< 0.0001	< 0.0001

m_i - mark event.

The metric scores presented in Table A8 demonstrate that the Bernoulli GLM (Equation 3.2), fitted with an interaction term to assess variations in homing status, achieved good discrimination between classes, showed insignificant evidence of poor fit, and exhibited high predictive capacity and overall accuracy. The likelihood ratio test results (Table A9) further confirm that the selected model specification (Equation 3.2) was the most appropriate for the data.

Table A8: Metric scores assessing the overall Bernoulli GLM performance for the variation in homing status between species across the different relocation treatments.

metric	value
roc_auc (%)	70.60000
hos-lem (p)	0.99996
brier score	0.09300
accuracy (%)	88.90000

roc_auc (%) - receiver operating characteristic value, hos-lem - hosmer-lemeshow test score, accuracy (%) - model accuracy.

Table A9: Model selection results for the Bernoulli GLM used to determine differences in the Homing rates of both sample species as a function of relocation treatment.

model	Df	AIC	BIC	logLik	deviance	Chisq	Chi Df	p.value
model1	4	2,297.5	2,322.3	-1,144.7	2,289.5	NA	NA	NA
model2	6	2,292.6	2,329.8	-1,140.3	2,280.6	8.8	2	< 0.0001

model1 - no interaction between variables, model2 - two-way interaction between species and relocation treatment.

The performance metrics shown in Figure A10 and A11 indicate that the Multinomial GLMs used to evaluate variations in post-relocation distribution patterns of *Siphonaria capensis* and *S. serrata* across microhabitats, respectively (Equation 3.3), demonstrated high overall accuracy and strong discrimination among classes.

Table A10: Metric scores assessing the overall Multinomial GLM performance for *Siphonaria capensis* distribution among recapture microhabitats.

metric	estimator	estimate
accuracy	multiclass	0.85
roc_auc	hand_till	0.96

accuracy - overall accuracy of the models predictions, roc_auc - evaluates how well a classifier can distinguish between classes.

Table A11: Metric scores assessing the overall Multinomial GLM performance for *Siphonaria serrata* distribution among recapture microhabitats.

metric	estimator	estimate
accuracy	multiclass	0.85
roc_auc	hand_till	0.96

accuracy - overall accuracy of the models predictions, roc_auc - evaluates how well a classifier can distinguish between classes.

In the roc plots for both species (Figure A21 and A22), the model's sensitivity versus (1 – specificity) performance is clearly better than random chance. Furthermore, the overall separation of the curves (sensitivity versus (1 – specificity)) from the diagonal confirms that the model discriminates among classes reasonably well.

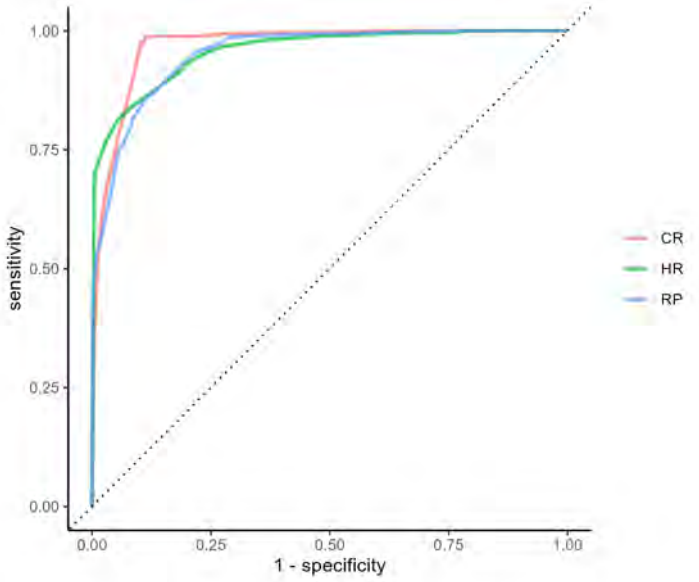

Figure A21: Receiver operating characteristic (roc) curve generated from the Multinomial GLM output used to evaluate the distribution of *S. capensis* among recapture microhabitats (CR - crevices, HR - horizontal rocks, RP - rock pools) as a function of relocation direction, site and season.

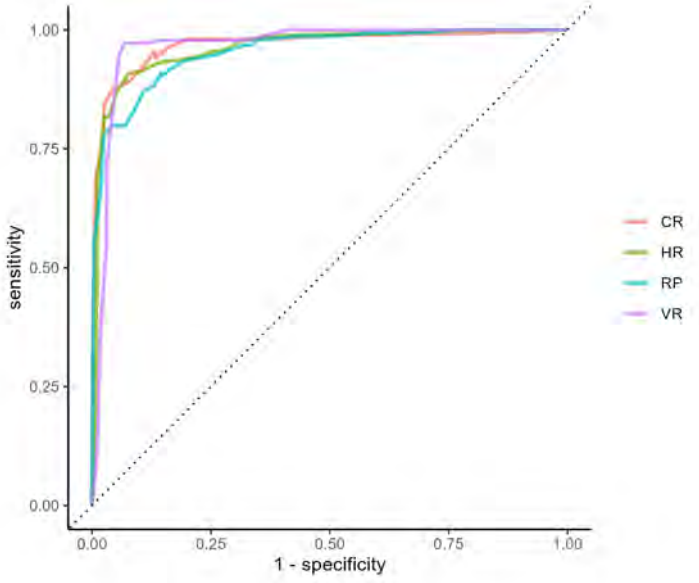

Figure A22: Receiver operating characteristic (roc) curve generated from the Multinomial GLM output used to evaluate the distribution of *S. serrata* among recapture microhabitats (CR - crevices, HR - horizontal rocks, RP - rock pools, VR - vertical rocks) as a function of relocation direction, site and season.

The confusion matrix generated from the Multinomial GLM for *Siphonaria capensis* shows that the model correctly predicts most crevice observations but had moderate misclassification rates for horizontal surfaces and rock pools (Table A12). Therefore, the model was generally suitable for inference. For *S. serrata*, the matrix indicated similarly accurate predictions for crevices and horizontal surfaces as in the *S. capensis* data, along with low misclassification for vertical surfaces, but revealed a particularly high misclassification rate for rock pools (Table A13). High misclassification in a single class often signals missing predictors, structural model issues, insufficient ability of the predictors to distinguish response variable classes, and/or a high class imbalance in the response variable (Manel et al. 2001, Allouche et al. 2006). In this case, rock pool outcomes for the categorical response variable, recapture microhabitat, were relatively few compared to other levels (Figure 3.4). This may have biased the model towards predicting the recapture of relocated individuals in more common categories, even when, in reality, they were recaptured from rock pools (Allouche et al. 2006). The most straightforward approaches to remedying these model performance issues are the inclusion of additional predictors or collecting more data (Manel et al. 2001, Burnham & Anderson 2002). Here, however, the model remains acceptable to use due to the strong overall performance indicated by the other model metrics (Table A10 and Figure A21), the model's moderately-to-highly accurate classification for other microhabitat classes (Table A13), and because the model was primarily intended for inference rather than perfect prediction (Burnham & Anderson 2002).

Table A12: Classification performance, based on a confusion matrix of observed and predicted outcomes, of the Multinomial GLM used to describe the distribution of *Siphonaria capensis* among recapture microhabitats.

Truth	maxfreq	sumotherfreq	missclass%
HR	421	124	29.5
CR	511	12	2.3
RP	415	95	22.9

Truth - target predictor class against which model predictions are compared (HR - horizontal rocks, CR - crevices, RP - rock pools), maxfreq - the maximum frequency of predictions made involving the target predictor class, sumotherfreq - frequency of incorrect predictions, missclass% - the model misclassification rate.

Table A13: Classification performance of the Multinomial GLM used to describe the distribution of *Siphonaria serrata* among recapture microhabitats, based on a confusion matrix of observed and predicted outcomes.

Truth	maxfreq	sumotherfreq	missclass %
HR	421	93	22.1
CR	490	59	12.0
RP	103	51	49.5
VR	176	5	2.8

Truth - target predictor class against which model predictions are compared (HR - horizontal rocks, CR - crevices, RP - rock pools), maxfreq - the maximum frequency of predictions made involving the target predictor class, sumotherfreq - frequency of incorrect predictions, missclass% - the model misclassification rate.

A3 Thermal preference analysis

An examination of the performance metrics in Table A14 reveals that the Bernoulli GLM analyzing changes in *Siphonaria capensis* movement status (Equation 4.1) achieves moderate discrimination and acceptable calibration (Hosmer-Lemeshow $p > 0.05$),

though the predictive capacity and overall model accuracy are relatively low. Potential reasons for these moderate performance metrics include missing predictors, unmodeled heterogeneity, or inherently high individual-level variability (Bolker et al. 2009). As with the Multinomial GLM described in Section A2, additional predictors or expanded datasets are typically required to address suboptimal performance scores and improve model fit (O'Hara & Kotze 2010, Harrison 2014). In the absence of such refinements, however, the model can still be deemed acceptable for further use, as it was specified to prioritize hypothesis testing and inferential clarity over predictive precision (Burnham & Anderson 2002). Furthermore, the current model specification, without additional complexity such as interaction terms, provides the best fit for the available data, as confirmed by a likelihood ratio test (Table A15).

Table A14: Metric scores assessing the overall performance of the Bernoulli GLM analyzing the influence of microhabitat and start temperature status on the movement status of *S. capensis*.

metric	**value**
roc_auc (%)	61.60000
hos-lem (p)	0.98547
brier score	0.23200
accuracy (%)	59.50000

roc_auc (%) - receiver operating characteristic value, hos-lem - hosmer-lemeshow test score, accuracy (%) - model accuracy.

Table A15: Model selection results for the Bernoulli GLM analyzing the influence of microhabitat and start temperature status on the movement status of *Siphonaria capensis* collected from Kommetjie.

model	Df	AIC	BIC	logLik	deviance	Chisq	Chi Df	p.value
mh+sts	6	274.6	294.4	-131.3	262.6	NA	NA	NA
mhxsts	10	280.7	313.7	-130.4	260.7	1.9	4	0.8

mh - microhabitat, sts - start temperature status.

mh+sts - model excluding interaction between microhabitat and start temperature status, mhxsts - model including interaction between microhabitat and start temperature status.

Table A16 and A17 confirm that the Chi-square test assumption, that all expected cell counts should be more than 5, is satisfied for the interactions between microhabitat and temperature shift and also, between start temperature status and temperature shift, respectively.

Table A16: Verification of Chi-square test assumption that expected cell counts for all levels of the combination of microhabitat (hr - horizontal rock, rp - rock pool) and temperature shift (nc - no change) are ≥ 5.

	temperature shift		
mh	**cold**	**hot**	**nc**
hr	18	23.5	58.5
rp	18	23.5	58.5

mh - microhabitat

Table A17: Verification of Chi-square test assumption that expected cell counts for all levels of the combination of start temperature status (hr - horizontal rock, rp - rock pool) and temperature shift (nc - no change) are ≥ 5.

	temperature shift		
sts	**cold**	**hot**	**nc**
cold	7.2	9.4	23.4
cool	7.2	9.4	23.4
hot	7.2	9.4	23.4
moderate	7.2	9.4	23.4
warm	7.2	9.4	23.4

sts - start temperature status

The *post hoc* analysis results in Table A18 revealed a significant positive association between rock pool origins and shifts to cooler temperatures, as well as between horizontal surface origins and shifts away from cooler temperatures in *Siphonaria capensis*. In contrast, no meaningful associations were observed between microhabitat origin and temperature shift state (Table A18), nor between the initial temperature state of *S. capensis* and its temperature shift status (Table A19).

Table A18: *Post hoc* pairwise comparisons for the Pearson's Chi-square test of independence on the relationship between microhabitat and temperature shift status in *S. capensis*.

Dimension	Value	cold	hot	nc
hr	Residuals	-4.4173	1.1674	2.4397
hr	p values	0.0001	1.0000	0.0882
rp	Residuals	4.4173	-1.1674	-2.4397
rp	p values	0.0001	1.0000	0.0882

nc - No change

Table A19: *Post hoc* pairwise comparisons for the 3x5 Pearson's Chi-square test of independence, examining the relationship between the initial temperature and temperature shift status of *S. capensis*.

Dimension	Value	cold	hot	nc
cold	Residuals	0.3681	-0.5837	0.2153
cold	p values	1.0000	1.0000	1.0000
cool	Residuals	0.3681	-1.4176	0.9328
cool	p values	1.0000	1.0000	1.0000
hot	Residuals	-0.5522	0.2502	0.2153
hot	p values	1.0000	1.0000	1.0000
moderate	Residuals	-0.0920	1.9179	-1.5786
moderate	p values	1.0000	0.8269	1.0000
warm	Residuals	-0.0920	-0.1668	0.2153
warm	p values	1.0000	1.0000	1.0000

nc - no change

A4 Thermal limit analysis

A4.1 Imputation results

Multiple imputation produced mostly unbiased estimates across the three analysis models. Although only two estimators in the first (Table A20) and third (Table A22) analysis models showed substantial bias, the second analysis model exhibited a few more biased parameter estimates (Table A21).

A4.1.1 Key performance indicator comparisons

Overall, the parameter estimates for the first model run on the incomplete data exhibited a greater degree of bias compared to estimates from the same model run on the imputed data. The RMSE values for the estimates were also generally smaller for the imputed data. Furthermore, no differences in significance outcomes of the parameter estimates produced by the analysis on the complete/“reference” data and both test datasets were detected (Table A20).

Table A20: Comparison of the key performance indicators, for the imputed versus incomplete data, derived from the coefficients of the initial linear mixed model fit using FLT (°C) as the response variable. Highlighted cells indicate larger BIAS and RMSE values for imputed estimates and significance outcome values (SO) that did not match those of the reference dataset (N) versus those that did (Y).

	BIAS		RMSE		STC	
Parameter	**Missing1**	**Imputed1**	**Missing2**	**Imputed2**	**Missing3**	**Imputed3**
INT	-0.2036	-0.1905	8.2489	7.7172	Y	Y
FBT	-0.4266	-0.4026	0.2203	0.2079	Y	Y
SUM	-4.0889	-0.5562	3.6611	0.4980	Y	Y
ts	-25.9077	-13.9089	10.7705	5.7823	Y	Y
km	-0.0004	-0.6396	0.0009	1.6254	Y	Y
L	-1.5680	-1.4592	0.8041	0.7483	Y	Y
FBT.SUM	-4.5499	-0.1497	0.0787	0.0026	Y	Y
FBT.ts	-5.2373	-3.1462	0.2895	0.1739	Y	Y
FBT.km	44.8979	8.8687	0.0490	0.0097	Y	Y
RE.MH	0.5299	-0.5904	0.1000	0.1113	NA	NA

INT - Intercept; SUM - Summer; SPR - Spring; L - length (mm); FLT - flatline temperature (°C); FBT - final breakpoint temperature (°C); zk - Zinkwazi; ts - Three Sisters; km - Kommetjie; RE.MH - microhabitat random effect.

In the second model, more of the parameter estimates from the imputed data analysis exhibited higher bias compared to estimates from the incomplete data when contrasted with the first model. This trend was mirrored in the RMSE values, which showed similar disparities between the two datasets, as observed in the estimate bias. Unlike the first model, however, when comparing the significance outcomes of the parameter estimates produced by the analysis on the complete/"reference" data and the test data, a difference in significance outcomes were detected between the reference and both test datasets (Table A21). Specifically, the significance outcome for the parameter Three Sisters, produced from the analysis of the test datasets did not match those of the corresponding

predictors from the analysis on the reference data. Nevertheless, these parameter estimates were less biased in the imputed data than those produced by the incomplete dataset.

Table A21: Comparison of the key performance indicators, for the imputed versus incomplete data, derived from the coefficients of the initial linear mixed model fit using FBT (°C) as the response variable. Highlighted cells indicate larger BIAS and RMSE values for imputed estimates and significance outcome values (SO) that did not match those from the reference dataset (N) versus those that did (Y).

	BIAS		RMSE		STC	
Parameter	**Missing1**	**Imputed1**	**Missing2**	**Imputed2**	**Missing3**	**Imputed3**
INT	0.1311	0.1050	4.4592	3.5713	Y	Y
CSR	3.3069	3.4782	0.1787	0.1879	Y	Y
SUM	0.2484	0.2073	0.4547	0.3795	Y	Y
ts	-2.4940	-2.5363	4.9054	4.9887	N	N
km	-1.2141	-1.2202	4.0786	4.0992	Y	Y
L	-0.4948	-0.2884	0.1155	0.0674	Y	Y
CSR.SUM	-4.8683	-3.8145	0.1755	0.1375	Y	Y
CSR.ts	3.6841	2.1212	0.1482	0.0853	Y	Y
CSR.km	-0.2503	-0.0096	0.0141	0.0005	Y	Y
RE.MH	-0.0200	1.2347	0.0482	2.9708	NA	NA

INT - Intercept; SUM - Summer; SPR - Spring; L - length (mm); FBT - final breakpoint temperature (°C); CSR - cardiac suppression range (°C); zk - Zinkwazi; ts - Three Sisters; km - Kommetjie; RE.MH - microhabitat random effect.

Key performance indicator analysis results for the third model were similar to those of the first two models. Specifically, when considering overall bias and RMSE across all parameters of the third model, the analysis model performed better on the imputed dataset than the incomplete dataset. The imputed dataset, however, had a slightly higher number of discrepancies between its significance outcomes and those of the reference dataset (Table A22).

Although some coefficient estimates derived from multiple imputation were suboptimal, they were generally more accurate than those obtained from the incomplete data. This suggests that final inferences and conclusions based on the imputed data would likely be more reliable than those drawn from the incomplete data.

Table A22: Comparison of the key performance indicators, for the imputed versus incomplete data, derived from the coefficients of the ANOVA analysis on FBT (°C). Highlighted cells indicate larger BIAS and RMSE values for imputed estimates and significance outcome values (SO) that did not match those from the reference dataset (N) versus those that did (Y).

	BIAS		RMSE		STC	
Parameter	**Missing1**	**Imputed1**	**Missing2**	**Imputed2**	**Missing3**	**Imputed3**
SZN	-0.4118	0.3079	89.7113	67.0788	Y	Y
SITE	-0.6060	0.0478	132.6592	10.4586	Y	Y
MH	-0.2536	-0.9998	286.1945	1,128.4799	Y	N
SZN.SITE	-0.9659	-0.5835	2.4534	1.4822	Y	Y
SITE.MH	-0.6696	-0.8850	10.5969	14.0061	Y	Y

SZN - season; MH - microhabitat

A4.1.2 Principal components analysis

In the PCA summary table generated from the imputed data for both *Siphonaria capensis* (Table A23) and *S. serrata* (Table A24), the first two principal components collectively explained slightly less than 75% of the total variance, which is commonly considered an acceptable threshold. Nevertheless, because the shortfall was marginal, only these two principal components were selected to generate the biplots for both species' imputed data (Figure A23 and Figure A24).

Table A23: PCA summary, generated using only the first multiply imputed dataset for *Siphonaria capensis*.

Content	PC1	PC2	PC3	PC4	PC5	PC6
Standard deviation	1.6529	1.3000	0.9233	0.6276	0.5214	0.2440
Proportion of variance	0.4553	0.2817	0.1421	0.0656	0.0453	0.0099
Cumulative proportion	0.4553	0.7370	0.8791	0.9448	0.9901	1.0000

Table A24: PCA summary, generated using only the first multiply imputed dataset for *Siphonaria serrata*.

Content	PC1	PC2	PC3	PC4	PC5	PC6
Standard deviation	1.7010	1.1932	0.9895	0.7048	0.3647	0.2721
Proportion of variance	0.4822	0.2373	0.1632	0.0828	0.0222	0.0123
Cumulative proportion	0.4822	0.7195	0.8827	0.9655	0.9877	1.0000

For *S. capensis*, most of the variability was captured by principal component one at 45.5% in Figure A23, with principal component two accounting for an additional 28.2%. Notable collinearity was observed among the size variables and between the three thermal limit variables (Figure A23). Consequently, to mitigate potential model fit issues, height and width were excluded from subsequent analyses of the *S. capensis* dataset. The thermal limit variables, however, were retained given the specific interest in their interrelationships. No correlation was expressed between these two groups of variables. Along principal component one, two distinct clusters materialized, with Kommetjie being distinguished from the other sites primarily due to size differences.

Kommetjie had larger individuals compared to the other two sites, which did not exhibit obvious differences in limpet size (Figure A23). In contrast, no site-specific clusters were observed along principal component two. Instead, separation on this component was more uniform and primarily influenced by the thermal limit variables. Although clustering along principal component two might become more discernible in a biplot colour-coded by one of the other categorical variables, such determination was outside the scope of the PCA as it was not the primary focus of this analysis.

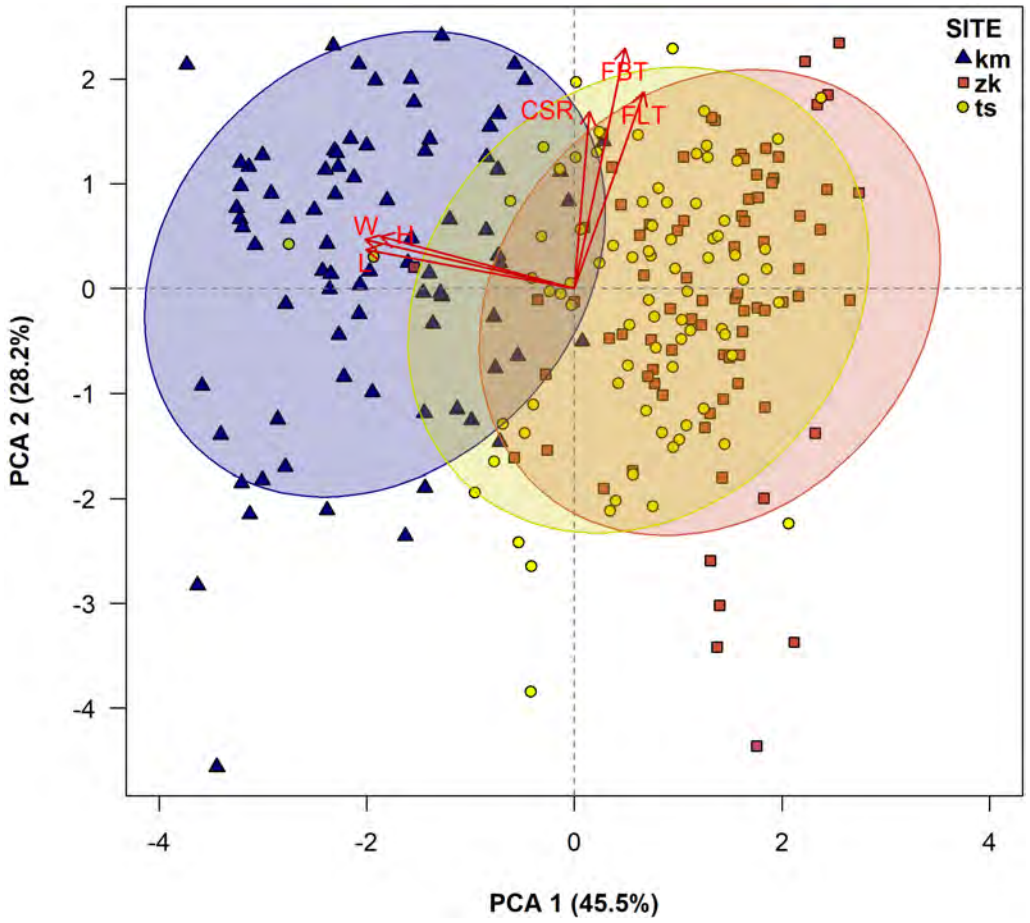

Figure A23: PCA biplot displaying clusters coded by site (zk - Zinkwazi; ts - Three Sisters; km - Kommetjie) in the first imputed dataset for *Siphonaria capensis*. Arrows indicate the direction and magnitude of the size (L - length (mm); H - height (mm); W - width (mm)) and thermal limit (FLT - flatline temperature (°C); FBT - final breakpoint temperature (°C); CSR – cardiac suppression range (°C)) variables.

The biplot derived from the *Siphonaria serrata* data reveals trends similar to those

observed in the *S.capensis* dataset (Figure A24). Principal component one accounted for the majority of the variability in the *S. serrata* dataset, capturing 48.2% of the variance, while the second principal component contributed a significant 23.7%. As with the *S.capensis* data, this dataset showed notable collinearity among thermal limit and size variables, indicating that a subset of the variables from each group may provide redundant information. Therefore, height and width were also removed from further analysis of the *S. serrata* dataset without the risk of losing significant insights. A distinct clustering along the first principal component suggests that larger *S.serrata* individuals are predominantly found at Kommetjie.

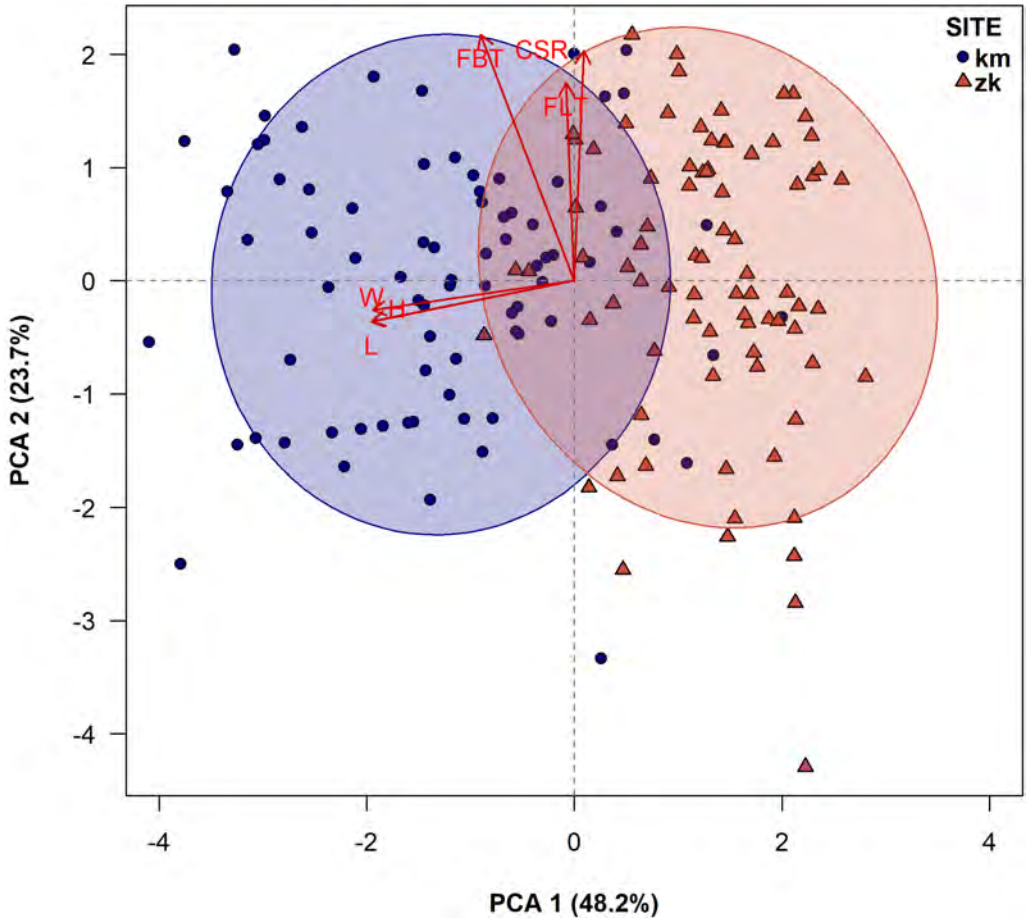

Figure A24: PCA biplot displaying clusters coded by site (zk - Zinkwazi; km - Kommetjie) in the first imputed dataset for *Siphonaria serrata*. Arrows indicate the direction and magnitude of the size (L - length (mm); H - height (mm); W - width (mm)) and thermal limit (FLT - flatline temperature (°C); FBT - final breakpoint temperature (°C); CSR – cardiac suppression range (°C)) variables.

A4.2 Model diagnostics

Model assumptions for all analyses in Chapter 5 were assessed using a range of graphical tools. The diagnostics were computed using the first imputed dataset for both species because there are no recognized methods available to perform regression diagnostics on pooled data.

A4.2.1 First model

Examination of the residuals vs fits plots from the linear mixed models, which focused on the covariance of FLT with FBT, revealed no evident heteroscedasticity for the extracted datasets of either *Siphonaria capensis* or *S. serrata* (Figure A25 and A26).

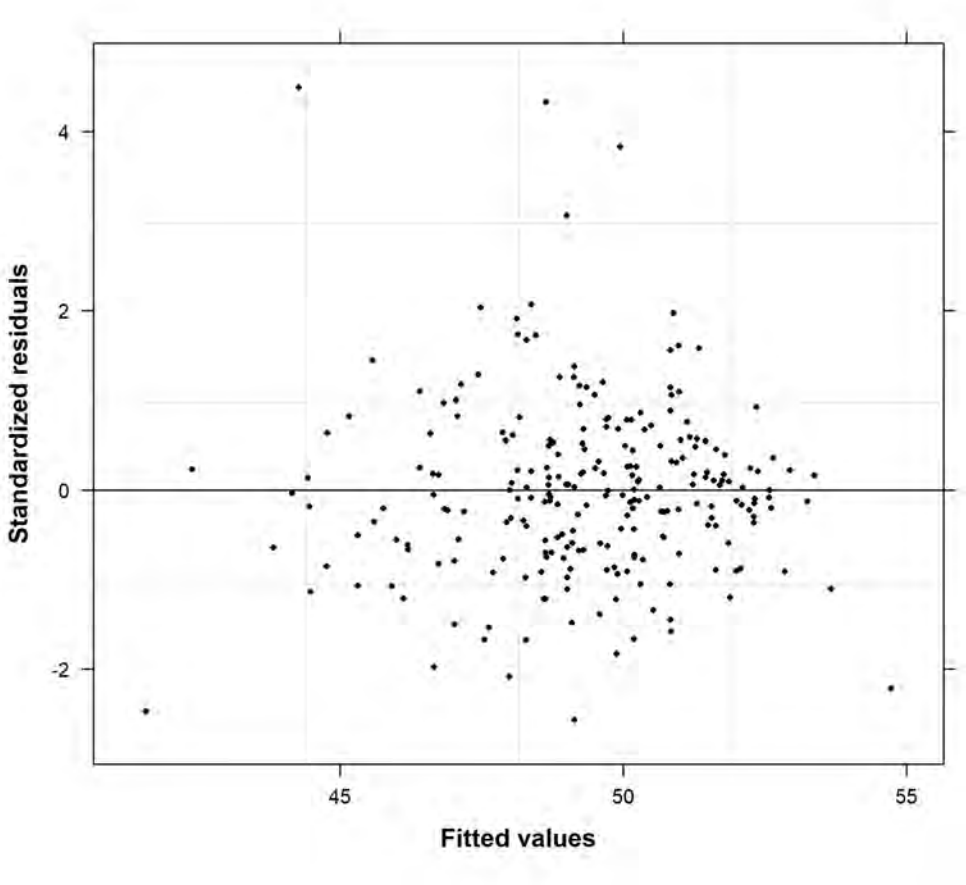

Figure A25: Plot of residuals vs fits for model 1 of the first imputed *S. capensis* dataset.

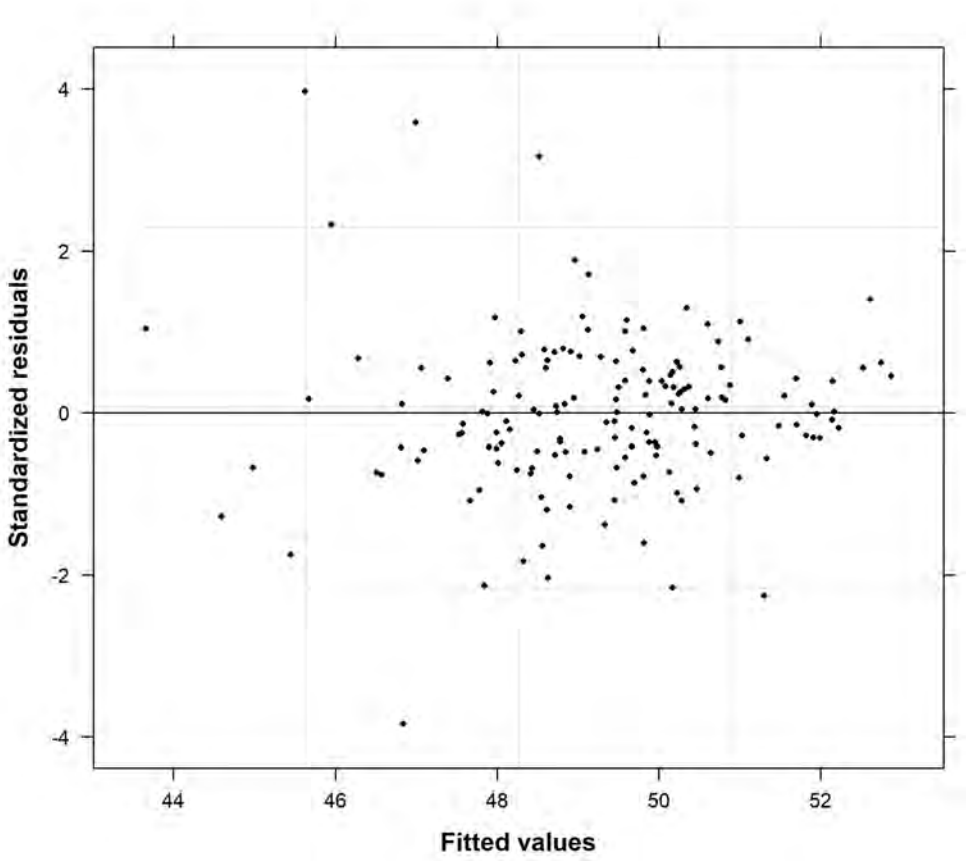

Figure A26: Plot of residuals vs fits for model 1 of the first imputed *S. serrata* dataset.

Consistent with the observations for the full datasets mentioned above, the variance among the levels of the random effect was homogeneous for both species (Figure A27 and A28).

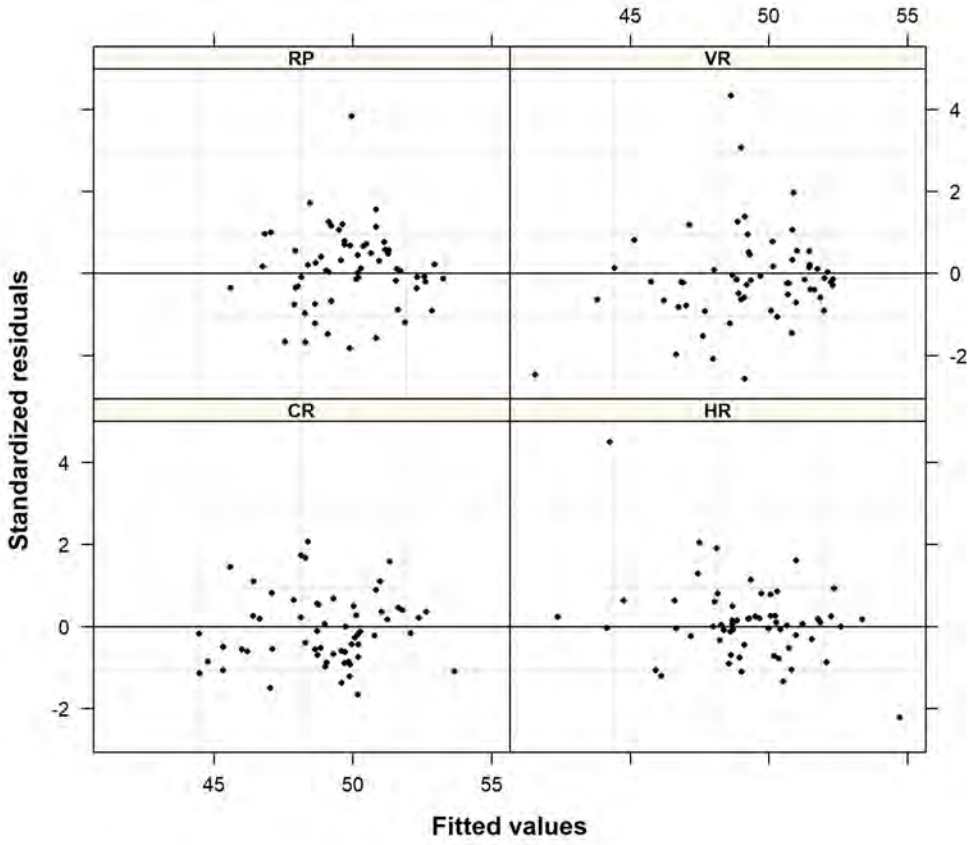

Figure A27: Plot of residuals vs fits by random effect (HR - Horizontal rock; VR - Vertical rock; CR - Crevice; RP - Rock pool) for model 1 of the first imputed *Siphonaria capensis* dataset.

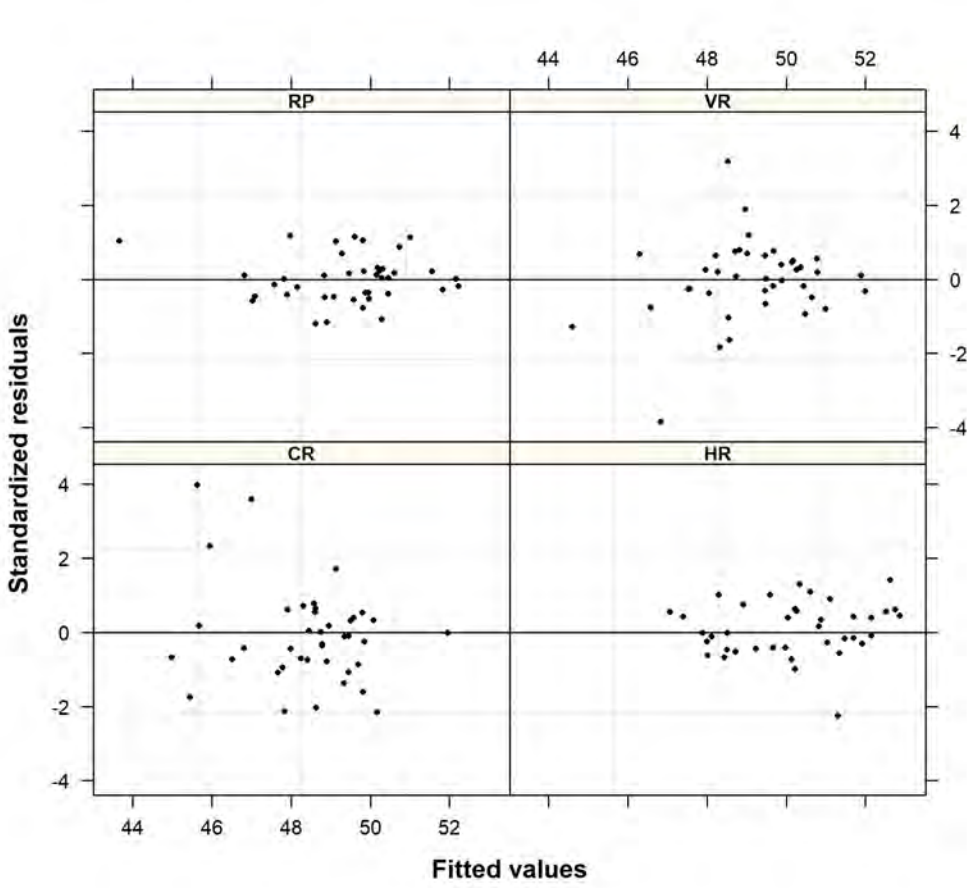

Figure A28: Plot of residuals vs fits by random effect (HR - Horizontal rock; VR - Vertical rock; CR - Crevice; RP - Rock pool) for model 1 of the first imputed *Siphonaria serrata* dataset.

The dotplot function from the lattice package, which represents standardized random effect distributions, indicated low variability across its levels in the plots for both species (Figure A29 and A30), supporting the Gaussian assumption. Although the confidence intervals for horizontal rocks in Figure A30 do not include zero, they overlap with those of the random effect levels for rock pools and vertical surfaces, which themselves overlap with one another and include zero. This pattern suggests that horizontal rocks were only marginally different from zero and remains consistent with the overall minimal variability observed (Figure A30).

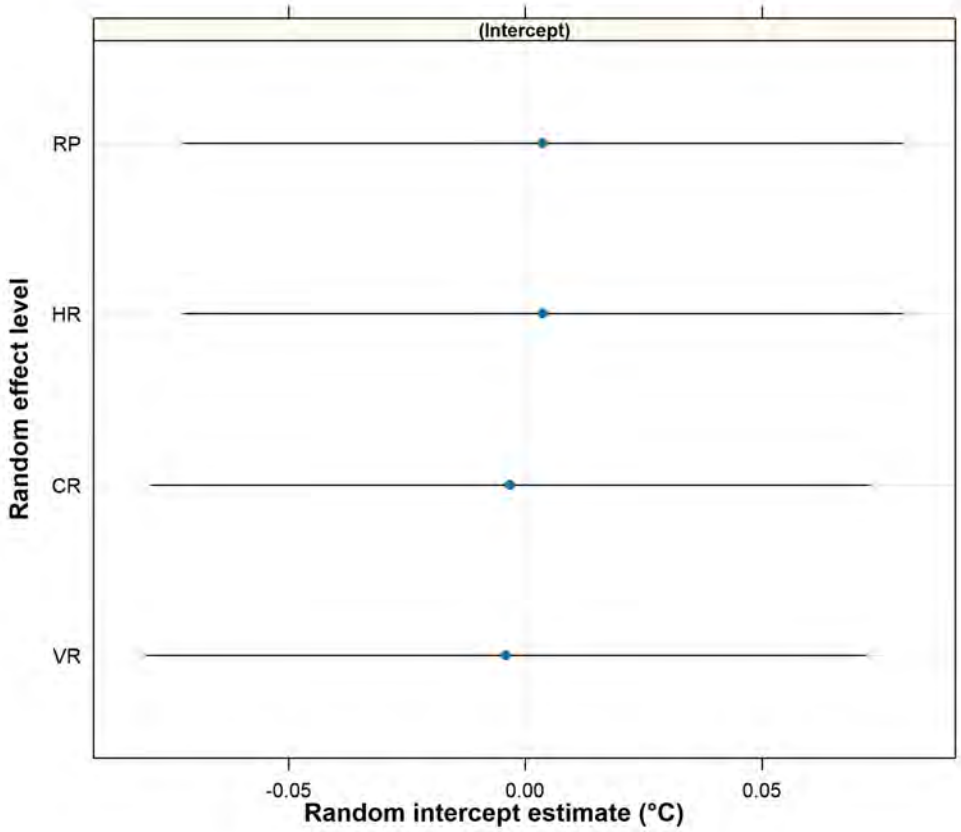

Figure A29: Standardized random effect distribution for the first model of the first imputed *S. capensis* dataset. HR - Horizontal rock; VR - Vertical rock; CR - Crevice; RP - Rock pool.

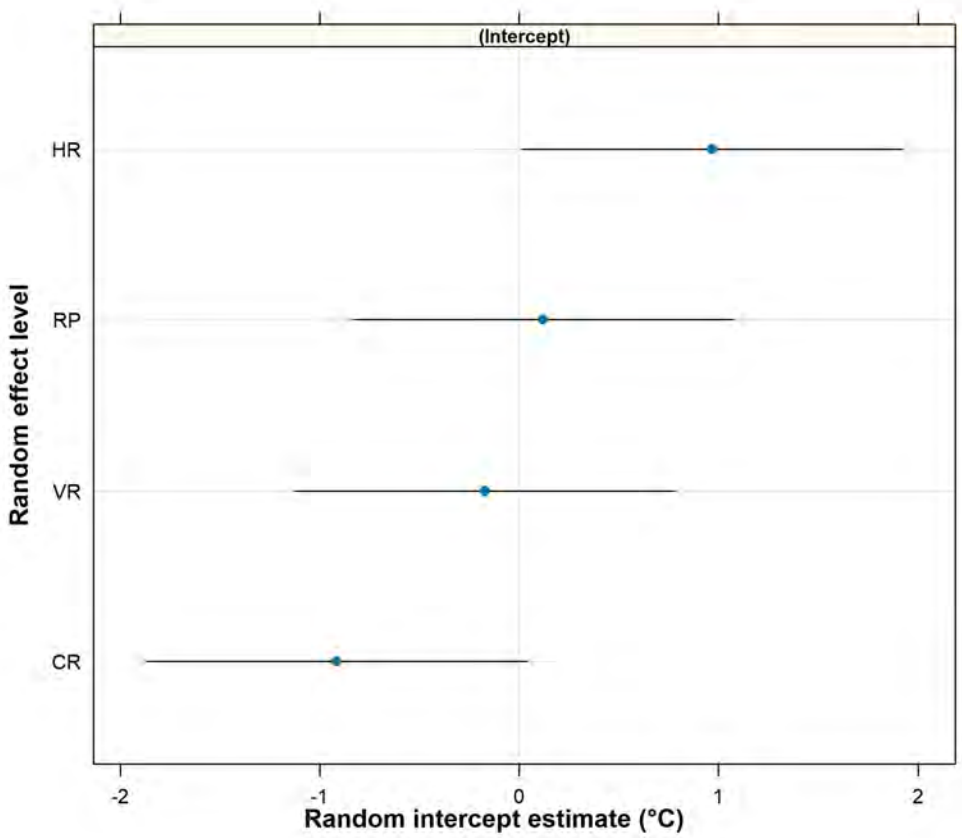

Figure A30: Standardized random effect distribution for the first model of the first imputed *S. serrata* dataset. HR - Horizontal rock; VR - Vertical rock; CR - Crevice; RP - Rock pool.

Although the quantile-quantile plot (qqplot), produced with the qqnorm function from base R, for the *Siphonaria capensis* and *S. serrata* data showed pronounced deviations from the reference line, these deviations were primarily concentrated at the tails (Figure A31 and A32). This suggests that the assumptions of normality for this model were reasonably met.

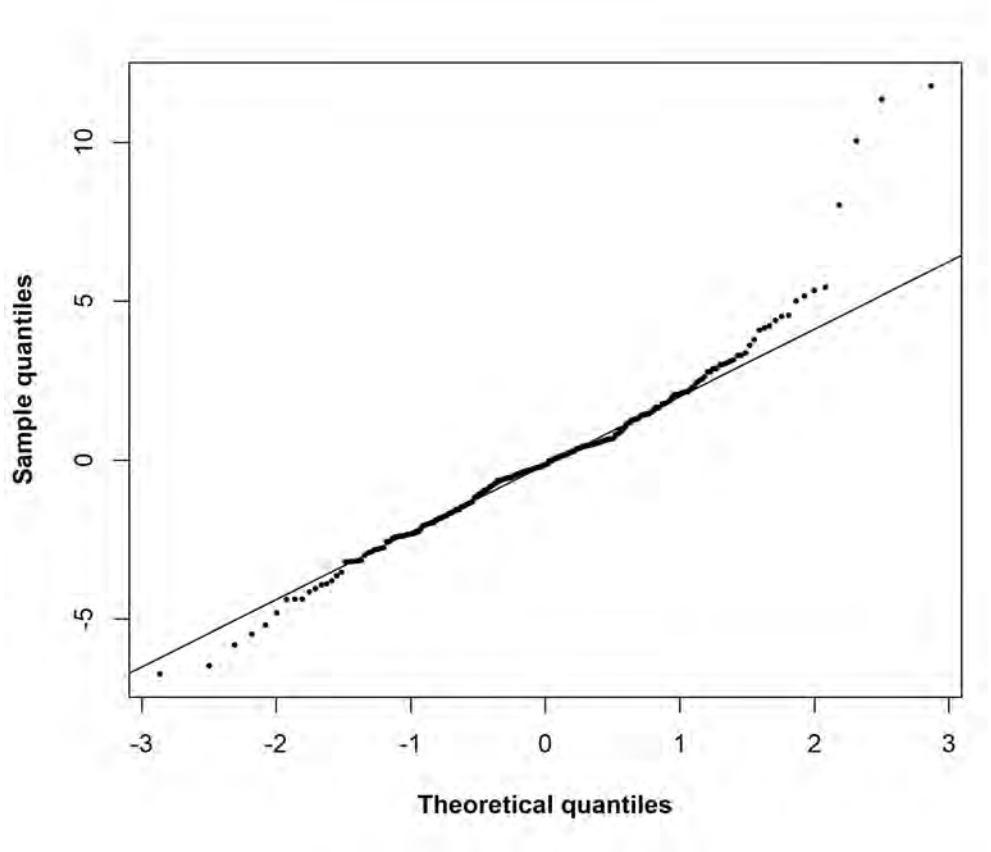

Figure A31: Normal QQ-Plot from the first model of the first imputed *S. capensis* dataset.

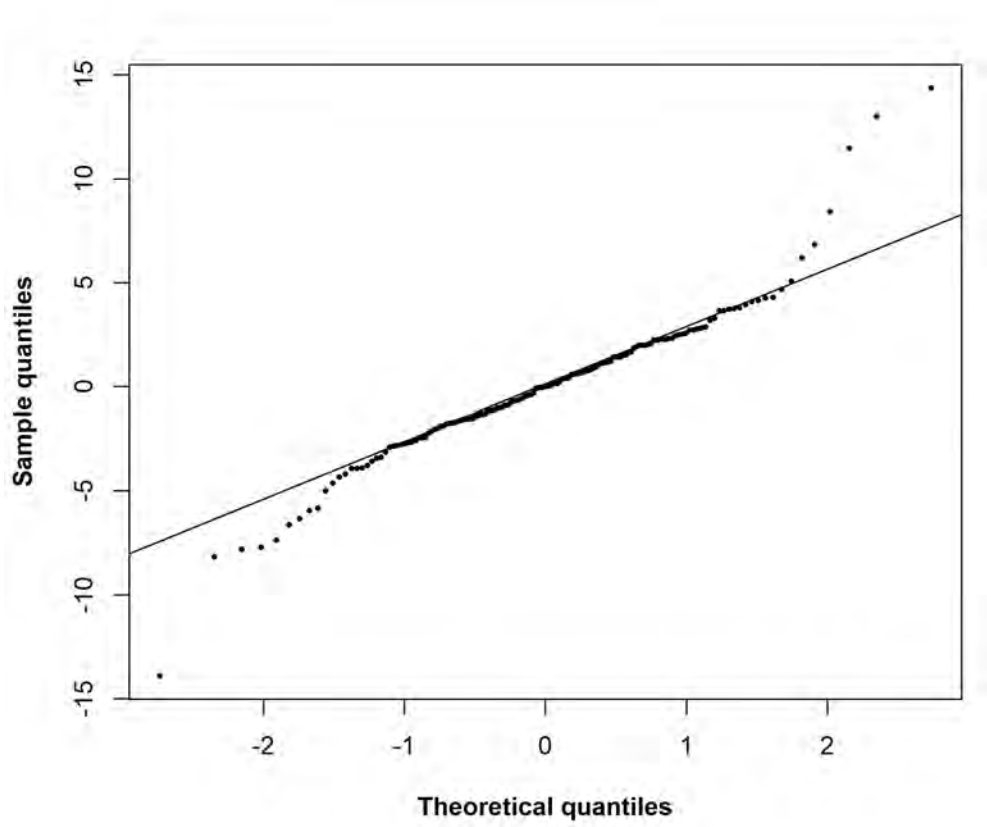

Figure A32: Normal QQ-Plot from the first model of the first imputed *S. serrata* dataset.

Apart from a few observations with high hat-values (leverage > 0.167) for both species (Figure A33 and A34), the majority of observations showed low standardized residuals (Cook's distance < 1) and low hat-values. The observations with high hat-values were not removed, as they did not appear to substantially affect the model's assumptions or overall fit. Hat-values measure the influence of individual observations on the fitted values in a regression model (Cook 1977, Fox & Monette 2002).

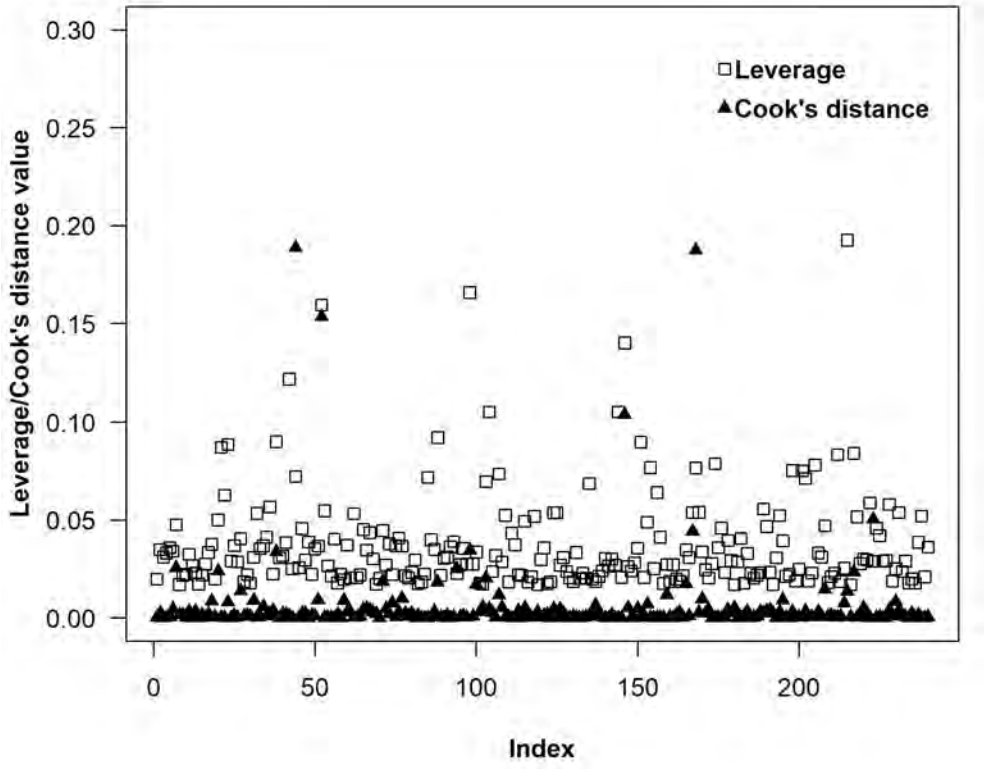

Figure A33: Plot of Cook's distance and Leverage to identify influential outliers from the first model of the first imputed *Siphonaria capensis* dataset.

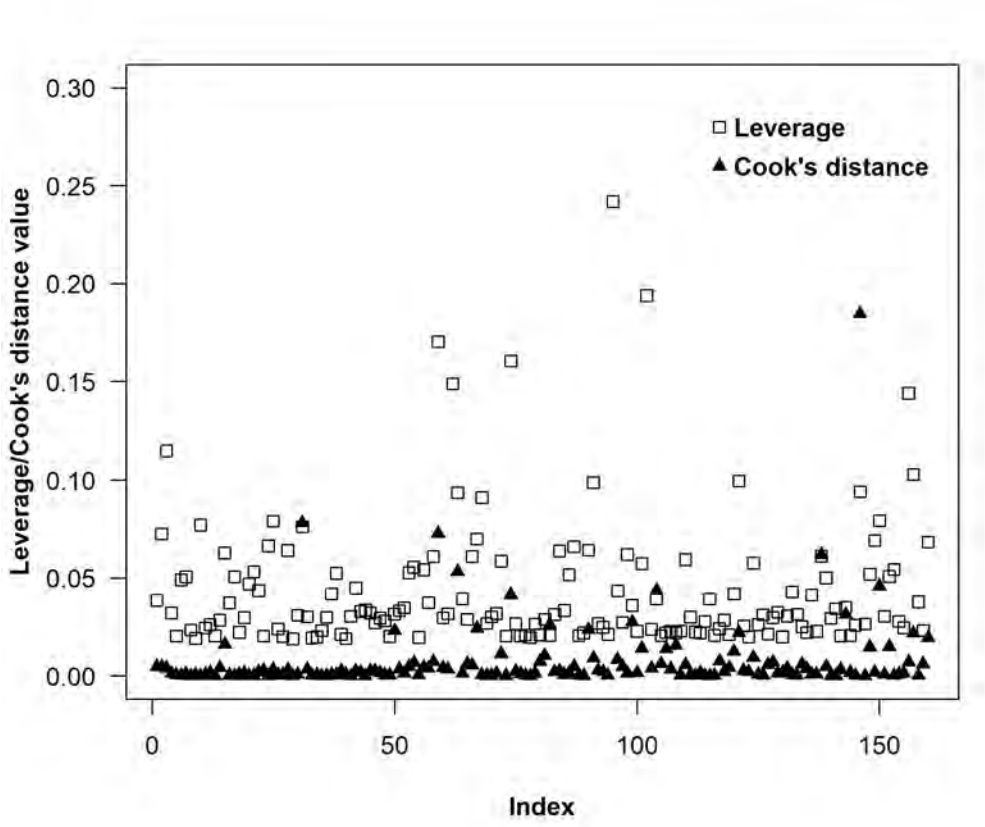

Figure A34: Plot of Cook's distance and Leverage to identify influential outliers from the first model of the first imputed *S. serrata* dataset.

A4.2.2 Second model

Upon reviewing the residuals vs fits plots from the second model, which explored the covariance between FBT and CSR, no clear signs of heteroscedasticity was found in the datasets extracted for either *Siphonaria capensis* or *S. serrata* (Figure A35 and A36).

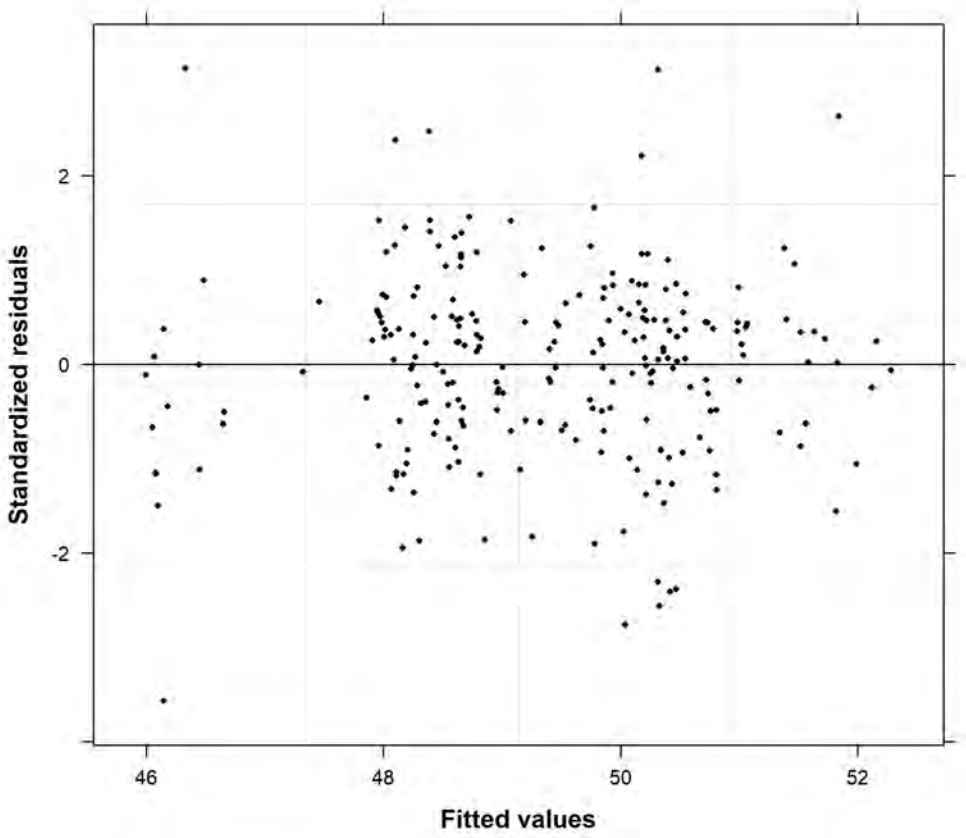

Figure A35: Plot of residuals vs fits for model 2 of the first imputed *S. capensis* dataset.

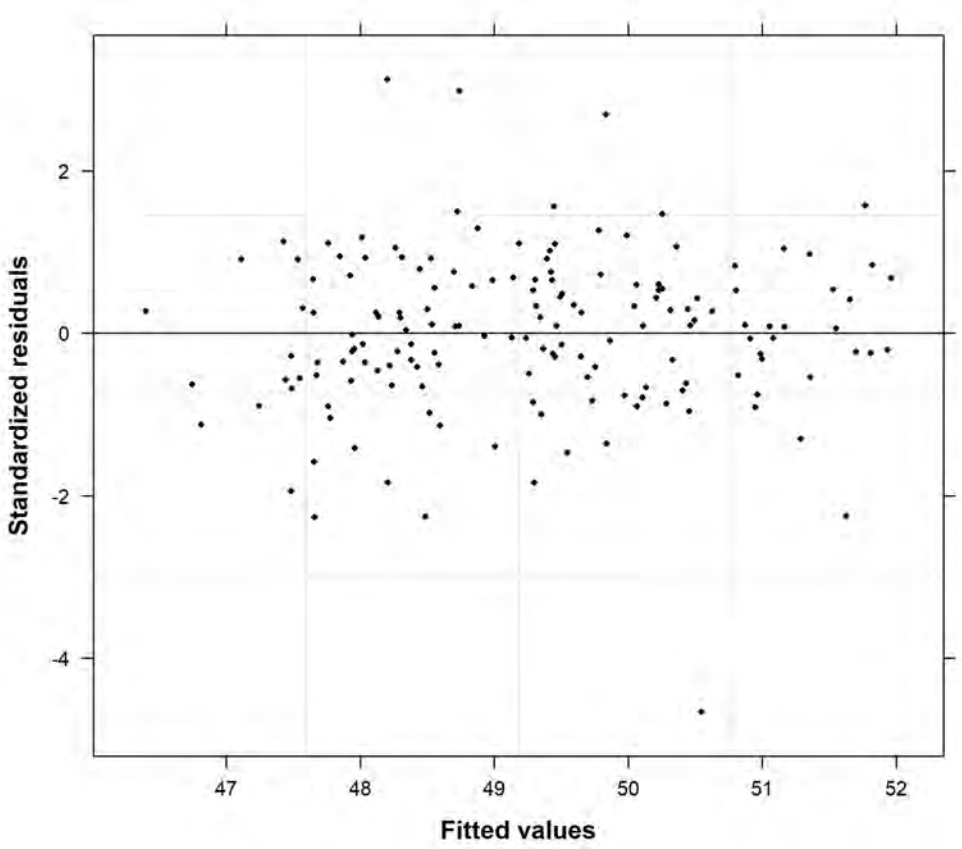

Figure A36: Plot of residuals vs fits for model 2 of the first imputed *S. serrata* dataset.

In line with earlier findings regarding heteroscedasticity in the imputed datasets, variance across the random effect levels was also uniform for both species (Figure A37 and A38).

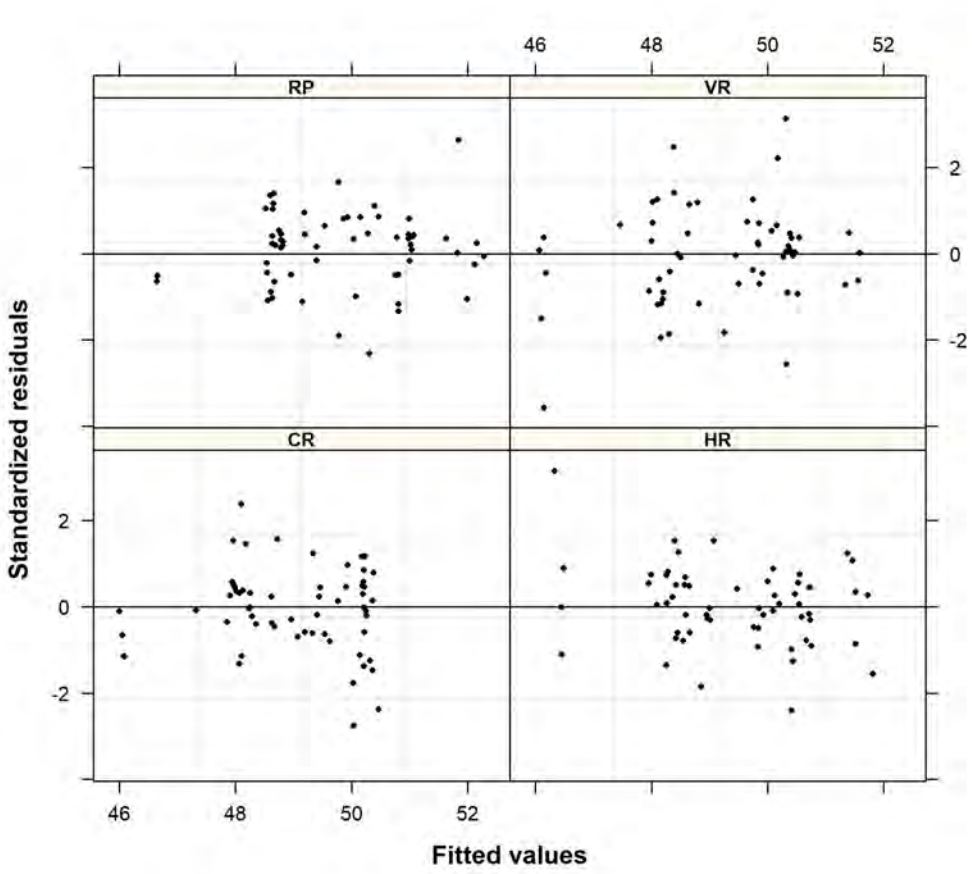

Figure A37: Plot of residuals vs fits by random effect for model 2 of the first imputed *Siphonaria capensis* dataset. HR - Horizontal rock; VR - Vertical rock; CR - Crevice; RP - Rock pool.

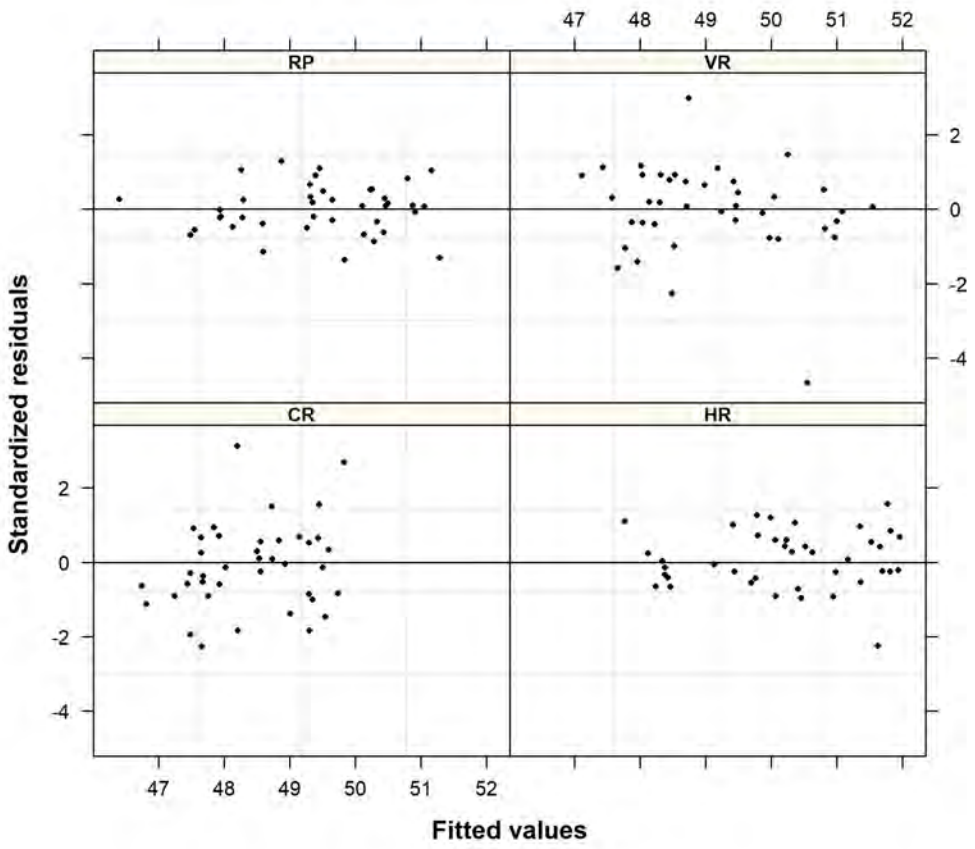

Figure A38: Plot of residuals vs fits by random effect for model 2 of the first imputed *Siphonaria serrata* dataset. HR - Horizontal rock; VR - Vertical rock; CR - Crevice; RP - Rock pool.

Similar to the estimated effects in the standardized random effect distribution plots for the first model (Figure A29 and A30), the second model's estimated effects also supported the Gaussian assumption (Figure A39 and A40). Furthermore, the confidence intervals for horizontal surfaces and crevices in the *Siphonaria serrata* data (Figure A40) do not include zero, but as described for Figure A30, they remain consistent with the overall minimal variability that was expected.

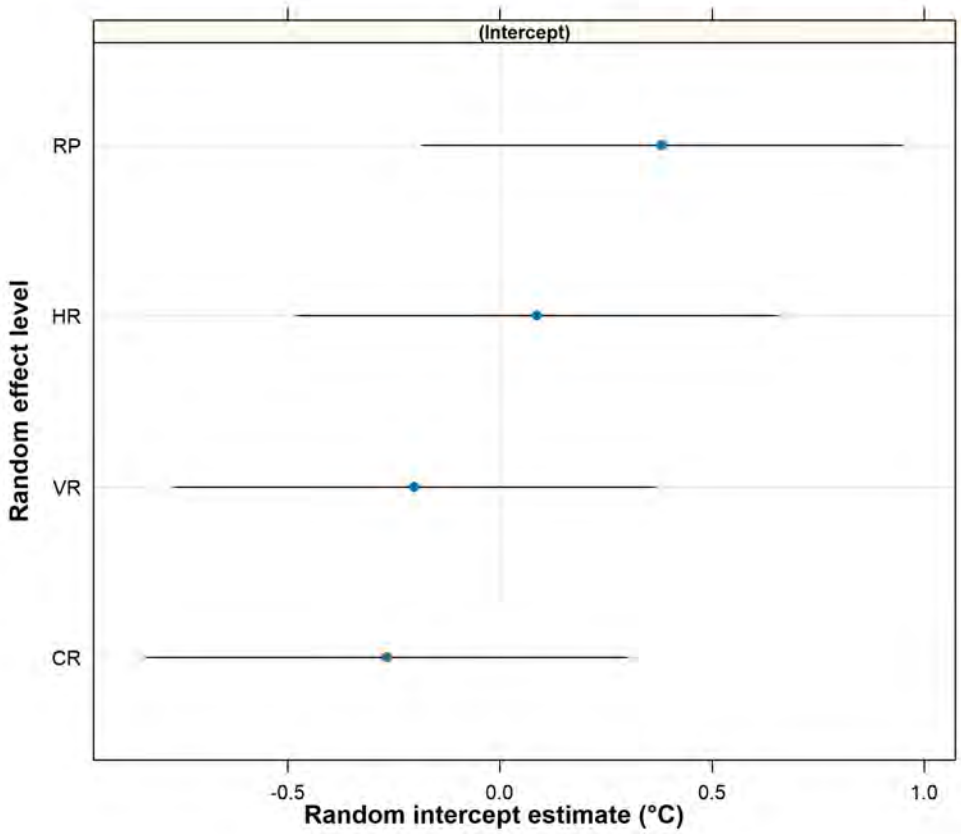

Figure A39: Standardized random effect distribution for the second model of the first imputed *S. capensis* dataset. HR - Horizontal rock; VR - Vertical rock; CR - Crevice; RP - Rock pool.

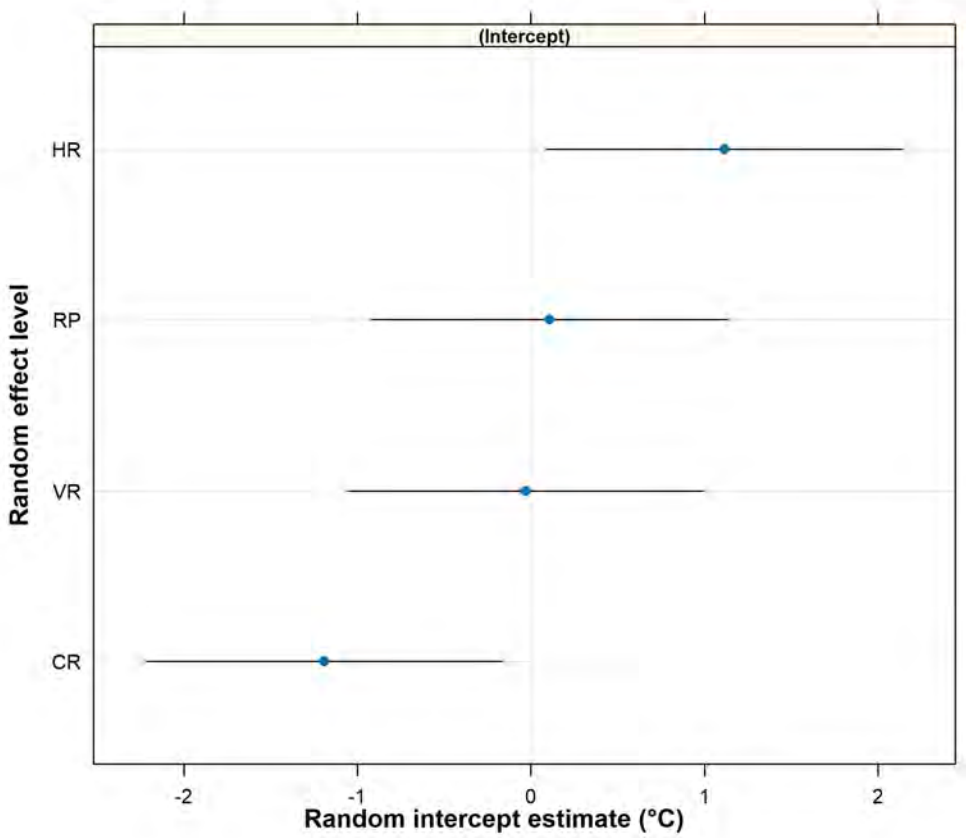

Figure A40: Standardized random effect distribution for the second model of the first imputed *S. serrata* dataset. HR - Horizontal rock; VR - Vertical rock; CR - Crevice; RP - Rock pool.

The quantile-quantile plots for both *Siphonaria capensis* and *S. serrata* displayed points largely aligned with the reference line, indicating that the residuals were predominantly normally distributed, despite slight deviations at the tails (Figure A41 and A42).

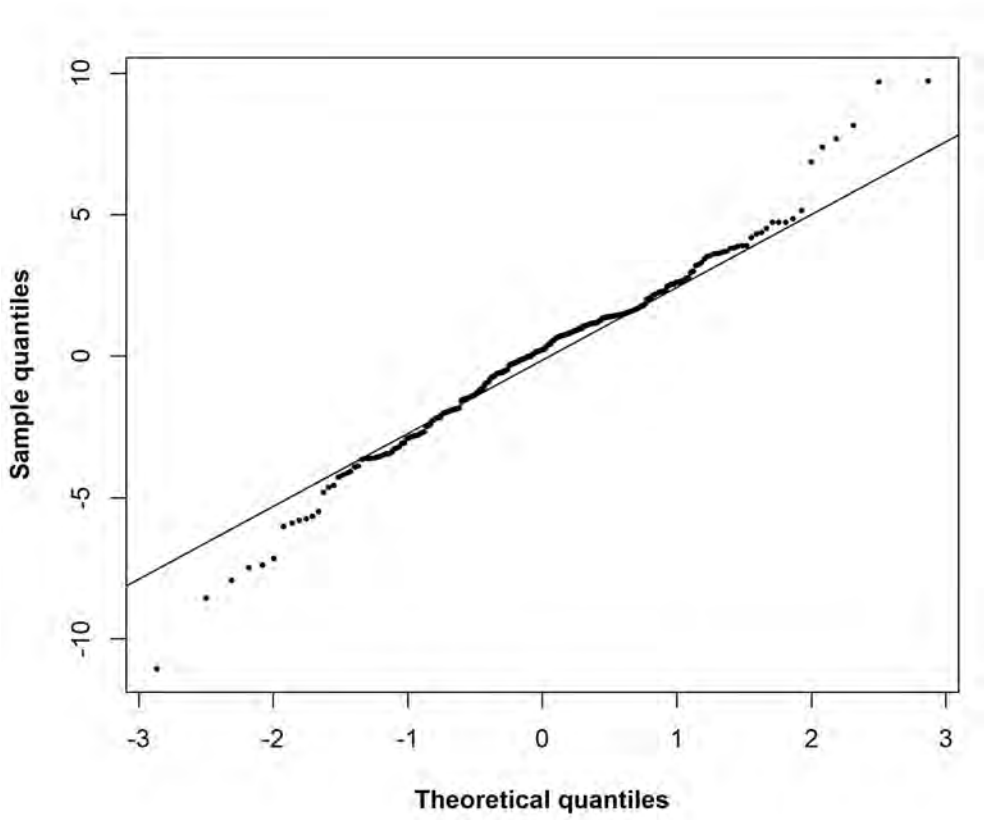

Figure A41: Normal QQ-Plot from the second model of the first imputed *S. capensis* dataset.

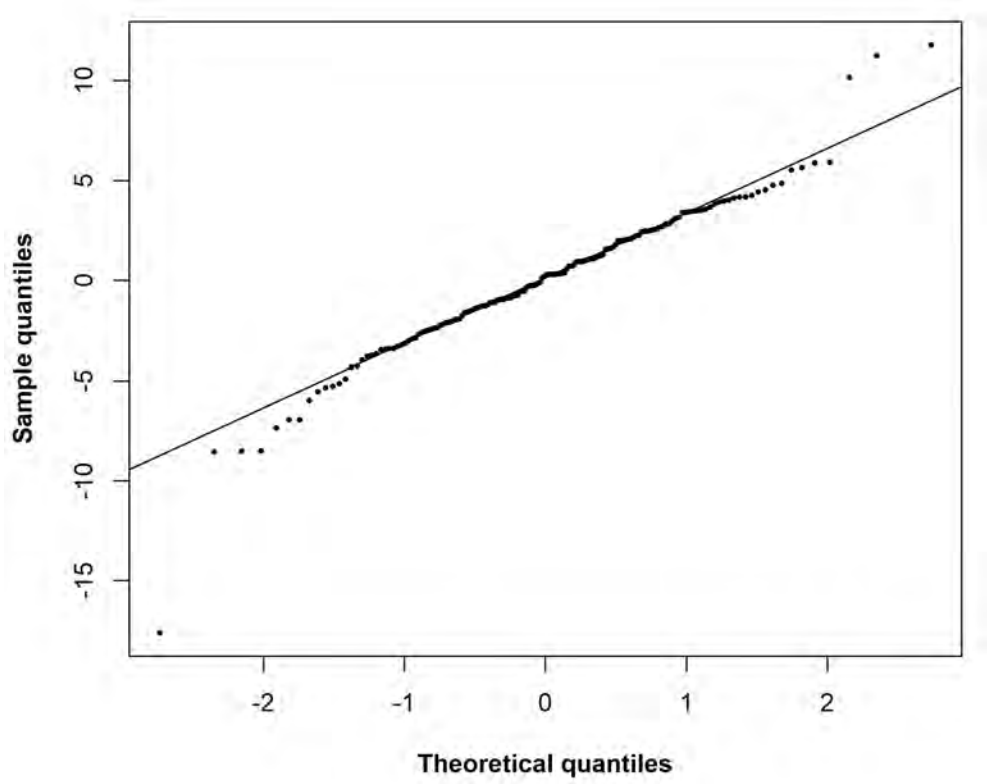

Figure A42: Normal QQ-Plot from the second model of the first imputed *S. serrata* dataset.

For both species, most observations had low Cook's distances and Leverage values, with only a few mildly increased Cook's distances for *Siphonaria serrata* that were not sufficiently high to regard them as influential outliers (Figure A43 and A44).

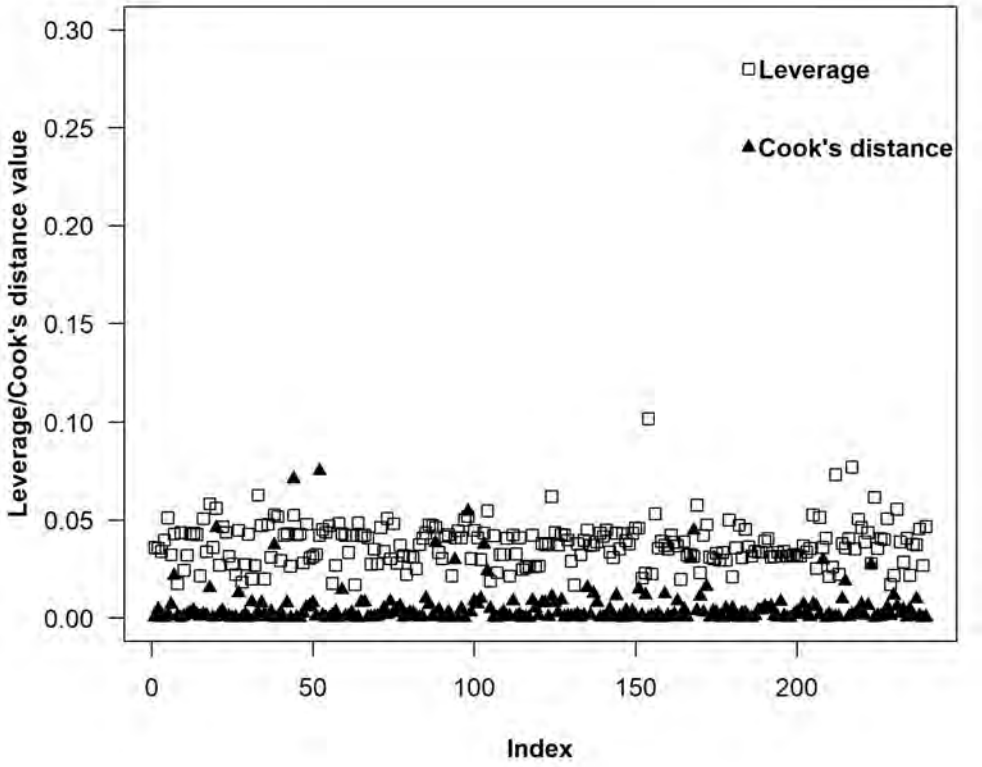

Figure A43: Plot of Cook's distance and Leverage to identify influential outliers from the second model of the first imputed *S. capensis* dataset.

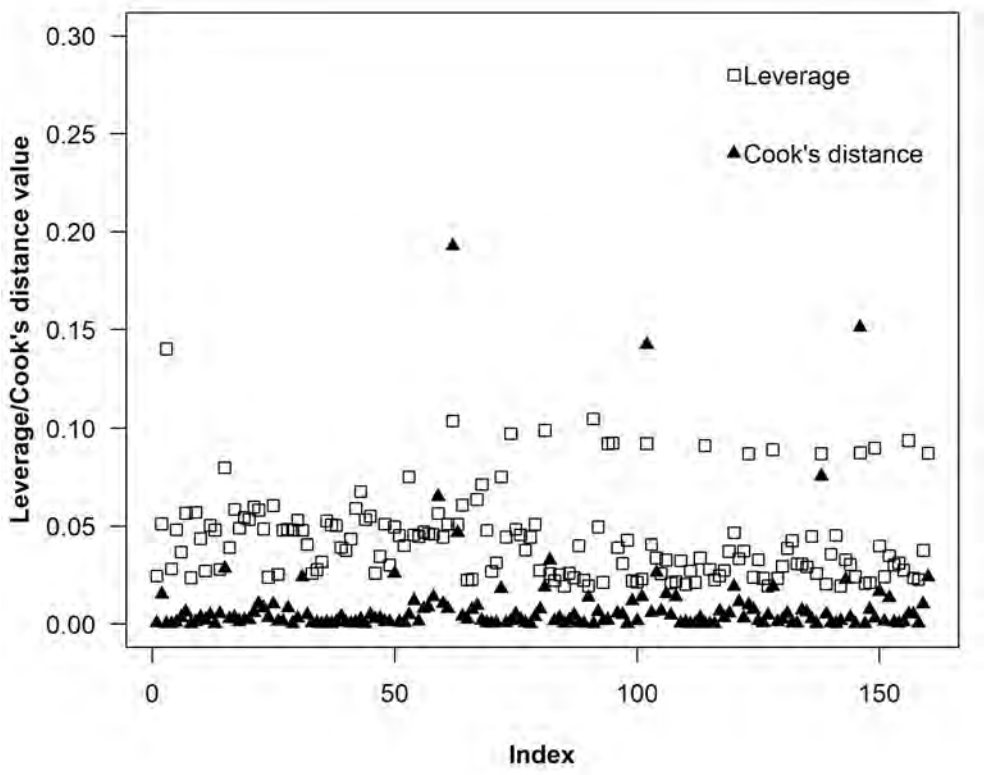

Figure A44: Plot of Cook's distance and Leverage to identify influential outliers from the second model of the first imputed *S. serrata* dataset.

A4.2.3 Third and fourth models

The diagnostic plots indicate that the assumptions of linearity (residuals vs fitted), normality (quantile-quantile normal), and constant variance (scale-location) for the ANOVA fit using the response variable FBT, were upheld for both *Siphonaria capensis* and *S. serrata* (Figure A45 and A46). The numbered observations in Figure A45 and A46 represent data points from the dataset that were flagged by the various diagnostic measures (e.g., high Cook's distance, large standardized residuals) as potentially being outliers or influential outliers. As with the outliers shown in Figure A33 and A34, I chose not to remove them from the dataset and re-run the model. In this case, although these observations are flagged as outliers under more recent thresholds for identifying

influential points (e.g., Cook's distance d = 4/n, where n = 240 observations), they do not exceed the original threshold proposed by Cook (1977) (Cook's distance d = 1) for determining influence.

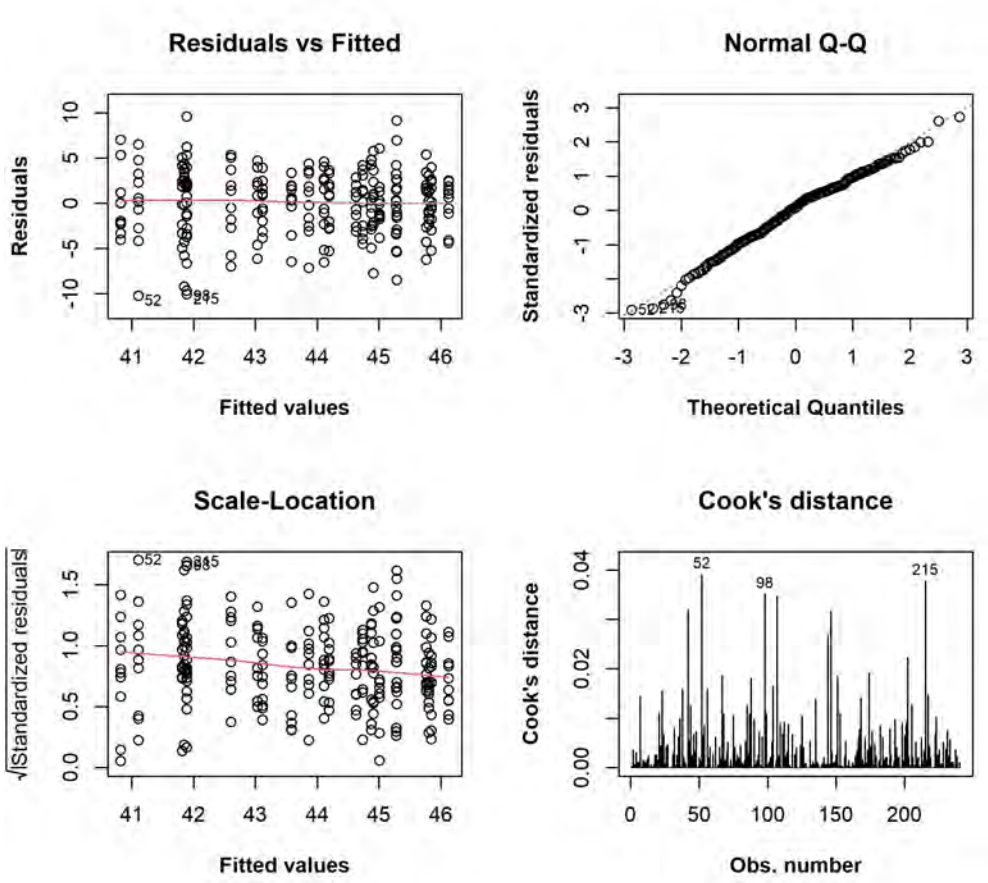

Figure A45: Diagnostic plots from the factorial ANOVA conducted on FBT (°C) values derived from TRCs of *S. capensis*.

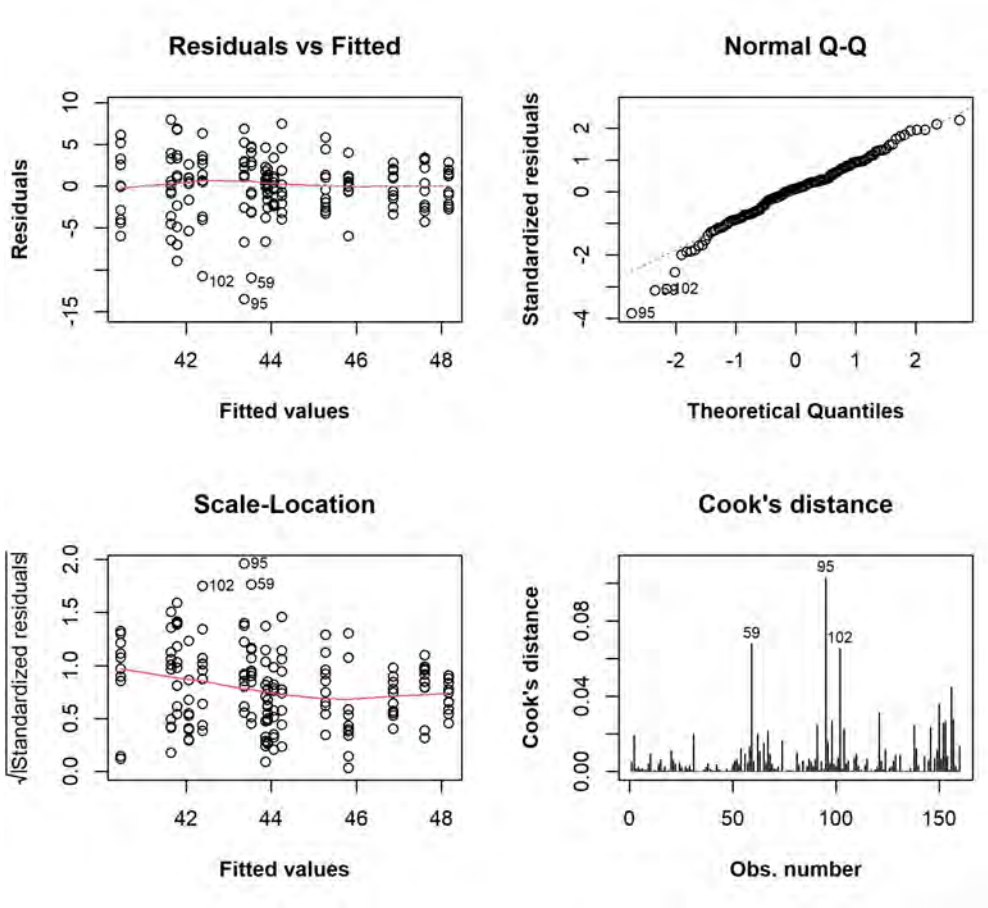

Figure A46: Diagnostic plots for the factorial design ANOVA analyzing FBT (°C) values from TRCs of *S. serrata*.

For both species, no model violations were detected for the ANOVA fit with Length as the response variable (Figure A47 and A48). Similar to Figure A45 and A46, the numbered observations in these figures represent data points that were flagged by diagnostic measures. Furthermore, these observations were treated in the same manner as those in Figure A45 and A46.

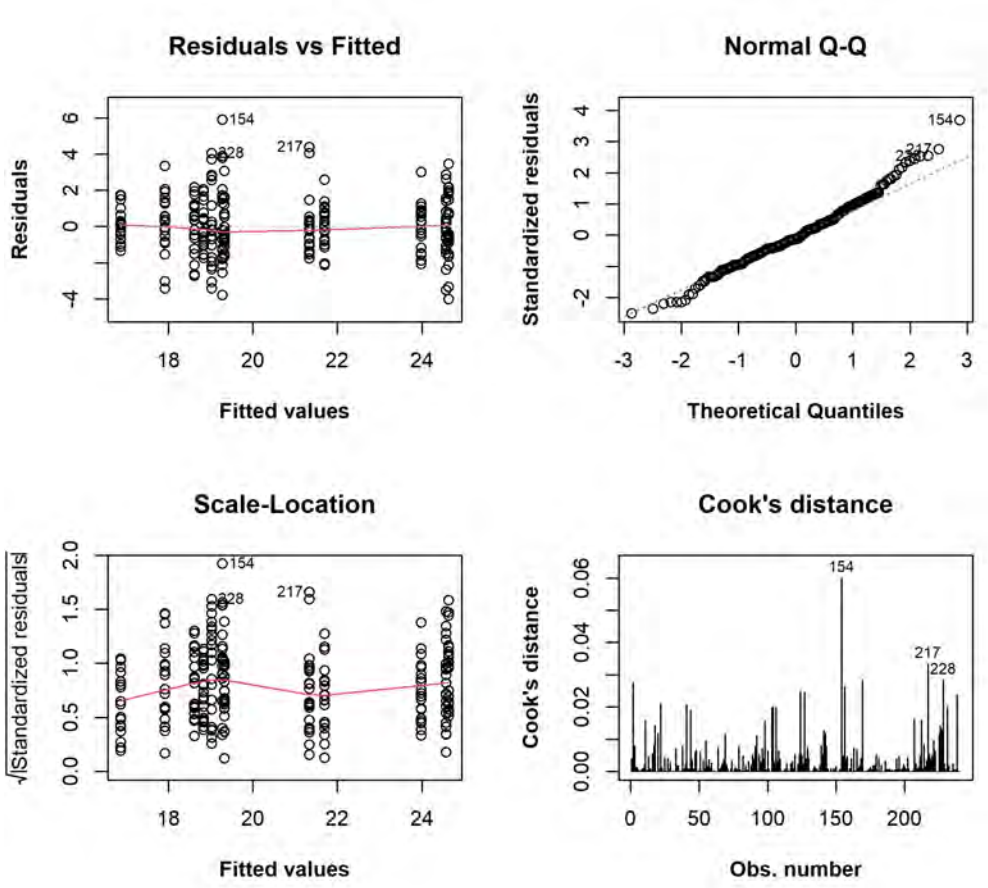

Figure A47: Diagnostic plots from the factorial ANOVA analyzing the Length (mm) of *S. capensis* individuals.

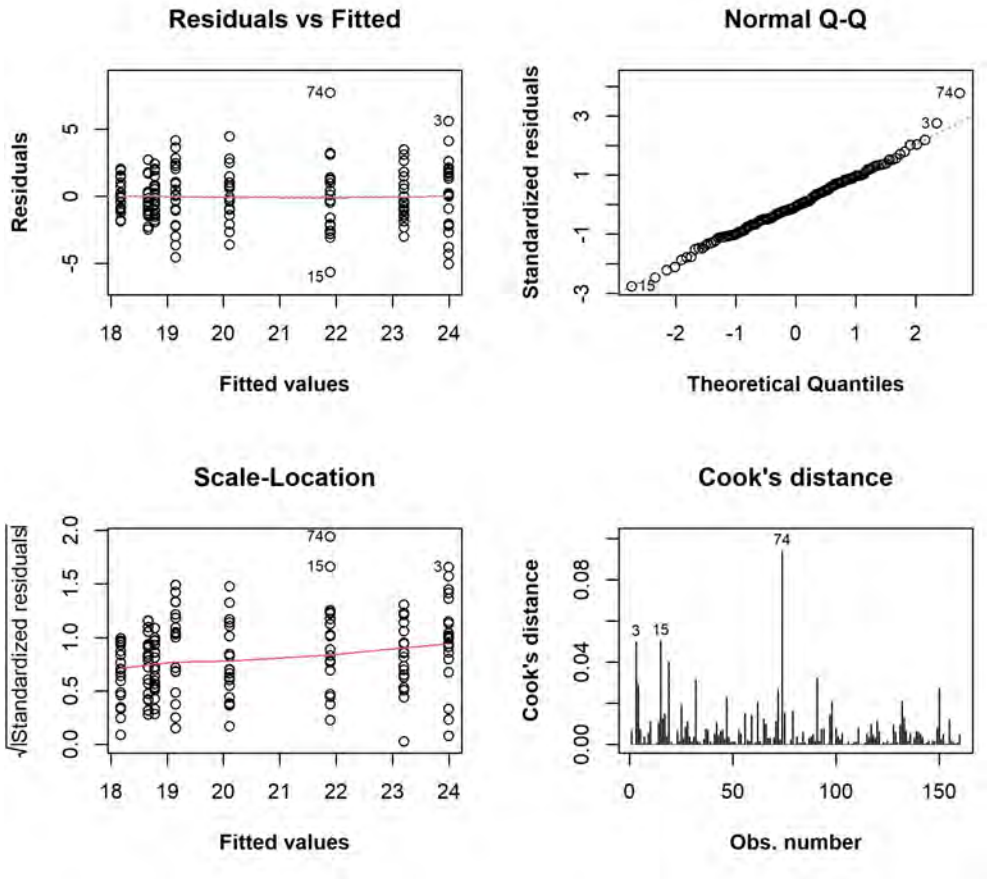

Figure A48: Diagnostic plots for the factorial ANOVA analyzing the Length (mm) of *S. serrata* individuals.

A5 Ethical clearance declaration

At the time of my experimental research, ethical approval was not required for research on non-cephalopod molluscs.